Kiyoshi Tomioka · Takayuki Shioiri
Hironao Sajiki *Editors*

New Horizons of Process Chemistry

Scalable Reactions and Technologies

Springer

New Horizons of Process Chemistry

Kiyoshi Tomioka · Takayuki Shioiri
Hironao Sajiki
Editors

New Horizons of Process Chemistry

Scalable Reactions and Technologies

Springer

Editors
Kiyoshi Tomioka
Doshisha Women's College of Liberal Arts
Kyotanabe
Japan

Hironao Sajiki
Gifu Pharmaceutical University
Gifu
Japan

Takayuki Shioiri
Meijo University
Nagoya
Japan

ISBN 978-981-10-3420-6 ISBN 978-981-10-3421-3 (eBook)
DOI 10.1007/978-981-10-3421-3

Library of Congress Control Number: 2016963739

Printed on acid-free paper

This Springer imprint is published by Springer Nature
The registered company is Springer Nature Singapore Pte Ltd.
The registered company address is: 152 Beach Road, #21-01/04 Gateway East, Singapore 189721, Singapore

Preface

Process chemistry will be one of the most important sciences in the twenty-first century. It passes the baton in a relay race from discovery of useful new materials to their industrial production. Economic and environmentally benign procedures are essential. Because the stagnation of process chemistry is estimated to cause industrial depression and excessive loss, chemists focus on process chemistry consistently to provide a stimulus by the development of novel and efficient new methods, reactions, and technologies applicable to scalable production.

In December 2015, the International Chemical Congress of Pacific Basin Societies 2015 (Pacifichem 2015) was held in Hawaii, and the symposium "New Horizon of Process Chemistry by Scalable Reactions and Technologies" was convened as one of the technical programs, supported by the Japanese Society for Process Chemistry. A series of interesting lectures by 35 speakers was delivered, and 33 topics were presented at the poster session. Topics of these lectures and presentations included new catalysts, reactions, and methods for the synthesis of functional materials including pharmaceuticals, agrochemicals, chemical raw materials, and other materials oriented toward process chemistry, with green and sustainable chemistry as one of the major topics. Furthermore, various isolation methods including crystallization, development of reactors and equipment, direct observational methods of the progress in reactions, and process design to increase scale were also important topics.

This book is a selection of the above-mentioned presentations; however, it is not a proceedings of the symposium but rather a collection of mini-reviews based on the presentations. Readers will be able to enjoy reading about the latest developments in the field of process chemistry, new methodology intended for process chemistry, and medicinal chemistry.

We hope process chemistry will be more productive and will flourish in the near future.

Kyotanabe, Japan — Kiyoshi Tomioka
Nagoya, Japan — Takayuki Shioiri
Gifu, Japan — Hironao Sajiki

Contents

Recent Advances in Rare Earth Metal Asymmetric Catalysis Toward Practical Synthesis of Therapeutics

Naoya Kumagai and Masakatsu Shibasaki

Abstract Two case studies regarding the development of rare earth metal-based asymmetric catalysts are summarized, with particular focus on the process of refining catalysts amenable to industrial applications. Amide-based chiral ligands in combination with lanthanum or neodymium cations furnished robust catalytic systems for asymmetric amination or nitroaldol reactions, respectively. Although rare earth metal catalysis is generally characterized by a peculiar coordination chemistry and Lewis acidic catalytic functions, its wide availability and moderate tolerance to moisture are also important features to be noted, making the application of rare earth metal catalysis beneficial for industrial large-scale synthesis.

Keywords Amination · Asymmetric catalysis · Flow reaction · Nitroaldol · Rare earth metals

1 Introduction

Homochirality has become an indispensable feature for the manufacture of active pharmaceutical ingredients (APIs), attracting increasing attention to enantioselective catalysis in medicinal and process chemistry as an efficient method for producing chiral building blocks of interest. Efficiency in lab-scale synthesis and feasibility in large-scale operations, however, are often difficult to achieve in parallel; the majority of newly developed methods in enantioselective catalysis are rarely applied to industrial applications. Particularly for chiral hard Lewis acid catalysts, the requirement for rigorous drying of the substrates and reaction vessels to achieve high fidelity in the reaction severely hampers industrial application.

N. Kumagai (✉) · M. Shibasaki (✉)
Institute of Microbial Chemistry (BIKAKEN), 3-14-23 Kamiosaki,
Shinagawa-ku Tokyo 141-0021, Japan
e-mail: nkumagai@bikaken.or.jp

M. Shibasaki
e-mail: mshibasa@bikaken.or.jp

K. Tomioka et al. (eds.), *New Horizons of Process Chemistry*,
DOI 10.1007/978-981-10-3421-3_1

Herein we document chiral rare earth metal catalysts that are promising for prospective application in large-scale industrial operations. Despite the term 'rare', not all 'rare' earth metal are expensive and available in only small quantities [1]; indeed, the natural abundance of lanthanum, one of the most representative rare earth metals, in the earth's crust is close to that of zinc or boron. The relatively low toxicity concerns of rare earth metals are also favorable for application to the manufacture of APIs. This chapter summarizes two rare earth metal-based asymmetric catalysts featuring lanthanum and neodymium as key components responsible for catalytic functions.

2 La-based Catalysis: Catalytic Asymmetric Amination

Nitrogen is a key element embedded in carbon-based skeletons in a myriad of natural products and therapeutics, thereby the development of synthetic methodologies to incorporate nitrogen functionalities have been a sustained topic in organic synthesis. Electrophilic amination utilizing azodicarboxylates as electrophiles is commonly exploited to install nitrogen functionality in certain nucleophiles, including latent enolates [2]. Despite its early discovery [3–5], no enantioselective variants were reported until Evans et al. disclosed catalytic asymmetric α-amination of *N*-acyloxazolidines and enolsilanes promoted by Mg and Cu complexes in the late 90s [6, 7]. Since this demonstration of enantioselective introduction of nitrogen functionality, the flurry of reports on catalytic asymmetric amination appeared based on both organocatalysts and metal catalysts, and has been compiled in various review articles [8–12].

In this context, we were particularly intrigued by the fact that simple succinimide-type substrate **1** eluded the introduction of a nitrogen functionality in a catalytic and enantioselective manner (Scheme 1). Amination product **2** is a known key intermediate of ranirestat (AS-3201) [13, 14], which is under clinical trials led by Dainippon-Sumitomo Pharma for the treatment of diabetic neuropathy. Previously identified organocatalysts and metal-based catalysts in the literature

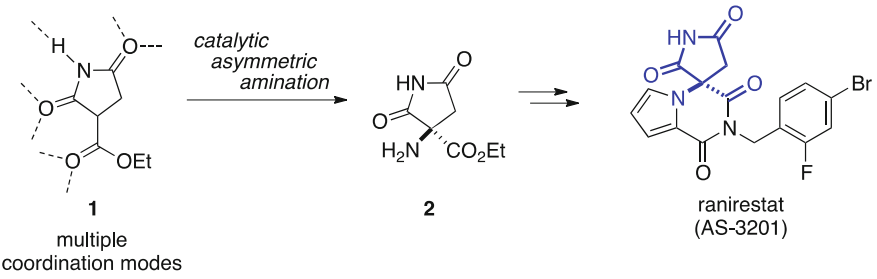

Scheme 1 Catalytic asymmetric amination of succinimide derivative **1** for the enantioselective synthesis of ranirestat, a candidate drug for diabetic neuropathy

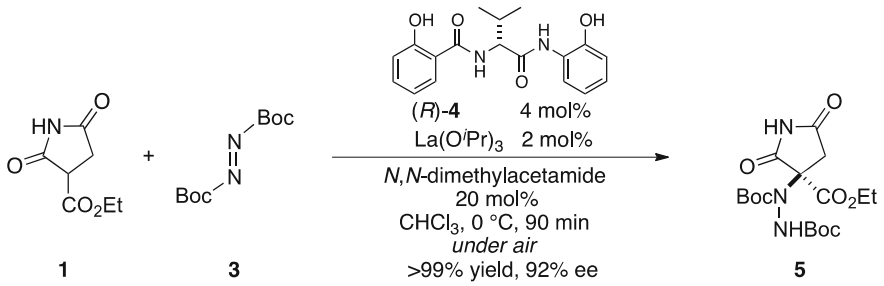

Scheme 2 Catalytic asymmetric amination of **1** and azodicarboxylate **3** promoted by La(O^{i}Pr)$_3$/(*R*)-**4**

promote the amination of **2** with insufficient enantioselectivity, presumably because the multiple coordination modes of **2** compromise enantiodifferentiation controlled by asymmetric catalysts. The high potency of ranirestat as an aldose reductase inhibitor and the prospective requirement for large quantities of the compound prompted us to initiate the development of a practical catalytic asymmetric amination of a highly coordinative substrate like **1** [15–19]. We aimed to develop a catalytic system that could incorporate a highly coordinative substrate as a ligand to build a highly ordered transition state architecture through multiple non-bonding interactions that might drive the reaction through a specific stereochemical course to achieve high enantioselectivity. Screening of the amination reaction of **1** and di-*tert*-butyl azodicarboxylate **3** revealed that a catalytic system comprising La(O^{i}Pr)$_3$ and amide-based chiral ligand (*R*)-**4** effectively afforded product **5** with 92% ee (Scheme 2) [20–23]. La^{3+}, a rare earth metal cation, accepts up to 12 coordinating Lewis basic functionalities, and its coordination pattern is flexible depending on the chemical environment [1]. Substrate **1**, azodicarboxylate **3**, and ligand (*R*)-**4**, a highly coordinative bisamide with multiple hydrogen bonding sites and Lewis basic sites, forms an ordered assembly with La^{3+} at the center to render amination predominantly at the *Re*-face of the enolate generated from **1**.

The reaction promoted by La(O^{i}Pr)$_3$/(*R*)-**4** could be reproducibly performed under air, and the chiral ligand (*R*)-**4** was readily prepared from D-Val without chromatographic purification. On the other hand, the cost, limited supply, and moisture sensitivity of La(O^{i}Pr)$_3$ impeded large-scale application. To develop a cost effective and more robust catalytic protocol, we evaluated neutral La^{3+} salts, which are generally inexpensive and readily available in large quantities. For solubility in common organic solvents, neutral $La(NO_3)_3 \cdot 6H_2O$ was optimal, and the combined use of amines was tested to promote the enolization of **1** [24]. Interestingly, the amine structure, including the chirality, was determinant of the reaction rate and enantioselectivity, suggesting that the additional amine participated in the transition state assembly. This assumption was consistent with the observed large negative activation entropy determined by Eyring's plot. H-D-Val-O^{t}Bu proved optimal as an amine co-catalyst, which was used in 3-fold excess to La^{3+}, and the reaction was reproducibly performed in less toxic ethyl acetate at 0 °C on 100 g scale (Scheme 3).

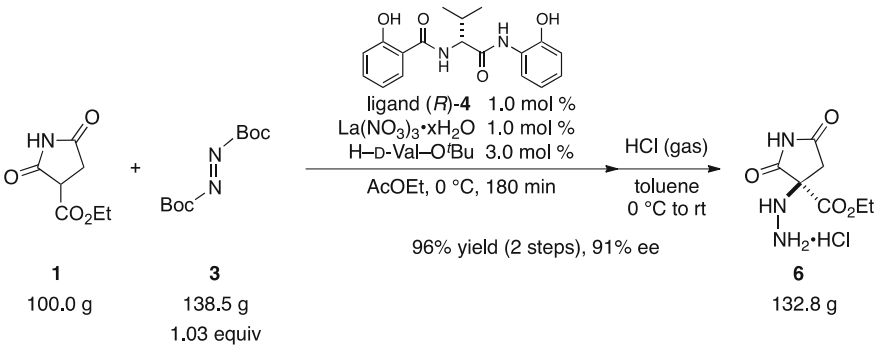

Scheme 3 Catalytic asymmetric amination of **1** and azodicarboxylate **3** promoted by La $(NO_3)_3 \cdot xH_2O$/(*R*)-**4**/H-D-Val-O^{t}Bu

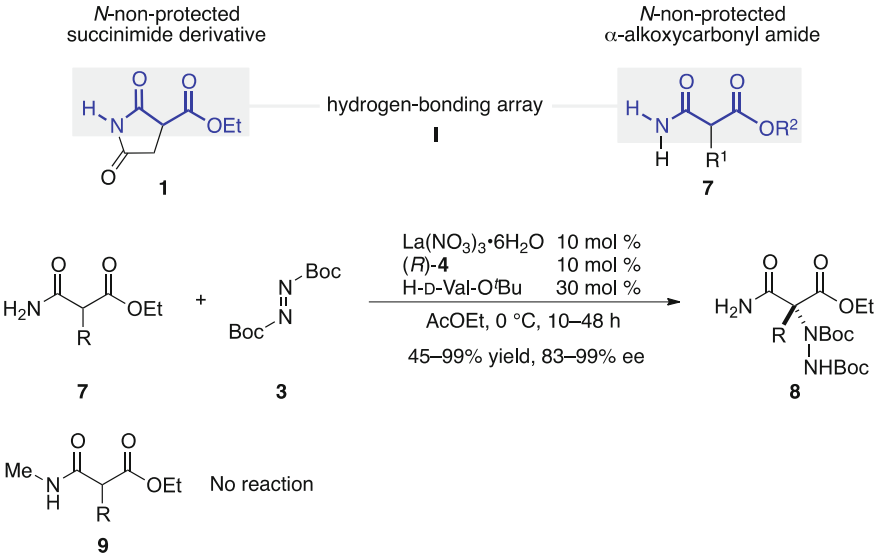

Scheme 4 Catalytic asymmetric amination of *N*-nonsubstituted α-alkoxycarbonyl amides **7** and azodicarboxylate **3** promoted by La$(NO_3)_3 \cdot 6H_2O$/(*R*)-**4**/H-D-Val-O^{t}Bu

H-D-Val-O^{t}Bu was separated and recovered by partitioning the reaction mixture. The crude product was then treated with HCl gas, which allowed us to isolate the hydrazine hydrochloric salt **6** with 91% ee by filtration. The reaction and a ternary complex of La$(NO_3)_3 \cdot 6H_2O$/(*R*)-**4**/H-D-Val-O^{t}Bu, which would be formed in equilibrium in dynamic association/dissociation kinetics, was observed in high-resolution mass spectrometry [25]. The thus-identified ternary catalytic system was uniquely effective for catalytic asymmetric amination of substrates bearing the hydrogen-bonding array shown in **I** (Scheme 4). *N*-Nonsubstituted α-alkoxycarbonyl amides **7** were competent substrates for affording the desired products **8** with high

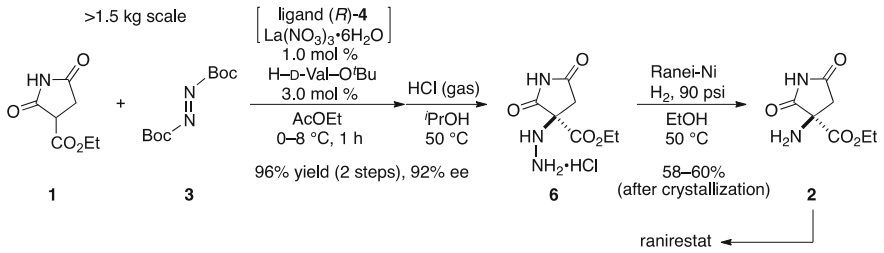

Scheme 5 Large-scale application of catalytic asymmetric amination and transformation into key intermediate **2**

enantioselectivity, but *N*-Me derivatives **9** failed the reaction, likely due to an insufficient coordination propensity to participate in the organized structure at the transition state. The ternary catalytic system allowed for easy set-up under an ambient atmosphere from readily available and bench-stable materials. Reaction conditions were further refined by process chemists to be feasible for industrial application; the amination of **1** over a 1.5-kg scale completed with 1 mol% of catalyst in ethyl acetate at 0–8 °C for 1 h, and the product **3** was safely converted to **2** by acidic removal of the Boc groups followed by Raney-Ni reduction of the N–N bond (Scheme 5) [26].

3 Nd-Based Catalysis: Catalytic Asymmetric Nitroaldol Reaction

Although nitroaldol (Henry) reaction is one of the most classical carbon-carbon bond-forming reactions, which was discovered more than a century ago [27], the reaction is still commonly used in organic synthesis. The substrates, aldehydes and nitroalkanes, are readily available in large quantities and the products provide vicinal amino alcohols, which constitute an important class of compounds frequently used in the synthesis of natural products and therapeutics [28–31]. Stereoselectivity is crucially important to the synthetic utility of the reaction, and several recently developed asymmetric catalysts afford *syn* [32–41] and *anti* [42–55] nitroaldol products in an enantioselective fashion.

Based on our exploration of the synthetic utility of amide-based ligand **4** described above [22, 23, 56–65], we disclosed that slightly modified ligand (*S*)-**10** constitutes a heterobimetallic complex comprising neodymium and sodium cations, which exhibit high catalytic activity and stereoselectivity in an asymmetric *anti*-selective nitroaldol reaction (Scheme 6) [66, 67]. In contrast to common asymmetric catalysts, the Nd/Na heterobimetallic catalyst serves as a heterogeneous catalyst and inspired us to further refine the catalyst toward practical applications. The Nd/Na heterogeneous catalyst was readily prepared via self-assembly (Scheme 7a); sequential addition of $NdO_{1/5}(O^iPr)_{13/5}$ (oxo complex of $Nd(O^iPr)_3$) and NaHMDS to a THF solution of ligand **10** gave the insoluble precatalyst, which was dissolved by the addition of

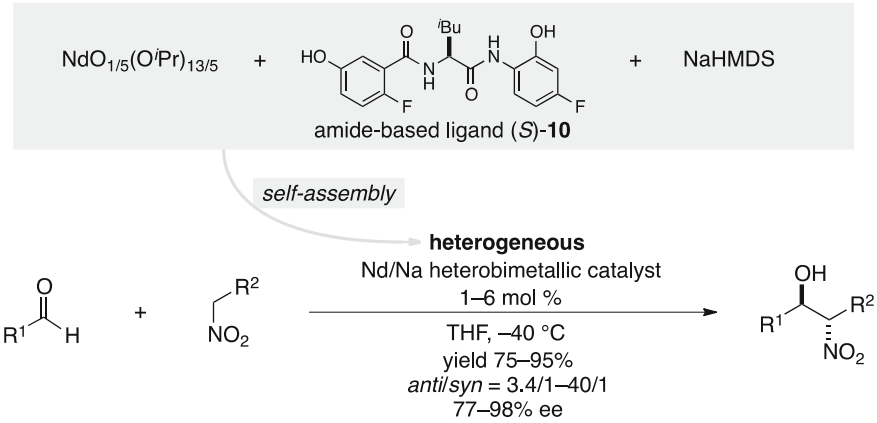

Scheme 6 *anti*-Selective catalytic asymmetric nitroaldol reaction promoted by the Nd/Na heterobimetallic catalyst

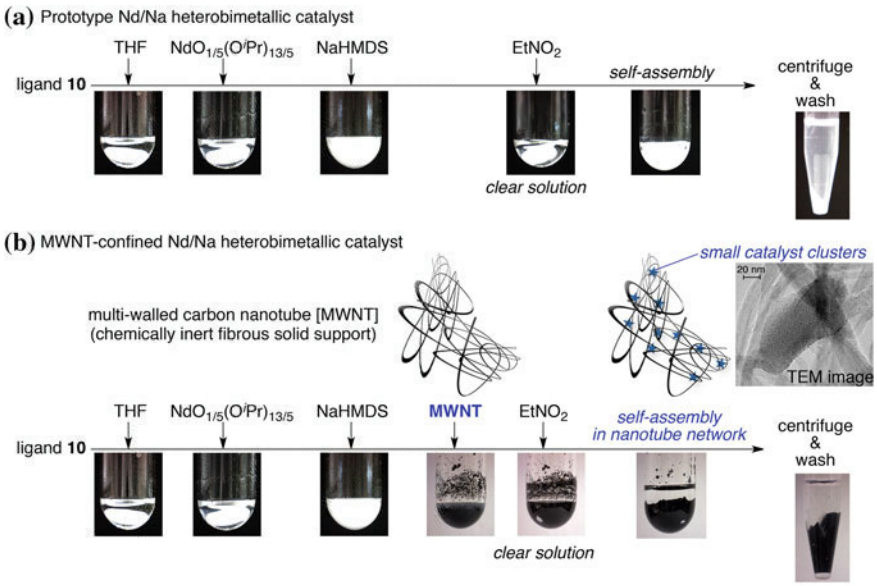

Scheme 7 Preparation procedure of the prototype Nd/Na heterobimetallic catalyst and the MWNT-confined Nd/Na recyclable catalyst

nitroethane. Self-assembly gradually proceeded to furnish heterogeneous catalyst as a white solid. Inductively coupled plasma–atomic emission spectroscopy (ICP-AES) and X-ray fluorescence (XRF) analyses indicated the composition of the heterogeneous catalyst as ca. Nd:**10**:Na = 1:1:2, and high resolution mass spectrometry (HRMS) revealed that the nitroethane used for catalyst preparation was incorporated

into the catalyst. Unsuccessful trials of catalyst reuse prompted us to produce a more durable heterogeneous catalyst. By taking advantage of the self-assembly process, we reasoned that self-assembly in the presence of a chemically inert solid support with a minute matrix would allow the catalyst to grow inside the matrix. With the judicious choice of multi-walled carbon nanotubes (MWNT) as the solid support for the additive during catalyst preparation, the self-assembled catalyst was efficiently trapped in the fibrous network of MWNT to furnish a recyclable heterogeneous catalyst (Scheme 7b) [65, 68, 69]. Transmission electron microscopy (TEM) revealed that 20–200 nm small catalyst clusters were dispersed on the MWNT surfaces. In contrast to the usual solid support catalysts, the Nd/Na catalyst confined within MWNT was prepared through a simple operation (mixing and centrifugation) by harnessing self-assembly without covalent bond linkage.

The discovery of heterogeneous asymmetric catalysts directed us to use a continuous-flow platform for the nitroaldol reaction. Continuous-flow reactions have received growing attention as an alternative to batch reactions with high practical impact [70–78]. The number of reports on the applications of flow technologies to the synthesis of APIs is increasing [79–83], and chiral catalyst modules amenable to concatenation in a flow system are in high demand [70, 76, 84, 85]. Catalytic asymmetric nitroaldol reactions generally require cryogenic control to prevent retro reactions and erosion of stereoselectivity. Implementing the continuous-flow nitroaldol reaction using a chiral catalyst module significantly reduces the cooling volume, decreasing the electric cost expected for such a large-scale reaction. Preliminary application of a MWNT-confined Nd/Na catalyst in a continuous-flow platform proved effective for miniaturization of the reactor with a turnover number of 200 (Scheme 8) [86]. Nitroaldol adduct **12** was produced in 12.4 g yield using a small (15.7 mL) catalyst column, a 20-fold smaller reaction volume than in a batch reaction for a comparable amount of product. Similarly to the case of $La(O^iPr)_3$, the cost and limited availability of moisture-sensitive $NdO_{1/5}(O^iPr)_{13/5}$ were bottlenecks for prospective large-scale application. Re-examination the catalyst preparation procedure revealed that the use of readily available $NdCl_3 \cdot 6H_2O$ and NaO^tBu in place of $NdO_{1/5}(O^iPr)_{13/5}$ and NaHMDS, respectively, was feasible for preparing the Nd/Na catalyst with comparable catalytic activity and stereoselectivity, leading to a 120-fold decrease in the cost [87]. The Nd/Na heterobimetallic catalyst exhibited

Scheme 8 *anti*-Selective catalytic asymmetric nitroaldol reaction in a continuous-flow platform

broad substrate generality and played a pivotal role in the enantioselective synthesis of zanamivir (relenza), an anti-influenza drug [88]. Further improvement and engineering of the flow reaction process to achieve a higher turnover number are anticipated to streamline the production of enantioenriched *anti*-vicinal amino alcohols for the synthesis therapeutic agents.

4 Conclusion

Recent advances of rare earth metal-based asymmetric catalysts with prospective industrial application are discussed. Rare earth nitrates and halides are inexpensive, easy-to-handle, and available in large quantities, and thus promising primary components of metal-based catalysts. Despite the additional notable characteristics of rare earth metals, such as their unique coordinating properties and durable Lewis acidity in the presence of amines, their utility in asymmetric catalysis has been underestimated in both academia and industry. The two examples described herein represent the potential utility of rare earth metal-based catalysts in manufacturing APIs in an enantioselective manner. More intensive research of rare earth metal-based catalysts will elicit hidden chemical properties of these intriguing metals to advance the art of asymmetric catalysis for prospective use in practical synthesis.

References

1. Cotton SA (2006) Lanthanide and actinide chemistry. Wiley, Chichester, England ; Hoboken, NJ.
2. Nair V, Biju AT, Mathew SC, Babu BP (2008) Chem Asian J 3:810.
3. Diels O (1922) Justus Liebigs Annalen der Chemie 429:1.
4. Diels O, Behncke H (1924) Chem Ber 57:653.
5. Huisgen R, Jakob F (1954) Justus Liebigs Ann Chem 590:37.
6. Evans DA, Nelson SG (1997) J Am Chem Soc 119:6452.
7. Evans DA, Johnson DS (1999) Org Lett 1:595.
8. Duthaler RO (2003) Angew Chem Int Ed 42:975.
9. Greck C, Drouillat B, Thomassigny C (2004) Eur J Org Chem 2004:1377.
10. Janey JM (2005) Angew Chem Int Ed Engl 44:4292.
11. Cativiela C, Ordonez M (2009) Tetrahedron: Asymmetry 20:1.
12. Polanc S, Košmrlj J, Kočevar M (2009) Synlett 2009:2217.
13. Negoro T, Murata M, Ueda S, Fujitani B, Ono Y, Kuromiya A, Komiya M, Suzuki K, Matsumoto J-I (1998) J Med Chem 41:4118.
14. Kurono M, Fujiwara I, Yoshida K (2001) Biochemistry 40:8216.
15. Bril V, Buchanan RA (2004) Diabetes Care 27.
16. Bril V, Buchanan RA (2006) Diabetes Care 29:68.
17. Giannoukakis N (2006) Curr Opin Investig Drugs 7:916.
18. Matsumoto T, Ono Y, Kurono M, Kuromiya A, Nakamura K, Bril V (2008) Journal of Pharmacological Sciences 107:231.

19. Bril V, Hirose T, Tomioka S, Buchanan R, Ranirestat Study G (2009) Diabetes Care 32:1256.
20. Mashiko T, Hara K, Tanaka D, Fujiwara Y, Kumagai N, Shibasaki M (2007) J Am Chem Soc 129:11342.
21. Shibasaki M, Kumagai N, Mashiko T (2009) Curr Opin Drug Discov Dev 12:862.
22. Kumagai N (2011) Chem Pharm Bull 59:1.
23. Kumagai N, Shibasaki M (2013) Angew Chem Int Ed 52:223.
24. Mashiko T, Kumagai N, Shibasaki M (2008) Org Lett 10:2725.
25. Mashiko T, Kumagai N, Shibasaki M (2009) J Am Chem Soc 131:14990.
26. Toshima M, Watanabe S, Uchiyama K, Takasaki T, Bhogle NN, Zhao H, Filios M, Takahashi K, Snoonian JR, Saranteas K (2016) Org Process Res Dev.
27. Henry LCR (1895) Hebd. Seances Acad. Sci. 120:1265.
28. Ager AJ, Prakash I, Schaad DR (1996) Chem Rev 96:835.
29. Bergmeier SC (2000) Tetrahedron 56:2561.
30. Fache F, Schulz E, Tommasino ML, Lemaire M (2000) Chem Rev 100:2159.
31. Juaristi E, Anaya De Parrodi C (2006) Synlett 2006:2699.
32. Sasai H, Suzuki T, Arai S, Arai T, Shibasaki M (1992) J Am Chem Soc 114:4418.
33. Sasai H, Tokunaga T, Watanabe S, Suzuki T, Itoh N, Shibasaki M (1995) J Org Chem 60:7388.
34. Sohtome Y, Hashimoto Y, Nagasawa K (2006) Eur J Org Chem 2006:2894.
35. Arai T, Watanabe M, Yanagisawa A (2007) Org Lett 9:3695.
36. Sohtome Y, Takemura N, Takada K, Takagi R, Iguchi T, Nagasawa K (2007) Chem Asian J 2:1150.
37. Arai T, Takashita R, Endo Y, Watanabe M, Yanagisawa A (2008) J Org Chem 73:4903.
38. Kim HY, Oh K (2009) Org Lett 11:5682.
39. Jin W, Li X, Wan B (2011) J Org Chem 76:484.
40. White JD, Shaw S (2012) Org Lett 14:6270.
41. Qin DD, Yu W, Zhou JD, Zhang YC, Ruan YP, Zhou ZH, Chen HB (2013) Chem Eur J 19:16541.
42. Uraguchi D, Sakaki S, Ooi T (2007) J Am Chem Soc 129.
43. Handa S, Nagawa K, Sohtome Y, Matsunaga S, Shibasaki M (2008) Angew. Chem., Int. Ed. 47:3230.
44. Sohtome Y, Kato Y, Handa S, Aoyama N, Nagawa K, Matsunaga S, Shibasaki M (2008) Org Lett 10:2231.
45. Uraguchi D, Nakamura S, Ooi T (2010) Angew Chem Int Ed 49:7562.
46. Lang K, Park J, Hong S (2012) Angew Chem Int Ed 51:1620.
47. Xu K, Lai G, Zha Z, Pan S, Chen H, Wang Z (2012) Chem Eur J 18:12357.
48. Blay G, Domingo LR, Hernandez-Olmos V, Pedro JR (2008) Chem Eur J 14:4725.
49. Ube H, Terada M (2009) Bioorg Med Chem Lett 19:3895.
50. Blay G, Hernández-Olmos V, Pedro JR (2010) Org Lett 12:3058.
51. Noole A, Lippur K, Metsala A, Lopp M, Kanger T (2010) J Org Chem 75:1313.
52. Qiong Ji Y, Qi G, Judeh ZMA (2011) Eur J Org Chem:4892.
53. Boobalan R, Lee G-H, Chen C (2012) Adv Synth Catal 354:2511.
54. Yao L, Wei Y, Wang P, He W, Zhang S (2012) Tetrahedron 68:9119.
55. Arai T, Joko A, Sato K (2014) Synlett 26:209.
56. Nojiri A, Kumagai N, Shibasaki M (2008) J Am Chem Soc 130:5630.
57. Nojiri A, Kumagai N, Shibasaki M (2009) J Am Chem Soc 131:3779.
58. Kawato Y, Takahashi N, Kumagai N, Shibasaki M (2010) Org Lett 7:1484.
59. Matsuzawa A, Nojiri A, Kumagai N, Shibasaki M (2010) Chem Eur J 16:5036.
60. Nitabaru T, Kumagai N, Shibasaki M (2010) Molecules 15:1280.
61. Matsuzawa A, Mashiko T, Kumagai N, Shibasaki M (2011) Angew Chem Int Ed 50:7616.
62. Takechi S, Kumagai N, Shibasaki M (2011) Tetrahedron Lett 52:2140.
63. Nojiri A, Kumagai N, Shibasaki M (2012) Angew. Chem., Int. Ed. 51:2137.
64. Nojiri A, Kumagai N, Shibasaki M (2013) Chem Commun 49:4628.
65. Hashimoto K, Kumagai N, Shibasaki M (2015) Chem Eur J 21:4262.

66. Nitabaru T, Kumagai N, Shibasaki M (2008) Tetrahedron Lett 49:272.
67. Nitabaru T, Nojiri A, Kobayashi M, Kumagai N, Shibasaki M (2009) J Am Chem Soc 131:13860.
68. Ogawa T, Kumagai N, Shibasaki M (2013) Angew Chem Int Ed 52:6196.
69. Sureshkumar D, Hashimoto K, Kumagai N, Shibasaki M (2013) J Org Chem 78:11494.
70. Mak XY, Laurino P, Seeberger PH (2009) Beilstein J Org Chem 5:19.
71. Webb D, Jamison TF (2010) Chemical Science 1:675.
72. Wegner J, Ceylan S, Kirschning A (2011) Chem Commun 47:4583.
73. Wegner J, Ceylan S, Kirschning A (2012) Adv Synth Catal 354:17.
74. Baxendale IR (2013) J Chem Technol Biotechnol 88:519.
75. Pastre JC, Browne DL, Ley SV (2013) Chem Soc Rev 42:8849.
76. Tsubogo T, Ishiwata T, Kobayashi S (2013) Angew Chem Int Ed 52:6590.
77. Zhao D, Ding K (2013) ACS Catalysis 3:928.
78. Munirathinam R, Huskens J, Verboom W (2015) Adv Synth Catal 357:1093.
79. Baumann M, Baxendale IR (2015) Beilstein J Org Chem 11:1194.
80. Adamo A, Beingessner RL, Behnam M, Chen J, Jamison TF, Jensen KF, Monbaliu J-CM, Myerson AS, Revalor EM, Snead DR, Stelzer T, Weeranoppanant N, Wong SY, Zhang P (2016) Science 352:61.
81. Fitzpatrick DE, Battilocchio C, Ley SV (2016) ACS Cent Sci 2:131.
82. Kobayashi S (2016) Chem Asian J 11:425.
83. Porta R, Benaglia M, Puglisi A (2016) Org Process Res Dev 20:2.
84. Ishitani H, Saito Y, Kobayashi S (2016) Top Organomet Chem 57:213.
85. Atodiresei I, Vila C, Rueping M (2015) ACS Catalysis 5:1972.
86. Hashimoto K, Kumagai N, Shibasaki M (2014) Org Lett 16:3496.
87. Nonoyama A, Hashimoto K, Saito A, Kumagai N, Shibasaki M (2016) Tetrahedron Lett 57:1815.
88. Nitabaru T, Kumagai N, Shibasaki M (2012) Angew Chem Int Ed 51:1644.

Metal Catalyzed Synthetic Reactions via Aerobic Oxidation as a Key Step

Mitsuru Shindo and Kenji Matsumoto

Abstract New aerobic oxidative metal catalyzed synthetic reactions are described: The Cu(II) complex catalyzed the acylation of thioester in Wittig lactonization under neutral conditions and the dissymmetrization of symmetric dithiomalonates via selective monoacylation. The key step in this reaction was the formation of an acylketene, the stability of which would contribute to selectivity. The aerobic Rh/C-catalyzed oxidative homo- and cross-coupling of aryl amines was developed. The coupling reactions afforded symmetrical and nonsymmetrical biaryl amines in excellent yields. These reactions provide a mild, operationally simple, and efficient approach for the synthesis of biaryls which are important to pharmaceutical and materials chemistry.

Keywords Aerobic oxidation · Metal catalysts · Acylation · Coupling · Heterogeneous catalysts · Recyclable

1 Introduction

Metal-catalyzed reactions are one of the main topics in synthetic organic chemistry and process chemistry. Needless to say, numerous metal-catalyzed reactions have achieved highly efficient C–C, C–O, and C−heteroatom bond formations. Oxidative (or oxidation) reactions are frequently used in not only functional group transformation but also C–C or C–O bond formation along with C–H bond cleavage (oxidative coupling). In the oxidative metal-catalyzed reactions, if air or oxygen is an oxidant, usage of hazardous peroxides or toxic high valence metals can be

M. Shindo (✉)
Institute for Materials Chemistry and Engineering, Kyushu University,
6-1 Kasugako-en, Kasuga, Fukuoka 816-8580, Japan
e-mail: shindo@cm.kyushu-u.ac.jp

K. Matsumoto
Faculty of Pharmaceutical Sciences, Tokushima Bunri University,
180 Nishihama-Boji, Yamashiro-cho, Tokushima 770-8514, Japan

K. Tomioka et al. (eds.), *New Horizons of Process Chemistry*,
DOI 10.1007/978-981-10-3421-3_2

avoided. In terms of green chemistry as well as practical synthesis, aerobic conditions would be favorable. Furthermore, reaction control would be more easily accomplished under aerobic conditions than inert gas atmosphere.

In this chapter, we describe our recent results on aerobic Cu(II) catalyzed acylation, in which catalyst deactivator is eliminated by oxidation, and aerobic metal catalyzed oxidative coupling reactions.

2 Aerobic Cu-Catalyzed Acylation-Wittig Reaction Under Neutral Conditions

2.1 Acylation-Wittig Reaction Under Neutral Conditions

During the course of our synthesis of xanthanolide sesquiterpenoids [1, 2], we found one-pot acylation-Wittig lactonization of acyloins (Fig. 1). A mixture of the acyloin **1** (α-hydroxy-cyclic hemiacetal as its equivalent) and excess amount of Wittig reagent **2** was heated in xylene at 150 °C to form a butenolide **3** in excellent yield. When the ester moiety was replaced to more acidic eliminating group like thiophenol, the reaction was fairly accelerated, albeit under harsh conditions (Fig. 2). These results indicated a reaction mechanism of the initial rate-determining acylation and the following intramolecular Wittig reaction.

2.2 Cu(II)-Catalyzed Acylation-Wittig Reaction [3]

In this successive lactonization, harsh conditions of an excess amount of the Wittig reagent and high temperatures were still required to complete the reaction. We then examined metal catalyzed reactions of this acylation-Wittig reaction under mild and neutral conditions [4, 5]. We focused on thioesters, which are easily handled, stable acylating agents of alcohols in organic syntheses and biological systems. Acylations with a thioester should be carried out under basic conditions for activation of the

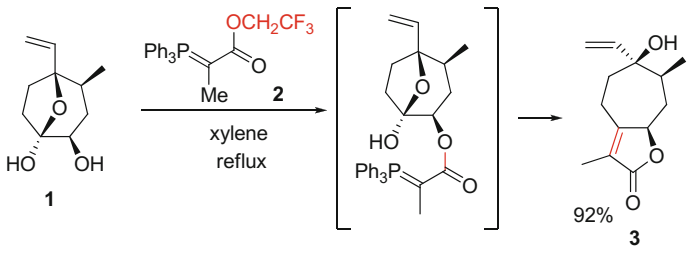

Fig. 1 One-pot acylation-Wittig lactonization of acyloins

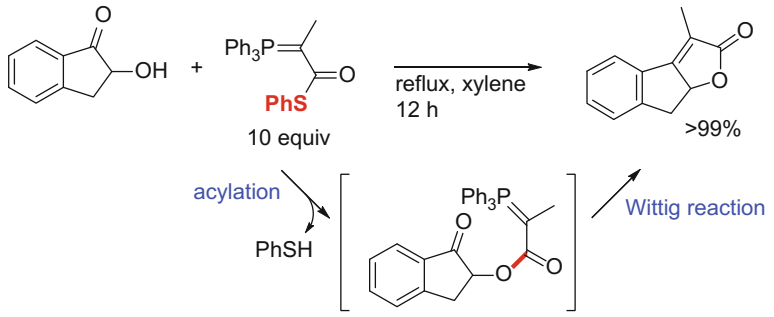

Fig. 2 One-pot lactonization using Wittig reagent with a thioester

Table 1 Acceleration of acylation by metal salts

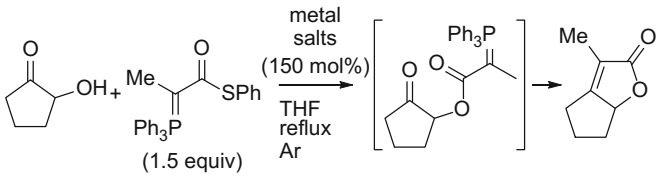

Entry	Metal salt	Time (h)	Yield (%)
1	None	–	No reaction
2	$Mg(OAc)_2$	3.5	Trace
3	$Fe(OAc)_2$	3.5	11
4	$Zn(OAc)_2$	3.5	61
5	$Ag(OAc)_2$	3.5	51
6	$Cu(OAc)_2$	0.5	80
7	$CuCl_2$	–	No reaction
8	$Cu(OTf)_2$	–	No reaction

alcohols. Although there have been several reports on *O*-acylations using thioesters accelerated by stoichiometric or substoichiometric amounts of soft metal salts, such as Hg(II), Ag(I), Cu(I), and Cu(II) [6–9], no catalytic reactions under neutral conditions were reported, because the thiolates eliminated by the acylation would deactivate the metal salts.

The reaction did not proceed in the absence of metal salts (Table 1, entry 1), and the hard metal salt such as magnesium acetate did not promote the reaction (entry 2). In contrast, 150 mol% of soft metal salts promoted the reaction to give the desired lactone **6** in good to moderate yields, (entries 3–6). And among the metals, $Cu(OAc)_2$ provided the best result (entry 6). The other Cu(II) salts did not almost accelerate the reaction (entries 7 and 8).

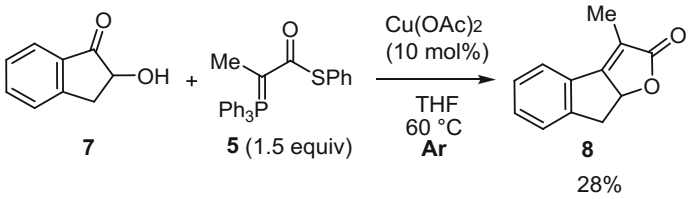

Fig. 3 Cu(II)-catalyzed acylation-Wittig reaction of acyloin **7**

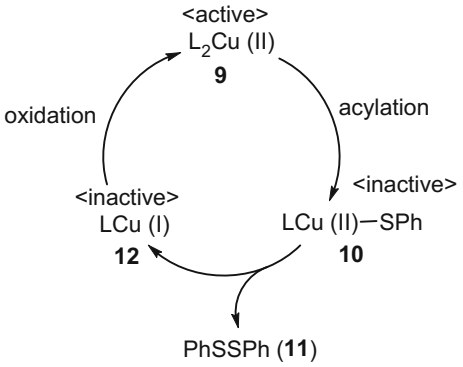

Fig. 4 Concept for catalytic cycle

The next issue was how to develop the catalytic reaction. 10 mol% of $Cu(OAc)_2$ promoted the model reaction (Fig. 3) to yield the product **8** in only 28% *under argon*.

In the reaction cycle, thiophenol is eliminated. This byproduct forms an inactive thiophenol-Cu complex **10**. Therefore, the generation of this complex must be suppressed for the catalytic system. A small amount of diphenyl disulfide (**11**) was detected as a side product, which was formed by oxidation of the thiol along with reduction of the catalyst (Cu(II) to Cu(I)). We anticipated that in order to regenerate the active catalyst Cu(II) **9**, the thiolate should be oxidized to the disulfide **11**, possibly a poorer ligand for Cu(II), and the resulting Cu(I) **12** should be oxidized to Cu(II) (Fig. 4) [10].

Based on this concept, we attempted the Cu(II)-catalyzed Wittig lactonization of 2-hydroxyindanone (**7**) *under air* to achieve catalytic turnover using 10 mol% of $Cu(OAc)_2$ (Table 2, entry 1). After screening of ligands, the bidentate-type salicylate complex (**14**) provided **8** in higher yields (entry 2). Furthermore, OXONE® accelerated the catalytic reaction to provide **8** in 2 h in high yield (entry 3). Even when 2 mol% of the catalyst **14** was used, **8** was obtained in good yield (entry 4). These results suggested the rate determining step being re-oxidation of Cu(I) to Cu (II) in this catalytic system. Finally, the Wittig reagent **13** having 2,6-dimethylphenylthioester afforded **8** in excellent yield catalyzed by only 2 mol% of the copper complex **14**, probably because the sterically more hindered ArS–Cu (II) complex was more readily converted into disulfide and Cu(I).

Table 2 Optimization of Cu (II)-catalyzed acylation-Wittig lactonization

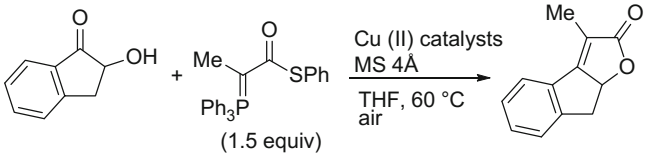

7 **5** **8**

Entry	Catalyst	mol%	Wittig reagent	Oxidants	Time (h)	Yield (%)
1	$Cu(OAc)_2$	10	**5**	Air	6	82
2	**14**	10	**5**	Air	5	97
3	**14**	10	**5**	OXONE[@a]	2	92
4	**14**	2	**5**	OXONE[@a]	5	76
5	**14**	2	**13**	OXONE[@a]	4	91

[a]3 equivalents

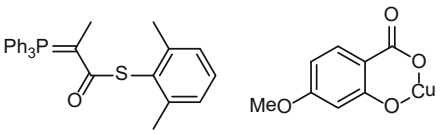

13 **14**

Various kinds of acyloins were treated with **13** in the presence of the catalyst **14** in toluene, which was safer than THF under oxidative conditions, to provide the lactones in high yields (Fig. 5). Not only hydroxyketones (**15a–f**) but also a hydroxylactone **15g** could be employed to afford butenolides **16**. The hemiacetal **15h** was also transformed into the butenolide under much milder conditions than the original conditions. The sterically labile precursor **15i** of heritonin [11] was converted into the corresponding butenolide in high yield, without epimerization [12], because of mild and neutral conditions. Therefore, base or acid-labile substrates could be subjected to this acylation without decomposition or isomerization. This reaction was applied to synthesis of karrikinolide [13].

Figure 6 shows a proposed mechanism for this catalytic cycle. The Cu(II) catalyst **14** would activate the thioester **13** [6, 7], which is converted into the phosphonium ketene intermediate **17** by double activation of the C–S and O–H bonds. The soft Lewis acidic Cu(II) specifically interacts with the thioester to accelerate elimination of the thiolate with the aid of electron-donating phosphorus ylide. Simultaneously, the alcohol **15** is deprotonated by salicylate to be converted into alkoxide **18**, which is acylated by **17**, followed by the intramolecular Wittig reaction, to furnish the lactone **16**. The resulting thiolate complex **19** would be homolytically cleaved into a thiyl radical **20** and the Cu(I) complex **21**. The former species would form the disulfide **22**, and the latter would be oxidized to regenerate the catalyst **14**. Molecular sieves could trap the water generated by oxidation. Accordingly, the Cu(II) catalyst would play a double role: activation of the thioester and oxidative removal of the thiolate.

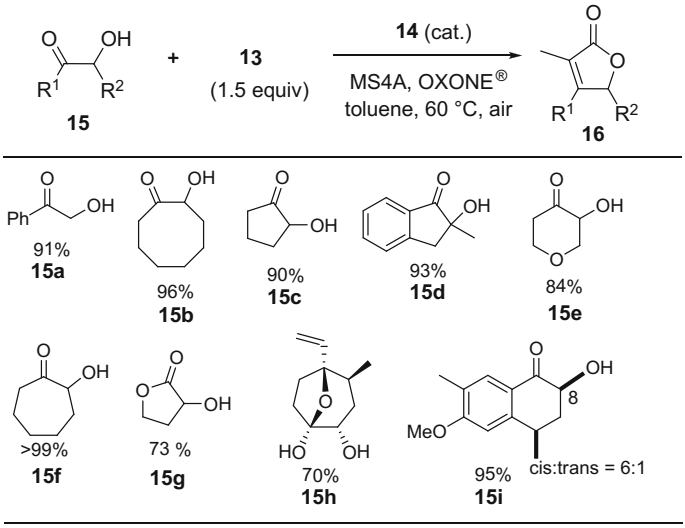

Fig. 5 Cu(II)-catalyzed one-pot lactonization

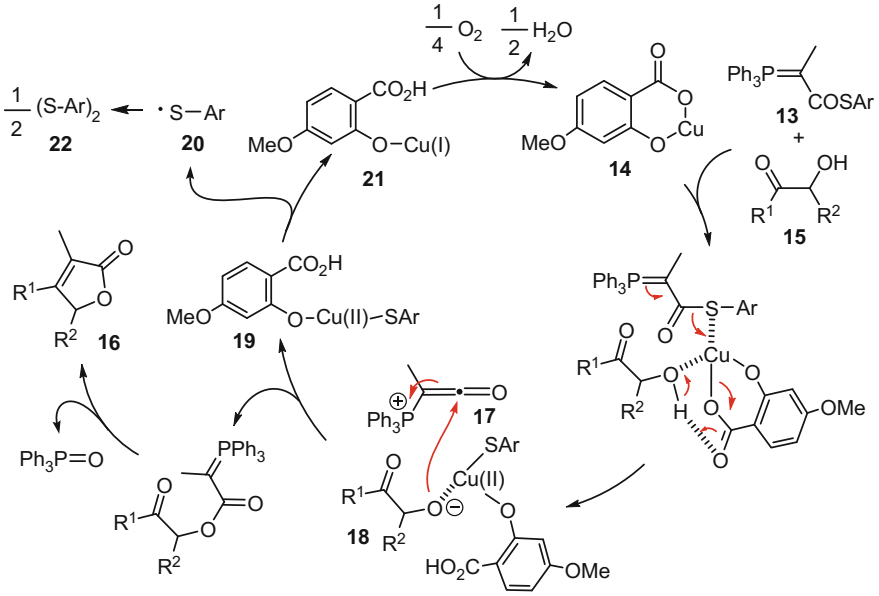

Fig. 6 Proposed mechanism for Cu(II)-catalyzed acylation

2.3 Cu(II) Catalyzed Dissymmetrization of Dithiomalonates [14]

Selective synthesis of dissymmetric malonates from the symmetric malonates is sometimes uncontrollable because esterification of malonic acid frequently produces the corresponding diester as well as the mono-ester, even if it is executed with an equimolar alcohol. Enzymatic methods are common for this conversion, but with the drawback of strong substrate specificity [15]. Nucleophilic ring-opening of Meldrum's acid have also been used [16, 17]; however, they are not always efficient due to facile decarboxylation. Niwayama's selective mono-hydrolysis of diesters including malonates successfully gives the dissymmetric half esters [18, 19]. A more efficient dissymmetrization of malonates that provides mono-esters (e.g. **24**) with *an activated acyl group* such as a thioester would be a valuable synthon directing to functionalized malonates **25** from inexpensive symmetrical malonates (Fig. 7) [20, 21].

A dithiomalonate **26** was found to be selectively converted into a malonic acid *S*, *O*-ester **27** in excellent yield in the presence of the catalyst **14** (Fig. 8), although the Cu(II) catalyst did not activate simple thiol esters.

Interestingly, even in the absence of the Cu(II) catalyst **14**, the reaction was completed under the similar conditions to give the dissymmetric product **27** in excellent yield. This result suggested that the selective mono-alcoholysis was attributed to the intrinsic properties of dithiomalonates. Therefore, we started studies on this reaction under non-catalytic conditions.

The solvent effect was important because only polar solvents accelerated the reaction (Table 3). Finally, acetonitrile was the best solvent for mono-alcoholysis, giving the dissymmetric *S*,*O*-ester **27** quantitatively (entry 4).

The non-catalytic mono-alcoholysis of diphenyl dithiomalonates (**26**) with various alcohols provided the corresponding *S*,*O*-malonates **29** in 5–24 h in excellent

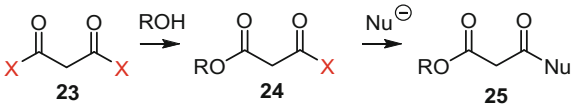

Fig. 7 Preparation of dissymmetric malonates

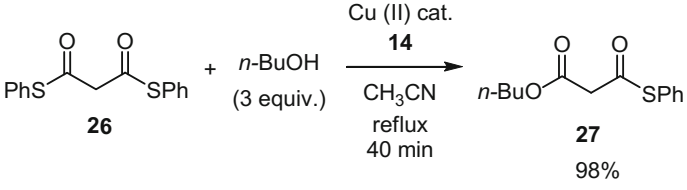

Fig. 8 Dissymmetrization of dithiomalonate **26**

Table 3 Screening of solvents

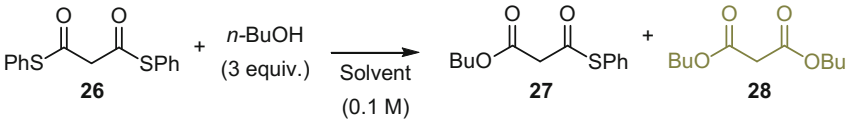

Entry	Solvent	Temperature (°C)	Time (h)	Ratio (**27/28**)	Yield (%)
1	Toluene	60	3.5		0
2	CH_2Cl_2	40	3.5		0
3	THF	60	3.5		Trace
4	CH_3CN	60	2	>20:1	96
5	DMF	60	1.2	>20:1	83

Table 4 Dissymmetrization of diphenyl dithiomalonate (**26**)

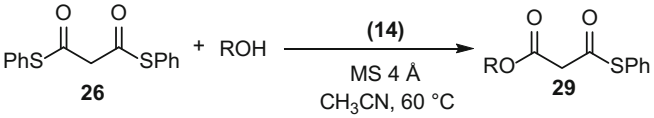

Entry	Alcohol	Without **14**		With **14** (1 mol%)	
		Time (h)	Yield (%)	Time (h)	Yield (%)
1	*n*-BuOH	2	96	0.6	91
2	*i*-PrOH	24	93	2	88
3	*t*-BuOH	24	70	1	82
4	$HC{\equiv}CCH_2OH$	24	0	4	71
5	$CH_2{=}CHCH_2OH$	24	0	2.5	82

yields with high selectivities except for propargyl and allyl alcohols (Table 4). The copper catalyst **14** significantly accelerated this mono-acylation with the aid of MS4A for trapping water, described section in Sect. 2.2. The reactions were completed within several hours, and even the less reactive allyl and propargyl alcohols gave the dissymmetric *S,O*-esters in excellent yields.

α-Alkyl-substituted dithiomalonates were also converted into dissymmetric *S,O*-malonates catalyzed by **14,** although the reaction was retarded (Fig. 9). The α-fluoromalonate showed much lower reactivity than α-alkylmalonate, even though its steric factor could be negligible. Neither α,α-dimethylmalonate **30** nor diphenyl dithiosuccinate (**31**) were inert to this reaction.

The thermal transesterification of ethyl acetoacetate has been known to proceed through an acylketene intermediate [22, 23]. In the alcoholysis of dithiomalonates, acylketenes would also be a key intermediate owing to the inertness of α,α-dimethylmalonate **30** and dithiosuccinate **31**. Rate constants of the reaction of **26** with *n*-butanol in acetonitrile were independent of the concentration of *n*-butanol. Therefore, the key intermediates in this alcoholysis were the ketenes **32**, and the ketene formation (**26** → **32**) was the rate-determining step in the case of

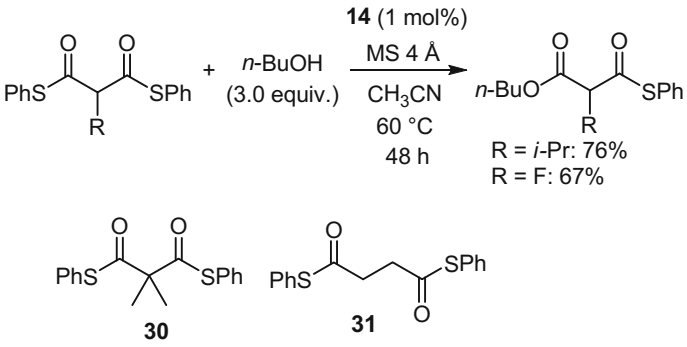

Fig. 9 Cu-catalyzed mono-butanolysis of α-substituted dithiomalonates

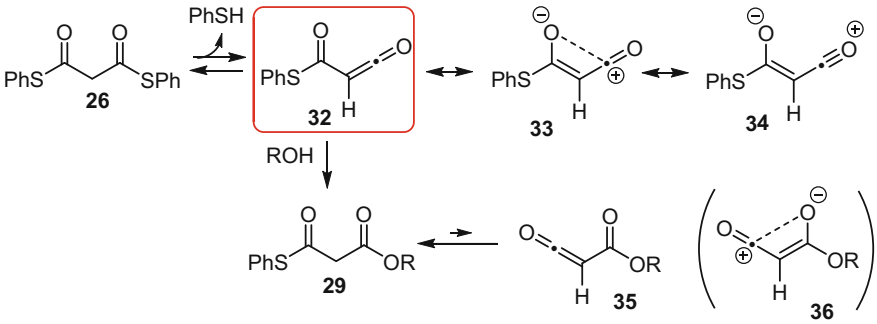

Fig. 10 Proposed mechanism for mono-alcoholysis of dithiomalonates

n-butanol (Fig. 10). The pronounced stability of **32** would be attributed to resonance structures (**33** and **34**) in addition to a intramolecular electrostatic interaction in **33,** according to the Tidwell's reports [24, 25]. The ketene **32** would be more stable than the oxocarbonylketene **35**; therefore, zwitterionic stabilization in **36** was relatively ineffective. Consequently, the high selectivity of mono-alcoholysis could be attributed to the different stabilities of the acylketenes. The copper catalyst accelerated the conversion to **32** by activating the thioester. In the case of the less reactive alcohols and less reactive sterically hindered malonates, the rate-determining step may be shifted to acylation (**32** → **29**).

In this section, aerobic Cu(II)-catalyzed acylations of Wittig lactonization and dissymmetrization of dithiomalonates were described. The Cu(II) complex-catalyzed reaction was the first catalytic acylation using thioesters under aerobic neutral conditions. Although this catalytic reaction is thus far limited to the Wittig reagent and dithiomalonates as thioesters, it may become a new principle for catalytic acylation. Further development of more efficient catalysts can be expected in the future. Since acylation is a conventional and fundamental method for C–C, C–O, and C–N bond formation, these aerobic catalytic methods will be valuable in synthetic organic chemistry and process chemistry.

3 Heterogeneous Metal-Catalyzed Aerobic Oxidative Biaryl Coupling

3.1 Aerobic Oxidative Homo-Coupling of Aryl Amines [26]

Biaryl compounds are privileged structural motifs found in many biologically important natural products, synthetic pharmaceuticals, and functional materials. In recent years, with the increasing pressure to develop environmentally friendly and sustainable methodologies, direct arylation, aryl–aryl bond formation through C–H bond activation, has captured growing attention as a very attractive methods for preparation of biaryls because the reactants do not have to be pre-functionalized, and because of the atom- and step-economy (Fig. 11) [27–33]. Among direct arylation methodologies, oxidative biaryl coupling is a simple and direct method for aryl–aryl bond formations. The oxidative coupling of naphthols and phenols leading to BINOL and biphenol derivatives has been well studied [34–37]. In strictly contrast, the oxidative coupling of aryl amines remains largely unexplored [38, 39], because aryl amines are easily oxidized, generating many side products. At the start of our study, catalytic processes are particularly limited and only an example of catalytic process was reported by Yang using catalytic amounts of $FeCl_3$ in combination with *m*CPBA [40]. Furthermore, the use of molecular oxygen as clean, safe, and inexpensive oxidant represents an important advance [41].

We anticipated that upon protonation of aryl amines under acidic conditions, the resulting ammonium salts may prevent side reactions induced by the high nucleophilicity or oxidation potential of aryl amines and undergo the desired oxidative coupling smoothly to yield homo-coupled products. The feasibility of this concept was confirmed by the oxidative coupling of 2-aminoanthracene (**37**) under heterogeneous aerobic conditions using 5% Rh/C catalyst (Table 5). To our delight, the use of methanesulfonic acid afforded the desired product **38**, but the yield was low (entry 1). Following this result, we examined various acidic solvents and found that trifluoroacetic acid (TFA) afforded the best result for obtaining dimer **38** in high yield (entry 2), whereas either difluoroacetic acid or acetic acid, the acidities of which are weaker than that of TFA, led to the reduced yields of **38** (entries 3 and 4). Interestingly, the reaction in hexafluoroisopropanol (HFIP) resulted in the exclusive formation of carbazole **39** in 76% yield (entry 5), but ethanol was unsuitable solvent (entry 6). The other aprotic solvents did not afford the coupling products (entries 7

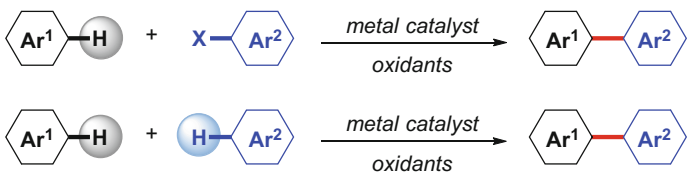

Fig. 11 Aryl–aryl bond formation via direct arylation

Table 5 Solvent effect for oxidative homo-coupling of aryl amines

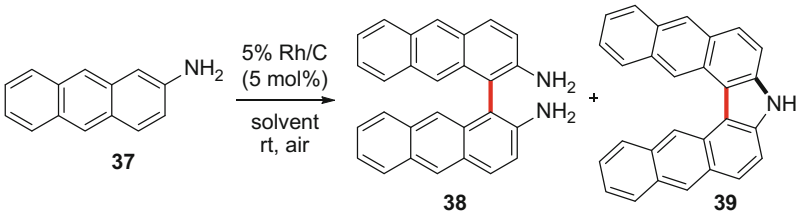

Entry	Solvent	pKa	Time (h)	Yield (%)	
				38	**39**
1	CH_3SO_3H	−2.6	26	Low yield	
2	CF_3CO_2H	−0.2	0.8	90	2
3	CF_2HCO_2H	1.2	4	60	14
4	CH_3CO_2H	4.8	34	51	36
5	$(CF_3)_2CHOH$	9.3	6	0	76
6	EtOH	15.5	24	15	6
7	THF	–	26	No reaction	
8	CH_2Cl_2	–	26	No reaction	

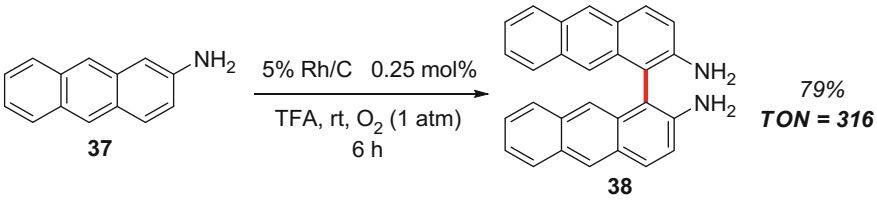

Fig. 12 Rh/C–catalyzed oxidative homo-coupling of 2-aminoanthracene

and 8). These results indicate that the acidic properties of solvents not only accelerate the reaction, but also control the product selectivity.

Besides Rh/C, other heterogeneous catalysts such as Rh/Al_2O_3, Ru/C, Pd/C, and PtO_2 also afforded **38** in high yields. Under 1 atm of oxygen, the reaction proceeded faster to give **38** in excellent yield. Furthermore, even using 0.25 mol% of 5% Rh/C, **38** was obtained in good yield and the turnover number (TON) reached up to 300 (Fig. 12). This is the first heterogeneously catalyzed aerobic oxidative coupling of aryl amines, which would provide the operationally simple and greener methodology for the efficient preparation of biaryl diamines.

With the optimized conditions in hand, the substrate scope was investigated with various aryl amines (Fig. 13). Using *N*-substituted-2-aminoanthracenes and

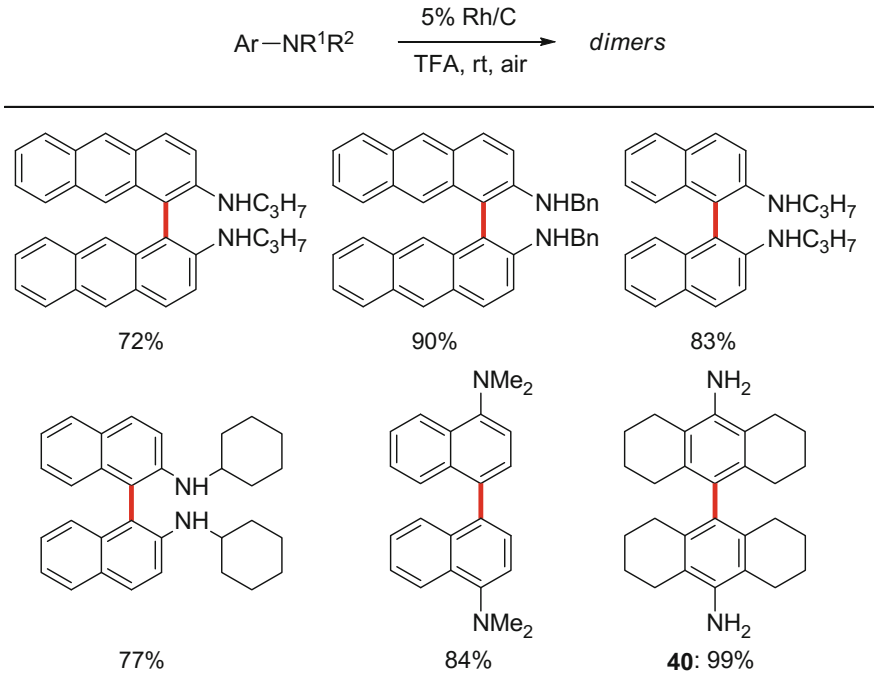

Fig. 13 Rh/C–catalyzed oxidative homo-coupling of aryl amines

2-aminonaphthalenes, dimers were obtained in good yields. Interestingly, 1-aminonaphthalenes underwent C–C bond formation at 4-position, generating dimers in excellent yields. The octahydroanthracene derivative, which is not a fused arene, also dimerized to afford the corresponding product **40** in quantitative yield. Thus, the anthracenes as well as naphthalene and aniline derivatives underwent oxidative coupling to afford the corresponding dimers in good yields, which show that this catalytic coupling reactions are highly versatile.

To gain insights into the reaction mechanism, the electron spin resonance (ESR) spectrum of the reaction using **37** and 5% Rh/Al_2O_3 under air was measured at room temperature, which indicated that the radical species are generated in the reaction mixture. Accordingly, the proposed mechanism is shown in Fig. 14. The catalytic cycle begins with a one-electron transfer from the ammonium salt **41** to the rhodium catalyst to produce the radical cation intermediate **42** and reduced rhodium, which is oxidized by molecular oxygen to regenerate the active rhodium metal. The radical cation **42** dimerizes to give the diiminium salt **43**, which tautomerizes to afford the coupled product **45** after work-up. Unlike the TFA system, in the presence of HFIP, the carbazole **39** is preferably produced. Probably owing to the higher pK_a value of HFIP, amino iminium intermediate **44** undergoes cyclization to produce **46**, which release ammonium to afford carbazole **47**.

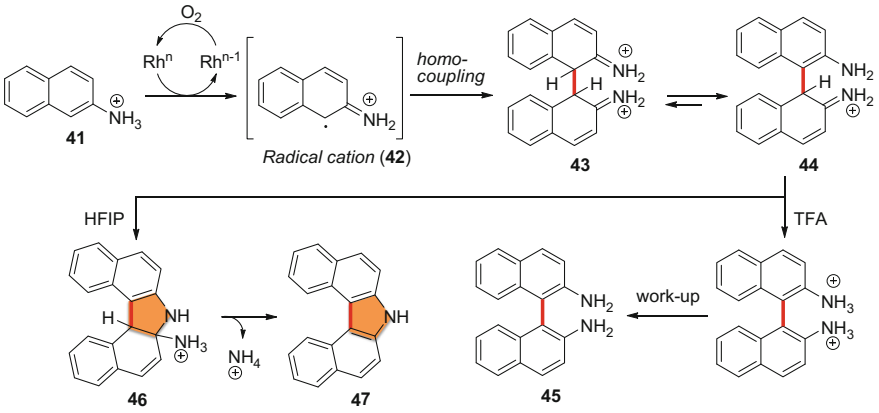

Fig. 14 Proposed mechanism for aerobic oxidative coupling of aryl amines

3.2 Aerobic C–H/C–H Cross-Coupling of Aryl Amines [42]

The C–H/C–H cross-coupling between two distinct aromatic compounds, also known as cross-dehydrogenative coupling (CDC), has recently attracted great attention as an efficient and promising strategy to synthesize a broad array of unsymmetrical biaryls [43–45]. In spite of significant development, the vast majority of C–H/C–H cross-coupling reactions are still limited by the high temperatures and stoichiometric amounts of strong oxidants that are required [46–49]. In particular, the oxidative C–H/C–H cross-coupling between two arenes with similar chemical and physical properties, such as phenol–phenol or aniline–aniline, are difficult to achieve due to the concomitant formation of homo-coupling products [50–53]. Kita and co-workers reported the metal-free oxidative cross-coupling of *N*-Ms protected aryl amines using hypervalent iodine reagents as the stoichiometric strong oxidant and developed the catalytic transformation in combination with *m*CPBA [54]. Waldvogel and co-workers have developed electrochemical oxidative phenol–aniline cross-coupling with high selectivity [55–57]. Despite these advances, since oxidative coupling of aryl amines are particularly difficult, there remains no general method for aniline–aniline cross-coupling [58].

We envisioned extending the above oxidative homo-coupling of aryl amines to CDC reaction. In comparison to homo-coupling, the control of selectivity for desired cross-coupling over homo-coupling represents a great challenge. Based on our previous results, we hypothesized that the homo-coupling could be suppressed if **48** had sterically hindered substituents on the amino group; the resulting radical cations **49** would preferentially react with sterically less hindered arenes **50** to provide cross-coupled biaryls **51** (Fig. 15).

Thus, we selected *N,N*-dimethylamino-2-naphthalene (**52**) as a substrate with a bulky amino group and optimized the cross-coupling of **52** with 3 equivalents of **53** in TFA under 1 atm of oxygen (Fig. 16). In the presence of 5% Rh/C (5 mol% of

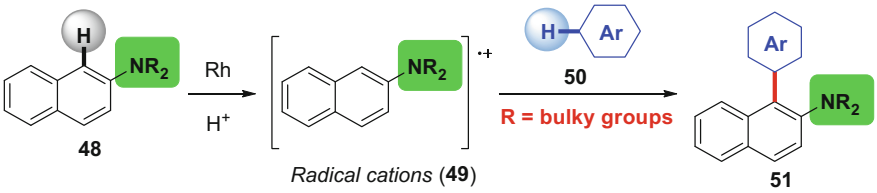

Fig. 15 Working hypothesis for C–H/C–H cross-coupling of aryl amines

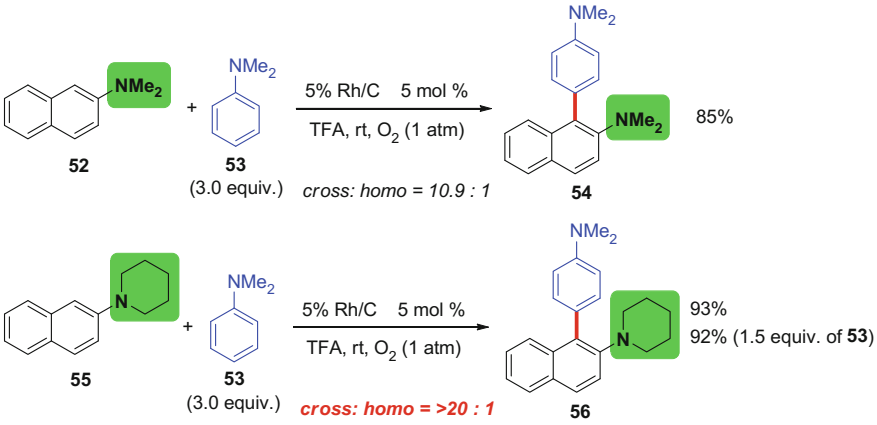

Fig. 16 Oxidative C–H/C–H cross-coupling of aryl amines

rhodium), the desired cross-coupled product **54** was obtained in 85% along with a small amount of the dehydrodimer of **52**. Following this result, we investigated the cross-coupling using various 2-naphthyl amines and found that amino substituents played important role on the selectivity of the reaction. When piperidino analog **55** was employed, the homo-coupling product was not observed and desired product **56** was obtained in 93% yield. Furthermore, even using a small amount of **53**, the reaction of **55** provided **56** in excellent yield.

Since high selectivity was obtained with **55**, the substrate scope was investigated with various aryl amines (Fig. 17). Several kinds of anilines, phenols and anisoles were reacted with **55** to give unsymmetrical biaryls in excellent yields and selectivities. *N,N*-Dibenzylamino-2-naphthalene also reacted with aniline to give **57** efficiently. Furthermore, even using 0.27 mol% of 5% Rh/C, **57** was obtained in good yield and the turnover number (TON) reached up to 280 [59].

To demonstrate the potential applications of the present cross-coupling, the preparation of versatile 1,1′-binaphtyl-based ligands was examined (Fig. 18). Cross-coupling of **52** with an excess of 2-naphthol proceeded to give NOBIN analog **58** in 62%. NOBIN is used not only in asymmetric catalysis, but is also used as a source of various 1,1′-binaphthyl-based ligands [60]. Additionally, since the amino groups can be used for further transformations, our methodology provides efficient access to a variety of biaryls with interesting functions and biological activities.

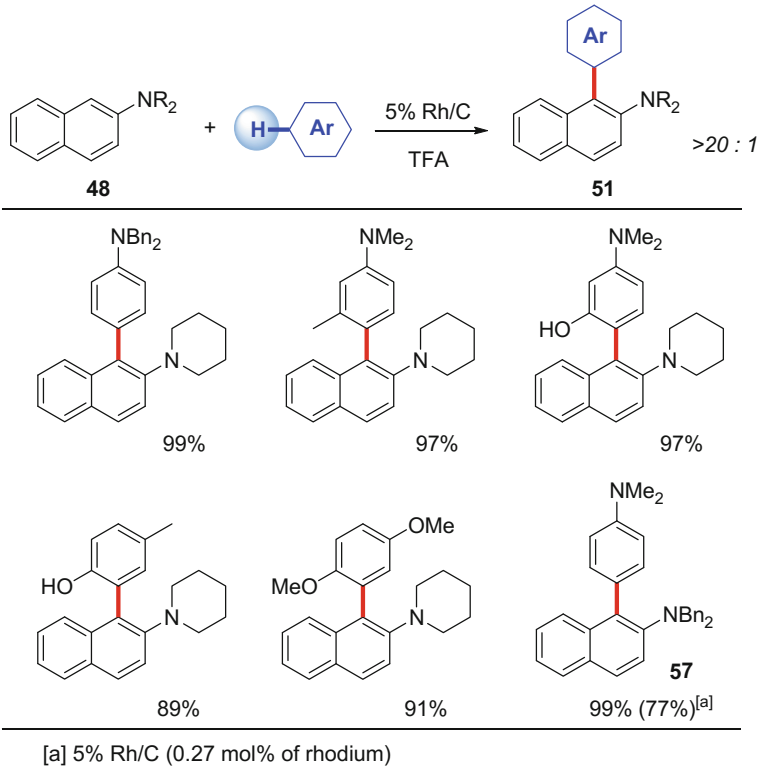

Fig. 17 Oxidative C–H/C–H cross-coupling of aryl amines

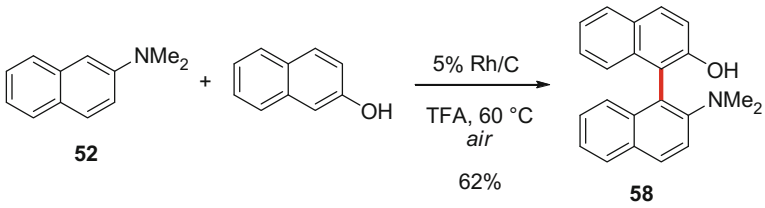

Fig. 18 Synthetic utility of the cross-coupling reaction

4 Conclusion

We demonstrated two kinds of aerobic oxidative metal catalyzed synthetic reactions that we recently developed. The homogeneous Cu(II) complex catalyzed acylations present new synthetic strategies of one-pot lactonization and dissymmetrization of malonate. These reactions can be carried out under mild and neutral conditions, which are compatible with acid- or base-labile functionality, especially for synthesis

of complex molecules. The aerobic oxidative metal catalyzed coupling reactions provide not only homo-coupled biaryl products but also cross coupled ones, which are highly useful for materials and medicinal chemistry. Furthermore, the reaction has special features including dehydrogenative direct C–C coupling, recyclable heterogeneous catalysts used, and oxygen as an oxidant. The current catalytic reactions will provide benign and scalable processes in synthetic organic chemistry.

Acknowledgements This work was partially supported by KAKENHI (No. JP22659023, No. JP26670003, No. JP16H01157 and No. JP26293004), Science and Technology Research Promotion Program for Agriculture, forestry, fisheries and food industry (M.S.), the Cooperative Research Program of the Network Joint Research Center for Materials and Devices, and the Asahi Glass Foundation (K.M.).

References

1. Ohtsuki, K.; Matsuo, K.; Yoshikawa, T.; Moriya, C.; Tomita-Yokotani, K.; Shishido, K.; Shindo, M. *Org. Lett.* **2008**, *10*, 1247–1250.
2. Matsuo, K.; Ohtsuki, K.; Yoshikawa, T.; Shishido, K.; Yokotani-Tomita, K.; Shindo, M. *Tetrahderon* **2010**, *66*, 8407–8419.
3. Matsuo, K.; Shindo, M. *Org. Lett*. **2010**, *12*, 5346–5349.
4. Bonadies, F.; Cardilli, A.; Lattanzi, A.; Pesci, S.; Scettri, A. *Tetrahedron Lett*. **1995**, *36*, 2839–2840.
5. Bestmann, H. J. *Angew. Chem. Int. Ed.* **1977**, *16*, 349–364.
6. Masamune, S.; Kamata, S.; Schilling, W. *J. Am. Chem. Soc.* **1975**, *97*, 3515–3516.
7. Masamune, S.; Hayase, Y.; Schilling, W.; Chan, W. K.; Bates, G. S. *J. Am. Chem. Soc.* **1977**, *99*, 6756–6758.
8. Gerlach, H.; Thalmann, A. *Helv. Chim. Acta* **1974**, *57*, 2661–2663.
9. Kim, S.; Lee, J. I. *J. Org. Chem.* **1984**, *49*, 1712–1716.
10. Witt, D. *Synthesis* **2008**, *16*, 2491–2509.
11. Miles, D. H.; Ly, A-M.; Ghittawong, V.; de la Cruz, A. A.; Gomez, E. D. *J. Nat. Prod*. **1989**, *52*, 896–898.
12. Irie, H.; Matsumoto, R.; Nishimura, M.; Zhang, Y. *Chem. Pharm. Bull*. **1990**, *38*, 1852–1856.
13. Matsuo, K.; Shindo, M. *Tetrahedron* **2011**, *67*, 971–975.
14. Matsuo, K.; Shindo, M. *Org. Lett.* **2011**, *13*, 4406–4409.
15. Gais, H.-J., Theil, F. In *Enzyme Catalysis in Organic Synthesis*; Drauz, K., Waldman, H., Eds.; Wiley-VCH: Weinheim, 2002; Vol. II, pp. 335–578.
16. Junek, H.; Ziegler, E.; Herzog, U.; Kroboth, H. *Synthesis* **1976**, 332–334.
17. Rigo, B.; Fasseur, D.; Cauliez, P.; Couturier, D. *Tetrahedron Lett.* **1989**, *30*, 3073–3076.
18. Niwayama, S.; Cho, H.; Lin, C. *Tetrahedron Lett*. **2008**, *49*, 4434–4436.
19. Niwayama, S.; Hanjoung, C. *Chem. Pharm. Bull*. **2009**, *57*, 508–510.
20. Mashiko, T.; Kumagai, N.; Shibasaki, M. *J. Am. Chem. Soc.* **2009**, *131*, 14990–14999.
21. Clerici, P.; Wennemers, H. *Org. Biomol. Chem.* **2012**, *10*, 110–113.
22. Clemens, R. J.; Witzeman, J. S. *J. Am. Chem. Soc.* **1989**, *111*, 2186–2193.
23. Witzeman, J. S. *Tetrahedron Lett.* **1990**, *31*, 1401–1404.
24. Gong, L.; McAllister, M. A.; Tidwell, T. T. *J. Am. Chem. Soc.* **1991**, *113*, 6021–6028.
25. Tidwell, T. T. *KETENES 2nd Ed.*, John Wiley & Sons: New Jersey, 2006; pp. 244–258.
26. Matsumoto, K.; Dougomori, K.; Tachikawa, S.; Ishii, T.; Shindo, M. *Org. Lett.* **2014**, *16*, 4754–4757.
27. Dick, A. R.; Sanford, M. S. *Tetrahedron* **2006**, *62*, 2439–2463.

28. Alberico, D.; Scott, M. E.; Lautens, M. *Chem. Rev*. **2007**, *107*, 174–238.
29. Santoro, S.; Kozhushkov, S. I.; Ackermann, L.; Vaccaro, L. *Green Chem.* **2016**, *18*, 3471–3493.
30. Yeung, C. S.; Dong, V. M. *Chem. Rev.* **2011**, *111*, 1215–1292.
31. Liu, C.; Zhang, H.; Shi, W.; Lei, A. *Chem. Rev.* **2011**, *111*, 1780–1824.
32. Cho, S. H.; Kim, J. Y.; Kwak, J.; Chang, S. *Chem. Soc. Rev.* **2011**, *40*, 5068–5083.
33. Kuhl, N.; Hopkinson, M. N.; Wencel-Delord, J.; Glorius, F. *Angew. Chem. Int. Ed.* **2012**, *51*, 10236–10254.
34. Nakajima, M.; Miyoshi, I.; Kanayama, K.; Hashimoto, S.; Noji, M.; Koga, K. *J. Org. Chem.* **1999**, *64*, 2264–2271.
35. Guo, Q.-X.; Wu, Z.-J.; Luo, Z.-B.; Liu, Q.-Z.; Ye, J.-L.; Luo, S.-W.; Cun, L.-F.; Gong, L.-Z. *J. Am. Chem. Soc.* **2007**, *129*, 13927–13938.
36. Egami, H.; Katsuki, T. *J. Am. Chem. Soc.* **2009**, *131*, 6082–6083.
37. Matsushita, M.; Kamata, K.; Yamaguchi, K.; Mizuno, N. *J. Am. Chem. Soc.* **2005**, *127*, 6632–6640.
38. Smrčina, M.; Lorenc, M.; Hanuš, V.; Kočovský, P. *Synlett* **1991**, 231–232.
39. Vyskočil, Š.; Smrčina, M.; Lorenc, M.; Tišlerová, I.; Brooks, R. D.; Kulagowski, J. J.; Langer, V.; Farrugia, L. J.; Kočovský, P. *J. Org. Chem.* **2001**, *66*, 1359–1365.
40. Li, X.-L.; Huang, J.-H.; Yang, L.-M. *Org. Lett.* **2011**, *13*, 4950–4953.
41. Wang, D.; Izawa, Y.; Stahl, S. S. *J. Am. Chem. Soc.* **2014**, *136*, 9914–9917.
42. Matsumoto, K.; Yoshida, M.; Shindo, M. *Angew. Chem. Int. Ed.* **2016**, *55*, 5272–5276.
43. Ackermann, L.; Vicente, R.; Kapdi, A. R. *Angew. Chem. Int. Ed.* **2009**, *48*, 9792–9826.
44. McGlacken, G. P.; Bateman, L. *Chem. Soc. Rev.* **2009**, *38*, 2447–2464.
45. Ashenhurst, J. A. *Chem. Soc. Rev.* **2010**, *39*, 540–548.
46. Stuart, D. R.; Fagnou, K. *Science* **2007**, *316*, 1172–1175.
47. Kitahara, M.; Umeda, N.; Hirano, K.; Satoh, T.; Miura, M. *J. Am. Chem. Soc.* **2011**, *133*, 2160–2162.
48. Wencel-Delord, J.; Nimphius, C.; Patureau, F. W.; Glorius, F. *Angew. Chem. Int. Ed.* **2012**, *51*, 2247–2251.
49. Sanhueza, I. A.; Wagner, A. M.; Sanford, M. S.; Schoenebeck, F. *Chem. Sci.* **2013**, *4*, 2767–2775.
50. Lee, Y. E.; Cao, T.; Torruellas, C.; Kozlowski, M. C. *J. Am. Chem. Soc.* **2014**, *136*, 6782–6785.
51. Libman, A.; Shalit, H.; Vainer, Y.; Narute, S.; Kozuch, S.; Pappo, D. *J. Am. Chem. Soc*. **2015**, *137*, 11453–11460.
52. Kita, Y.; Morimoto, K.; Ito, M.; Ogawa, C.; Goto, A.; Dohi, T. *J. Am. Chem. Soc.* **2009**, *131*, 1668–1669.
53. Morimoto, K.; Sakamoto, K.; Ohshika, T.; Dohi, T.; Kita, Y. *Angew. Chem. Int. Ed.* **2016**, *55*, 3652–3656.
54. Ito, M.; Kubo, H.; Itani, I.; Morimoto, K.; Dohi, T.; Kita, Y. *J. Am. Chem. Soc.* **2013**, *135*, 14078–14081.
55. Elsler, B.; Wiebe, A.; Schollmeyer, D.; Dyballa, K. M.; Franke, R.; Waldvogel, S. R. *Chem. Eur. J.* **2015**, *21*, 12321–12325.
56. Kirste, A.; Elsler, B.; Schnakenburg, G.; Waldvogel, S. R. *J. Am. Chem. Soc.* **2012**, *134*, 3571–3576.
57. Morofuji, T.; Shimizu, A.; Yoshida, J. *Angew. Chem. Int. Ed.* **2012**, *51*, 7259–7262.
58. Smrčina, M.; Vyskočil, Š.; Máca, B.; Polášek, M.; Claxton, T. A.; Abbott, A. P.; Kočovský, P. *J. Org. Chem.* **1994**, *59*, 2156–2163.
59. The preliminary recycling experiment for the cross-coupling of **48** (R = Bn) with **53** in the presence of recovered 5% Rh/C at 50 °C under oxygen (1 atm) provided 93% of **57**. This result revealed that Rh/C can be reused in the present reaction.
60. Ding, K.; Li, X.; Ji, B.; Guo, H.; Kitamura, M. *Curr. Org. Synth.* **2005**, *2*, 499–545.

Heterogeneous Platinum Metal Catalyzed Deuterium Generation and Labeling Methods Using Hydrogen Gas and Deuterium Oxide as Key Reagents

Hironao Sajiki

Abstract Deuterium (heavy hydrogen, D or ^{2}H), a stable isotope of hydrogen (^{1}H) consists of one proton, one neutron and one electron and used extensively in a wide range of fields including science, chemistry, medicine, etc. We have developed quite simple and post-synthetic D labeled methods using a combination of platinum metal on carbon and deuterium oxide (D_2O) as the catalyst and a D source in the presence of organic substrates, and a highly pure D_2 gas preparation method occurred at room temperature (rt) via the catalytic H_2–D_2 exchange reaction between the H atom of the H_2 gas with the D atom of D_2O without any substrates. This review illustrates and describes such straightforward and useful methodologies.

Keywords Deuterium labeling · H–D exchange · C–H activation · Platinum-group metal on carbon · Deuterium gas preparation · Deuterium oxide · Hydrogen gas

Deuterated products have received attention not only as useful tools for the investigation of drug metabolisms [1, 2] or reaction mechanisms [3, 4] as tracers or surrogate compounds, but also as functional materials such as fully deuterated polymers as components of optical fibers for high-speed telecommunication, which are virtually free of any optical absorption based on the C–H stretching vibration [5]. Multi-deuterated alkanes are anticipated as internal markers to prevent the distribution of illegal (illicit) light diesel oil [6] and deuterated medicines are expected to become new drugs having a longer duration of action based on the isotopic effect (resistant to the drug metabolism) [7]. Since the atomic nucleus of D can be fused with a tritium (T or ^{3}H) nucleus into a helium (He) and a neutron together with the emission of a massive amount of energy (fusion energy) [8], it is expected as one of the most useful new sources of energy that avoids CO_2 generation.

H. Sajiki (✉)
Laboratory of Organic Chemistry, Gifu Pharmaceutical University,
1-25-4 Daigaku-Nishi, Gifu 501-1196, Japan
e-mail: sajiki@gifu-pu.ac.jp

K. Tomioka et al. (eds.), *New Horizons of Process Chemistry*,
DOI 10.1007/978-981-10-3421-3_3

As summarized above, D is widely used in a variety of scientific fields as a representative nuclide of a stable isotope. The precedent preparation methods of D-labeled compounds can be classified into three types: (1) total synthetic methods starting from small deuterated raw materials; (2) reduction of reducible functionalities using deuterated reducing agents; and (3) post-synthetic direct deuteration (H–D exchange reaction). It is patently obvious that the catalytic reduction using D_2 gas (deuterogenation) as a part of (2) and the catalytic H–D exchange reaction of non-deuterated compounds as (3) are preferable and practical methodologies associated with less waste. By the way, what kind of deuterium source is desired to achieve the H–D exchange reactions? The cheapest and most productive one is D_2O. Natural water contains ca. 0.015% (150 ppm) of the D atom [9], which exists in the form of HDO by a disproportionation equilibrium. The D-abundance ratio that is highly enriched by the dual temperature isotope exchange process utilizing the difference in the chemical equilibrium constant between HDS and HDO in a temperature-dependent manner [H_2S obtains a deuterium atom from HDO at a higher temperature (ca. 125 °C) and H_2O obtains a deuterium from HDS at a lower temperature (ca. 25 °C); Girdler-Sulfide (GS) method] [10, 11]. Although nearly pure D_2O has been industrially manufactured using the GS method, D_2 gas is still produced by electrolysis of the incrassate (nearly pure) D_2O using an enormous amount of electric energy. Since D_2 gas, D_2O and some deuterated compounds are designated as international controlled materials and subject to rigid control regarding import and export under security trade control, the development of efficient, mild, easily handled and catalytic preparation methods of regulated and combustible D_2 gas would have to be developed in the respective countries, or even, each manufacturing site including laboratories in order to avoid the export, import and transportation problems.

In this review, we would like to describe the efficient platinum metal on carbon-catalyzed post-synthetic direct H–D exchange reactions using D_2O as the deuterium source under a H_2 atmosphere and a simple replacement method of sealed H_2 gas by D_2 gas via the Pd/C-catalyzed H_2–D_2 exchange reaction between H_2 and D_2O developed by us.

1 Heterogeneous Platinum Metal Catalyzed Post-synthetic Deuterium Labeling Method Using D_2O as the Deuterium Source in the Presence of Hydrogen Gas

We have discovered that the H-atoms on the benzylic position of the substrate were time-dependently and site-selectively replaced with an equal number of D-atoms derived from D_2O under mild and Pd/C-catalyzed hydrogenation conditions (Fig. 1) [12–14].

The catalyst activity for the H–D exchange reaction under Pd/C–H_2–D_2O conditions was dramatically enhanced by the application of heat which facilitated the

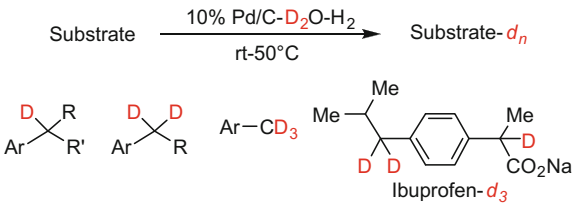

Fig. 1 H–D exchange reaction at the benzylic positions

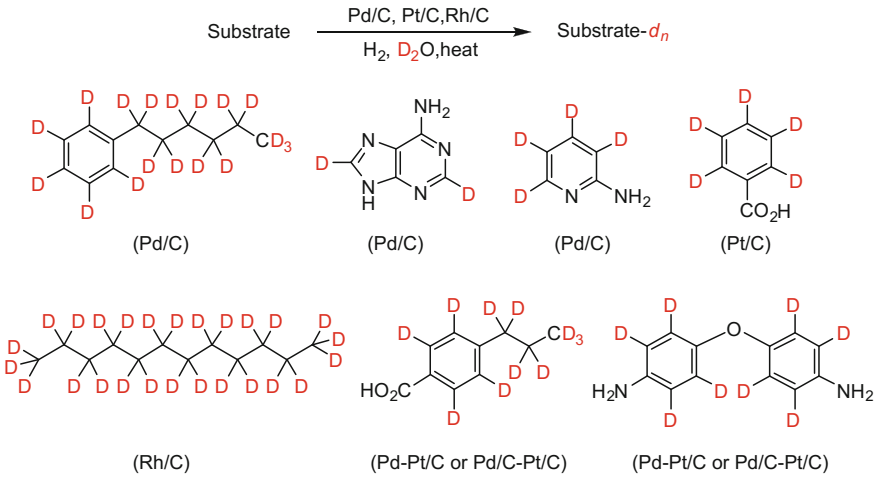

Fig. 2 Catalyst activity for the H–D exchange reaction

H–D exchange reaction at not only the benzylic sites, but also the inactive C–H bonds of alkyl-substituted aromatic compounds and heterocyclic nuclei [15–20]. Pt/C is an appropriate catalyst for the deuteration of aromatic nuclei, and the H–D exchange reaction smoothly proceeded under milder conditions [21, 22]. Furthermore, the mixed use of Pd/C and Pt/C or a bimetallic Pd–Pt on carbon was also found to be more efficient for the H–D exchange reaction in comparison to the independent use of Pd/C or Pt/C [23–25]. Furthermore, simple alkanes, which are inactive substrates by most definitions, could also be efficiently deuterated under the Rh/C-catalyzed heating conditions in a sealed tube (Fig. 2) [26].

The use of Ru/C enabled the regiospecific and efficient D incorporation at the α-position of alcohols at rt −80 °C and the results were applied as a regio- and stereoselective multi-deuteration method of sugar derivatives (Fig. 3) [27, 28].

H_2 gas is essential as an activating agent of the zero valent platinum group metal on carbon. Moreover, these H–D exchange methodologies are available to apply to the H–T (tritium, ^3H) exchange reaction using highly diluted tritiated water (THO) indicating a low level of radioactivity, and the multi-tritium incorporated products indicates a higher specific radioactivity in comparison to the HTO based on the suppression of the reverse reaction due to the isotope effect of T (Fig. 4) [29].

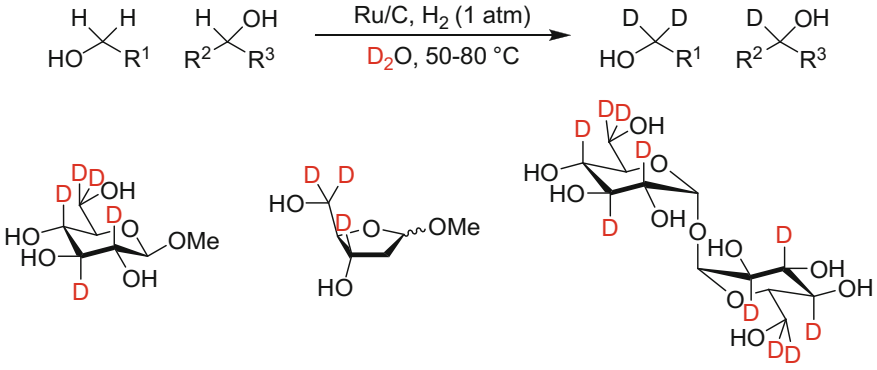

Fig. 3 Regiospecific deuterium incorporation at the α-positions of alcohols

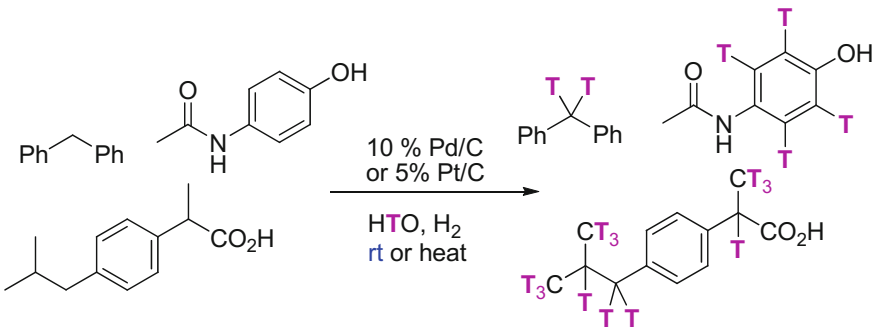

Fig. 4 H–T exchange reaction in highly diluted tritiated water

These deuterium and tritium labeling methods using the platinum group metal on carbon–D_2O–H_2 combination can be achieved under simple and mild conditions in comparison to conventional methods, and a wide variety of labeled compounds are obtained in good to quantitative yields and deuterium efficiencies [30–32].

2 Replacement of Hydrogen Gas by Deuterium Gas via Pd/C-Catalyzed H_2–D_2 Exchange Reaction Between H_2 and D_2O

As for the preparation methods of D_2 gas on a laboratory scale, the reaction of metals, such as sodium [33], iron [34], and magnesium [35] with D_2O, have been reported in the literature, although a large quantity of metal sludge is produced and drastic reaction conditions (several hundred degrees Celsius) are required. While numerous catalytic H_2–D_2 exchange reactions between H_2 and D_2O have also been

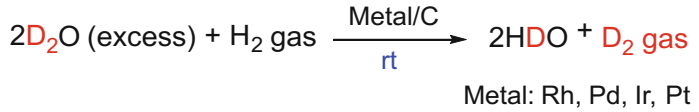

Fig. 5 Quantitative transmutation of H_2 gas into D_2 gas at room temperature

reported in the literature [36–44], such methods could not produce highly pure D_2 gas and also required a high pressure, the use of a special catalyst, and/or strongly basic or acidic reaction conditions.

We have developed an efficient and quantitative in situ transmutation reaction of H_2 gas into D_2 gas utilizing the heterogeneous platinum group metal-catalyzed H_2–D_2 exchange reaction derived from D_2O as the deuterium source that occurs at rt [30–32, 45, 46]. H_2 gas sealed in the reaction flask is totally converted into nearly pure D_2 gas (Fig. 5), which can be used for the one-pot reductive deuteration (deuterogenation) of a wide variety of substrates possessing reducible functionalities within the molecule. Since Rh/C indicates the highest activity and Pd/C, Ir/C and Pt/C are also effective as catalysts, the H_2–D_2 exchange study was effected by the selection of Pd/C as the catalyst from the aspect of cost and ready availability.

The H_2–D_2 exchange efficiency after 24 h of stirring of 7.4 mg of 10% Pd/C in D_2O (3.0 mL, 166 mmol) in a hydrogen filled sealed flask with an effective internal volume of 160 mL (6.5 mmol/H_2 at 25 °C; that is to say commercially designated as a 100 mL eggplant flask) at rt was determined by the incorporation ratio of the deuterium into dihydrocinnamic acid (**2-*d*$_n$**) by the 10% Pd/C-catalyzed hydrogenation and/or deuterogenation of cinnamic acid (**1**) at rt for 6 h in the H_2–D_2 exchanged sealed flask (Table 1). The deurterogenation of **1** efficiently proceeded by a 24 h pre-stirring (H_2–D_2 exchange reaction), and nearly 50% deuterium efficiencies (theoretical value) were observed on both the C1 and C2 methylenes (**2-*d*$_n$**, Entry 1). On the other hand, little deuteration was observed without the 24 h pre-stirring (Entry 2). The deuterium efficiency was reduced with an inclease in volume of H_2 using a larger flask (Entries 3 and 4). The D_2 purity is significantly affected by the use a ratio of H_2 and D_2O based upon the H_2–D_2 exchange efficiency under the same time frame and reaction temperature.

The replacement efficiency of H_2 by D_2 decreased with the deterioration in the deuterium content of D_2O (Entries 5–8). The significant decrease in the deuterium efficiency of the deuterogenated product was observed and 50% D_2O (HDO) led to virtually no incorporation of deuterium (Entry 7). Since the deterioration in purity of the D_2O caused a significant drop in the H_2–D_2 exchange efficiency, an excess amount of D_2O (3 mL, 166 mmol vs. 160 mL, 6.5 mmol of H_2) should be required to circumvent the drastic degradation of the D_2O purity.

The Pd/C-catalyzed H_2–D_2 exchange reaction is very likely proceeding via the illustrated reaction pathway shown in Fig. 6. The oxidative addition of the O–D bond of D_2O to the H_2-activated Pd metal on charcoal (**I**) produced the Pd(II) complex (**II**). Subsequently, the H–D exchange on a Pd(II) complex (**III**) and reductive elimination to give a HD-activated Pd metal on charcoal (**IV**).

Table 1 H_2–D_2 exchange efficiency under various conditions[a]

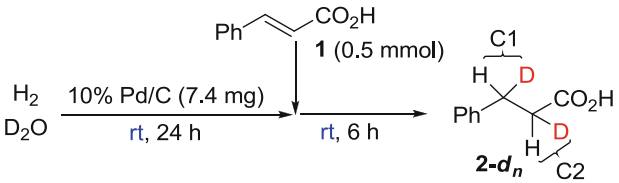

Entry	H_2 (mL/mmol)	D_2O (mL)	H_2O (mL)	D efficiency (%)[b]		Isolated yield (%)
				C1	C2	
1	160/6.5	3.0	0	48	46	98
2[c]	160/6.5	3.0	0	2	0	97
3	285/12.2	3.0	0	44	42	100
4	690/28.2	3.0	0	31	29	100
5	160/6.5	2.7	0.3	30	26	98
6	160/6.5	2.1	0.9	13	12	94
7	160/6.5	1.5	1.5	5	6	98
8	160/6.5	0.9	2.1	0	0	95

[a]The reaction was performed in a hydrogen-charged sealed flask using 7.4 mg of 10% Pd/C in D_2O or D_2O–H_2O mixed solvents (each 3.0 mL) at room temperature (25 °C) for 24 h. Subsequently, *trans*-cinnamic acid (**1**, 0.5 mmol) was added, and the reaction was quenched after 6 h

[b]The D content was determined by ^1H NMR on the basis of the integration of the aromatic protons

[c]Without initial 24 h-stirring prior to the addition of *trans*-cinnamic acid (**1**)

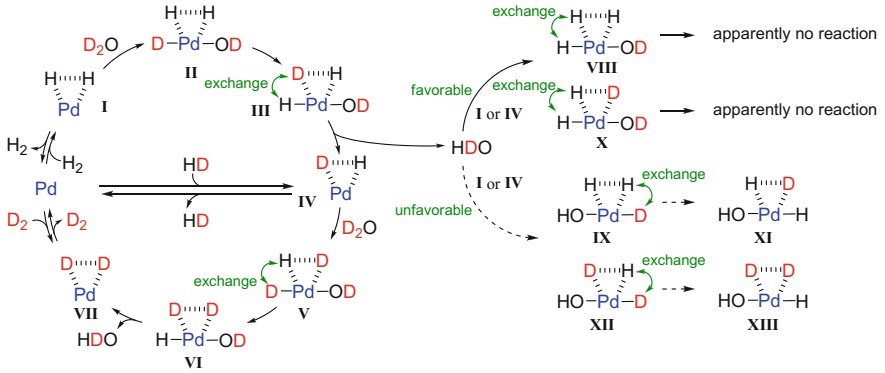

Fig. 6 Plausible reaction mechanism

Further oxidative addition of excess D_2O to **IV**, H–D exchange, reductive elimination and discharge of D_2 gas could turn over the catalyst cycle.

The reaction progress is clearly controlled by the isotopic effect between H and D. The oxidative addition of HDO to H_2 or HD-activated Pd metal on charcoal (**I** or **IV**) should preferably occur at the O–H bonds (**VIII** or **X**) compared to the O–D bond (**IX** or **XII**) and virtually no reaction was observed as a result of the H–H exchange on **VIII** or **X**. Therefore, the formation of the complex (**II** or **V**) derived from D_2O and **I** or **IV** should be necessary to generate HD or D_2. The oxidative addition of the HD–activated Pd metal (**IV**) to D_2O gave the complex (**V**), which would undergo the intramolecular H–D exchange, leading to the D_2 generation via complex **VI**. Namely, increasing the H_2O content in D_2O with the ratio of 50% or more would result in no reaction due to the complexation with HDO or H_2O and Pd metal (**I** or/and **IV**) followed by the intramolecular H–H exchange based on the isotopic effect (see also Table 1, Entries 7 and 8). Therefore, the use of a reasonably excess molar number of D_2O compared with the use of H_2 to avoid the unfavorable H–H exchange process should be required for the efficient generation of pure D_2 gas.

The generated deuterium gas in a sealed flask is easily applicable for the one-pot deuterogenation of various substrates possessing a wide variety of reducible functionalities within the molecule, and the desired deuterium-incorporated products are obtained in excellent to quantitative deuterium efficiencies as shown in Table 2. The heterogeneous catalyst can be recovered by simple filtration, and the acidic deuterium atoms on the carboxylic acid, alcohol and amine functionalities were replaced by hydrogen atoms during the aqueous workup.

The *chemoselective* one-pot deuterogenation was also possible by the addition of a catalyst poison [47–53]. For example, the chemoselective one-pot deuterogenation of an olefin in the presence of an aromatic ketone or benzyl ester within the molecule proceeded with excellent deuterium efficiencies by the addition of a very low loading (0.01 equiv) of diphenylsulfide (Ph_2S) as a catalyst poison (Table 2, **14-*d*$_2$** and **16-*d*$_2$**), while the deuterogenation of the aromatic ketone or benzyl ester cannot be avoided without the addition of Ph_2S (Table 2, **13-*d*$_4$** and **15-*d*$_2$**) [45, 46]. Furthermore, a quite mild and fruitful deuterogenation of an aromatic nucleus is also possible. A partially (nearly 50%) deuterated cyclohexane derivative (**17-*d*$_6$**) can be easily obtained by the use of 10% Rh/C as a catalyst under gentle heating conditions (50 °C) [54–57].

It is noteworthy that almost pure and dried (waterless) D_2 gas can be collected in a rubber balloon or gas collection bag via a drying tube from a pressure-resistant reaction vessel with an internal volume of 170 mL after the H_2–D_2 exchange reaction at rt although the increased use of 10% Pd/C (30–40 mg) and D_2O (6–10 mL) under medium H_2 pressure (3–4 atm) was required. The collected waterless D_2 gas can be applied to the anhydrous deuterogenation and deuteration reactions, while the one-pot and in situ method is not applicable to water-sensitive substrates and reactions.

Table 2 Deuterium efficiency of deuteration using in-situ generated D_2 gas[a,b,]

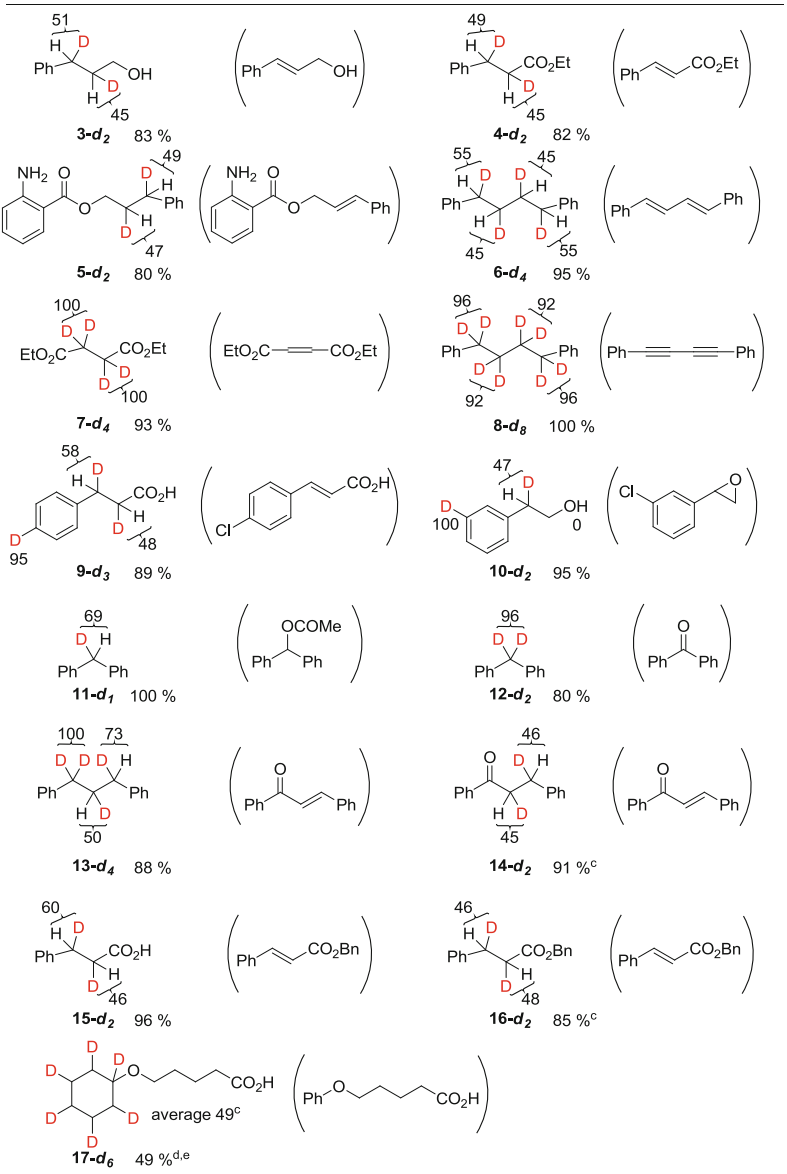

[a]The substrate is indicated in parentheses

[b]Digits located adjacent to each D atom indicate the deutrium efficiency

[c]0.01 equiv of Ph_2S were added as a catalyst poison

[d]10% Rh/C was used as a catalyst instead of 10% Pd/C

[e]The theoretical D-efficiency is 55%

In summary, the H–D and H_2–D_2 exchange reactions introduced in this manuscript are readily and independently available at each laboratory and manufacturing site when necessary. Interestingly, these results strongly indicate that the H–H exchange reaction between the H_2 gas, substrates and protic solvents, such as H_2O, MeOH, etc. without the influence of the isotopic effect must frequently and continuously occur under the hydrogenation conditions, while the reaction seems to apparently undergo no reaction. This review should be helpful for the various international research groups who need the presented methodologies to prepare D labeled compounds and D_2 gas. Since the methodologies in this review have already been put to practical use by Wako Pure Chemical Industries, Ltd. (deuterium labeled reagents and contract manufacturing service), it is possible to use such a service according to your needs.

References

1. Foster, A. B., "Deuterium Isotope Effects in Studies of Drug Metabolism" Trends Pharmacol. Sci. (1984) **5**, 524–527.
2. Davidova, I. A.; Gieg, L. M.; Nanny, M.; Kropp, K. G.; Suflita, J. M., "Stable Isotopic Studies of n-Alkane Metabolism by a Sulfate-Reducing Bacterial Enrichment Culture" Appl. Environ. Microbiol. (2005) **71**, 8174–8182.
3. Lowry, T. H.; Richardson, K. S., "Mechanism and Theory in Organic Chemistry", Harper & Row, New York (1987).
4. Perrin, C. L.; Dong, Y., "Secondary Deuterium Isotope Effects on Acidity of Carboxylic Acids and Phenols", J. Am. Chem. Soc. (2007) **129**, 4490–4497.
5. Kondo, A.; Ishigure, T.; Koike, Y., "Fabrication Process and Optical Properties of Perdeuterated Gradedindex Polymer Optical Fiber" J. Lightwave Technol. (2005) **23**, 2443–2448.
6. Suzuki, Y.; Korenaga, T.; Chikaraishi, Y., "A Novel Method to Identify Illegal Diesel Fuel, II: the Use of [1-D] N-Alkane with Stable Hydrogen Isotope Analysis" Chem. Lett. (2006) **35**, 532–533.
7. Sanderson, K., "*Big Interest in Heavy Drugs*" Nature (2009) **458**, 269.
8. Harms, A. A.; Schoepf, K. F.; Miley, G. H.; Kingdon, D. R., "Principles of Fusion Energy: An Introduction to Fusion Energy for Students of Science and Engineering", World Scientific, Singapore (2000).
9. Scrimgeour, C. M.; Rollo, M. M.; Mudambo, S. M. K. T.; Handley, L. L.; Prosser, S. J., "A Simplified Method for Deuterium/Hydrogen Isotope Ratio Measurements on Water Samples of Biological Origin", Biol. Mass Spectrom., (1993) **22**, 383–387.
10. Benedict, M; Pigford, T. H., "Nuclear Chemical Engineering", McGraw-Hill, New York, (1957).
11. Kikuchi, M.; Azumi, M., "Frontiers in Fusion Research II: Introduction to Modern Tokamak Physics", Tritium and Deuterium Chemistry, pp. 327–333, Springer, Heidelberg, (2015).
12. Sajiki, H.; Hattori, K.; Aoki, F.; Yasunaga, K.; Hirota, K., "Pd/C–H_2–Catalyzed Deuterium Exchange Reaction of the Benzylic Site in D_2O", Synlett (2002) 1149–1151.
13. Maegawa, T.; Akashi, A.; Esaki, H.; Aoki, F.; Sajiki, H.; Hirota, K., "Efficient and Selective Deuteration of Phenylalanine Derivatives Catalyzed by Pd/C", Synlett (2005) 845–847.
14. Kurita, T.; Hattori, K.; Seki, S.; Mizumoto, T.; Aoki, F.; Yamada, Y.; Ikawa, K.; Maegawa, T.; Monguchi, Y.; Sajiki, H., "Efficient and Convenient Heterogeneous Palladium-Catalyzed Regioselective Deuteration at the Benzylic Position", Chem. Eur. J., (2008) **14**, 664–673.

15. Sajiki, H.; Aoki, F.; Esaki, H.; Maegawa, T.; Hirota, K., "Efficient C–H/C–D Exchange Reaction on the Alkyl Side Chain of Aromatic Compounds Using Heterogeneous Pd/C in D_2O", Org. Lett. (2004) **6**, 1485–1487.
16. Sajiki, H.; Esaki, H.; Aoki, F.; Maegawa, T.; Hirota, K., "Palladium-Catalyzed Base-Selective H–D Exchange Reaction of Nucleosides in Deuterium Oxide", Synlett (2005) 1385–1388.
17. Esaki, H.; Aoki, F.; Maegawa, T.; Hirota, K.; Sajiki, H., "Synthesis of Base-Selectively Deuterium-Labeled Nucleosides by the Pd/C-Catalyzed H–D Exchange Reaction in Deuterium Oxide", Heterocycles (2005) **66**, 361–369.
18. Esaki, H.; Ito, N.; Sakai, S.; Maegawa, T.; Monguchi, Y.; Sajiki, H., "General Method of Obtaining Deuterium Labelling heterocyclic Compounds Using Neutral D_2O with Heterogeneous Pd/C", Tetrahedron (2006) **62**, 10954–10961.
19. Esaki, H.; Aoki, F.; Umemura, M.; Kato, M.; Maegawa, T.; Monguchi, Y.; Sajiki, H., "Efficient H–D Exchange Reaction of Alkyl-substituted Benzene Derivatives Using Pd/C–H_2–D_2O System", Chem. Eur. J. (2007) **13**, 4052–4063.
20. Modutlwa, N.; Tada, H.; Sugahara, Y.; Shiraki, K.; Hara, N.; Deyashiki, Y.; Maegawa, T.; Monguchi, Y.; Sajiki, H., "Deuterium-Labelled Benzyladenine: Synthesis and Application as a Surrogate", Heterocycles (2012) **84**, 419–429.
21. Sajiki, H.; Ito, N.; Esaki, H.; Maesawa, T.; Maegawa, T.; Hirota, K., "Aromatic Ring Favorable and Efficient H–D Exchange Reaction Catalyzed by Pt/C", Tetrahedron Lett. (2005) **46**, 6995–6998.
22. Ito, N.; Esaki, H.; Maesawa, T.; Imamiya, E.; Maegawa, T.; Sajiki, H., "Pt/C-Catalyzed Efficient H–D Exchange Reaction of Aromatic Rings And its Scope and Limitations", Bull. Chem. Soc. Jpn. (2008) **81**, 278–286.
23. Ito, N.; Watahiki, T.; Maesawa, T.; Maegawa, T.; Sajiki, H., "Synergistic Effect of a Palladium-on-Carbon/Platinum-on-Carbon Mixed Catalyst in Hydrogen/Deuterium Exchange Reactions of Alkyl-Substituted Aromatic Compounds", Adv. Synth. Catal. (2006) **348**, 1025–1028.
24. Ito, N.; Watahiki, T.; Maesawa, T, Maegawa, T.; Sajiki, H., "H–D Exchange Reaction Taking Advantage of a Synergistic Effect of a Heterogeneous Pd and Pt Mixed Catalyst", Synthesis (2008) **9**, 1467–1478.
25. Maegawa, T.; Ito, N.; Ohno, K.; Monguchi, Y.; Sajiki, H., "Bimetallic Palladium-Platinum on Carbon Catalyzed H–D Exchange Reaction: Synergistic Effect on Multiple Deuterium Incorporation", Synthesis (2009) **16**, 2674–2678.
26. Maegawa, T.; Fujiwara, Y.; Inagaki, Y.; Esaki, H.; Monguchi, Y.; Sajiki, H., "Mild and Efficient H–D Exchange of Alkanes Based on C–H Activation Catalyzed by Heterogeneous Rhodium on Charcoal", Angew. Chem. Int. Ed. (2008) **47**, 5394–5397.
27. Maegawa, T.; Fujiwara, Y.; Inagaki, Y.; Monguchi, Y.; Sajiki, H., "A Convenient and Effective Method for the Regioselective Deuteration of Alcohols", Adv. Synth. Catal. (2008) **350**, 2215–2218.
28. Fujiwara, Y.; Iwata, H.; Sawama, Y.; Monguchi, Y.; Sajiki, H., "Regio-, Chemo- and Stereoselective Deuterium Labeling Method of Sugars Based on Ruthenium-Catalyzed C–H Bond Activation", Chem. Commun. (2010) **46**, 4977–4979.
29. Maegawa, T.; Hirota, K.; Tatematsu, K.; Mori, Y.; Sajiki, H., "Facile and Efficient Postsynthetic Tritium Labeling Method Catalyzed by Pd/C in HTO" J. Org. Chem. (2005) **70**, 10581–10583.
30. Esaki, H.; Kurita, T.; Fujiwara, Y.; Maegawa, T.; Monguchi, Y.; Sajiki, H., "An Efficient Deuteration Method Catalyzed by Heterogeneous Platinum Group Metals", J. Synth. Org. Chem., Jpn. (2007), 65, 1179–1190.
31. Sawama, Y.; Monguchi, Y.; Sajiki, H., "Efficient H–D Exchange Reactions Using Heterogeneous Platinum-Group Metal on Carbon–H_2–D_2O System", Synlett (Account), (2012) **23**, 959–972.
32. Sajiki, H., "Development of Deuterium Labeling Method Based on the Heterogeneous Platinum Group Metal-Catalyzed C–H Activation", J. Pharm. Soc. Jpn. (2013) **133**, 1177–1193.

33. Mann, W. B.; Newell, W. C., "The Exchanges of Energy between a Platinum Surface and Hydrogen and Deuterium Molecules", Proc. Roy. Soc., A (1937) **158**, 397–403.
34. Coppock, J. B. M., "The Volume Coefficient of Expansion of Deuterium" Trans. Faraday Soc. (1935) **31**, 913–914.
35. Knowlton, J. W.; Rossini, F. D., "Method and Apparatus for the Rapid Conversion of Deuterium Oxide into Deuterium", J. Res. Nat. Bur. Stand. (1937) **19**, 605–612.
36. Farkas, A.; Farkas, L.; Yudkin, J., "Decomposition of Sodium Formate by E. coli in the Presence of Heavy Water", Proc. Roy. Soc. (1934) **B115**, 373–379.
37. von Hahn, H. E.; Peters, E., "Kinetics of Copper(II)- and Copper(I)-Catalyzed Deuterium Exchange in Sulfuric and Perchloric Acid Solutions" J. Phys. Chem. (1971) **75**, 571–579.
38. Palibroda, N.; Grecu, E.; Mărginean, P., "Catalytic Activity of Ni—Cr_2O_3 in the II_2–NH_3 and H_2–H_2O Deuterium Exchange Reactions" Isotopenpraxis (1986) **22**, 435–438.
39. El-Nour, F. A.; Belacy, N.; Abdel-Khalik, M.; Khalil, T.; Aly, H. F., "H/D Isotopic Exchange between Hydrogen and Water Vapour on Ni/Cr_2O_3/ThO_2 Catalysts" Isotopenpraxis (1990) **26**, 529–531.
40. Mochizuki, M.; Noda, S.; Morishima, T., "A Simple Method for Determination of Heavy Water by. Combined Use of Gas Chromatography and Platinum Catalyst", Radioisotopes (1987) **36**, 163–168.
41. Baba, A.; Nishikawa, M.; Eguchi, T., "Isotope Exchange Reaction on Li_2ZrO_3", J. Nucl. Mater. (1997), **250**, 29–35.
42. Yoshida, T.; Okano, T.; Saito, K.; Otsuka, S., "Activation of Water. 3. Oxidative Addition of Water to Rhodium(I) Hydrido Compounds and Application as Catalyst for Deuteration of Aromatic Hydrocarbons and Hydrogen with D_2O", Inorg. Chim. Acta. (1980) **44**, L135–L136.
43. Collman, J. P.; Wagenknecht, P. S.; Hembre, R. T.; Lewis, N. S., "Dihydrogen Complexes of Metalloporphyrins: Characterization and Hydrogen-transfer Reactivity" J. Am. Chem. Soc. (1990) **112**, 1294–1295.
44. Grundler, P. V.; Yazyev, O. V.; Aebischer, N.; Helm, L.; Laurenczy, G.; Merbach, A. E., "Kinetic Studies on the First Dihydrogen Aquacomplex, $[Ru(H_2)(H_2O)_5]^{2+}$: Formation under H_2 Pressure and Catalytic H/D Isotope Exchange in Water", Inorg. Chim. Acta. (2006) **359**, 1795–1806.
45. Sajiki H., Kurita T., Esaki H., Aoki F., Maegawa T., Hirota K., "Complete Replacement of H_2 by D_2 via Pd/C-Catalyzed H/D Exchange Reaction", Org. Lett., (2004) **6**, 3521–3523.
46. Kurita T., Aoki F., Mizumoto T., Maejima T., Esaki H., Maegawa T., Monguchi Y., Sajiki H., "Facile and Convenient Method of Deuterium Gas Generation Using a Pd/C Catalyzed H_2–D_2 Exchange Reaction and Its Application to Synthesis of Deuterium-Labeled Compounds", Chem. Eur. J., (2008) **14**, 3371–3379.
47. Sajiki, H., "Selective Inhibition of Benzyl Ether Hydrogenolysis with Pd/C Due to the Presence of Ammonia, Pyridine and Ammonium Acetate", Tetrahedron Lett., (1995) **36**, 3465–3468.
48. Sajiki, H.; Hattori, K.; Hirota, K., "The Formation of a Novel Pd/C-Ethylenediamine Complex Catalyst: Chemoselective Hydrogenation without Deprotection of the *O*-Benzyl and *N*-Cbz Groups", J. Org. Chem., (1998) **63**, 7990–7992.
49. Sajiki, H.; Hirota, K., "A Novel Type of Pd/C-catalyzed Hydrogenation Using a Catalyst Poison: Chemoselective Inhibition of the Hydrogenolysis of *O*-Benzyl Protective Groups by the Addition of a Nitrogen-containing Base", Tetrahedron (1998) **54**, 13981–13996.
50. Sajiki, H.; Hirota, K., "Pd/C-catalyzed Chemoselective Hydrogenation in the Presence of a Phenolic MPM Protective Group Using Pyridine as a Catalyst Poison", Chem. Pharm. Bull. (2003) **51**, 320–324.
51. Mori, A.; Miyakawa, Y.; Ohashi, E.,; Haga, T.; Maegawa, T.; Monguchi, Y.; Sajiki, H., "Pd/C-Catalyzed Chemoselective Hydrogenation in the Presence of Diphenylsulfide", Org. Lett. (2006) **8**, 3279–3281.

52. Mori, A.; Mizusaki, T.; Miyakawa, Y.; Ohashi, E.,; Haga, T.; Maegawa, T.; Sajiki, H., "Chemoselective Hydrogenation Method Catalyzed by Pd/C Using Diphenylsulfide as a Reasonable Catalyst Poison", Tetrahedron (2006) **62**, 11925–11932.
53. Yabe, Y.; Yamada, T.; Nagata, S.; Sawama, Y.; Monguchi, Y.; Sajiki, H., "Development of Palladium on Boron Nitride Catalyst and Its Application to Semihydrogenation of Alkynes", Adv. Synth. Catal. (2012) **354**, 1264–1268.
54. Maegawa, T.; Akashi, A.; Esaki, H.; Aoki, F.; Sajiki, H.; Hirota K., "Efficient and Selective Deuteration of Phenylalanine Derivatives Catalyzed by Pd/C", Synlett (2005) 845–847.
55. Maegawa, T.; Akashi, A.; Yaguchi, K.; Iwasaki, Y.; Shigetsura, M.; Monguchi, Y.; Sajiki, H., "Efficient and Practical Arene Hydrogenation by Heterogeneous Catalysts under Mild Conditions", Chem. Eur. J. (2009) 6953–6963.
56. Hattori, T.; Ida, T.; Tsubone, A.; Sawama, Y.; Monguchi, Y.; Sajiki, H., "Facile Arene Hydrogenation under Flow Conditions Catalyzed by Rhodium or Ruthenium on Carbon", Eur. J. Org. Chem.. (2015) 2492–2497.
57. Sawama, Y.; Mori, M.; Yamada, T.; Monguchi, Y.; Sajiki, H., "Hydrogen Self-Sufficient Arene Reduction to Cyclohexane Derivatives Using a Combination of Platinum on Carbon and 2-Propanol", Adv. Synth. Catal. (2015) 3667–3670.

Pd on Spherical Carbon (Pd/SC)-Catalyzed Chemoselective Hydrogenation

Hiroyoshi Esaki

Abstract It is well known that the activity of a supported catalyst is deeply dependent on the physicochemical properties of the support material that include fabric, size, shape, steric structure, and dispersion of the supported metal. We have developed a chemoselective hydrogenation method using a heterogeneous zero-valent palladium catalyst supported on spherical carbon (Pd/SC) with a large average diameter (0.36 mm). Pd/SC was found to be an efficient catalyst for the hydrogenation of alkyne, alkene, azido, nitro, and aliphatic *O*-*tert*-butyldimethylsilyl (TBS) functionalities without the hydrogenolysis of benzyl ester and ether, nitrile, aromatic ketone, aromatic *O*-TBS, and *N*-carbobenzyloxy (*N*-Cbz) functionalities. The present method is promising as a general, practical, and chemoselective hydrogenation process.

Keywords Pd/SC · Spherical carbon · Chemoselectivity · Hydrogenation · Solvent effect

1 Introduction

Selective transformation methods for specific functional groups among a variety of functionalities using economical and environmentally benign reaction conditions have been the subject of extensive studies in chemistry during the last decades. Chemoselective hydrogenation methods using transition metal catalysts have been extensively studied [1, 2]. Ever since Lindlar introduced a semi-hydrogenation method of alkynes using a calcium carbonate supported palladium catalyst partially deactivated with lead acetate and quinoline [3], suppression of catalyst activity through the use of coordination-induced catalyst poisoning effects using nitrogen- or sulfur-containing substances has received widespread attention [4–7]. Sajiki and

H. Esaki (✉)
Department of Chemistry, Hyogo College of Medicine, 1-1 Mukogawa-Cho, Nishinomiya 663-8501, Hyogo, Japan
e-mail: esaki@hyo-med.ac.jp

K. Tomioka et al. (eds.), *New Horizons of Process Chemistry*,
DOI 10.1007/978-981-10-3421-3_4

co-workers found that the addition of an appropriate catalyst poisons to the hydrogenation system using Pd on activated carbon (Pd/C) selectively suppressed the catalyst activity [8–14]. These results led to the development of novel and commercially available heterogeneous catalysts, which contain a nitrogen or sulfur component as a catalyst poison {e.g., Pd/C–ethylenediamine complex [Pd/C(en) (Wako Co., Ltd.; 169-21443)] [15–23], Pd–polyethyleneimine complex [Pd/PEI (Wako Co., Ltd.; 167-22223) [24], and Pd/C–diphenylsulfide complex [Pd/C(Ph_2S) (N.E. CHEMCAT Co.; SGS-10DR)] [25]}. It is also well known that the properties of supported catalysts are deeply influenced by the fabric, size, shape, and the physicochemical character of the support material, and/or the dispersivity of the supported noble metals [26–32]. A wide variety of substances such as silica [32–36], alumina [32, 37–39], zeolite [40–42], clays [43, 44], resins [45, 46], and organic polymers [47–53] are applicable as catalyst supports. Taking advantage of the properties of the support material, Sajiki and co-workers have also developed Pd supported on fibroin (a protein produced by silkworms) [Pd/Fib (Wako: 163-22183)] [54–56] and molecular sieves (Pd/MS) [57, 58] as chemoselective hydrogenation catalysts. Furthermore, they have focused on boron nitride (BN) as a catalyst support and found that Pd/BN enables the selective semi-hydrogenation of mono- as well as di-substituted alkynes to the corresponding alkenes in the presence of diethylenetriamine [59].

During the screening of new heterogeneous catalysts for chemoselective hydrogenation, we recently found that a zero-valent palladium catalyst supported on spherical carbon (Pd/SC, YMC Co., Ltd.), which had been developed as a catalyst for a continuous-flow hydrogenation reactor, achieved chemoselective hydrogenation without the addition of catalyst poisons [60]. 0.5% Pd/SC is commercially available from YMC Co., Ltd. (Kyoto, Japan), and the Pd species within Pd/SC consists mainly of Pd(0). Furthermore, electron probe microanalysis (EPMA) of 0.5% Pd/SC clarified that the Pd metal is distributed only on the surface of the SC (Fig. 1). Herein, we provide a brief account of Pd/SC-catalyzed chemoselective hydrogenation [60].

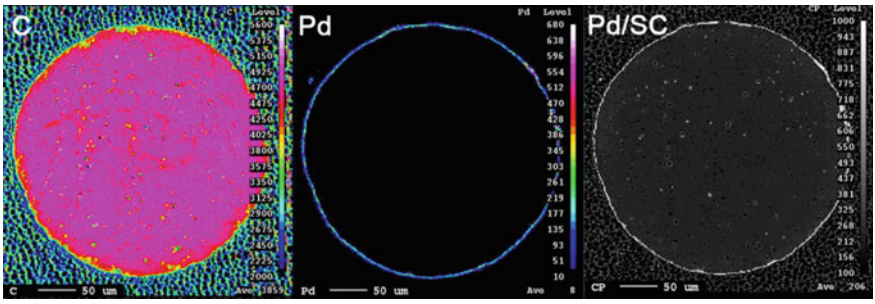

Fig. 1 EPMA images of 0.5% Pd/SC. Reproduced from ref. [60] by permission of John Wiley & Sons Ltd.

2 Results and Discussion

2.1 Catalytic Activity of Pd/SC for Hydrogenation Reactions

0.5% Pd/SC was indicated to have a chemoselective catalyst activity toward the hydrogenation of azido (Table 1, entries 1–3, and 6), nitro (entries 4 and 10), alkene (entries 9, 12, 14–16) and alkyne (entry 13) functionalities, and the desired products were obtained in excellent isolated yields.

Although it is well known that aromatic carbonyls are easily reduced to the corresponding methylene compounds via the intermediary benzyl alcohol under Pd/C-catalyzed hydrogenation conditions, the carbonyl group of benzophenone derivatives were tolerated by 0.5% Pd/SC as a catalyst (entries 5 and 6, hydrogenated products were observed in trace amounts in the case of acetophenone or acetonaphthone derivatives).

Aromatic benzyl ether (entry 7) and benzyl ester (entry 8) functionalities were found to undergo partial hydrogenolysis in methanol, while the benzyl ester functionality was completely tolerated in methanol in the presence of an azido group within the molecule (entry 1). This is probably owing to the catalyst poisonous effect of the liberated amine moiety produced by the rapid hydrogenation of the coexisting azido group.

tert-Butyldimethylsilyl (TBS) ether, one of the most widely used protecting group of hydroxyl groups, is generally removed by fluoride ion or acid treatment. Furthermore, the smooth Pd/C-catalyzed hydrogenolysis of *O*-TBS ethers under neutral conditions has also been reported [21, 61–63]. The TBS groups of aliphatic *O*-TBS ethers were easily cleaved by hydrogenolysis (entries 11 and 12), although the deprotection of aromatic *O*-TBS ethers never proceeded during the chemoselective hydrogenation of a coexisting alkene and nitro group within the molecule (entries 9 and 10).

N-Carbobenzyloxy (*N*-Cbz) protecting group is widely used for the protection of amino groups in organic synthesis because of its easy introduction as well as ease of removal under the mild Pd/C-catalyzed hydrogenolysis conditions. The results in entries 13–15 demonstrate the selective hydrogenation of the alkene and alkyne by the use of 0.5% Pd/SC in the presence of an *N*-Cbz group within the molecule.

Although the hydrodechlorination of 4-chlorobenzoic acid was not observed under the 0.5% Pd/SC-catalyzed conditions (entries 16 and 17), it was difficult to block the partial dechlorination of 4-chloro-2-methyl-1-nitrobenzene (entry 18). This result was presumably caused by the amine moiety derived from the nitro group, which could accelerate the hydrodechlorination as a single electron source [64, 65], since the similar result (partial dechlorination) could be arisen by the addition of triethylamine to the 5% Pd/SC-catalyzed hydrodechlorination of 4-chlorobenzoic acid (entry 19; compared to entry 17). It is interesting to note that the hydrogenolysis of the aromatic bromide is completely chemoselective in the presence of the aromatic carbonyl group by the addition of triethylamine (entry 20).

Table 1 Chemoselective hydrogenations[a] Substrate $\xrightarrow[\text{MeOH, 24 h}]{\text{0.5\% Pd/SC, H}_2\text{ (balloon)}}$ Product

Entry	Substrate	Product	Yield (%)[b]
1	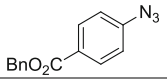	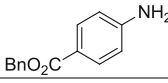	96
2	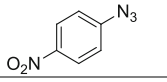	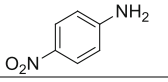	95
3	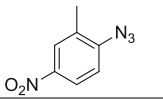	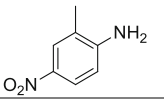	96
4	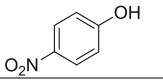	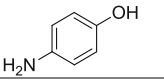	100
5	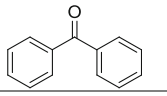	Recovery	96
6	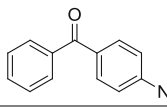	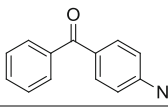	99
7	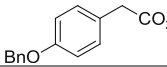	—[c]	–
8	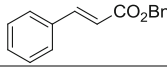	—[d]	–
9[e]	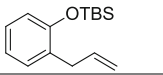	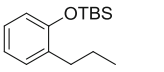	94
10[e]	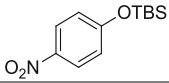	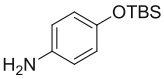	100
11[f]	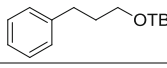	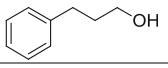	91
12[e]	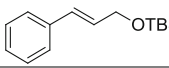	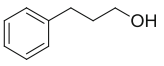	87
13	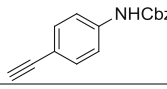	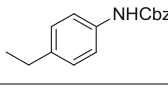	100
14[g]	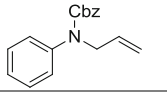	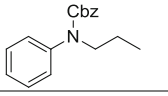	97[h]
15[g]	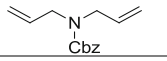	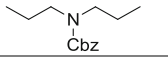	93
16[i]	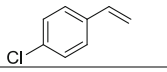	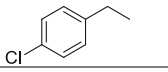	100[j]

(continued)

Table 1 (continued)

Entry	Substrate	Product	Yield (%)[b]
17	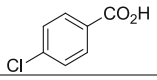	Recovery	95
18	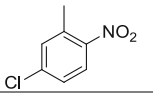	—[k]	–
19[l]	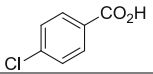	—[m]	–
20[l]	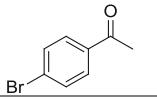	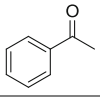	57[n]

[a]Reproduced from ref. [60] by permission of John Wiley & Sons Ltd. Unless otherwise noted, reactions were performed in methanol using 0.5% Pd/SC (0.05 mol% of the substrate) with stirring under ordinary hydrogen pressure and at room temperature for 24 h

[b]Isolated yield

[c]A 92:8 mixture of 4-benzyloxyphenylacetic acid and 4-hydroxyphenylacetic acid was obtained

[d]A complex mixture including benzyl 3-phenylpropionate and 3-phenylpropanoic acid was obtained

[e]The reaction time was 48 h

[f]The reaction time was 72 h

[g]The reaction time was 3 h

[h]A 98:2 mixture of *N*-benzyloxycarbonyl-*N*-propylaniline and *N*-propylaniline was obtained. The yield of the desired product in the mixture was determined by the calculation based on the ^{1}H NMR ratio, total weight of the mixture, and molecular weight of each material

[i]CD_3OD was used as the solvent, owing to the low boiling point of the products

[j]The quantitative formation of 1-chloro-4-ethylbenzene was observed by ^{1}H NMR in CD_3OD after removal of the catalyst

[k]A complex mixture including the substrate, 4-chloro-2-methylaniline, and 2-methylaniline was obtained

[l]Et_3N (1.2 eq. relative to the substrate) was added

[m]A 55:45 mixture of 4-chlorobenzoic acid and benzoic acid was obtained

[n]The low yield is due to the volatile nature

The solvent selection is also an effective way for preventing the undesirous over-hydrogenation. The coordinable ability and polarity of the solvents can drastically alter the catalyst activity. Sajiki and co-workers have reported that the solvents capable of mildly coordinating to the catalyst metal such as THF and 1,4-dioxane, decrease catalyst activity toward hydrogenation [12–15, 18, 20, 22–24, 54–56, 61]. With the expectation of the complete suppression of the hydrogenolysis of the benzyl ether, the hydrogenation of 4-benzyloxyphenylacetic acid was investigated in several solvents (Table 2). Although hydrogenation in methanol resulted in the formation of 8% of 4-hydroxyphenylacetic acid as an over-hydrogenation product together with 92% of unchanged starting material (entry 1, compared to Table 1, entry 7), EtOAc, THF, and acetonitrile indicated comparatively suppressive effects (entries 2–4), the benzyl ether was completely resistant to hydrogenolysis in 1,4-dioxane (entry 5).

Table 2 The solvent effect on the hydrogenolysis[a]

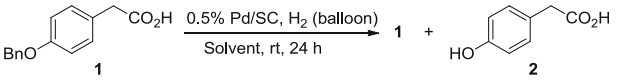

Entry	Solvent	**1**:**2**[b]
1	MeOH	92:8
2	EtOAc	95:5
3	THF	97:3
4	MeCN	97:3
5	1,4-dioxane	100:0

[a]Reproduced from ref. [60] by permission of John Wiley & Sons Ltd.
[b]Determined by ^{1}H NMR spectroscopy

The complete suppression of the hydrogenolysis of aromatic benzyl ether and aromatic carbonyl functionalities could be achieved by the use of 1,4-dioxane as a solvent instead of methanol, while the hydrogenation of olefins proceeded (Table 3, entries 1–3, 7, 8). Furthermore, benzyl esters are also completely tolerated in 1,4-dioxane or acetonitrile as a solvent (entries 2, 4–6, compared to Table 1, entry 8).

A diagrammatic summary of the catalyst activity of 0.5% Pd/SC in comparison with other hydrogenation catalysts developed by Sajiki and co-workers is provided in Fig. 2. Unsaturated C–C bonds, azido, and nitro groups can easily be hydrogenated by the use of 0.5% Pd/SC as a catalyst in the presence of benzyl ethers and esters, nitriles, aromatic ketones, and *N*-Cbz protective groups. The distinctive feature of the 0.5% Pd/SC is its catalyst activity toward the hydrogenolysis of *O*-TBS ethers and aromatic halides and the chemoselective hydrogenation of an azido group in distinction from a nitro group within the molecule (Table 1, entries 2 and 3). When an azido group coexists with a nitro group, only the azido group is expeditiously reduced to the corresponding amine with the nitro group intact on the basis of the suppressive effect of the amine moiety derived from the azide as an appropriate catalyst poison.

2.2 Reuse of Pd/SC

Reusability is one of the most important properties of heterogeneous catalysts from an economical and environmental point of view. 0.5% Pd/SC could be reused a second time without any loss of catalyst activity, although activity significantly decreased after the third run (Table 4).

While the leaching of Pd species from the activated spherical carbon as the catalyst support was carefully investigated to determine the cause of the deterioration in catalyst activity of 0.5% Pd/SC after reuse test (Table 4), no Pd leaching (<1 ppm) was detected by ICP-AES. On the other hand, the SEM image of the catalyst after its second use showed that significant mechanical damage of the

Table 3 Chemoselective hydrogenation[a] Substrate $\xrightarrow[\text{Solvent, rt, 24 h}]{\text{0.5\% Pd/SC, } H_2 \text{ (balloon)}}$ Product

	Entry	Substrate	Solvent	Product
	Yield (%)[b]			
1	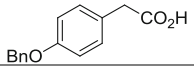	1,4-dioxane	Recovery	100[c]
2	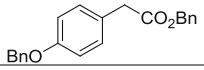	1,4-dioxane	Recovery	93[c]
3	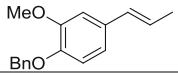	1,4-dioxane	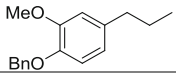	98
4	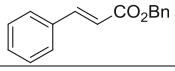	MeCN	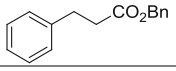	99
5	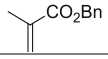	MeCN	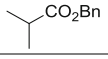	86
6	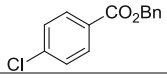	MeCN	Recovery	97[c]
7	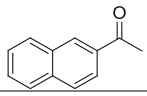	1,4-dioxane	Recovery	97[c]
8	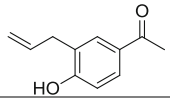	1,4-dioxane	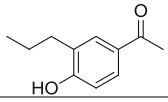	92

[a]Reproduced from ref. [60] by permission of John Wiley & Sons Ltd. Reactions were carried out using 1.0 mmol of substrate and 0.5% Pd/SC (0.05 mol% relative to the substrate) in each solvent (1.0 mL) under ordinary hydrogen pressure and at room temperature for 24 h

[b]Isolated yield

[c]Yield of the recovered starting material

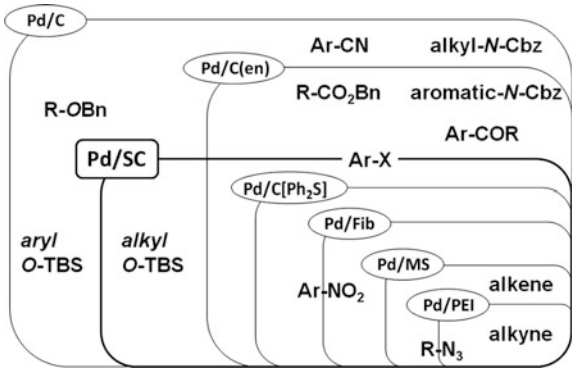

Fig. 2 Comparison of the catalyst activities of various heterogeneous platinum group metal catalysts for chemoselective hydrogenation: functional groups of within each frame are reducible by the captioned catalyst. Reproduced from ref. [60] by permission of John Wiley & Sons Ltd.

Table 4 Reuse of 0.5% Pd/SC[a]

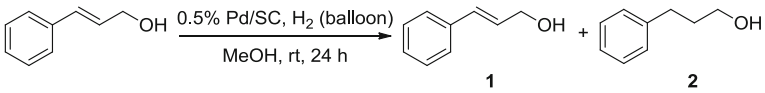

Run	Recovered Pd/SC (%)	**1**:**2**[b]
1st	100	0:100 (92)
2nd	91	0:100 (98)
3rd	99	79:21
4th	95	99:1

[a]Reproduced from ref. [60] by permission of John Wiley & Sons Ltd.
[b]Determined by ^{1}H NMR spectroscopy. Isolated yield is indicated in parentheses

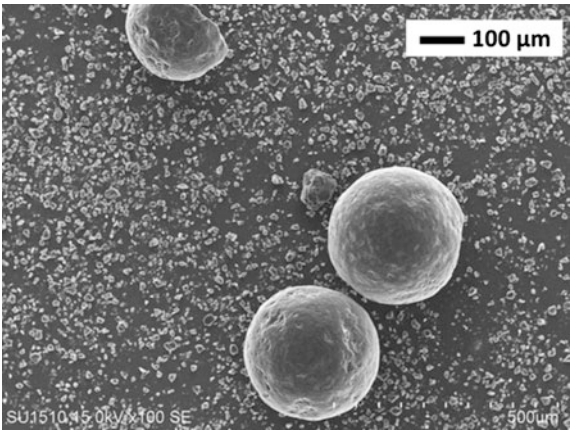

Fig. 3 SEM image of 0.5% Pd/SC after its second use test at 200 magnification

catalyst had occurred, and many small crushed particles were observed (Fig. 3). Consequently, the deterioration of the catalyst activity of 0.5% Pd/SC would be attributed to mechanical damage of the Pd rich surface during vigorous stirring.

3 Conclusions

In conclusion, 0.5% Pd/SC is an excellent chemoselective hydrogenation catalyst for alkyne, alkene, azido, nitro, aromatic bromide, and alkyl *O*-TBS functionalities, leaving nitrile, aromatic chloride, *N*-Cbz, and aryl *O*-TBS functionalities intact. We have also shown that the choice of solvent is important for the suppression of hydrogenation toward benzyl ether and ester, and aromatic ketone functionalities.

The use of 1,4-dioxane or acetonitrile instead of methanol resulted in desired chemoselective hydrogenations. 0.5% Pd/SC is expected to be a practical catalyst for the chemoselective hydrogenation process.

Acknowledgements This work was supported by JSPS KAKENHI Grant Number 24790031 and a Grant-in-Aid for Researchers, Hyogo College of Medicine, 2010. We thank the YMC Co., Ltd., for the kind gift of the catalysts. We also sincerely thank the N.E. CHEMCAT Corporation for the EPMA measurements.

References

1. James RB (1973) Homogeneous Hydrogenation, Wiley, New York.
2. Horváth IT (ed) (2002) Encyclopedia of Chemistry, Wiley, New York.
3. Lindlar, H (1952) Helv Chim Acta 35:446–450.
4. Rylander PN (1985) Hydrogenation methods, Academic Press, New York.
5. Hudlicky M (1996) Reductions in Organic Chemistry, 2nd ed, American Chemical Society, Washington, D.C.
6. Larock RC (1999) Comprehensive Organic Transformations, 2nd ed, Wiley-VCH, New York.
7. Nishimura S (2001) Handbook of Heterogeneous Catalytic Hydrogenation for Organic Synthesis, Wiley-Interscience, New York.
8. Sajiki H (1995) Tetrahedron Lett 36:3465–3468.
9. Sajiki H, Kuno H, Hirota K (1997) Tetrahedron Lett 38:399–402.
10. Sajiki H, Hirota K (1998) Tetrahedron 54:13981–13996.
11. Sajiki H, Kuno H, Hirota K (1998) Tetrahedron Lett 39:7127–7130.
12. Sajiki H, Hirota K (2003) Chem Pharm Bull 51:320–324.
13. Mori A, Miyakawa Y, Ohashi E, Haga T, Maegawa T, Sajiki H (2006) Org Lett 8:3279–3281.
14. Mori A, Mizusaki T, Miyakawa Y, Ohashi E, Haga T, Maegawa T, Monguchi Y, Sajiki H (2006) Tetrahedron 62:11925–11932.
15. Sajiki H, Hattori K, Hirota K (1998) J Org Chem 63:7990–7992.
16. Sajiki H, Hattori K, Hirota K (1998) J Chem Soc, Perkin Trans 1 4043–4044.
17. Sajiki H, Hattori K, Hirota K (1999) Chem Commun 1041–1042.
18. Sajiki H, Hattori K, Hirota K (2000) Chem Eur J 6:2200–2204
19. Hattori K, Sajiki H, Hirota K (2000) Tetrahedron Lett 41:5711–5714.
20. Hattori K, Sajiki H, Hirota K (2000) Tetrahedron 56:8433–8441
21. Hattori K, Sajiki H, Hirota K (2001) Tetrahedron 57:2109–2114.
22. Hattori K, Sajiki H, Hirota K (2001) Tetrahedron 57:4817–4824.
23. Maegawa T, Fujita Y, Sakurai A, Akashi A, Sato M, Oono K, Sajiki H (2007) Chem Pharm Bull 55:837–839.
24. Sajiki H, Mori S, Ohkubo T, Ikawa T, Kume A, Maegawa T, Monguchi Y (2008) Chem Eur J 14:5109–5111.
25. Mori A, Mizusaki T, Kawase M, Maegawa T, Monguchi Y, Takao S, Takagi Y, Sajiki H (2008) Adv Synth Catal 350:406–410.
26. Stiles AB (ed) (1987) Catalyst Supports and Supported Catalysts, Butterworths, Boston.
27. Che M, Bennett CO (1989) Adv Catal 36:55–172.
28. Feldheim DL, Foss CA Jr (2002) Metal Nanoparticles: Synthesis, Characterization, and Application, Marcel Dekker, New York.
29. White RJ, Luque R, Budarin VL, Clark JH, Macquarrie DJ (2009) Chem Soc Rev 38:481–494.
30. Shimizu K, Miyamoto Y, Kawasaki T, Tanji T, Tai Y, Satsuma A (2009) J Phys Chem C 113:17803–17810.
31. Jia CJ, Schüth F (2011) Phys Chem Chem Phys 13:2457–2487.

32. Wang Z, Pokhrel S, Chen M, Hunger M, Mädler L, Huang J (2013) J Catal 302:10–19.
33. Panpranot J, Pattamakomsan K, Goodwin JG Jr, Praserthdam P (2004) Catal Commun 5:583–590.
34. Lee H-Y, Ryu S, Kang H, Jun Y, Cheon J (2006) Chem Commun 1325–1327.
35. Jana S, Dutta B, Bera R, Koner S (2008) Inorg Chem 47:5512–5520.
36. Crudden CM, Sateesh M, Lewis R (2005) J Am Chem Soc 127:10045–10050.
37. Hutchings GJ, King F, Okoye IP, Padley MB, Rochester CH (1994) J Catal 148:464–469.
38. Trueba M, Trasatti SP (2005) Eur J Inorg Chem 3393–3403.
39. McInroy AR, Uhl A, Lear T, Klapötke TM, Shaikhutdinov S, Schauermann S, Rupprechter G, Freund H-J, Lennon D (2011) J Chem Phys 134:214704.
40. Djakovitch L, Koehler K (2001) J Am Chem Soc 123:5990–5999.
41. Okumura K, Nota K, Yoshida K, Niwa M (2005) J Catal 231:245–253.
42. Djakovitch L, Rollet P (2004) Adv Synth Catal 346:1782–1792.
43. Shimizu K, Kan-no T, Kodama T, Hagiwara H, Kitayama Y (2002) Tetrahedron Lett 43:5653–5655.
44. Mas-Marzá E, Segarra AM, Claver C, Peris E, Fernandez E (2003) Tetrahedron Lett 44:6595–6599.
45. Barbaro P, Bianchini C, Giambastiani G, Oberhauser W, Bonzi LM, Rossi F, Dal Santo V (2004) Dalton Trans 1783–1784.
46. Diwakar MM, Deshpande RM, Chaudhari RV (2005) J Mol Catal A Chem 232:179–186.
47. Kobayashi S, Endo M, Nagayama S (1999) J Am Chem Soc 121:11229–11230.
48. Akiyama R, Kobayashi S (2003) J Am Chem Soc 125:3412–3413.
49. Uozumi Y, Nakao R (2003) Angew Chem 115:204–207; Angew Chem Int Ed 42:194–197.
50. Ley SV, Mitchell C, Pears D, Ramarao C, Yu J-Q, Zhou W (2003) Org Lett 5:4665–4668.
51. Corma A, Garcia H, Leyva A (2005) J Mol Catal A Chem 230:97–105.
52. Okamoto K, Akiyama R, Yoshida H, Yoshida T, Kobayashi S (2005) J Am Chem Soc 127:2125–2135.
53. Yamada YMA, Arakawa T, Hocke H, Uozumi Y (2007) Angew Chem 119:718–720; Angew Chem Int Ed 46:704–706.
54. Sajiki H, Ikawa T, Yamada H, Tsubouchi K, Hirota K (2003) Tetrahedron Lett 44:171–174.
55. Sajiki H, Ikawa T, Hirota K (2003) Tetrahedron Lett 44:8437–8439.
56. Ikawa T, Sajiki H, Hirota K (2005) Tetrahedron 61:2217–2231.
57. Maegawa T, Takahashi T, Yoshimura M, Suzuka H, Monguchi Y, Sajiki H (2009) Adv Synth Catal 351:2091–2095.
58. Takahashi T, Yoshimura M, Suzuka H, Maegawa T, Sawama Y, Monguchi Y, Sajiki H (2012) Tetrahedron 68:8293–8299.
59. Yabe Y, Yamada T, Nagata S, Sawama Y, Monguchi Y, Sajiki H (2012) Adv Synth Catal 354:1264–1268.
60. Esaki H, Hattori T, Tsubone A, Mibayashi S, Sakata T, Sawama Y, Monguchi Y, Yasuda H, Nosaka K, Sajiki H (2013) ChemCatChem 5:3629–3635.
61. Sajiki H, Ikawa T, Hattori H, Hirota K (2003) Chem Commun 654–655.
62. Sajiki H, Ikawa T, Hirota K (2003) Tetrahedron Lett 44:7407–7410.
63. Ikawa T, Sajiki H, Hirota K (2004) Tetrahedron 60:6189–6195.
64. Sajiki H, Kume A, Hattori K, Hirota K (2002) Tetrahedron Lett 43:7247–7250.
65. Monguchi Y, Kume A, Hattori K, Maegawa T, Sajiki H (2006) Tetrahedron 62:7926–7933.

Environment-Friendly Iron-Catalyzed Reactions

Yoshinari Sawama

Abstract Aromatics composed of benzene, naphthalene, heteroarene etc., are useful backbones in various scientific fields, such as the pharmaceutical and material chemistries. Iron (Fe) metal is one of the bountiful resources on the earth and iron trichloride ($FeCl_3$) is widely utilized as an inexpensive and commercially available reagent for organic synthesis. Meanwhile, the reactions generating neutral wastes and/or reducing wastes are valuable methods from the viewpoint of green chemistry. We have continuously investigated the $FeCl_3$-catalyzed benzylic activations of various substrates to construct highly-functionalized aromatics. The reactions that only generate water, methanol or silanol derived from substrates as a neutral waste are regarded to be environmentally friendly and green sustainable in comparison with the similar reported reactions, which generate acidic waste and/or require the use of rare metals. In this review, our recent results, related to the chemo-selective transformations and construction of highly-substituted aromatics, etc., are summarized.

Keywords Iron catalyst · Neutral waste · Aromatics · Benzylic activation

From the viewpoint of process chemistry, the synthetic methodologies using inexpensive and easily available catalysts and enabling the reduction of wastes are recognized as green sustainable reactions. Meanwhile, $FeCl_3$ is utilized as a versatile Lewis acid catalyst in many organic reactions. Although the nucleophilic substitutions are also widely adapted to construct highly-functionalized target molecules, the general leaving groups cause the generation of acidic wastes originating from their elimination process. We have recently revealed that $FeCl_3$ could efficiently activate various benzylic carbon (C)-oxygen (O) bonds as a catalyst and highly-substituted aromatic products could be effectively constructed in a regio- and/or chemo-selective manner accompanied by the generation of methanol

Y. Sawama (✉)
Gifu Pharmaceutical University, Gifu, Japan
e-mail: sawama@gifu-pu.ac.jp

K. Tomioka et al. (eds.), *New Horizons of Process Chemistry*,
DOI 10.1007/978-981-10-3421-3_5

(MeOH), silanol (*Si*OH) or water (H_2O) as a nearly neutral waste. These $FeCl_3$-catalyzed environmentally-friendly methods are summarized in this review.

1 Use of Siloxy and Alkoxy Groups as Leaving Groups

Silyl and alkyl ethers are generally utilized as protected alcohols [1]. Therefore, the nucleophilic substitution via the elimination of the corresponding siloxy or alkoxy group has not been reported. Since the nucleophilic substitutions generally require good and well-known leaving groups, such as acetoxy (AcO), tosyloxy (TsO), halogen, etc., accompanied by the formation of acidic wastes by their eliminations, a neutralization process is necessary after the reactions (Fig. 1). Meanwhile, if the silyl and methoxy ethers are utilized in the nucleophilic substitutions, the nearly neutral silanol and methanol are generated as byproducts (Fig. 1). Namely, the corrosion of the reaction apparatus due to the acidic wastes can be suppressed and the neutralization process is avoidable. Furthermore, these methodologies are useful from the viewpoint of the direct transformation of protected substrates resulting in a reduction of the number of synthetic steps.

1.1 Nucleophilic Substitutions of Benzylic Silyl Ethers

1.1.1 Azidation

The secondary benzylic trimethylsilyl (TMS) ether effectively underwent the $FeCl_3$-catalyzed nucleophilic substitution using $TMSN_3$ as a nucleophile at room temperature to produce the corresponding azido product in good yield within a short time (Fig. 2) [2]. Meanwhile, the free alcohol as a substrate was less reactive under the same reaction conditions to form the azido product in low yield and the dimer product as a byproduct in 40% yield (calculated by the consumption of two molecules of substrate), which indicated that this reaction proceed by the

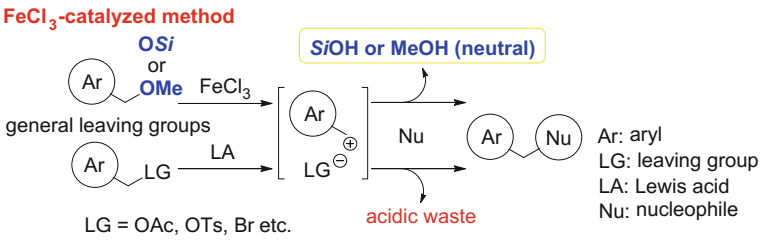

Fig. 1 Concept

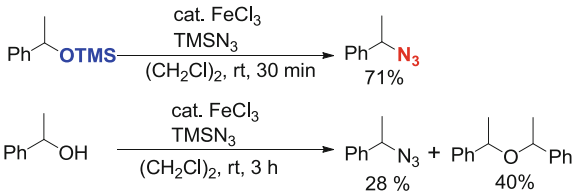

Fig. 2 Azidation of benzylic silyl ether

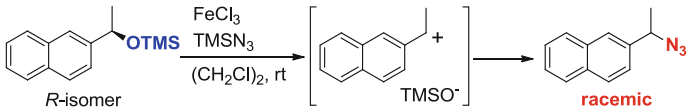

Fig. 3 Mechanistic study

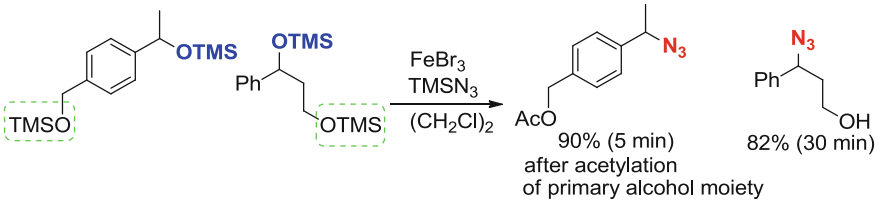

Fig. 4 Chemoselective azidation

elimination of the siloxy group, and the reaction path via the acid-mediated deprotection of the silyl ether to the alcohol may be minor.

Since the *R*-isomer of TMS ether was transformed into the racemic azido product under the $FeCl_3$-catalyzed conditions, the S_N1 reaction via the carbocation intermediate generated by elimination of the siloxy group is considerable in the nucleophilic azidation (Fig. 3).

The $FeCl_3$ (or $FeBr_3$)-catalyzed azidation of silyl ethers can be a powerful tool to transform the secondary and tertiary benzylic alcohols in the presence of other alcoholic hydroxyl groups (Fig. 4). Although the primary TMS ethers were acid labile and deprotection of the TMS group easily occurred during the aqueous work-up, secondary and tertiary aliphatic silyl ethers were also tolerant under the reaction conditions. Because $FeBr_3$ is sometimes more reactive to give the product in higher yield than $FeCl_3$, the chemoselective transformations were carried out using $FeBr_3$ instead of $FeCl_3$. The former product was isolated after acetylation of the resulting primary benzyl alcohol moiety resulting from the deprotection of the primary benzylic TMS ether during the reaction, because the unidentified byproduct was contaminated with primary benzyl alcohol product.

1.1.2 Friedel-Crafts Benzylation

Although the Friedel-Crafts reaction using non-activated arenes is an environment-friendly method to introduce an aromatic moiety, harsh reaction conditions are sometimes required depending on the nucleophilicity grade of the arenes. Actually, the Friedel-Craft benzylation is a valuable method to construct the pharmaceutically-useful biarylmethane skeleton, and heating conditions and/or strong Lewis acids were generally required even with the use of highly-removable leaving groups [3–5]. On the other hand, the $FeCl_3$-catalyzed Friedel-Craft benzylation of silyl ethers could proceed at room temperature for a short time to form various biarylmethane derivatives possessing highly-substituted arenes including the halogen-containing arenes, which are known to be less reactive for the Friedel-Crafts benzylation (Fig. 5) [6].

It is noteworthy that the excess use of the silyl ether towards an arene directly provided a bis-benzylated arene derivative by the double Friedel-Craft benzylation (Fig. 6). The related compounds can be the core of dendoritic molecules [7] and the previous method based on the Friedel-Crafts benzylation cannot be applied to synthesize the bis-benzylated arenes.

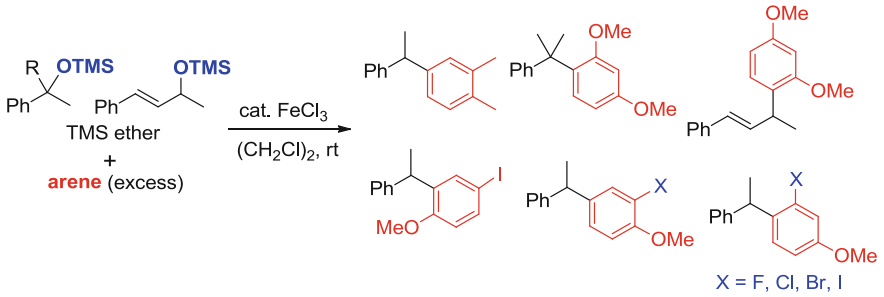

Fig. 5 Friedel-Crafts benzylation of silyl ethers

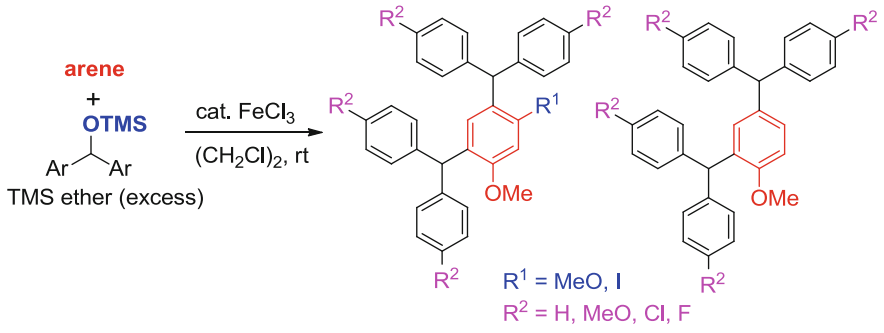

Fig. 6 Double Friedel-Crafts benzylation

1.2 *Site-Selective Nucleophilic Substitution of Secondary/Tertiary Benzylic Methyl or Benzyl Ethers*

Although methyl ethers are also utilized as stable protected alcohols, strong acidic conditions are required for deprotection of the mother alcohols. Therefore, the direct transformation of methyl ethers is useful due to avoiding the deprotection process. The secondary and tertiary benzylic methyl ethers were efficiently converted to the corresponding azido derivatives in the presence of the catalytic $FeCl_3$ and $TMSN_3$ at room temperature (Fig. 7) just like the reaction of silyl ethers (Sect. 1.1) [8]. Additionally, the azidation of the allyl and propargyl alcohol methyl ethers possessing a conjugated phenyl group also sufficiently occurred.

The chemo-selective elimination was perfectly accomplished by the use of unsymmetric dibenzyl ethers possessing secondary and primary benzylic moieties (Fig. 8). In the presence of the catalytic $FeCl_3$, the more stable secondary carbocation intermediate was generated in a perfect chemo-selective manner. Therefore, the $FeCl_3$-catalyzed azidation efficiently proceeded at the secondary benzylic positions, while the primary benzylic and aliphatic benzyl ether moieties in the same molecule remained completely unchanged (Fig. 9).

Other nucleophiles, such as allylTMS, TMSCN and TMS phenylacetylene, were also applied in the $FeCl_3$-catalyzed transformation of methyl and benzyl ethers to form the corresponding products (Fig. 10) [8].

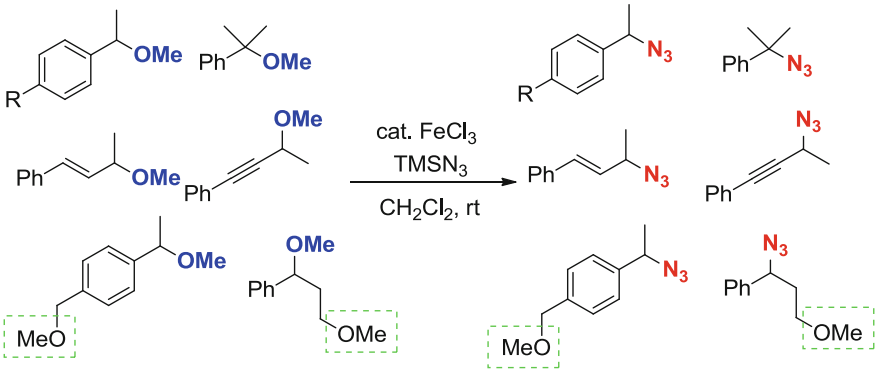

Fig. 7 Azidation of benzylic methyl ethers

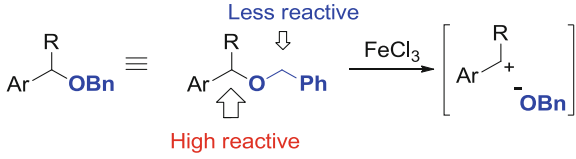

Fig. 8 Comparison of reactivities

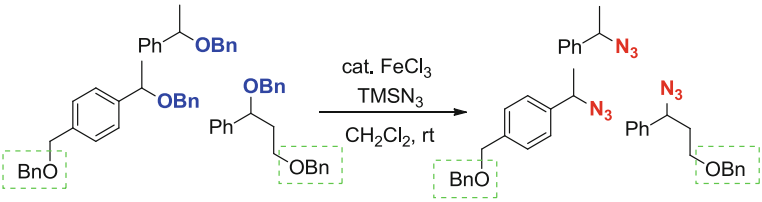

Fig. 9 Chemoselective azidation of benzylic ethers

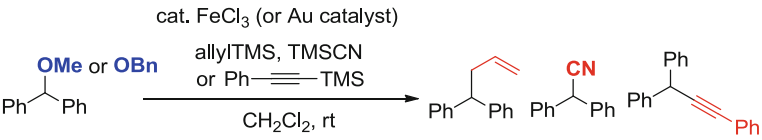

Fig. 10 Application using other nucleophiles

1.3 Deprotection of Methoxyphenylmethyl Type-Protected Alcohols and Carboxylic Acids

Although the primary benzylic position is obviously less reactive (Sects. 1.1 and 1.2), the introduction of an electron-donating methoxy (MeO) group on the benzene ring of the primary benzyl ether can facilitate the generation of the cation intermediate by cleavage of the benzylic C–O bond. Namely, a 4-methoxyphenylmethyl (MPM)-protected alcohol (4-methoxybenzyl alkyl ether) could be effectively deprotected into the mother alcohol (Fig. 11, top) [9]. The 4-MPM-protected alcohols are generally deprotected by the use of stoichiometric oxidants, such as ceric ammonium nitrate (CAN) and 2,3-dichloro-5,6-dicyano-*p*-benzoquinone (DDQ), or nucleophiles in the presence of catalytic Lewis acids, and the wastes derived from the stoichiometric reagents should be removed by purification using silica-gel column chromatography [2]. Meanwhile, the $FeCl_3$-catalyzed deprotection could proceed without any additional nucleophiles by the self-cleaving

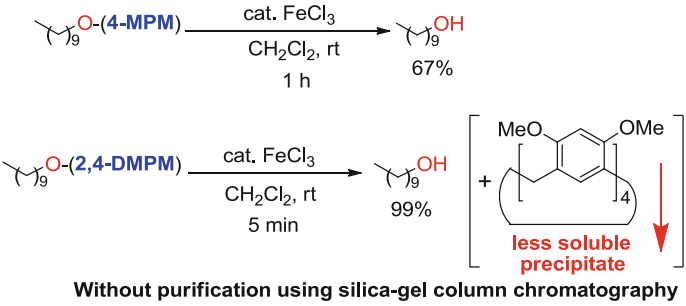

Fig. 11 Iron-catalyzed deprotection of MPM type-protected alcohols

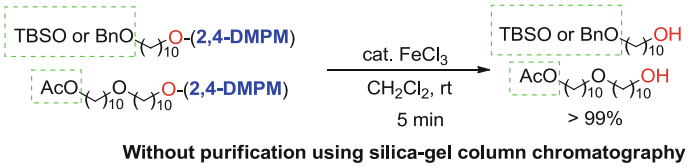

Fig. 12 Mild deprotection of 2,4-DMPM-protected alcohols

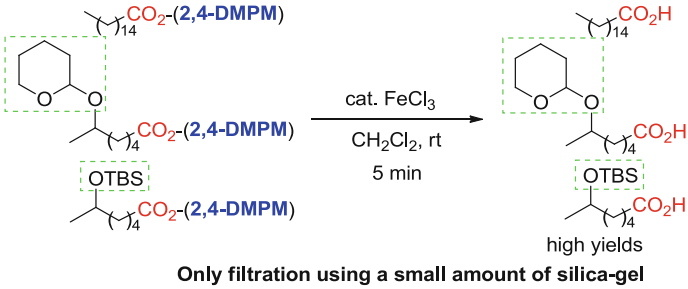

Fig. 13 Deprotection of 2,4-DMPM-protected carboxylic acids

mechanism, in which the electron-rich benzene ring of the 4-MPM group could work as an embedded nucleophile. It is noteworthy that the deprotection of a 2,4-dimethoxyphenylmethyl (DMPM)-protected alcohol was also catalyzed by $FeCl_3$ to give the deprotected alcohol accompanied by the generation of resorcin[4]arene octamethyl ether as a hardly-soluble precipitate, which was easily removed by simple filtration (Fig. 11, bottom). The $FeCl_3$-catalyzed deprotection method using 2,4-DMPM as a protecting group is green sustainable without purification using silica-gel column chromatography [9, 10].

tert-Butyldimethylsilyl (TBS) ether, benzyl ether, acetoxy group, etc., could be tolerant under the $FeCl_3$-catalyzed deprotection conditions of 2,4-DMPM-protected alcohols, and the corresponding mother alcohols were obtained in excellent yields within 5 min without silica-gel column chromatography (Fig. 12) [9, 10].

Furthermore, the 2,4-DMPM-protected carboxylic acids were also sufficiently deprotected in the presence of the catalytic $FeCl_3$ to give the corresponding mother carboxylic acids in high yields. The resulting reaction mixtures were directly filtered through a small amount of silica-gel to provide high purity carboxylic acids (Fig. 13) [10].

2 Ring-Opening Substitutions

Aromatic (Ar)-Ar linked compounds, such as biaryls, etc., are well-known to be important backbones in the material and pharmaceutical sciences. Although the transition metal-catalyzed cross coupling reactions of two different preliminarily

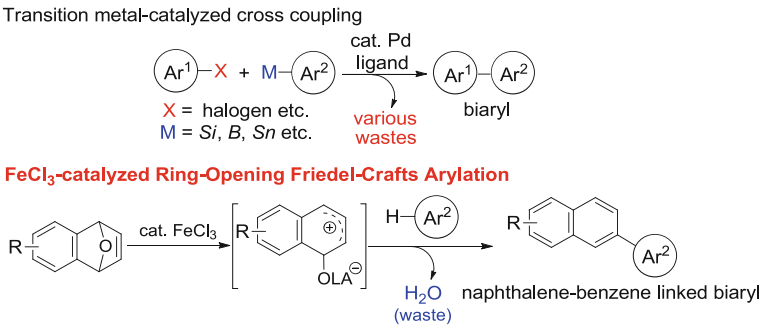

Fig. 14 Ring-opening arylation

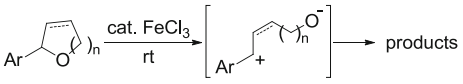

Fig. 15 Iron-catalyzed ring-opening of cyclic ether derivatives

substituted arenes are powerful tools to construct a variety of biaryl products, a large quantity of waste derived from the substrates and ligands are still problematic issues (Fig. 14, top). Biaryls possessing a naphthalene core are also useful compounds in various fields, and we designed environment-friendly construction methods of naphthalene-arene from the 1,4-epoxy-1,4-dihydronaphthalenes, which are easily prepared by the cycloaddition between benzynes and furans (Fig. 14, bottom). Biaryl derivatives can be obtained by traping of the corresponding cation intermediate generated by the $FeCl_3$-catalyzed cleavage of the benzylic C–O bond of the 1,4-epoxy moiety with arene nucleophiles. During the reaction, H_2O should be the only generated waste.

We have previously revealed that $FeCl_3$ effectively activated the benzylic positions of 2-aryl-dihydrofuran and tetrahydrofuran to generate the corresponding zwitterionic intermediates, which could be trapped with various nucleophiles (Fig. 15) [11, 12]. We planned that these discoveries would be applied to the ring-opening functionalizations of the 1,4-epoxy-1,4-dihydronaphthalenes.

Since the zwitterionic intermediates derived from the 1,4-epoxy-1,4-dihydronaphthalenes were short-lived, the electron-donating substituents (R^1 and R^2) on both bridge-heads were necessary to adequately stabilize the intermediates and provide enough time for the introduction of the arene nucleophiles (Fig. 16) [13]. Various arenes including heteroarenes (e.g., benzofuran, pyrrole, indole, etc.) could be adapted to form the corresponding biaryls. Especially, sulfur-containing heteroarenes (e.g., thiophene, thieno[3,2-*b*]thiophene, 2,2′:5,2″-terthiophene, etc.) were highly reactive to produce the binaphthyl thiophene derivatives. Allylic, cyano and azido groups were also introduced to give the corresponding naphthalene or 1,2-dihydronaphthalene derivatives [14, 15].

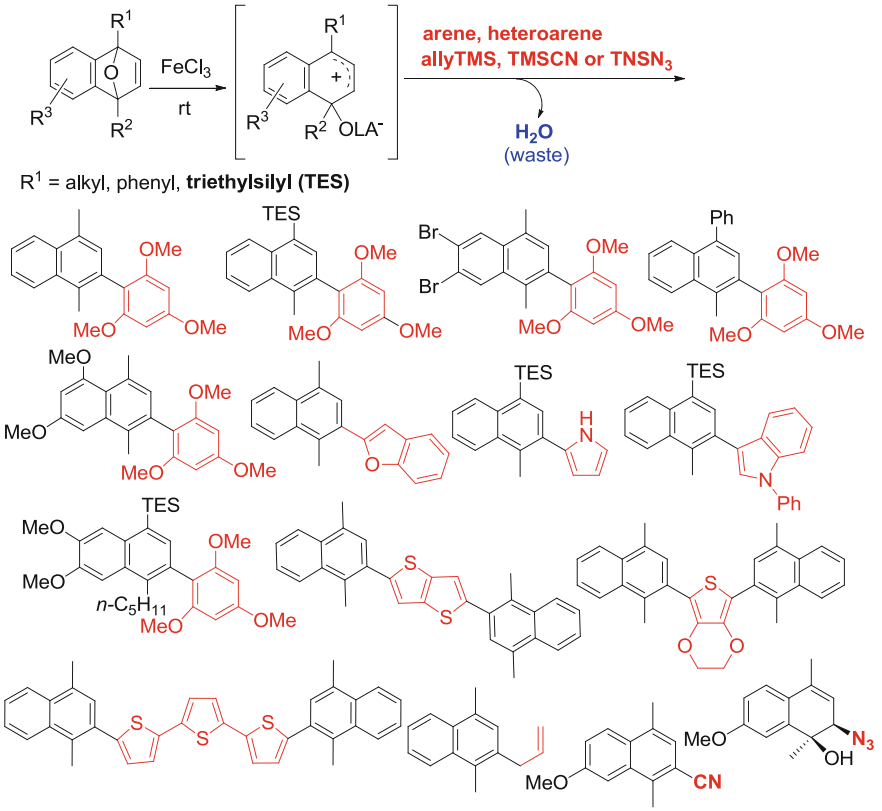

Fig. 16 Iron-catalyzed ring-opening functionalizations of 1,4-epoxy-1,4-dihydronaphthalenes

3 Application of Ring-Opening Reaction and Elimination of Siloxy Group to Form Naphthoquinone Methides

Quinone methides (QMs) are reactive intermediates and typically prepared from phenol derivatives bearing an activated benzylic carbon [16]. The introduction of easily-removable leaving groups, such as AcO, TsO, halogen, etc., producing acidic wastes are necessary on the benzylic carbon (Fig. 17, top). On the other hand, the 1-siloxymethyl-1,4-epoxy-1,4-dihydronaphthalenes, prepared by the Diels-Alder reaction of the corresponding benzynes and furans, were efficiently transformed in the presence of $FeCl_3$ into naphthoquinone methide (NQM) intermediates via a tandem reaction mechanism accompanied by the elimination of a silanol (Fig. 17, bottom; Fig. 18) [17, 18].

The substituents (R) on the bridge-head carbon strongly influence the structure of NQM [*ortho*-NQM (**A**) or *para*-NQM (**B**)] (Fig. 18). In the case of the 4-alkyl or silyl-1-siloxymethyl-1,4-epoxy-1,4-dihydronaphthalene, the benzylic C–O bond is

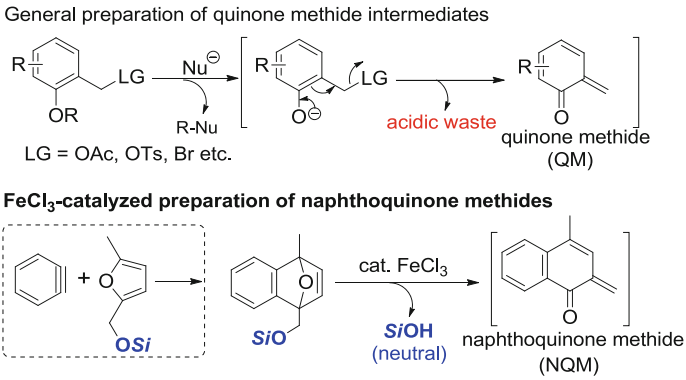

Fig. 17 Preparation of quinone methides

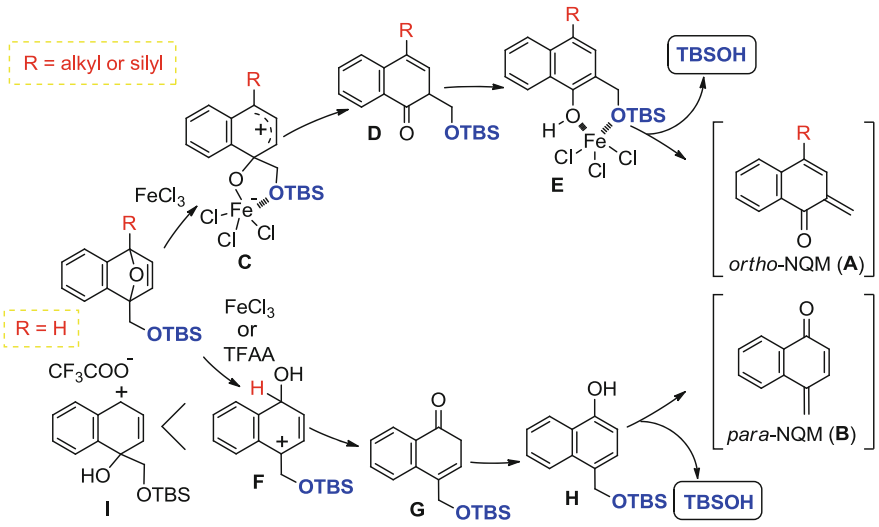

Fig. 18 Selective constructions of *ortho*- or *para*-naphthoquinone methides

regio-selectively cleaved by the coordination control between the iron metal and two oxygen atoms to form the zwitterionic intermediate (**C**). The subsequent rearrangement of the siloxymethyl group and aromatization produce the intermediate **E**. The elimination of the siloxy group then furnishes the *ortho*-NQM (**A**) [17]. Alternatively, 1-siloxymethyl-1,4-epoxy-1,4-dihydronaphthalene (R=H) possessing only a hydrogen substituent on the bridge-head carbon is completely converted into the *para*-NQM (**B**). The more stable tertiary carbocation intermediate (**F**) is generated by the regio-selective cleavage of the benzylic C–O bond, and the following hydride shift and aromatization provide the 4-siloxylmethyl-1-naphthol (**H**), which is transformed into the *para*-NQM (**B**) accompanied by the elimination of silanol [18].

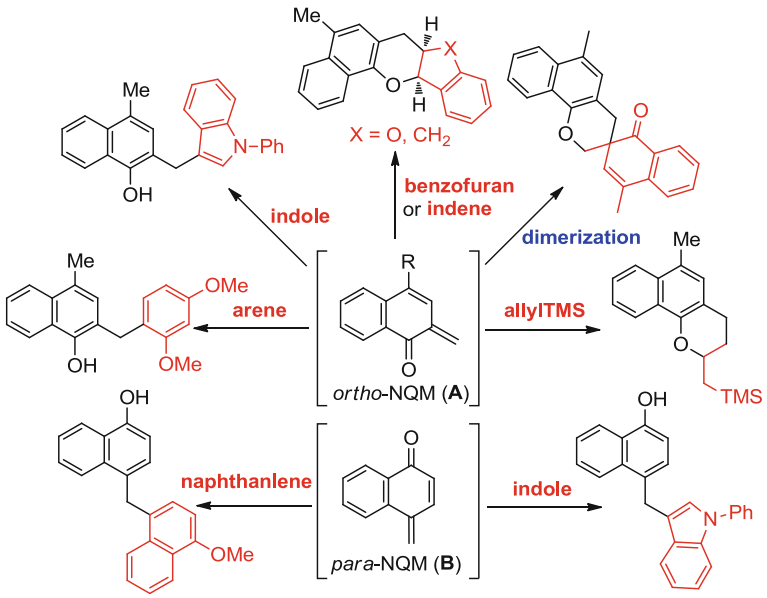

Fig. 19 Various transformation of naphthoquinone methides

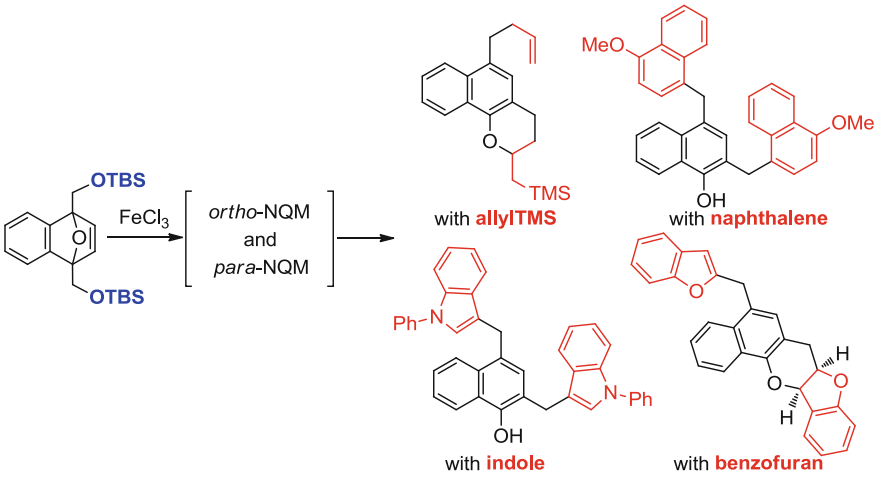

Fig. 20 Double functionalizations via *ortho*- and *para*-naphthoquinone methides

The obtained *ortho*-NQM (**A**) and *para*-NQM (**B**) were sufficiently transformed into a wide variety of materially useful basic skeletons (Fig. 19). Arene nucleophiles, such as the electron-rich benzene, naphthalene, indole derivatives, etc., were efficiently reacted with **A** and **B** to form various biarylmethane derivatives (Fig. 19) [17, 18]. Meanwhile, allylTMS, benzofuran or indene assumed the role of

a dienophile to promote the annulation with **A** and produce fused and complicated heterocycles.

Furthermore, 1,4-disiloxymethyl-1,4-epoxy-1,4-dihydronaphthalene was effectively transformed into the highly-functionalized naphthalene derivatives via both the *ortho*- and *para*-NQM intermediates (Fig. 20) [17, 18].

In summary, we have developed a variety of $FeCl_3$-catalyzed environment-friendly methods accompanied with the generation of H_2O, methanol (alcohol) or silanol as a nearly neutral waste. These regio- and chemo-selective reactions could easily supply highly-functionalized and materially useful aromatic compounds. We eagerly expect that our developed methods will be able to contribute to many scientific fields.

References

1. Wuts P. G. M.; Greene T. W., "*Greene's Protective Groups in Organic Synthesis*", 5th Edition, Wiley, Hoboken, (2007).
2. Sawama, Y.; Nagata, S.; Yabe, Y.; Morita, K.; Monguchi, Y.; Sajiki, H., "*Iron-Catalyzed Chemoselective Azidation of Benzylic Silyl Ethers*", Chem. Eur. J. (2012) **18**, 16608–16611.
3. Niggemann, M.; Meel, M. J., "*Calcium-Catalyzed Friedel–Crafts Alkylation at Room Temperature*", Angew. Chem. Int. Ed. (2010) **49**, 3684–3687.
4. Iovel, I.; Mertins, K.; Kischel, J.; Zapf, A.; Beller, M., "*An Efficient and General Iron-Catalyzed Arylation of Benzyl Alcohols and Benzyl Carboxylates*", Angew. Chem. Int. Ed. (2005) **44**, 3913–3917.
5. Schäfer, G.; Bode, J. W., "Friedel–Crafts Benzylation of Activated and Deactivated Arenes", Angew. Chem. Int. Ed. (2011) **50**, 10913–10916.
6. Sawama, Y.; Shishido, Y.; Kawajiri, T.; Goto, R.; Monguchi, Y.; Sajiki, H., "*Iron-Catalyzed Friedel-Crafts Benzylation with Benzyl TMS Ethers at Room Temperature*", Chem. Eur. J. (2014) **20**, 510–516.
7. Nokami, T.; Ohata, K.; Inoue, M.; Tsuyama, H.; Shibuya, A.; Soga, K.; Okajima, M.; Suga, S.; Yoshida, J., "*Iterative Molecular Assembly Based on the Cation-Pool Method. Convergent Synthesis of Dendritic Molecules*", J. Am. Chem. Soc. (2008) **130**, 10864–10865.
8. Sawama, Y.; Goto, R.; Nagata, S.; Shishido, Y.; Monguchi, Y.; Sajiki, H., "*Chemoselective and Direct Functionalization of Methyl Benzyl Ethers and Unsymmetrical Dibenzyl Ethers by Using Iron Trichloride*", Chem. Eur. J. (2014) **20**, 2631–2636.
9. Sawama, Y.; Masuda, M.; Asai, S.; Goto, R.; Nagata, S.; Nishimura, S.; Monguchi, Y.: Sajiki, H., "*$FeCl_3$-Catalyzed Self-Cleaving Deprotection of Methoxyphenylmethyl-Protected Alcohols*", Org. Lett. (2015) **17**, 434–437.
10. Sawama, Y.; Masuda, M.; Honda, A.; Yokoyama, H.; Park, K.; Yasukawa, N.; Monguchi, Y.; Sajiki, H., "*Additional Nucleophile-Free $FeCl_3$-Catalyzed Green Deprotection of 2,4-Dimethoxyphenylmethyl-Protected Alcohols and Carboxylic acids*", Chem. Pharm. Bull. (2016) **64**, 778–784.
11. Sawama, Y.; Sawama, Y.; Krause, N., "*Highly Regioselective Gold-Catalyzed Ring-Opening Allylation and Azidation of Dihydrofurans*", Org. Lett. (2009) **11**, 5034–5037.
12. Sawama, Y.; Shibata, K.; Sawama, Y.; Takubo, M.; Monguchi, Y.; Krause, N.; Sajiki, H., "*Iron-Catalyzed Ring-Opening Azidation and Allylation of O-Heterocycles*", Org. Lett. (2013) **15**, 5282–5285.

13. Sawama, Y.; Asai, S.; Kawajiri, T.; Monguchi, Y.; Sajiki, H., "*Biaryl Synthesis by Ring-Opening Friedel-Crafts Arylation of 1,4-Epoxy-1,4-dihydronaphthalenes Catalyzed by Iron Trichloride*", Chem. Eur. J. (2015) **21**, 2222–2229.
14. Sawama, Y.; Kawamoto, K.; Satake, H.; Krause, N.; Kita, Y., "*Regioselective Gold-Catalyzed Allylative Ring-Opening of 1,4-Epoxy-1,4-dihydronaphthalenes*", Synlett (2010) **14**, 2151–2155.
15. Sawama, Y.; Ogata, Y.; Kawamoto, K.; Satake, H.; Shibata, K.; Monguchi, Y.; Sajiki, H.; Kita, Y., "*Lewis Acid-Catalyzed Ring-Opening Functionalizations of 1,4-Epoxy-1,4-dihydronaphthalenes*", Adv. Synth. Catal. (2013) **355**, 517–528.
16. Rokita, S. E., "*Quinone Methides*", Vol. 1, John Wiley & Sons Ltd, New Jersey, (2009).
17. Sawama, Y.; Shishido, Y.; Yanase, T.; Kawamoto, K.; Goto, R.; Monguchi, Y.; Sajiki, H., "*Efficient Generation of ortho-Naphthoquinone Methides from 1,4-Epoxy-1,4-dihydronaphthalenes and Their Annulation with Allyl Silanes*", Angew. Chem. Int. Ed. (2013) **52**, 1515–1519.
18. Sawama, Y.; Kawajiri, T.; Asai, S.; Yasukawa, N.; Shishido, Y.; Monguchi, Y.; Sajiki, H., "*Biarylmethane and Fused Heterocyclic Arene Synthesis via in situ Generated o- and/or p-Naphthoquinone Methides*", J. Org. Chem. (2015) **80**, 5556–5565.

Tetranuclear Zinc Cluster-Catalyzed Transesterification

Takashi Ohshima

Abstract Our studies on tetranuclear zinc cluster-catalyzed environmentally friendly transesterification are presented here. The newly developed μ-oxo-tetranuclear zinc cluster is a highly efficient catalyst for the transesterification of various methyl esters including α-amino esters, β-keto esters, and even highly unstable α,β-unsaturated esters; for the acetylation of alcohols in EtOAc; and for the deacylation of esters in MeOH. A unique hydroxy group-selective acylation in the presence of inherently much more nucleophilic amino groups was also achieved by this zinc cluster. Zinc cluster-catalyzed transesterification was drastically accelerated by the addition of alkyl amine and *N*-heteroaromatic ligands, which coordinate with the metals, stabilize the clusters with lower nuclearities, and enhance catalytic activity for the transesterification. Based on our mechanistic studies, the deprotonation of nucleophiles was the most important step in this process, not only for achieving high catalytic activity but also for determining chemoselectivity. In addition, we also developed the second generation zinc catalyst: bis(imidazole)/zinc complexes and the third generation zinc catalyst: heterogeneous zinc/imidazole catalyst, enabling the recovery of the catalyst through simple filtration with the same or higher catalytic activity.

Keywords Chemoselectivity · Cooperative mechanism · Atom economy · E-factor · Recycle · Heterogeneous catalyst

1 Introduction

Increasing the supply of scarce or inaccessible natural products is essential for the production of more sophisticated pharmaceutical agents and biological tools. Therefore, the development of catalyst-promoted atom-economical [1] and envi-

T. Ohshima (✉)
Graduate School of Pharmaceutical Sciences, Kyushu University, 3-1-1 Maidashi, Higashi-ku, Fukuoka 812-8582, Japan
e-mail: ohshima@phar.kyushu-u.ac.jp

K. Tomioka et al. (eds.), *New Horizons of Process Chemistry*,
DOI 10.1007/978-981-10-3421-3_6

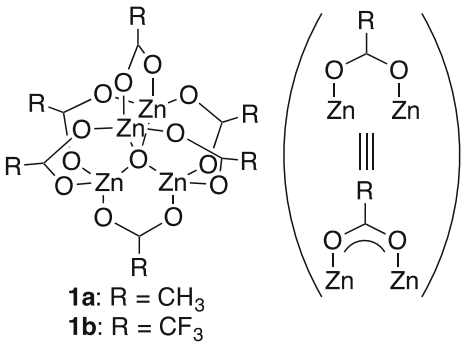

Fig. 1 The Structures of μ_4-oxo-tetranuclear zinc cluster: $Zn_4(OCOR)_6O$ (**1**)

ronmentally benign processes is in high demand [2, 3]. Among these processes, ester bond formation is a fundamental and well-studied methodology because it is a ubiquitous chemical bond, abundant in both natural and synthetic organic compounds [4–7]. Ester synthesis is commonly performed in synthetic organic chemistry using carboxylic acid with alcohol under stoichiometric amounts of condensation reagent, or by treatment with a highly reactive acylating reagent. An attractive alternative method of ester synthesis is transesterification promoted by a catalytic amount of metal reagent [8–11]. This process generates only nontoxic lower alcohols, and can be performed under almost neutral conditions, allowing for high functional group compatibility. Furthermore, ease of handling, as well as high solubility of the esters in most organic solvents compared with the corresponding carboxylic acids, makes them advantageous as a starting material. Several metal-catalyzed transesterification reactions have recently been reported [12–27]. Most of these methods, however, require the use of toxic metal salts or tediously strict reaction conditions. In addition, the application of sterically demanding alcohols to catalytic transesterification remains difficult. Therefore, the development of highly active nontoxic metal-catalyzed transesterification reactions is highly desirable for practical utility. Recently, we developed a μ-oxo-tetranuclear zinc cluster, $Zn_4(OCOCF_3)_6O$ (**1b**), which efficiently catalyzed the transesterification of various methyl esters under mild conditions, and exhibited high tolerance for various functional groups (Fig. 1) [28–43]. This review presents our studies on tetranuclear zinc cluster-catalyzed environmentally friendly reactions, including the unprecedented *O*-selective acylation of aminoalcohols, and further development of more reactive and recyclable zinc catalysts.

2 Tetranuclear Zinc Cluster

An acetate-bridged tetranuclear zinc cluster $Zn_4(OCOCH_3)_6O$ (**1a**) was first synthesized by Auger and Robin in 1924, [44] and its μ-oxo structure was later determined by X-ray crystallographic analysis [45, 46]. Other tetranuclear zinc

clusters with different carboxylate ligands (R = Et, *n*-Pr, *t*-Bu, Ph, etc.) were subsequently prepared using similar pyrolytic methods [47–51]. Although these zinc clusters were inefficient catalysts in almost all the reactions we examined, during our studies on catalytic oxazoline formation, we found that trifluoroacetate-bridged tetranuclear zinc cluster $Zn_4(OCOCF_3)_6O$ (**1b**) dramatically improved the catalytic activity [28]. We synthesized **1b** as white solid in good yield by pyrolysis of the corresponding zinc carboxylates and purification by vacuum distillation (<0.02 mmHg). These preparation methods can be performed in gram-scale. Later, we aimed to develop a practical large scale synthesis of **1b**, and we revealed that construction of the μ_4-oxo tetranuclear zinc trifluoroacetate motif proceeded smoothly even at 110 °C. Heating zinc trifluoroacetate hydrate **2b** under toluene reflux conditions, and simple filtration of the resulting precipitates, afforded a white solid, which was a mixture of trifluoroacetate-bridged tetranuclear zinc cluster **1b** and its TFA adduct $Zn_4(OCOCF_3)_6O{\cdot}CF_3CO_2H$ [35]. The catalytic activity and functional group tolerance of the TFA adduct in transesterification and oxazoline formation were almost identical to those of **1b**. Currently, the TFA adduct is commercially available under the name of ZnTAC24™, and more than 200 kg of ZnTAC24™ have been produced to date.

3 Transesterification

3.1 Introduction

Transesterification is an equilibrium reaction, therefore, it is difficult to attain high conversions. The following methods have been used to force the reaction toward the product side: (i) the use of excess amounts of either of the reactants, (ii) the use of an enol ester as a reactant, and (iii) the removal of the resulting lower alcohol by molecular sieves or continuous distillation. The last approach is the most ideal method, and several catalytic transesterifications at high temperature using esters of lower alcohols were developed [8–11]. There is great demand, however, for the development of a versatile transesterification under mild and harmless conditions to produce highly functionalized compounds such as pharmaceutical agents.

3.2 Scope and Limitations

Using zinc cluster **1b** as a catalyst, we first examined various reaction conditions, including solvent effects and reaction temperature, and finally, we decided to use diisopropyl ether (bp = 68 °C) reflux conditions as the optimal conditions in terms of mildness and functional compatibility [52]. Then, the scope and limitations of alcohols **3a–i** were examined (Table 1) [30]. Transesterification with a variety of

primary and secondary aliphatic alcohols **3a–i**, including benzylic alcohols and allylic alcohols, was efficiently catalyzed by **1b** to afford the corresponding esters **4** in high yield (up to 99% yield). We also estimated the substrate generality of the ester component (Table 2) [30]. Aromatic esters with various substituents at the para position were converted to the corresponding butyl esters **4** in good to excellent yield (Entries 1–7). Due to the large reactivity difference between aliphatic and aromatic alcohols, the reaction of 4-hydroxybenzoate **2g** provided the corresponding product **4gb** in good yield without the formations of a phenol ester (Entry 6). Because the reaction conditions are almost neutral, various functional groups, including acid sensitive TBDMS (Table 1, Entry 5) and tetrahydropyranyl ethers (Table 2, Entry 10), were compatible under the catalytic conditions.

α-Amino esters are widely present in natural and unnatural bioactive compounds, and play an important role in the development of pharmaceuticals. Therefore, the transesterification of α-amino acid esters with a broader scope of *N*-protective groups (Cbz, Boc, Fmoc, Ns, Bz, Pht, etc.) and side chains were investigated [30, 36]. Transesterification of the methyl esters of alanine (**5b**), leucine (**5e**), and phenylalanine (**5f**) proceeded smoothly to give the corresponding butyl esters in high yield (Table 3, Entries 1, 4, and 5). In contrast, the reaction rates of methyl esters of valine (**5c**) and isoleucine (**5d**), both of which have congested secondary aliphatic side chains, were retarded, and the transformations were suppressed, resulting in rather low yields (Entries 2 and 3). These reactions were later

Table 1 Transesterification of various alcohols

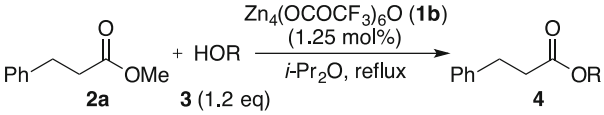

Entry	Alcohol (HOR)	Time (h)	Yield (%)
1	**3a**: HOBn	18	79 (**4aa**)
2	**3b**: $HO(CH_2)_3CH_3$	18	92 (**4ab**)
3	**3c**: $HO(CH_2)_5CH_3$	24	94 (**4ac**)
4	**3d**: $HO(CH_2)_{17}CH_3$	18	99 (**4ad**)
5	**3e**: 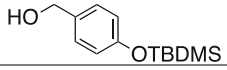	24	92 (**4ae**)
6	**3f**: 	40	76 (**4af**)
7	**3g**: 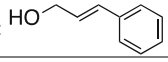	40	91 (**4ag**)
8	**3h**: 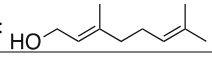	40	91 (**4ah**)
9	**3i**: 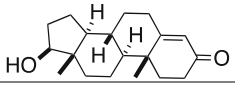	40	96 (**4ai**)

Table 2 Transesterification of various methyl ester

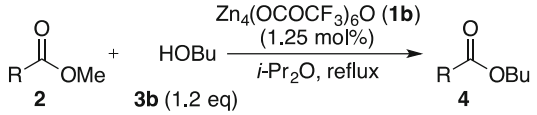

Entry	Ester (RCO_2Me)		Time (h)	Yield (%)
1	**2b**: R′ = H	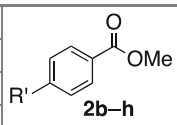	40	96 (**4bb**)
2	**2c**: R′ = Cl		24	91 (**4cb**)
3	**2d**: R′ = Br		40	90 (**4db**)
4	**2e**: R′ = CN		24	77 (**4eb**)
5	**2f**: R′ = NO_2		40	>99 (**4fb**)
6	**2g**: R′ = OH		40	76 (**4gb**)
7	**2h**: 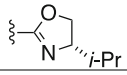		44	93 (**4hb**)
8	**2i**: 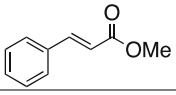		24	86 (**4ib**)
9	**2j**: $CH_3(CH_2)_{16}CO_2Me$		24	92 (**4jb**)
10	**2k**: $THPO(CH_2)_9CO_2Me$		44	87 (**4kb**)
11	**2l**: *c*-Hex-CO_2Me		40	97 (**4lb**)
12	**2m**: 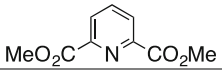		40	>99 (**4mb**)
13	**2n**: 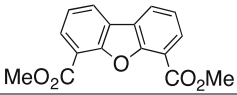		40	97 (**4nb**)

improved by the addition of DMAP (vide infra). This catalyst system was applied to the transesterification of other *N*-Cbz-protected amino acid methyl esters bearing an additional protective group, such as MOM ether (**5i**) (Entry 8), thioether (**5j** and **5k**) (Entries 9 and 10), a trityl group on imidazole (**5o**) (Entry 14), and those with different functionalities such as cyano (**5m**) (Entry 12) and indole (**5n**) (Entry 13) groups. Phenylglycine derivatives are racemized much more easily than any natural amino acid esters in peptide coupling reactions conducted under basic conditions because of the higher acidity of the proton at the benzylic chiral center. Zinc catalyst **1b** was advantageous in that no racemization was observed for the smooth transesterification of *N*-Cbz-protected phenylglycine methyl ester **5q** with **3b** to give **6qb** (Entry 16). The reactions of dipeptides also proceeded in good yield with no epimerization of the stereocenters (Entries 17 and 18).

β-Keto esters are highly useful for various transformations, such as condensation reactions and alkylation, because of their electrophilic and nucleophilic nature; they are thus used as organic building blocks for the synthesis of complex bioactive

Table 3 Transesterification of various *N*-protected α-amino esters

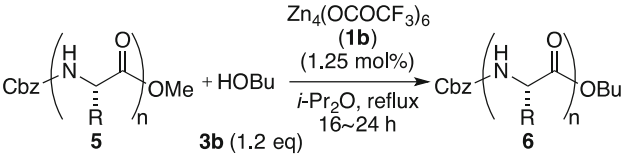

Entry	Ester	Yield (%)	Entry	Ester	Yield (%)
1	**5b**: 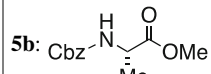	96 (**6bb**)	9	**5j**: 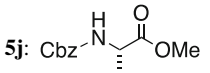	84 (**6jb**)
2	**5c**: 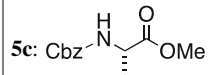	41 (**6cb**)	10	**5k**: 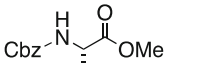	84 (**6kb**)
3	**5d**: 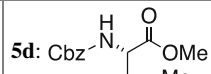	44 (**6db**)	11[a]	**5l**: 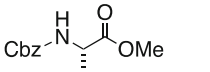	91 (**6lb**)
4	**5e**: 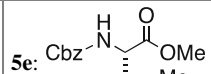	97 (**6eb**)	12	**5m**: 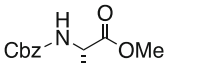	79 (**6mb**)
5	**5f**: 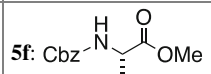	96 (**6fb**)	13	**5n**: 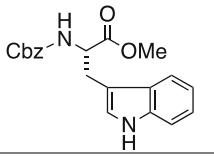	99 (**6nb**)
6	**5g**: 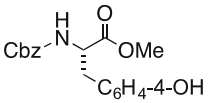	87 (**6gb**)	14	**5o**: 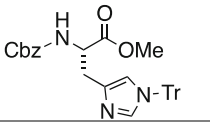	99 (**6ob**)
7	**5 h**: 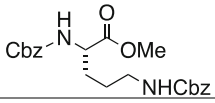	90 (**6hb**)	15	**5p**: 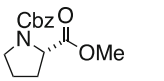	97 (**6pb**)
8	**5i**: 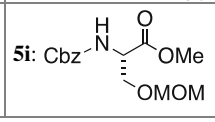	87 (**6ib**)	16	**5q**: 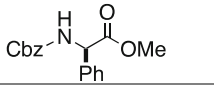	90 (**6qb**)

(continued)

Table 3 (continued)

Entry	Ester	Yield (%)	Entry	Ester	Yield (%)
17	**5r**: 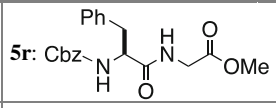				92 (**6rb**)
18	**5s**: 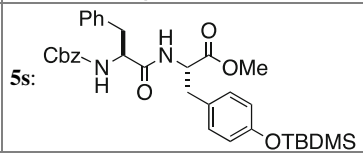				82 (**6sb**)

[a]4 eq of **3b** was used

natural products [53]. The transesterification of β-keto esters is sluggish and requires an excess of β-keto ester and high boiling alcohols [8–11]. In addition, unlike simple esters, the chelation nature of β-keto esters suppresses the activity of metal catalysts through the formation of a coordinate bond to metal ions, and the acidic nature of β-keto esters (pK_a ca. 14 in DMSO) suppresses the activity of the base catalyst. Fortunately, zinc cluster **1b** was highly effective for the transesterification of β-keto esters as well [40]. Under toluene reflux conditions, the reactions of various primary alcohols, including sterically congested neopentyl alcohol (**3j**), gave the desired products in high yield (Table 4, Entries 1–3). Although β-keto esters of allylic alcohols such as **8ag** are difficult to prepare because they readily proceed to Carroll rearrangement, the reaction of cinnamyl alcohol (**3g**) under *i*-Pr_2O refluxed conditions to give **8ag** in 86% yield (Entry 4). The highly acid-sensitive THP ether group was partially decomposed due to the acidity of β-keto ester **7a**, but the addition of 10 mol% of DMAP (vide infra) efficiently suppressed the decomposition of THP ether to provide **8an** in 94% yield (Entry 8). Notably, the reactions of sterically more congested secondary and the tertiary alcohol adamantanol (**3s**) and *tert*-butanol (**3t**) also proceeded smoothly (Entries 9–13). This zinc catalysis was highly effective for β-keto esters as well as for other active β-dicarbonyl derivatives, including β-diesters, Meldrum's acid, methyl-*N*-hexyl malonamide, and trimethyl phosphonoacetate [40].

There is another way to look at zinc cluster-catalyzed transesterification: We used ethyl acetate as an acetylation reagent [32]. The acetylation of alcohols is one of the most important and fundamental reactions in organic synthesis. In general, the acetylation of hydroxyl groups is conducted with acetyl chloride or acetic anhydride in the presence of greater than stoichiometric amounts of a base, resulting in the formation of greater than stoichiometric amounts of unwanted chemical waste. Alternatively, catalytic transesterification has been applied to acetylation. High conversion, however, is difficult to attain with the direct use of methyl acetate and ethyl acetate for acetylation because of the low electrophilicity of these simple acetates and the existence of a reverse reaction [54–60]. Thus, most reported acetylations by transesterification use enol esters as the acetyl donor to improve

Table 4 Transesterification of β-keto ester with various alcohols

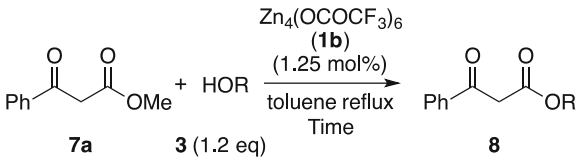

Entry	Alcohol (HOR)	Time (h)	Yield (%)
1	**3a**: HOBn	45	89 (**8aa**)
2	**3c**: $HO(CH_2)_5CH_3$	48	86 (**8ac**)
3	**3j**: $HOCH_2$-*t*-Bu	44	89 (**8aj**)
4[a]	**3g**: 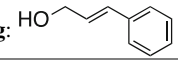	65	86 (**8ag**)
5	**3k**: 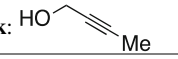	48	82 (**8ak**)
6	**3l**: $HO(CH_2)_6OCO$-*t*-Bu	60	89 (**8al**)
7	**3m**: $HO(CH_2)_6OTBDMS$	48	86 (**8am**)
8[b]	**3n**: $HO(CH_2)_6OTHP$	48	94 (**8an**)
9	**3o**: $HOCH(Pr)_2$	44	89 (**8ao**)
10	**3p**: HO-*c*-Hex	45	95 (**8ap**)
11	**3q**: 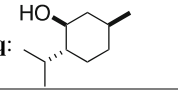	44	93 (**8aq**)
12[c]	**3r**: 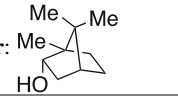	44	97 (**8ar**)
13[d]	**3s**: 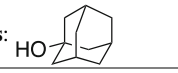	72	85 (**8as**)
14[e]	**3t**: HO-*t*-Bu	72	82 (**8at**)

[a] *i*-Pr_2O was used as the solvent
[b] 10 mol% of DMAP was added
[c] 1.5 eq of **3r** was used
[d] 2.0 eq of **3s** was used
[e] 5.0 eq of **3t** was used

reactivity and prevent the reverse reaction. In contrast, our zinc catalysis uses ethyl acetate as the acetyl donor based on its high stability, accessibility, and economic advantages. Acetylation of a variety of alcohols using ethyl acetate was efficiently promoted by only 1.25 mol% of zinc catalyst **1b** (Table 5). Of particular note is that highly acid-sensitive TES ether survived under the reaction conditions (Entry 5). Moreover, the benzoyl (Entry 7) and pivaloyl (Entry 8) groups were not scrambled. Acetylation of the D-glucose derivative **3α**, which has both isopropylidene and benzylidene acetal functionalities, proceeded in quantitative yield without cleavage

Table 5 Catalytic acetylation of various alcohols

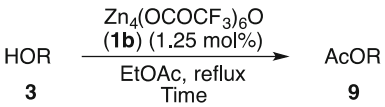

Entry	Alcohol (HOR)		Time (h)	Yield (%)
1	**3a**: R′ = H	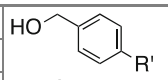	18	98 (**9a**)
2	**3u**: R′ = Cl		38	76 (**9u**)
3	**3v**: R′ = Br	**3a**,**e**,**u**–**z**	38	81 (**9v**)
4	**3e**: R′ = OTBDMS		24	97 (**9e**)
5	**3w**: R′ = CH_2OTES		18	89 (**9w**)
6	**3x**: R′ = CH_2OMEM		36	96 (**9x**)
7	**3y**: R′ = CH_2OCOPh		40	83 (**9y**)
8	**3z**: R′ = CH_2OCO-*t*-Bu		36	89 (**9z**)
9	**3d**: $HO(CH_2)_{17}CH_3$		38	>99 (**9d**)
10	**3g**: 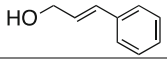		38	94 (**9g**)
11	**3h**: 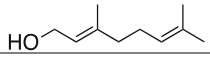		24	97 (**9h**)
12	**3α**: 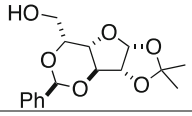		18	>99 (**9α**)
13	**3q**: 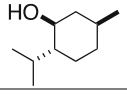		18	75 (**9q**)
14	**3β**: 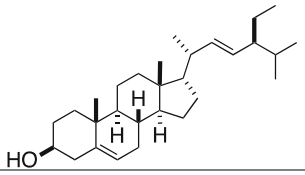		40	>99 (**9β**)
15	**3γ**: 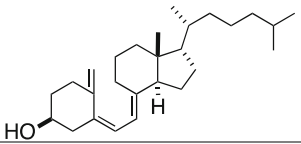		40	>99 (**9γ**)
16	**3δ**: 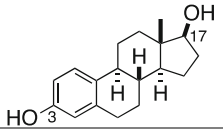		40	>99 (**9δ**)[a]
17	**3i**: 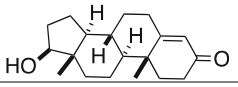		40	93 (**9i**)

[a]Yield of the corresponding 17-OAc product

of the acetal protecting groups (Entry 12). To the best of our knowledge, this is the first example of a highly chemoselective catalytic acetylation of secondary aliphatic alcohols over that of aromatic alcohols through transesterification.

Deacylation reaction, which is the reverse reaction of the above mentioned acetylation reaction, was also promoted by zinc catalyst **1b** by employing methanol as the solvent [33].

4 Chemoselective Acylation of Alcohols Over Amines

4.1 Introduction

Esters and amides are ubiquitous functional groups in natural and synthetic organic compounds, and they are commonly synthesized by acylation of the corresponding alcohol and amine, respectively, with carboxylic acid, acid chloride, or acid anhydride. As the nucleophilicity of the amino group is much greater than that of the hydroxyl group, the amine can be selectively acylated to give the corresponding amide, even in the presence of excess alcohol and/or water. This chemoselectivity has been well utilized for several highly efficient amidation reactions, such as the Schotten-Baumann reactions (Scheme 1, *path a*, **10** → **11**) [61]. On the other hand, selective *O*-acylation (*path b*, **10** → **12**) is quite difficult to perform under ordinary organic reactions. When aminoester **12** was targeted, the only feasible route was an indirect protection-deprotection process including in situ protection with acid (*path c*). The requirement for such a multistep transformation decreases the atom-economy of this process. To comply with the demand for an environmentally benign process, reversing the normal chemoselectivity of *path a* and minimizing waste are very important. The ideal method leading to the development of a new transformation without using protecting groups is a direct catalytic conversion of aminoalcohol **10** to aminoester **12** in a highly chemoselective manner (*path b*); however, there were no examples of such a reaction using an artificial catalyst.

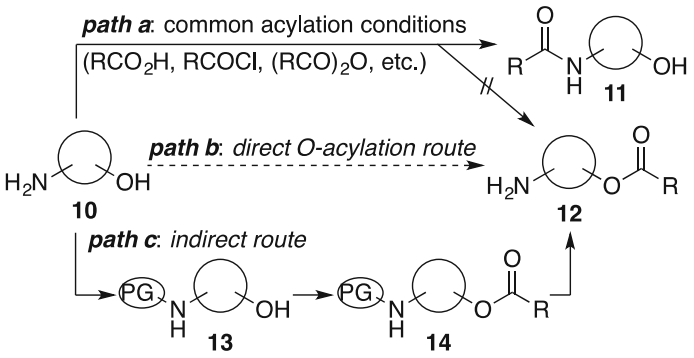

Scheme 1 Acylation of amino alcohol

4.2 Optimization of Reaction Conditions

We first investigated selective *O*-acylation using a 1:1 mixture of cyclohexanol (**3p**) and cyclohexylamine (**15p**) (Scheme 2) [29]. When PhCOCl or $(PhCO)_2O$ was used as an acylation reagent with base, the acylation of amine **15p** proceeded exclusively to give the corresponding *N*-cyclohexylbenzamide (**16bp**) in >99% yield, and cyclohexyl benzoate (**4bp**) was not detected (Eqs. 1 and 2), consistent with normal chemoselectivity. To tackle the issue of chemoselectivity, we focused on transesterification using the tetranuclear zinc cluster **1b** as a catalyst because during our studies on zinc cluster catalysis we found that **1b** was a highly efficient catalyst for transesterification, but not for amidation. Although so-called monomeric zinc complexes $Zn(OCOR)_2$ showed only moderate reactivity, when **1b** was used for this chemoselective acylation reaction, alcohol **3p** was selectively acylated to afford ester **4bp** in 96% yield, along with only 1% of amide **16bp** (Eq. 3).

4.3 Scope and Limitations

We performed the selective *O*-acylation using various combinations of alcohols and amines. All of the reactions that we evaluated using primary amines proceeded in a highly chemoselective manner [29]. To demonstrate the usefulness and effectiveness of this zinc catalysis in organic synthesis, we performed the *O*-selective acylation of amino alcohols **10** (Table 6). When β-amino alcohol **10a** was used as a

Scheme 2 Chemoselective acylation using a 1:1 mixture of alcohol and amine

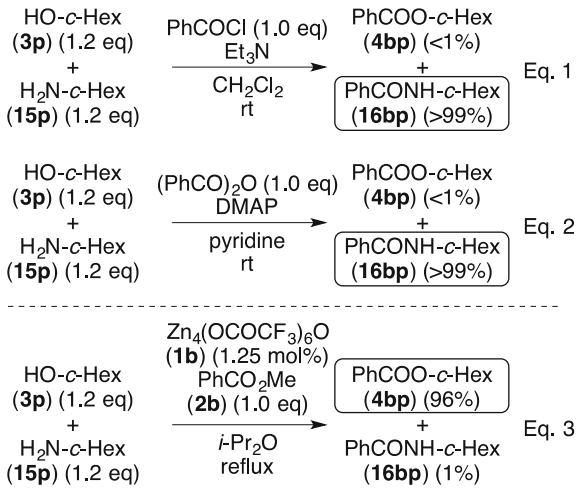

Table 6 Chemoselective acylation of various amino alcohols

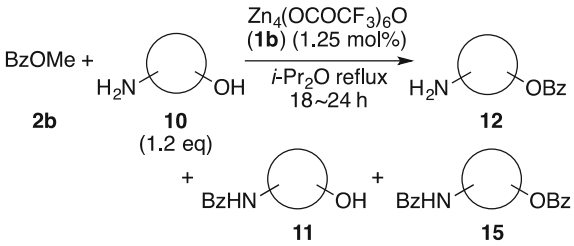

Entry	Aminoalcohol	Yield of **12** (%)	Yield of **11** (%)	Yield of **15** (%)
1	**10a**: 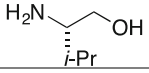	ND (**12ba**)	77 (**11ba**)	23 (**15ba**)
2	**10b**: H_2N–$(CH_2)_6$–OH	82 (**12bb**)	ND (**11bb**)	18 (**15bb**)
3	**10c**: H_2N–$(CH_2)_8$–OH	90 (**12bc**)	ND (**11bc**)	7 (**15bc**)
4	**10d**: H_2N–$(CH_2)_{10}$–OH	90 (**12bd**)	ND (**11bd**)	7 (**15bd**)
5[a]	**10e**: 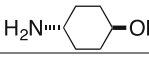	99 (**12be**)	ND (**11be**)	ND (**15be**)
6[a]	**10f**: 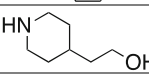	92 (**12bf**)	ND (**11bf**)	7 (**15bf**)

[a]Toluene was used as the solvent instead of *i*-Pr_2O

substrate, hydroxyamide **11ba** was obtained in 77% yield along with diacylation products **15ba** in 23% yield (Entry 1). The product **15ba** is produced through *O*-acylation (**10a** → **12ba**), with a subsequent complete *O* → *N* acyl transfer reaction (**12ba** → **11ba**) due to the instability of the resulting amino ester **12ba**. When amino alcohols **10b–d** tethered by long alkyl chains were treated, we obtained amino esters **12bb–bd** in good yield (82–90%) (Entries 2–4). Furthermore, the reaction of trans-4-aminocyclohexanol (**10e**) provided amino ester **10be** exclusively (99%), presumably due to trans-stereochemistry preventing the intramolecular *O* → *N* acyl transfer reaction. Even when amino alcohol **10f** with highly nucleophilic secondary amino group (piperidine unit) was used, the reaction proceeded in an *O*-acylation selective manner to give the corresponding amino esters **12bf** in high yield (92%).

Based on these results, we anticipated that this selectivity allowed for the transesterification of amino acid esters bearing a primary or secondary aliphatic amino group. In fact, transesterification of *N*-protection-free valine methyl ester (**16**) with 1-butanol (**3b**) afforded the butyl ester **18** in 69% yield upon treatment with CbzCl (Scheme 3) [36]. As a substrate with a secondary aliphatic amino group, the reaction of *N*-benzyl glycine methyl ester (**19**) gave the corresponding butyl ester **20** in 89% yield. Acylation of the amino group was not observed in either reaction.

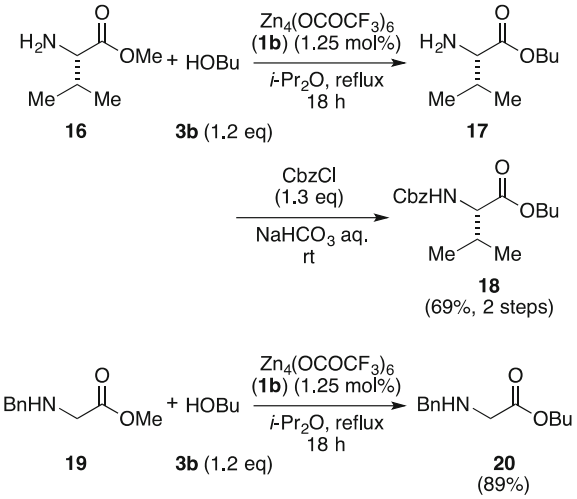

Scheme 3 Transesterification of α-amino esters bearing a primary or secondary aliphatic amino group

Scheme 4 Additive effects of amine on transesterification

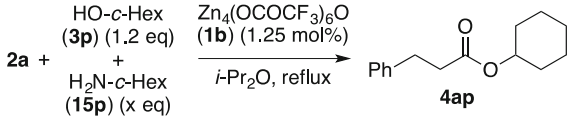

without **15p**: 22% yield (48 h)
with **15p** (1.2 eq): 94% yield (18 h)
with **15p** (0.2 eq): 90% yield (18 h)

5 Activation by *N*-Heteroaromatics

5.1 DMAP

Transesterification of sterically demanding substrates remains a difficult and challenging task. During the course of our studies on the above-mentioned chemoselective acylation of hydroxyl groups over amino groups, we discovered important clues to solving this problem. In the presence of an equivalent amount of cyclohexylamine (**15p**), for example, the acylation of cyclohexyl alcohol (**3p**) with methyl 3-phenylpropanoate (**2a**) provided the corresponding ester **4ap** in 94% yield after refluxing for 18 h, whereas in the absence of **15p**, the reaction provided the same product but in only 22% yield, even after refluxing for 48 h (Scheme 4) [34]. These results clearly indicate that under this acylation condition, highly nucleophilic alkylamine, which is in general acylated in preference to alcohol, greatly accelerates the acylation of alcohol without being converted to the corresponding amide. Further, the addition of only a catalytic amount of alkylamine (20 mol%) was sufficient to achieve satisfactory catalyst activity.

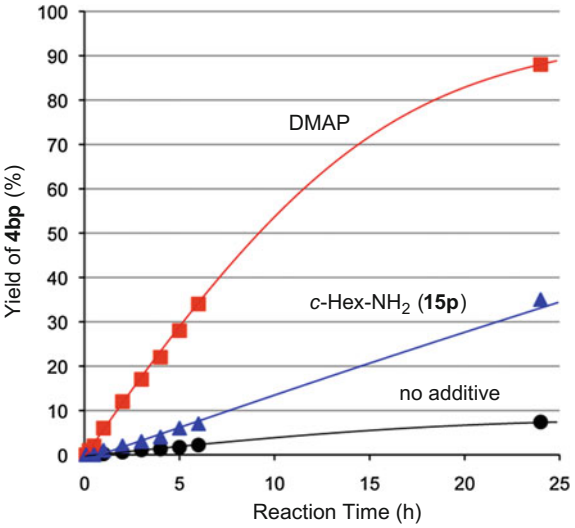

Fig. 2 Time-course for the **1b**-catalyzed transesterification of **2b** with **3p** in the presence of 20 mol% of **15p** (*filled triangle*), 20 mol% of DMAP (*filled square*) or in the absence of additives (*filled circle*)

Encouraged by such drastic additive effects of alkylamine **15p**, we further examined a variety of additives [34]. Based on the fact that metal ions in the active site of some metalloenzymes, such as aminopeptidase, are supported by both carboxylate and imidazole ligands, we examined heteroaromatics as additives as well, and found that *N*-methylimidazole (NMI), *N*,*N*-dimethylaminopyridine (DMAP) and 4-pyrrolidinopyridine were highly effective. The time-course for the reaction in the presence of the best alkylamine-type additive **15p** and the best *N*-heterocycle-type additive DMAP revealed that the addition of 20 mol% of these additives increased the initial rate of the reactions more than 3- and 15-fold, respectively (Fig. 2). The addition of these additives at any stage of the reaction sufficiently accelerated the reaction.

With the best additive, DMAP, in hand, we investigated the substrate generality of the transesterification of comparatively low reactive esters, as well as alcohols [34]. As shown in Table 7, DMAP had drastic positive effects on the reaction, resulting in great improvement of the chemical yield (up to 98%). The reactions of various methyl esters, including highly congested methyl 1-adamantanecarboxylate (**2r**), with 1-butanol (**3b**) in the presence of 20 mol% DMAP resulted in satisfactory yields, though sluggish reactions were observed for the corresponding substrates in the absence of the additive (Entries 1–4). The DMAP additive system was also superior for the less reactive alcohols (Entries 5–8). Notably, the addition of DMAP not only accelerated the catalytic rate but also suppressed undesirable side reactions because of the neutral reaction conditions; the reaction of **2b** with 1-indanol (**3u**) afforded the product 1-indanyl 3-phenylpropanoate (**4bu**) in 88% yield despite observations that the same reaction conducted in the absence of DMAP resulted in a complex mixture of decomposed products from **3u** via a carbocation intermediate (Entry 7). The addition of DMAP (20 mol%) also accelerated the transesterification

Table 7 Additive effects of DMAP on **1b**-catalyzed transesterification: scope and limitations

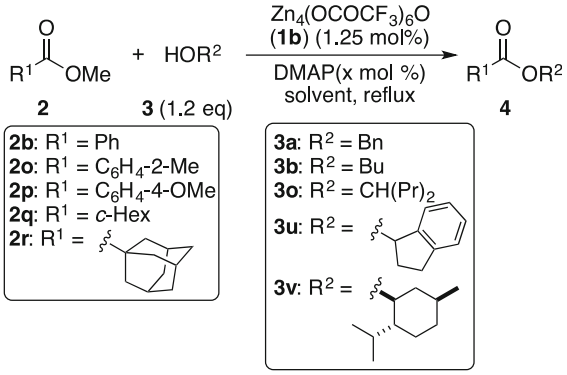

Entry	Ester	Alcohol	Solvent	Time (h)	Yield (%) (x = 0)	Yield (%) (x = 20)
1	**2o**	**3b**	Toluene	48	2	89
2	**2p**	**3b**	Toluene	18	7	89
3	**2q**	**3b**	*i*-Pr_2O	18	25	98
4	**2r**	**3b**	Toluene	90	<1	94
5	**2b**	**3a**	Toluene	18	58	92
6	**2b**	**3o**	*i*-Pr_2O	48	37	93
7	**2b**	**3u**	*i*-Pr_2O	18	5	88
8	**2b**	**3v**	*i*-Pr_2O	72	23	83

of less reactive α-amino esters, increasing the yield of **6cb** from 41% (Table 3, Entry 2) to 95%, and that of **6db** from 44% (Entry 3) to 90% yield, respectively.

5.2 Bis(imidazole) Ligand (2nd Generation Zn Catalyst)

Encouraged by the additive effects of DMAP, we next examined various bidentate and multidentate ligands having amines and/or *N*-heterocyclic units [38]. Because our mechanistic studies (vide infra) revealed the key intermediate: dinuclear metal complexes, we expected that proper multidentate *N*-heteroaromatic ligands could stabilize such active dinuclear metal complexes, leading to enhanced catalytic activity. Thus, several *N*-heteroaromatic additives were investigated with zinc cluster **1b**, and eventually we found that bis(imidazole)/zinc catalyst **22** (Fig. 3) was more active than **1b**/DMAP system [39]. Tertiary alcohol, previously not an applicable substrate for the transesterification of simple esters, could also be used, and the corresponding product was isolated in high yield (Table 8). Labile acrylate and methacrylate could be transesterificated in preference to 1,4-addition, indicating that the present zinc complex catalysis could be useful for the synthesis of various monomers using readily available methyl acrylate and methacrylate [39, 42].

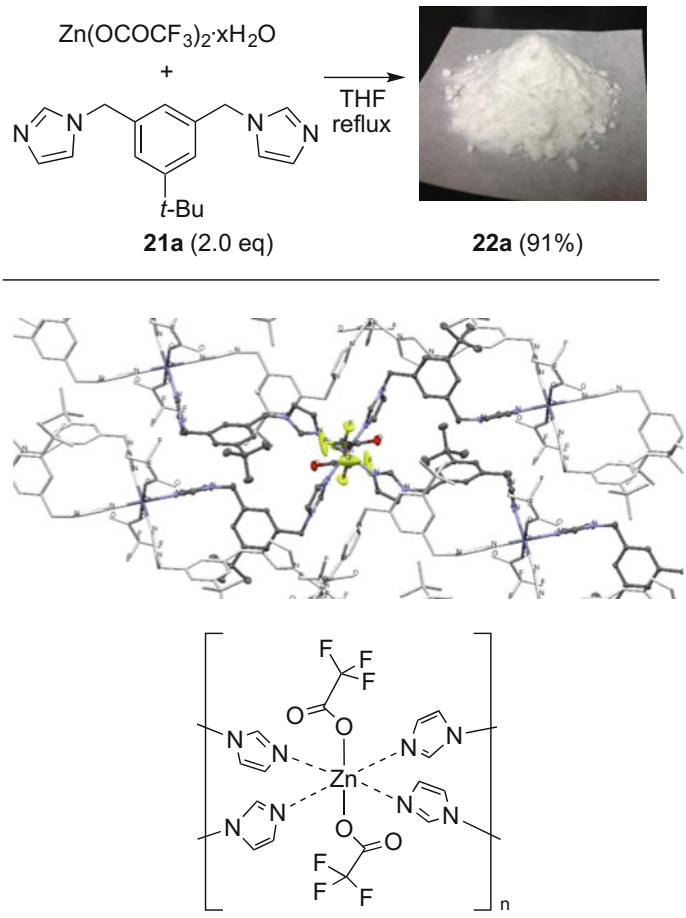

Fig. 3 Highly stable crystalline zinc complex **22a** and X-ray crystallographic structure

Zinc complex **22a** also catalyzed the transesterification using dimethyl or diethyl carbonate **23** to afford various linear carbonates **24**, cyclic carbonates **26**, and cyclic oxazolidinones **28** in high yield (Table 9) [39]. In addition, zinc complex **22a** also catalyzed the chemoselective transesterification of unprotected-amino alcohols using dimethyl carbonate with better chemoselectivity (*O*/*N* = ca. 12/1) than $Zn_4(OCOCF_3)_6O$ (**1b**) (*O*/*N* = ca. 2/1). To the best of our knowledge, this is the first example of chemoselective transesterification using dimethyl carbonate [39].

Zinc complex **22a** can be prepared in multigram scale using a simple procedure. A water addition experiment revealed the high stability of zinc complex **22a** compared to **1b**. The stable nature of zinc complex **22a** allowed for its recovery and reuse in transesterification reactions [39]. The recovered zinc complex was reused five times without a significant loss of catalytic activity (average over 95% yield;

Table 8 Bis(imidazole)/zinc-catalyzed transesterification of various methyl esters

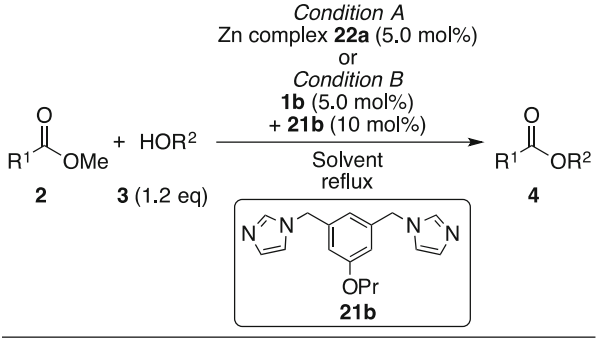

Structures of Products **4**

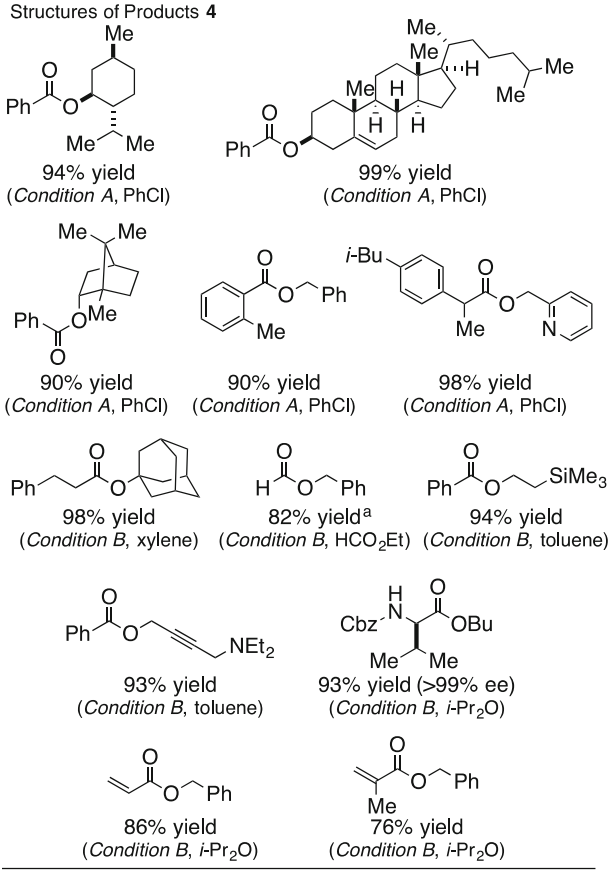

[a]HCO_2Et was used as an electrophile instead of HCO_2Me

Table 9 Transesterification using dimethyl or diethyl carbonates

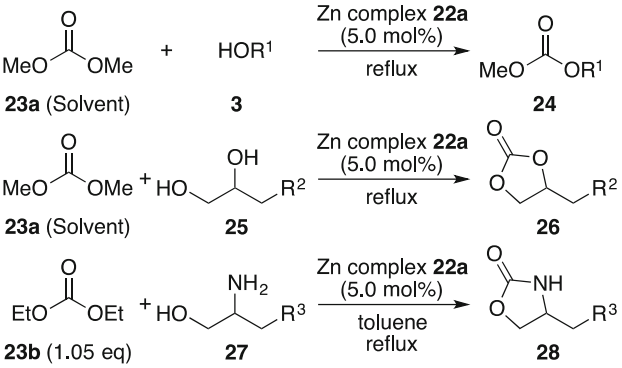

Structures of Products

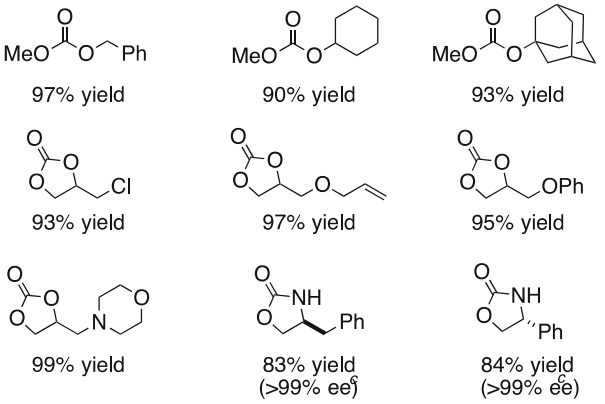

Scheme 5 Recovery and reuse experiment using zinc complex **22a**

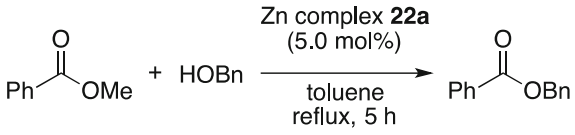

Run	Yield (%)
1	96
2	97
3	97
4	97
5	97

Scheme 5). Even after five runs, zinc complex **22a** could be recovered in 91% yield without any decomposition.

5.3 *Polystyrene Resin-Supported Imidazole Ligand (3rd Generation Zn Catalyst)*

The high stability of bis(imidazole)/zinc complex **22** enabled the practical use of **22** for transesterification reactions without strict concern regarding air and moisture. The highly crystalline nature of **22** stemming from its infinite network structure, however, limits the applicability of **22** in organic solvents. Moreover, because of high superiority of heterogeneous catalysts in catalyst recycling, we were interested in the development of a heterogeneous zinc catalyst for transesterification and transcarbonation reactions in a variety of organic solvents.

After several examinations, we found that newly developed heterogeneous zinc complex **30**, which was derived from Merrifield resin-supported imidazole ligand **29** and $Zn(OCOCF_3)_2$, was highly effective in a broad-spectrum of solvents, such as toluene, ethyl acetate, methanol, and dimethyl carbonate [41]. For complexation of imidazole resin **29** and zinc salt, the zinc/imidazole ratio and solvent selection were crucial for obtaining high catalytic activity. Very interestingly, although newly developed heterogeneous zinc/imidazole catalyst **30** was completely insoluble during the course of the reaction, it had comparable catalytic performance as the homogeneous zinc/NMI catalyst (Table 10). The recyclability of catalyst **30** was also demonstrated by recovery-reuse experiments, and catalyst **30** promoted various reactions in various solvents at least five times without loss of the activity (Scheme 6).

Table 10 Evaluation of zinc catalysts on transesterification

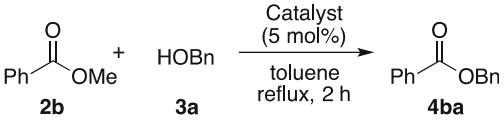

2b **3a** **4ba**

Entry	Catalyst	Yield (%)
1	$Zn(OCOCF_3)_2$	19
2	$Zn_4(OCOCF_3)_6O$ (**1b**)	21
3	Bis(imidazole)/zinc **22a**	38
4	$Zn(OCOCF_3)_2$ + NMI	97
5	Heterogeneous imidazole/zinc **30**	97
6	Imidazole resin **29**	ND

Scheme 6 Recovery and recuse experiments in various reaction

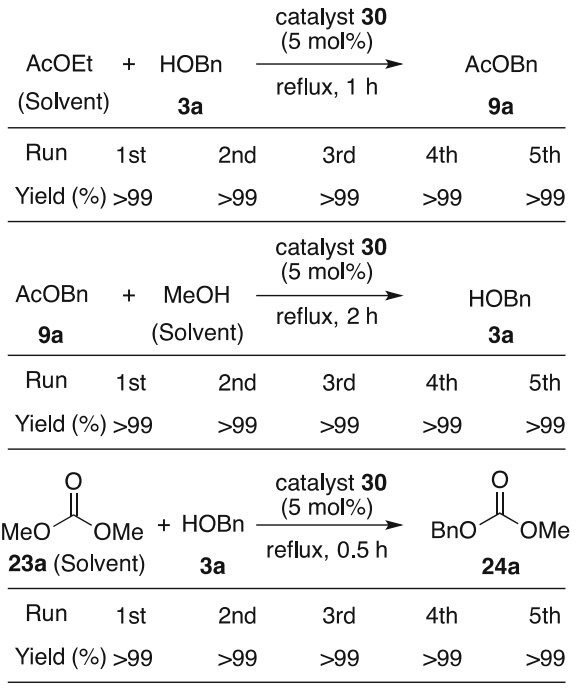

6 Mechanistic Studies

As presented here, we developed several environmentally friendly transesterification using μ-oxo-tetranuclear zinc cluster as the catalyst. Moreover, we achieved unprecedented *O*-selective acylations in the presence of much more nucleophilic primary and secondary alkyl amino groups, indicating that such innate chemoselectivity is reversible in a catalytic manner. Our intensive mechanistic studies using cobalt cluster [62] instead of zinc cluster revealed that the transesterification proceeds with Michaelis-Menten behavior through an ordered ternary complex mechanism similar to dinuclear metallo-enzymes, suggesting that the formation of metal alkoxide-bridged dinuclear metal complex, followed by coordination of the ester, is responsible for the unique *O*-selective acylation (Scheme 7) [38]. Because of the high efficiency in terms of atom economy and step economy, these direct new catalyses will be a powerful tool for organic synthesis, and I hope that the findings discussed herein will facilitate the development of new environmentally friendly reactions, including new catalyst-controlled chemoselective reactions [63].

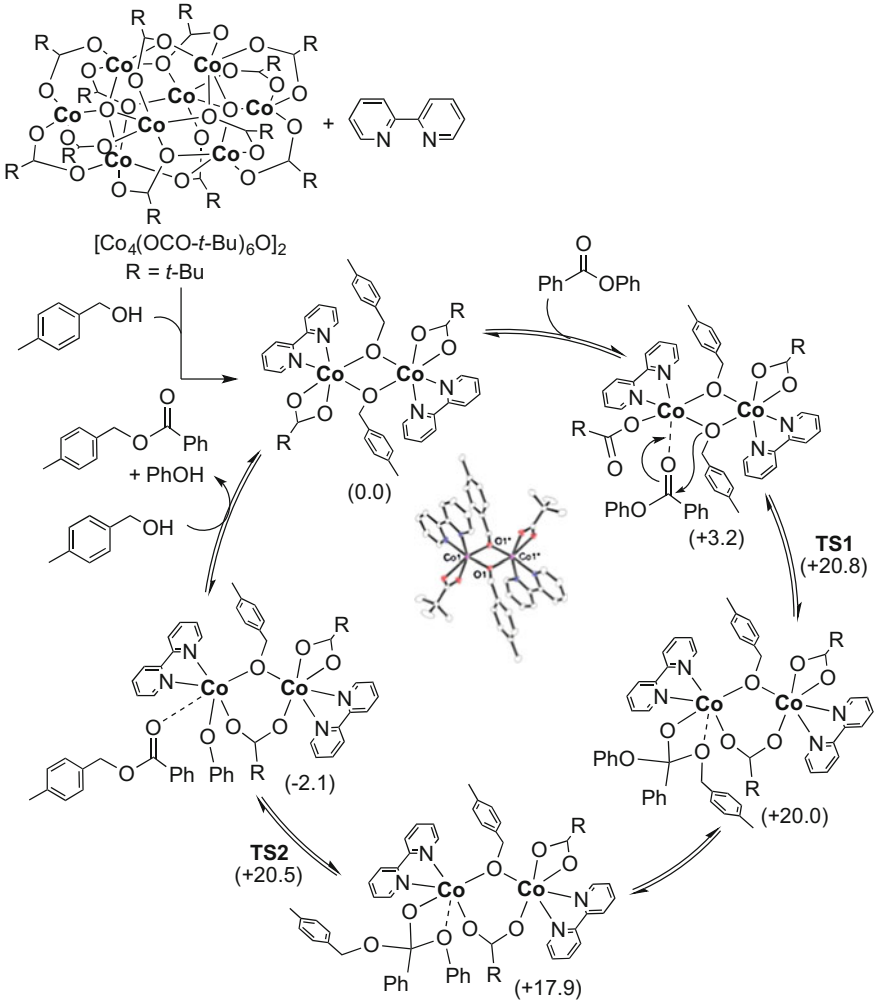

Scheme 7 Possible reaction mechanism for transesterification catalyzed by cobalt cluster

7 Conclusion

As presented here, we developed several environmentally friendly reactions using μ-oxo-tetranuclear zinc cluster (1st generation), bis(imidazole)/zinc complex (2nd generation), and heterogeneous PS-resin/zinc complex (3rd generation) as the catalyst. These zinc catalysts efficiently promoted the transesterification of various methyl esters including α-amino esters, β-keto esters, β-nonsubstituted-α,β-unsaturated esters (acrylate and methacrylate); the acetylation of alcohols in EtOAc; and the deacylation of esters in MeOH. Because the reaction conditions of

this method are almost neutral, this zinc catalysis has broad substrate generality wherein even in acid sensitive functional groups, such as THP ether and TES ether, catalysis persisted, and side reactions such as isomerization, cyclization, 1,4-addition, did not occur. Moreover, we achieved unprecedented *O*-selective acylations in the presence of much more nucleophilic primary and secondary alkyl amino groups.

Acknowledgements I would like to express my heartfelt respect and gratitude to Prof. K. Mashima of Osaka University for his kind and valuable advice. The research reviewed in this paper was possible only through the dedication, enthusiasm, and creativity of scores of co-workers: Dr. T. Iwasaki, Dr. Y. Maegawa, Miss A. Yoshiyama, Dr. Y. Hayashi, Prof. R. Dembinski (Oakland University), Dr. K. Agura, Miss Y. Fujii, Dr. Y. Matsushima (Takasago Co.), Dr. S. Santoro (Stockholm University), Prof. F. Himo (Stockholm University), Mr. D. Nakatake, Miss Y. Yokote, Dr. R. Yazaki, and Miss M. Wada.

References and Notes

1. B. M. Trost, Science, 254, 1471 (1991).
2. L. Jorgensen, S. J. McKerrall, C. A. Kuttruff, F. Ungeheuer, J. Felding, P. S. Baran, Science, 341, 878 (2013).
3. T. Mukaiyama, H. Ishikawa, H. Koshino, Y. Hayashi, Chem. Eur. J., 19, 17789 (2013).
4. K. C. Nicolaou, E. J. Sorensen, "Classics in Total Synthesis" Wiley-VCH, Weinheim, 1996.
5. K. C. Nicolaou, S. A. Snyder, "Classics in Total Synthesis II" Wiley-VCH, Weinheim, 2003.
6. K. C. Nicolaou, T. Montagnon, "Molecules That Changed the World" Wiley-VCH, Weinheim, 2008.
7. K. C. Nicolaou, J. S. Chan, "Classics in Total Synthesis III" Wiley-VCH, Weinheim, 2010.
8. J. Otera, Chem. Rev., 93, 1449 (1993).
9. H. E. Hoy-donckx, D. E. De Vos, S. A. Chavan, P. A. Jacobs, Top. Catal., 27, 83 (2004).
10. G. A. Grasa, R. Singh, S. P. Nolan, Synthesis, 971 (2004).
11. D. Enders, O. Niemeier, A. Henseler, Chem. Rev., 107, 5606 (2007).
12. N. A. Higgins, US-Patent 2676945 (1954).
13. R. C. Mehrotra, J. Am. Chem. Soc., 76, 2266 (1954).
14. K. Chimura, S. Takashima, M. Kawashima, Y. Shimoshinbara, JP-Patent 48049740 (1973).
15. D. Seebach, E. Hungerbuehler, R. Naef, P. Schnurrenberger, B. Weidmann, M. Zueger, Synthesis, 138 (1982).
16. J. Otera, T. Yano, A. Kawabata, H. Nozaki, Tetrahedron Lett., 27, 2383 (1986).
17. J. Otera, N. Danoh, H. Nozaki, J. Org. Chem., 56, 5307 (1991).
18. J. Otera, N. Dan-Oh, H. Nozaki, J. Chem. Soc., Chem. Commun., 1742 (1991).
19. L. A. Hobbs, P. J. Smith, Appl. Organomet. Chem., 6, 95 (1992).
20. P. Krasik, Tetrahedron Lett., 39, 4223 (1998).
21. J.-W. Chen, L.-W. Chen, J. Polym. Sci. Part A: Polym. Chem., 37, 1797 (1999).
22. J. Xiang, S. Toyoshima, A. Orita, J. Otera, Angew. Chem. Int. Ed., 40, 3670 (2001).
23. C.-T. Chen, J.-H. Kuo, C.-H. Ku, S.-S. Weng, C.-Y. Liu, J. Org. Chem., 70, 1328 (2005).
24. S. Magens, B. Plietker, J. Org. Chem., 75, 3715 (2010).
25. S.-S. Weng, C.-S. Ke, F.-K. Chen, Y.-F. Lyu, G.-Y. Lin, Tetrahedron, 67, 1640 (2011).
26. M. Hatano, Y. Furuya, T. Shimmura, K. Moriyama, S. Kamiya, T. Maki, K. Ishihara, Org. Lett., 13, 426 (2011).
27. M. Hatano, K. Ishihara, Chem. Commun., 49, 1983 (2013).
28. T. Ohshima, T. Iwasaki, K. Mashima, Chem. Commun., 2711 (2006).

29. T. Ohshima, T. Iwasaki, Y. Maegawa, A. Yoshiyama, K. Mashima, J. Am. Chem. Soc., 130, 2944 (2008).
30. T. Iwasaki, Y. Maegawa, Y. Hayashi, T. Ohshima, K. Mashima, J. Org. Chem., 73, 5147 (2008).
31. A. Sniady, A. Durham, M. S. Morreale, A. Marcinek, S. Szafert, T. Lis, K. R. Brzezinska, T. Iwasaki, T. Ohshima, K. Mashima, R. Dembinski, J. Org. Chem., 73, 5881 (2008).
32. T. Iwasaki, Y. Maegawa, Y. Hayashi, T. Ohshima, K. Mashima, Synlett, 10, 1659 (2009).
33. T. Iwasaki, K. Agura, Y. Maegawa, Y. Hayashi, T. Ohshima, K. Mashima, Chem. Eur. J., 16, 11567 (2010).
34. Y. Maegawa, T. Ohshima, Y. Hayashi, K. Agura, T. Iwasaki, K. Mashima, ACS Catal., 1, 1178 (2011).
35. Y. Hayashi, T. Ohshima, Y. Fujii, Y. Matsushima, K. Mashima, Catal. Sci. Technol., 1, 230 (2011).
36. Y. Maegawa, K. Agura, Y. Hayashi, T. Ohshima, K. Mashima, Synlett, 23, 137 (2012).
37. Y. Yang, Y. Hayashi, Y. Fujii, T. Nagano, Y. Kita, T. Ohshima, J. Okuda, K. Mashima, Catal. Sci. Tech., 2, 509 (2012).
38. Y. Hayashi, S. Santoro, Y. Azuma, F. Himo, T. Ohshima, K. Mashima, J. Am. Chem. Soc., 135, 6192 (2013).
39. D. Nakatake, Y. Yokote, Y. Matsushima, R, Yazaki, T. Ohshima, Green Chem., 18, 1524 (2016).
40. K. Agura, Y. Hayashi, M. Wada, D. Nakatake, K. Mashima, T. Ohshima, Chem. Asian. J., 11, 1548 (2016).
41. D. Nakatake, R. Yazaki, Y. Matsushima, T. Ohshima, Adv. Synth. Cat., 358, 2569 (2016).
42. D. Nakatake, R. Yazaki, T. Ohshima, Eur. J. Org. Chem., 3696 (2016).
43. T. Ohshima, Chem. Pharm. Bull., 64, 523 (2016).
44. V. Auger, I. Robin, Compt. Rend., 178, 1546 (1924).
45. J. Wyart, Bull. Soc. Fr. Mineral., 49, 148 (1926).
46. H. Koyama, Y. Saito, Bull. Chem. Soc. Jpn., 27, 112 (1954).
47. R. M. Gordon, H. B. Silver, Can. J. Chem., 61, 1218 (1983).
48. W. Clegg, D. R. Harbron, C. D. Homan, P. A. Hunt, J. R. Little, B. P. Straughan, Inorg. Chim. Acta, 186, 51 (1991).
49. Y. Ming-cai, M. Chi-wei, A. Chang-chun, Y. Liang-jie and S. Ju-tang, Wuhan University Journal of Natural Sciences, 9, 939 (2004).
50. S. Hermes, T. Witte, T. Hkov, D. Zacher, S. Bahnmüller, G. Langstein, K. Huber, R. A. Fischer, J. Am. Chem. Soc., 129, 5324 (2007).
51. O. Berkesi, I. Dreveni, A. Andor, Inorg. Chim. Acta, 181, 285 (1991).
52. CAUTION: Diisopropyl ether can form explosive peroxides upon standing in air for long periods. For safety, toluene or CPME can be used as an alternative solvent; these solvents usually give a higher yield, although they also require a higher reaction temperature.
53. S. Benetti, R. Romagnoli, C. De Risi, G. Spalluto, V. Zanirato, Chem. Rev., 95, 1065 (1995).
54. T. Nishiguchi, H. Taya, J. Am. Chem. Soc., 111, 9102 (1989).
55. N. Iranpoor, M. Shekarriz, Bull. Chem. Soc. Jpn., 72, 455 (1999).
56. A. Orita, K. Sakamoto, Y. Hamada, A. Mitsutome, J. Otera, Tetrahedron, 55, 2899 (1999).
57. B. C. Ranu, P. Dutta, A. Sarkar, J. Chem. Soc. Perkin Trans. 1, 2223 (2000).
58. M. H. Habibi, S. Tangestaninejad, V. Mirkhani, B. Yadollahi, Tetrahedron, 57, 8333 (2001).
59. R. Singh, R. M. Kissling, M.-A. Letellier, S. P. Nolan, J. Org. Chem., 69, 209 (2004).
60. R. Tayebee, M. H. Alizadeh, Monatsh. Chem., 137, 1063 (2006).
61. N. O. V. Sonntag, Chem. Rev., 52, 237 (1953).
62. A. A. Sidorov, I. G. Fomina, M. O. Ponina, G. G. Aleksandrov, S. E. Nefedov, I. L. Eremenko, I. I. Moiseev, Russ. Chem. Bull., Int. Ed., 49, 958 (2000).
63. S. Uesugi, Z. Li, R. Yazaki, T. Ohshima, Angew. Chem. Int. Ed., 53, 1611 (2014).

Vinyl Ruthenium Carbenes: Valuable Intermediates in Catalysis

Damián Padín, Jesús A. Varela and Carlos Saá

Abstract Vinyl ruthenium carbenes are easily prepared from the neutral Ru(II) complex $Cp^*RuCl(cod)$ in the presence of functionalized alkynes and diazoalkanes. These intermediates have been proposed for several transformations in which the nature of the products are strongly dependent of the functionality on the alkyne substituents. New modes of catalytic cyclizations due to the electrophilicity of these vinyl ruthenium carbene intermediates are presented in this chapter. Alkynyl acetals, ethers and amines gave rise to complex bicyclic structures, spiro- and fused, in an intramolecular redox, neutral process that involved [1,n]-hydrogen transfers/cyclization. New catalytic heterocyclizations have been also achieved by trapping the in situ generated vinyl ruthenium carbenes with O- and N-nucleophiles from alkynals/alkynones and alkynylamines.

Keywords Alkynyl derivatives · Benzoxazines · Bicyclic compounds · Carbenes · Catalysis · Cyclization · Heterocycles · Ruthenium · Vinyl ruthenium carbenes

1 Introduction

Metal carbene complexes have proven their value in synthetic chemistry due to the number of catalytic organometallic transformations in which they are involved [1]. For example, metal carbenes have been investigated in a wide variety of catalytic alkene metathesis transformations such as cross metathesis (CM), ring-closing metathesis (RCM), acyclic diene metathesis (ADMET), and ring-opening metathesis

D. Padín · J.A. Varela (✉) · C. Saá
Centro Singular de Investigación En Química Biolóxica e Materiais Moleculares (CIQUS), e Departamento de Química Orgánica, Universidade de Santiago de Compostela, 15782 Santiago de Compostela, Spain
e-mail: jesus.varela@usc.es

C. Saá
e-mail: carlos.saa@usc.es

K. Tomioka et al. (eds.), *New Horizons of Process Chemistry*,
DOI 10.1007/978-981-10-3421-3_7

polymerization (ROMP) [2–9], as well as in reactions involving alkynes such as alkyne polymerization [10–12], enyne metathesis [13–15], cyclopropenation [16], etc. Other in situ generated metal carbenes, either from diazo compounds or from activation of alkynes with electrophilic metals [1, 17, 18], have been considered as key intermediates for catalytic cyclopropa(e)nation reactions, X-H insertions or intricate skeleton rearrangements [19–26].

Conjugated vinyl ruthenium carbenes **D** (Scheme 1), smoothly prepared under mild conditions by treatment of neutral Ru(II) complex $Cp^*RuCl(cod)$ in the presence of functionalized alkynes and diazoalkanes, have been recently proposed in catalytic transformations that involve the formation of carbon-carbon bonds [27].

The type of the reaction products is strongly dependent on the nature of the alkyne functionality (Scheme 2). Functionalized 1,3-dienes could be catalytically obtained by (a) trapping the initially formed vinyl ruthenium carbene with a second molecule of a diazo compound [28, 29] and (b) Rautenstrauch rearrangement of propargylic carboxylates followed by trapping of the transient vinyl ruthenium carbene with a diazoalkane [30]. In addition, (c) enynes bearing terminal triple bonds led to alkenyl bicyclo[3.1.0]hexanes [31, 32], (d) disubstituted 1,6-enynes at

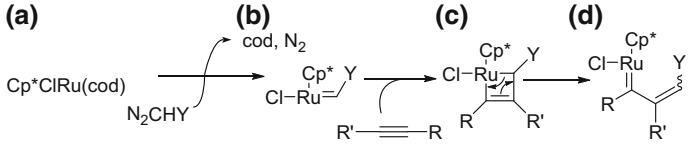

Scheme 1 Mechanistic hypothesis for the formation of vinyl ruthenium carbenes from $Cp^*ClRu(cod)$ in the presence of diazo compounds and alkynes

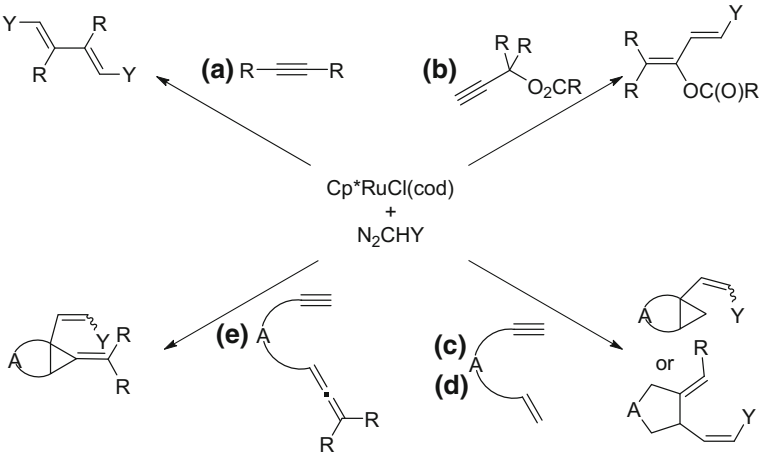

Scheme 2 Type of products obtained by reaction of catalytic amounts of $Cp^*RuCl(cod)$ with diazo compounds and alkynes

the propargylic positions afforded α-alkenyl alkylidene cyclopentanes [33], while (e) 1,6-allenynes were converted to *E*,*Z*-mixtures of α-alkenyl alkylidenes bicyclo [3.1.0]hexanes [34].

In all the previous transformations the vinyl ruthenium carbene intermediate evolves to the final products via non-polar mechanisms (reductive eliminations, [2+2] cycloadditions and 1,2-insertions). This chapter will be devoted to the synthetic opportunities (new catalytic cyclizations) derived from the polar chemistry of vinyl ruthenium carbene intermediates (electrophilic carbenes). New carbo- and heterocyclizations by intramolecular nucleophilic attack to the ruthenium carbene intermediates will be described. Specifically, the neutral redox processes in which an activated hydrogen (a "hydride") is intramolecularly transferred to the ruthenium carbene and the nucleophilic attack of oxygenated and nitrogenated nucleophiles will be presented. Finally, computational calculations would rationalize the stereoselectivity observed for such transformations.

2 Intramolecular Ruthenium Catalyzed Redox, Neutral [1,n]-Hydride Transfer/Cyclization Processes

The functionalization of relatively unreactive C–H bonds remains a major topic in organic synthesis, particularly from the viewpoint of sustainability and efficiency, since new C–C and C-heteroatom bonds can be directly formed without previous prefunctionalization [35–40]. For this purpose, a large number of methodologies have been developed, being most of them oriented to the transition metal-catalyzed C(sp^2)-H activation, while the most difficult C(sp^3)-H activation still remains a challenge owing to its high bond dissociation energy. The intramolecular redox, neutral [1,n]-hydride transfer/cyclization processes has emerged as one efficient and powerful method for selective activation and direct functionalization of inactive C(sp^3)-H bonds towards 5-, 6- and 7-membered carbo-, hetero-, spiro-, or fused cycles [41, 42].

Vinyl ruthenium carbene intermediates, obtained by treatment of catalytic $Cp^*RuCl(cod)$ with (trimethylsilyl)diazomethane and alkynylacetals, ethers or amines, can act as hydride acceptors in intramolecular [1,n]-hydride transfers to afford functionalized spiro- and fused bicycles [43]. Tertiary C(sp^3)-H of cyclic and acyclic acetal derivatives of alkynals could be activated under the mild conditions to generate vinyl ruthenium carbenes to give the corresponding functionalized cyclic compounds resulting from a [1,5] and [1,6]-hydride transfer/cyclization in good yields (Scheme 3).

Gratifyingly, the less activated tertiary C(sp^3)-H of alkynyl tetrahydrofurans and pyrans (X = O, n = 1, 2) or pyrrolidines (X = N) underwent the [1,5] and [1,6]-hydride transfer/cyclization processes to afford the oxa- and azaspiranic bicycles in

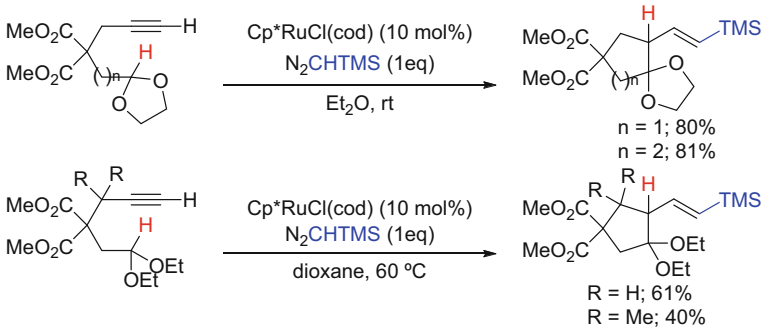

Scheme 3 Ruthenium-catalyzed tertiary [1,5]- an [1,6]-hydride transfer/cyclization in alkynyl acetals

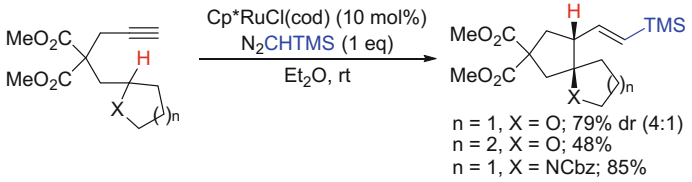

Scheme 4 Ruthenium-catalyzed tertiary [1,5]- and [1,6]-hydride transfer/cyclization in alkynyl tetrahydrofurans/pyrans and pyrrolidines

fairly good yields with good diastereoselectivity or as single diastereomer, respectively (Scheme 4).

Even the alkynyl ethers bearing secondary C(sp^3)-H also underwent [1,5]-hydride transfer/cyclization processes in moderate to good yields. *Trans* homoallylic ethers (mono- and bicyclic structures) could be obtained from acyclic ethers and tetrahydrofurans, respectively (Scheme 5). Secondary C(sp^3)-H of amines could also be activated to give the corresponding bicyclic piperidine derivative as a single diastereoisomer.

The proposed mechanism for the Ru-catalyzed intramolecular redox, neutral [1,n]-hydride transfer/cyclization processes is shown in Scheme 6. The starting neutral precatalyst ruthenium(II) complex in the presence of the (trimethylsilyl)-diazomethane and the alkyne would easily form the ruthenium carbene complex **I,** which smoothly evolves to the conjugated vinyl ruthenium carbene species **II**. This complex would undergo a [1,5]-hydride transfer to the electrophilic carbene assisted by the heteroatom(s) to afford a transient oxonium ion which is trapped to give the ruthenacycle **III**. Finally, reductive elimination would give rise to the spiro compound with recovery of the catalytic Ru(II) species.

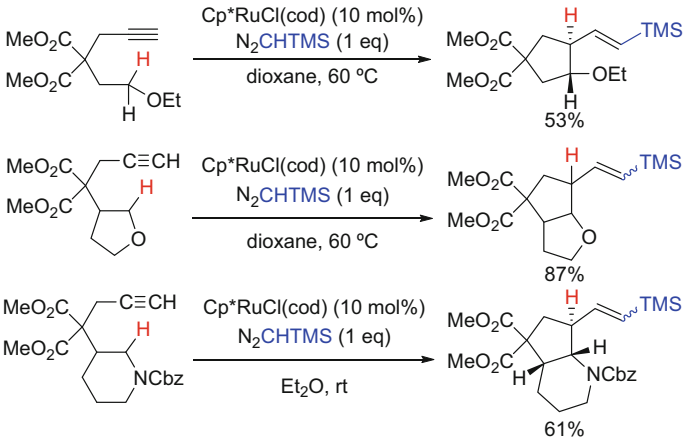

Scheme 5 Ruthenium-catalyzed secondary [1,5]-hydride transfer/cyclization in alkynyl ethers and piperidines

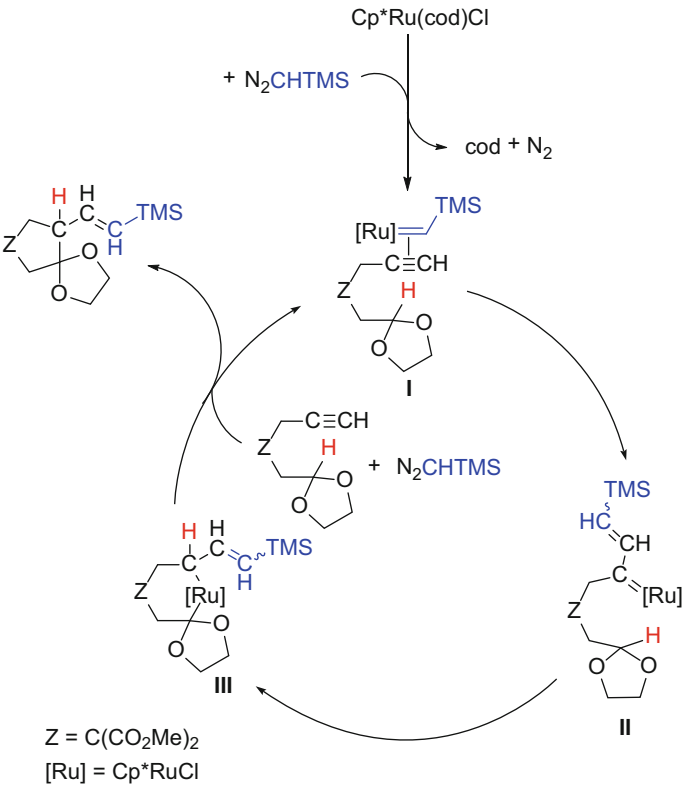

Scheme 6 Mechanistic hypothesis for the Ru-catalyzed intramolecular redox, neutral [1,n]-hydride transfer/cyclization processes

3 Heterocyclizations via Vinyl Ruthenium Carbene Intermediates from Alkynals and Alkynones

New catalytic heterocyclizations have been also achieved by trapping the in situ generated electrophilic vinyl ruthenium carbenes (obtained by treatment of catalytic amounts of $Cp^*RuCl(cod)$ with alkynals/alkynones and (trimethylsilyl)diazomethane) with *O*-nucleophiles from the carbonyl functionalities. Indeed, 3,3-disubstituted and 3,3,4-trisubstituted alkynals afforded the corresponding 2-vinyl-3,4-dihydropyrans in good yields with high diastereoselectivity (Scheme 7) [44].

The diastereoselectivity of the reaction was further evaluated by using 3-monosubstituted alkynals as starting materials. Alkynals bearing methoxycarbonyl, benzyloxymethyl and acetoxymethyl substituents gave rise to the corresponding 2-vinyl-3,4-dihydropyrans as single *cis* diastereomers (Scheme 8). However, alkynals bearing bulkier 3-silyloxy substituents showed lower diastereoselectivity for the heterocyclization process.

6-Substituted 2-vinyl-3,4-dihydropyrans could also be achieved by ruthenium catalyzed heterocyclization of alkynones instead of alkynals (Scheme 9). The heterocyclization of 3-monosubstituted alkynones showed complete diastereoselectivity to give the *cis* 2,4,6-trisubstituted dihydropyrans, which could be applied to the obtention of enantiomerically pure dihydropyrans by just starting from (*R*) 3-(*tert*-butylsilyloxy)alkynones (Scheme 9).

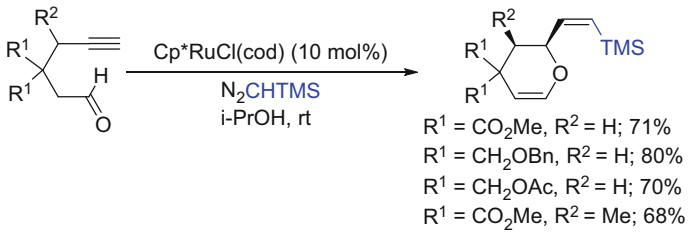

Scheme 7 Ruthenium-catalyzed heterocyclization of alkynals to 2-vinyl-3,4-dihydropyrans

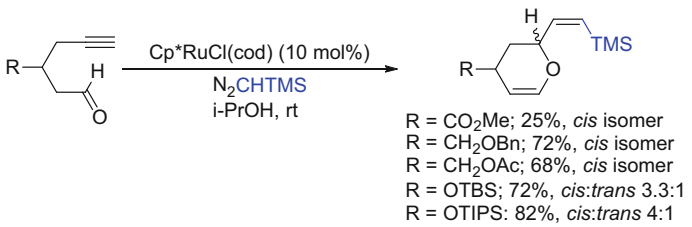

Scheme 8 Diastereoselectivity of the ruthenium-catalyzed heterocyclization of 3-alkynals to 2-vinyl-3,4-dihydropyrans

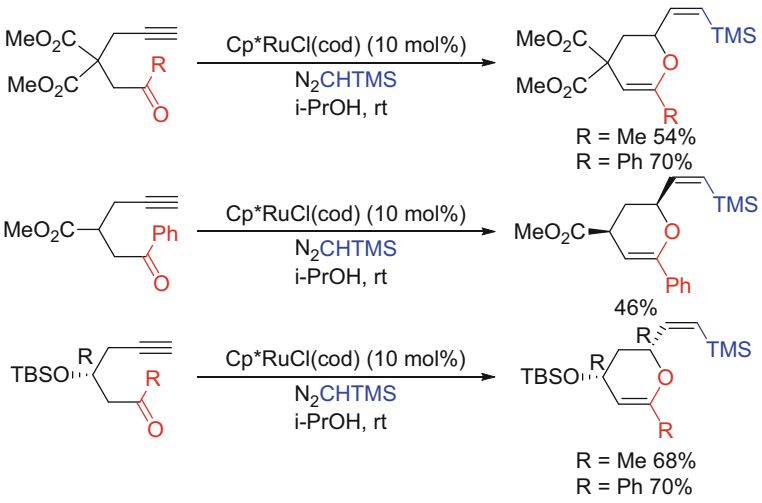

Scheme 9 Ruthenium-catalyzed heterocyclization of alkynones to 6-substituted 2-vinyl-3,4-dihydropyrans and studies of diastereoselectivity

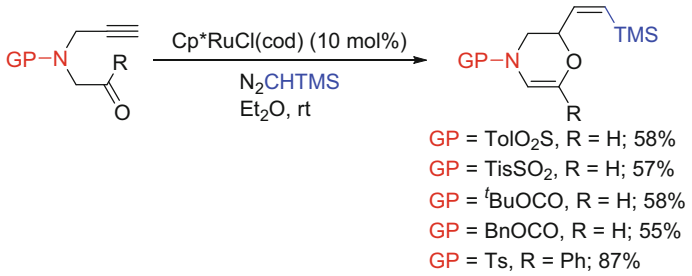

Scheme 10 Ruthenium-catalyzed heterocyclization of *N*-tethered alkynals and alkynones to 2-vinyl-3,4-dihydro-2*H*-1,4-dihydrooxazines

N-Tethered alkynals and alkynones also cyclized under the typical catalytic reaction conditions (diethyl ether as solvent) to give the corresponding 2-vinyl-3,4-dihydro-2*H*-1,4-oxazines in moderate to good yields (Scheme 10).

The proposed mechanism for the Ru-catalyzed heterocyclization of alkynals and alkynones to give 2-vinyl-3,4-dihydropyrans (and 2-vinyl-3,4-dihydrooxazines, not shown) is depicted in Scheme 11. It would start with the initial formation of the electrophilic vinyl ruthenium carbene intermediate **II** that undergoes a nucleophilic attack of the carbonyl to afford the zwitterionic intermediate **III**. The diastereoselectivity of the process could be rationalized if the nucleophilic attack of the carbonyl takes place through the more stable chair-like conformer of the ruthenium carbene **IIa** with all the substituents in equatorial position. Final deprotonation and reprotonation of the C–Ru bond would afford the observed dihydropyran with recovery of the catalytic species.

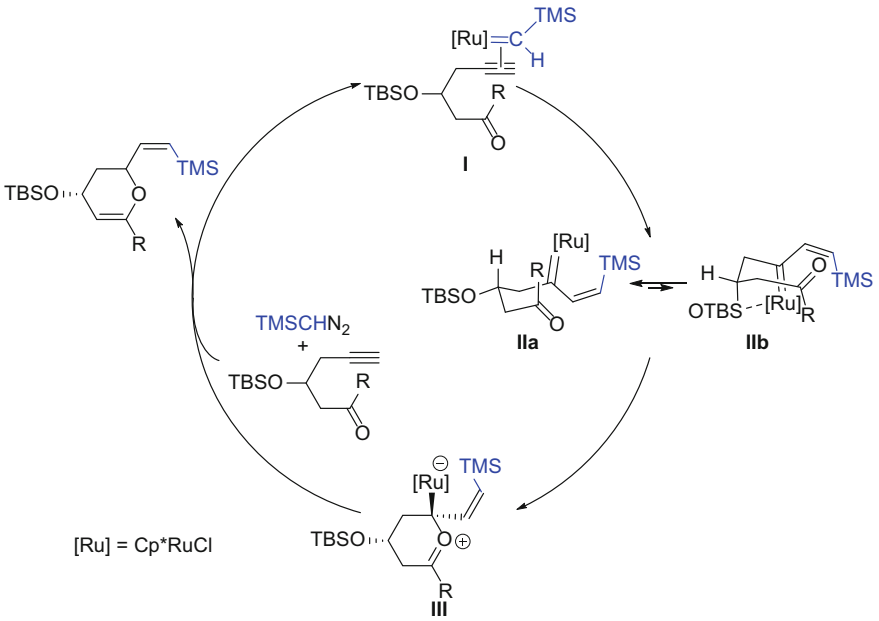

Scheme 11 Proposed mechanism for the ruthenium-catalyzed heterocyclization of alkynals and alkynones

4 Heterocyclizations via Vinyl Ruthenium Carbene Intermediates from *Ortho*-(Alkynyloxy)Benzylamines

Other catalytic heterocyclizations have been achieved by trapping the in situ generated electrophilic vinyl ruthenium carbenes (obtained by treatment of catalytic amounts of $Cp^*RuCl(cod)$ with ω-alkynyl benzylamines and (trimethylsilyl)diazomethane) with *N*-nucleophiles from benzylamine derivatives. Indeed, ruthenium-catalyzed intramolecular heterocyclization of *ortho*-(alkynyloxy)benzylamines gave rise to 2,2-disubstituted dihydro-1,3-benzoxazines, which would involve a nucleophilic attack of the amine to the in situ generated vinyl ruthenium carbene intermediate followed by a skeletal rearrangement (Scheme 12) [45]. The presence of the oxygenated tether was crucial for the rearrangement since the corresponding alkynyl benzylamine afforded the linear conjugated diene instead the cyclized product (probably by β-hydrogen elimination from the vinyl ruthenium carbene intermediate).

Substitution on the aromatic ring of benzylamines is well tolerated for this transformation (Table 1). Both electron-donating and electron-withdrawing substituents are well accepted since the corresponding 1,3-benzoxazines were obtained in reasonably good yields being slightly better for electron-poor aromatic rings. On the other hand, functionalized halo-1,3-benzoxazines could be easily prepared using

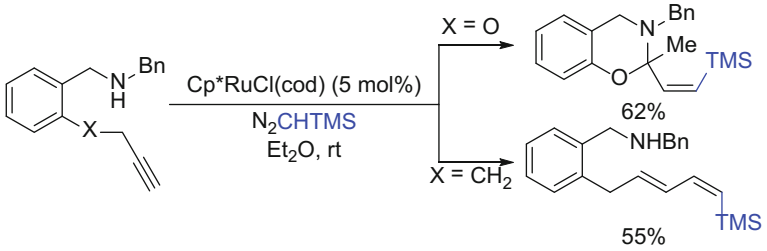

Scheme 12 Ruthenium-catalyzed reactions of C- and O-tethered *ortho*-alkynylbenzylamines

Table 1 Ruthenium-catalyzed heterocyclization of aryl substituted *ortho*-(alkynyloxy)-benzylamines to 1,3-benzoxazines

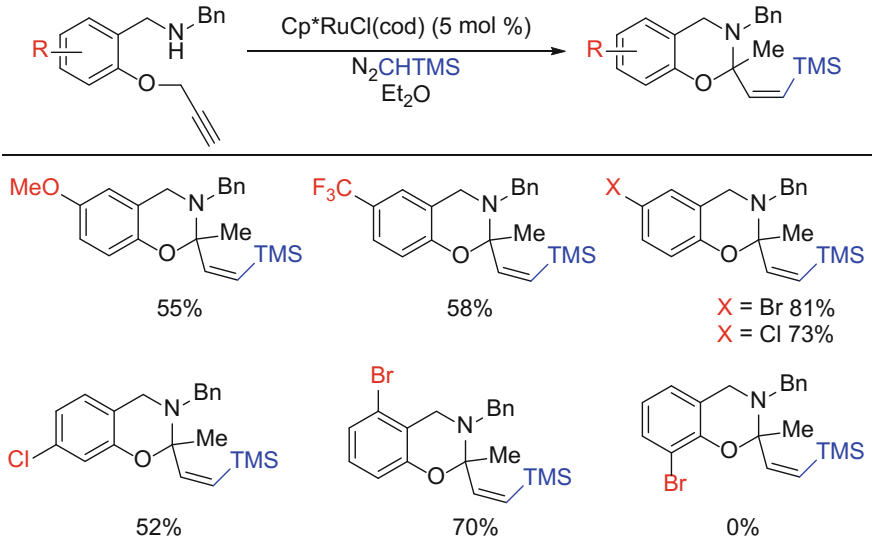

this methodology, which facilitates other functionalizations by further manipulations, with the exception of the *ortho* bromo substituted 1,3-benzoxazines due, most probably, to steric reasons.

Ortho-(Alkynyloxy)benzylamines bearing alkynyl substituents also cyclized to give the corresponding 1,3-benzoxazines in fairly good yields, although longer reaction times, high catalyst loadings and/or heating to 65 °C was necessary to proceed (Scheme 13).

Primary and secondary alkyl substituted benzylamines such as propyl and cyclohexyl are well tolerated and gave rise to the corresponding 1,3-benzoxazines in good yields. In the case of the *N*-allyl substituted benzylamine, the recovery of the allyl group intact seems to indicate that polar nucleophile/electrophile interactions dominate the reactivity of the putative carbene intermediate (Scheme 14).

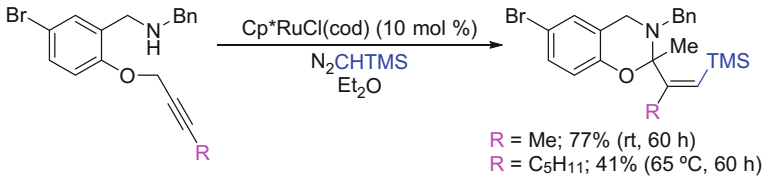

Scheme 13 Ruthenium-catalyzed heterocyclization of alkynyl substituted *ortho*-(alkynyloxy)-benzylamines to 1,3-benzoxazines

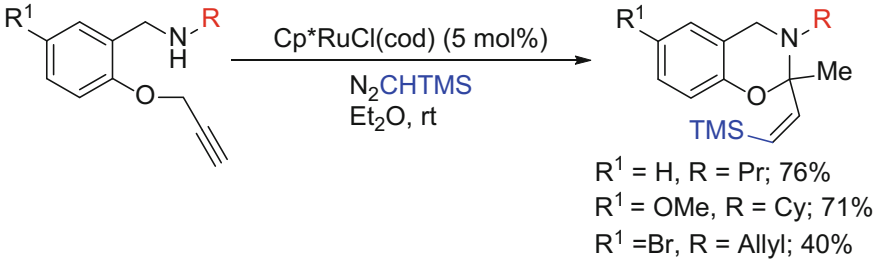

Scheme 14 Ruthenium-catalyzed heterocyclization of *N*-substituted *ortho*-(alkynyloxy)-benzylamines to 1,3-benzoxazines

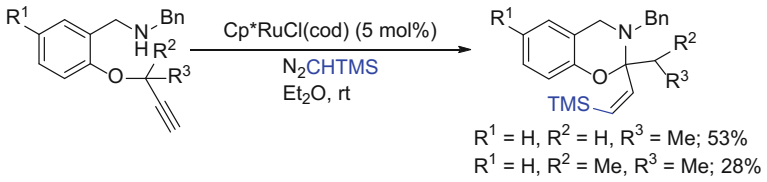

Scheme 15 Ruthenium-catalyzed heterocyclization of propargyl substituted *ortho*-(alkynyloxy)-benzylamines to 1,3-benzoxazines

The reaction also tolerates substrates substituted at the propargylic position. When the *ortho*-(alkynyloxy)benzylamine bears one methyl substituent at the propargylic position, the rearranged 2-ethyl substituted 1,3-benzoxazine was obtained in moderate yield. Similarly, when the *ortho*-(alkynyloxy)benzylamine bears two methyl substituents at the propargylic position, the rearranged 2-isopropyl substituted 1,3-benzoxazine was obtained in low yield (Scheme 15).

The proposed mechanism would start with the smooth formation of the vinyl ruthenium intermediate **II**, in which the nitrogen lone pair might coordinate to the ruthenium to give the 18 e^- complex. Then, nucleophilic attack of the nitrogen to the electrophilic ruthenium carbene would afford the zwitterionic species **III** which could evolve by ring opening (phenoxide as good leaving group) to a transient enamine **IV** with recovery of catalytic species **I**. Finally, iminium formation from **IV** is trapped with the phenoxide to afford the final 1,3-benzoxazine (Scheme 16).

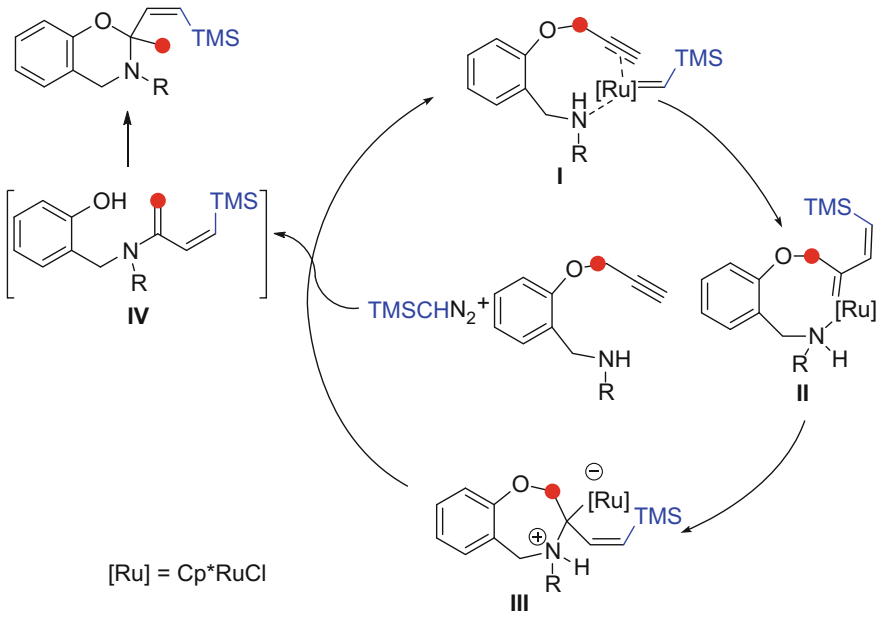

Scheme 16 Proposed mechanism for the ruthenium-catalyzed heterocyclization of *ortho*-(alkynyloxy)benzylamines to 1,3-benzoxazines

5 DFT Studies of the TMS-Substituted Vinyl Ruthenium Carbenes: Formation and Stereoselective Cyclizations

In all the previous transformations, the geometry of the double bond (stereoselectivity) of the in situ generated vinyl carbene intermediate and the final product seems to be dependent of the type of cyclization (type of mechanism), being *E* configuration in the case of the [1,n]-hydride transfer/cyclization and *Z* configuration for the oxygen and nitrogen nucleophilic trap of the electrophilic carbene. An early explanation for the origin of the stereoselectivity derives from the assumption of formation of the vinyl ruthenium carbene during the electrocyclic opening of ruthenacyclobutene (Scheme 1), in which the Cp^* and Y groups should be *anti* to avoid unfavorable steric interactions. If Y = $SiMe_3$, strong attractive interactions should be established between $SiMe_3$ and Cl groups forcing a favourable *Z* configuration after ring-opening. On the other hand, if Y ≠ $SiMe_3$ steric hindrance should be the major driving force for the torquoselectivity delivering favourable *E*-configuration of the double bond (Scheme 17) [28].

To clarify this early assumptions for the formation of vinyl ruthenium carbenes, we carried out DFT calculations for the [1,n]-hydride transfer/cyclization (Scheme 18) [46]. The calculations showed the presence of three conformers in equilibria for the initial ruthenium carbene complex coordinated to the alkyne:

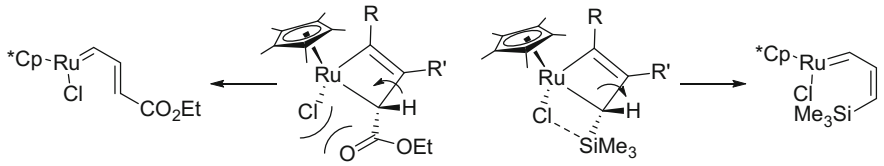

Scheme 17 *Z*- and *E*-vinyl ruthenium carbenes by ring-opening of ruthenacyclobutenes

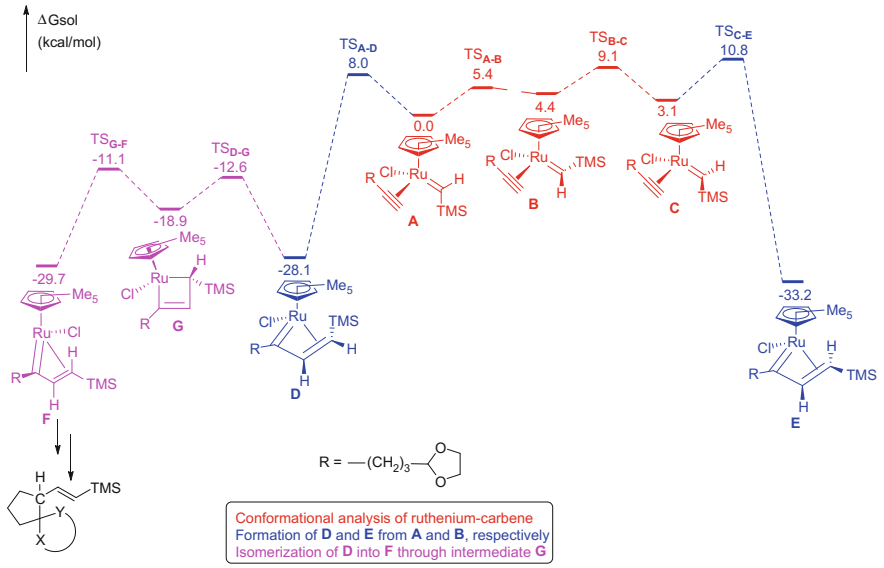

Scheme 18 Free energy profile for the conformational analysis of ruthenium carbene, formation of **D**, **E** and isomerization of **D** to **F** for the [1,5]-hydrogen migration/cyclization of alkynylacetals using the B3LYP-D3/LANL2DZ for Ru and 6-311++G(d,p) for all other atoms, SCRF using SMD model (diethyl ether). Energies are relative to **A** and are mass balanced

(a) the more stable conformer **A**, with the hydrogen pointing to the Cp^* ring, and (b) two less stable conformers **B** and **C**, with the TMS group pointing to the Cp^* ring backwards and forward, respectively.

This initial ruthenium carbene complex can evolve either to the *Z*- or *E*- vinyl ruthenium carbene species **D** and **E**, respectively, through transition states separated by 2.8 kcal mol^{-1} that favor the formation of *Z* isomer **D**. The most favorable pathway for the [1,5]-hydrogen transfer/cyclization process involved the initial isomerization of *Z* isomer **D** to the *E* isomer **F**, distinct stereoisomer of **E**, through ruthenacyclobutene intermediate **G**, which could explain the *E* geometry of the vinyl substituents of the final products in these transformations.

For the cases of vinyl ruthenium carbene intermediates that undergo nucleophilic attack either by an oxygenated (alkynals and alkynones) or nitrogenated (*ortho*-(alkynyloxy)benzylamines) nucleophile, the most favorable pathway would

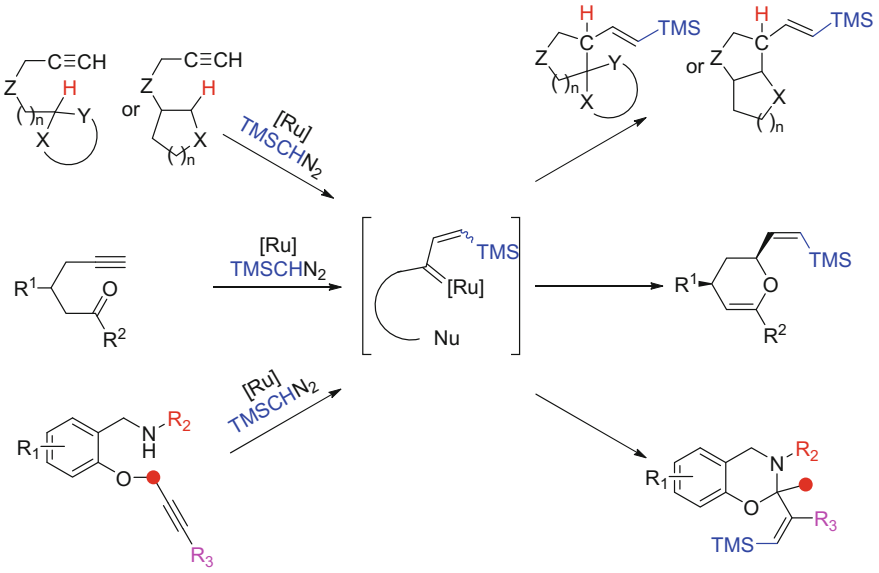

Scheme 19 New modes of catalytic cyclizations from vinyl ruthenium carbene intermediates

start from intermediates of type **D** without isomerization, which would explain the formation of the final products bearing vinyl substituents with *Z* geometry.

6 Conclusions

In summary, it has been described new modes of catalytic cyclizations from the in situ generated vinyl ruthenium carbene intermediates by the intramolecular nucleophilic attack to the carbene (Scheme 19). Complex spiro and fused bicyclic structures can be obtained by an intramolecular neutral/redox process which involves a mild formation of catalytic vinylic ruthenium carbenes from alkynyl acetals, ethers and amines which behave as hydride acceptors.

On the other hand, trapping the in situ generated catalytic vinyl ruthenium carbenes with carbonyl nucleophiles allowed the synthesis of valuable 2-vinyl dihydropyrans.

Finally, trapping the catalytic vinyl ruthenium carbenes with nitrogen nucleophiles generated from alkynyloxybenzylamines afforded the rearranged 2,2-disubstituted 1,3-benzoxazines.

Acknowledgements This work was supported by the Spanish MINECO (project CTQ2014-59015R), the Xunta de Galicia (project GRC2014/032) and the European Regional Development Fund (projects CTQ2014-59015R and GRC2014/032). We also thank the ORFEO-CINQA network (CTQ2014-51912REDC). D. P. thanks XUGA for a predoctoral contract. We are also grateful to the CESGA (Xunta de Galicia) for computational time.

References

1. Moss RA, Doyle MP (eds) (2014) Contemporary Carbene Chemistry. John Wiley & Sons, Inc., Hoboken.
2. Hoveyda AH, Malcolmson SJ, Meek SJ, Zhugralin AR (2010) Angew Chem Int Ed 49:34.
3. Kotha S, Dipak MK (2012) Tetrahedron 68:397.
4. Fuerstner A (2013) Science 341:1357.
5. Vougioukalakis GC, Grubbs RH (2010) Chem Rev 110:1746.
6. Connon SJ, Blechert S (2003) Angew Chem Int Ed 42:1900.
7. Nolan SP, Clavier H (2010) Chem Soc Rev 39:3305.
8. Kress S, Blechert S (2012) Chem Soc Rev 41:4389.
9. Grubbs RH (2004) Tetrahedron 60:7117.
10. Masuda T, Higashimura T (1984) Acc Chem Res 17:51.
11. Katz TJ, Sivavec TM (1985) J Am Chem Soc 107:737.
12. Fox HH, Wolf MO, O'Dell R, Lin BL, Schrock RR, Wrighton MS (1994) J Am Chem Soc 116:2827.
13. Diver ST, Giessert AJ (2004) Chem Rev 104:1317.
14. Katz TJ (2005) Angew Chem Int Ed 44:3010.
15. Li J, Lee D (2011) Eur J Org Chem 2011:4269.
16. Rubin M, Rubina M, Gevorgyan V (2007) Chem Rev 107:3117.
17. Zaragoza Dorwald F (1998) Metal Carbenes in Organic Synthesis. Wiley-VCH, Weinheim.
18. Doyle MP, McKervey MA, Ye T (1998) Modern Catalytic Methods for Organic Synthesis with Diazo Compounds: From Cyclopropanes to Ylides. Wiley, New York.
19. DeAngelis A, Panish R, Fox JM (2016) Acc Chem Res 49:115.
20. Ford A, Miel H, Ring A, Slattery CN, Maguire AR, McKervey MA (2015) Chem Rev 115:9981.
21. Hu F, Xia Y, Ma C, Zhang Y, Wang J (2015) Chem Commun 51:7986.
22. Dorel R, Echavarren AM (2015) J Org Chem 80:7321.
23. Archambeau A, Miege F, Meyer C, Cossy J (2015) Acc Chem Res 48:1021.
24. Qian D, Zhang J (2015) Chem Soc Rev 44:677.
25. Wei F, Song C, Ma Y, Zhou L, Tung C-H, Xu Z (2015) Sci Bull 60:1479.
26. Xia Y, Zhang Y, Wang J (2013) ACS Catal 3:2586.
27. Vovard-Le Bray C, Derien S, Dixneuf PH (2010) C R Chim 13:292.
28. Le Paih J, Vovard-Le Bray C, Derien S, Dixneuf PH (2010) J Am Chem Soc 132:7391.
29. Le Paih J, Derien S, Oezdemir I, Dixneuf PH (2000) J Am Chem Soc 122:7400.
30. Vovard-Le Bray C, Derien S, Dixneuf PH (2009) Angew Chem Int Ed 48:1439.
31. Eckert M, Monnier F, Shchetnikov GT, Titanyuk ID, Osipov SN, Toupet L, Derien S, Dixneuf PH (2005) Org Lett 7:3741.
32. Monnier F, Castillo D, Derien S, Toupet L, Dixneuf PH (2003) Angew Chem Int Ed 42:5474.
33. Monnier F, Vovard-Le Bray C, Castillo D, Aubert V, Derien S, Dixneuf PH, Toupet L, Ienco A, Mealli C (2007) J Am Chem Soc 129:6037.
34. Vovard-Le Bray C, Derien S, Dixneuf PH, Murakami M (2008) Synlett 193.
35. Girard SA, Knauber T, Li C-J (2014) Angew Chem Int Ed 53:74.
36. Rouquet G, Chatani N (2013) Angew Chem Int Ed 52:11726.
37. Jazzar R, Hitce J, Renaudat A, Sofack-Kreutzer J, Baudoin O (2010) Chem Eur J 16:2654.
38. Chen X, Engle KM, Wang D-H, Yu J-Q (2009) Angew Chem Int Ed 48:5094.
39. Bergman RG (2007) Nature 446:391.
40. Godula K, Sames D (2006) Science 312:67.
41. Wang L, Xiao J (2014) Adv Synth Catal 356:1137.
42. Haibach MC, Seidel D (2014) Angew Chem Int Ed 53:5010.
43. Cambeiro F, López S, Varela JA, Saá C (2012) Angew Chem Int Ed 51:723.
44. Cambeiro F, López S, Varela JA, Saá C (2014) Angew Chem Int Ed 53:5959.
45. González-Rodríguez C, Suárez JR, Varela JA, Saá C (2015) Angew Chem Int Ed 54:2724.
46. Cambeiro F, Martínez-Núñez E, Varela JA, Saá C (2015) ACS Catal 5:6255.

Radical-Based Late Stage C–H Functionalization of Heteroaromatics in Drug Discovery

Yuta Fujiwara and Phil S. Baran

Abstract The development of the radical-based C–H functionalization of heteroaromatics is in demand, since it can directly introduce medicinally important functionalities (Me, CF_3, etc.) to druggable compounds during the late stage of synthesis. Classical methods using alkyl carboxylic acids and alkyl halides as a radical precursor have been reported, however, they are still under development regarding the reaction conditions and the substrate scope. These drawbacks inspired us to invent two radical-based C–H functionalization methods. The first topic covers the C–H alkylation and arylation using boronic acids as a radical precursor, while the latter covers the C–H alkylation using sulfinate salts as a radical precursor. Additionally, new reagents for the C–H functionalization were invented during the course of these studies. Under ambient conditions using inexpensive reagents and simple procedures, our methods can supply a rapid access to complex molecules which are difficult to prepare by traditional methods. Due to these features and the growing demand for the late stage functionalization in drug discovery, our strategies have already been utilized by Pfizer and Sigma-Aldrich.

Keywords Late stage functionalization · C–H functionalization · Trifluoromethylation · Langlois salt · Minisci reaction · Sulfinate

Y. Fujiwara (✉)
Department of Medicinal Chemistry, Meiji Seika Pharma Co., Ltd.,
760 Morooka-Cho, Yokohama-shi, Kanagawa 222-8567, Japan
e-mail: yuuta.fujiwara@meiji.com

P.S. Baran
Department of Chemistry and Chemical Biology, The Scripps Research Institute,
10550 North Torrey Pines Rd, La Jolla, CA 92037, USA
e-mail: pbaran@scripps.edu

K. Tomioka et al. (eds.), *New Horizons of Process Chemistry*,
DOI 10.1007/978-981-10-3421-3_8

1 Introduction

With the progress in C–H functionalization, late stage functionalization (LSF) has become a powerful tool in drug discovery [1]. It can directly introduce small functionalities, such as a methyl group, to a pharmacophore and efficiently provide important information about structure-activity relationships (SAR), structure-property relationships (SPR), and absorption-distribution-metabolism-excretion (ADME), while traditional methods usually require multi-step syntheses to obtain them. It can also be useful for the preparation of radiolabelled molecules and large-scale synthesis in process chemistry to prepare drug candidates for preclinical safety studies using higher animal models.

The radical-based C–H functionalization of heteroaromatics is undeveloped, fruitful, and basic research for the LSF of druggable molecules, because their motifs are found in many pharmaceuticals. To demonstrate the potential of this methodology, we began with the synthesis of irinotecan. The radical-based C–H ethylation of a complex natural product was designed as the key step in the synthesis (Scheme 1a) [2]. Chemists developed this radical-based strategy in 1991, but this field has not been well-studied. Rapid progress has come to this field. In 2012, MacMillan reported C–H trifluoromethylation using trifluoromethanesulfonyl chlorides as a radical precursor with visible light and photoredox catalysts [3].

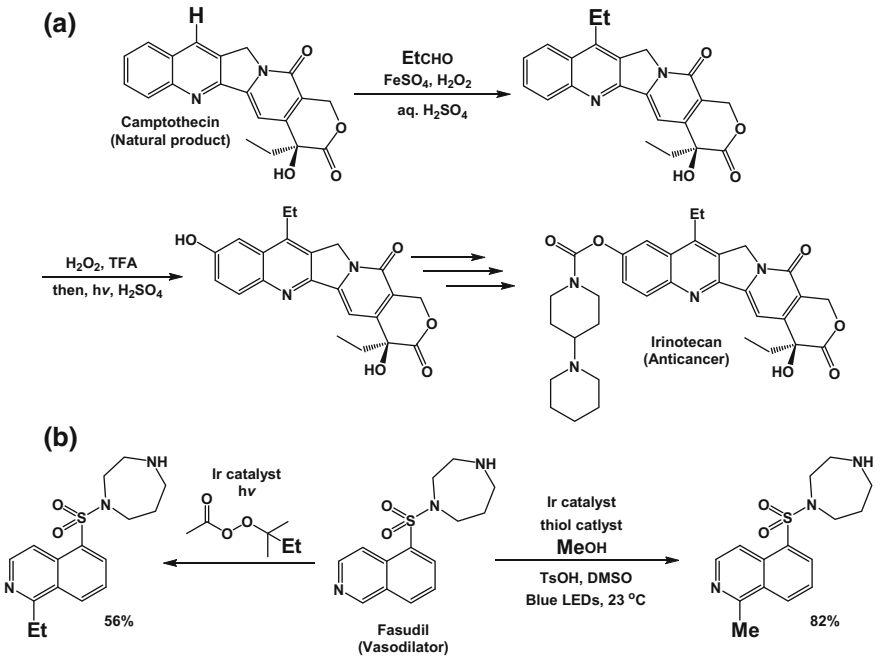

Scheme 1 Applications of radical-based C–H alkylation to pharmaceuticals

Under similar conditions, the alkyl peroxide-mediated C–H alkylation [4] and alkyl alcohol-mediated C–H alkylation [5] have been reported. They cover the C–H functionalization of complex pharmaceuticals, such as atorvastatin and fasudil (Scheme 1b), and highlighted that a radical-based C–H functionalization would be a powerful tool in drug discovery.

In this report, we describe the development of two radical-based C–H functionalization methods. The first topic covers the C–H alkylation and arylation using boronic acids as a radical precursor. The latter covers the C–H alkylation using sulfinate salts as a radical precursor.

2 C–H Functionalization with Aryl/Alkylboronic Acids

2.1 Direct C–H Arylation of Heteroaromatics with Arylboronic Acids

The introduction of aryl groups to heteroaromatics is widely employed in various scientific fields, such as natural product synthesis and drug discovery. General access to arylated heteroaromatics is the Pd-catalyzed cross coupling, such as the Suzuki coupling [6]. Recently, the transition metal catalyzed (Pd, Rh, Ni, etc.) direct C–H arylation methods for heteroaromatics have been reported [7]. On the other hand, the radical-based C–H functionalization is an underdeveloped area, and the mild protocol for the generation of aryl radicals is unknown.

Due to these drawbacks (Fig. 1) and our recent studies regarding the silver catalyzed regioselective oxidation, highly complex alkaloids, such as palau'amine, we designed a C–H arylation which is based on the Ag-catalyzed addition of radicals to heteroaromatics (Minisci reaction) [8]. A classical method can generate an alkyl or acyl radical through the oxidative decarboxylation of the corresponding carboxylic acids, while our first approach for the generation of an aryl radical using benzoic acid failed. We then postulated that arylboronic acid could be a significant radical precursor. Based on the report for the C–H arylation under the $Mn(OAc)_3$-mediated C–H functionalization of electron-rich heteroaromatics [9], the homolytic cleavage of the C–B bond could be induced in a manner similar to decarboxylation. Actually, the C–H arylation using arylboronic acids worked even at room temperature (rt) (Scheme 2a) [10]. The procedure is very simple. To a stirred solution of the in situ generated heteroaromatics/trifluoroacetic acid (TFA) salt (1 eq) and arylboronic acid (1.5 eq) in dichloromethane (DCM)/H_2O (1:1 v:v) were added silver nitrate ($AgNO_3$) and potassium persulfate ($K_2S_2O_8$) at rt. The reaction mixture was stirred at rt for 3–12 h. An inert atmosphere or purification of solvents/reagents is not necessary. These features [simplicity of procedure, mild conditions, inexpensive reagents ($AgNO_3$ ca. 1 \$/g, $K_2S_2O_8$ ca. 1 cent/g), solvents, and scalability] indicated the potential of this reaction in process chemistry. In addition, it can also be a powerful tool in medicinal chemistry. The reaction

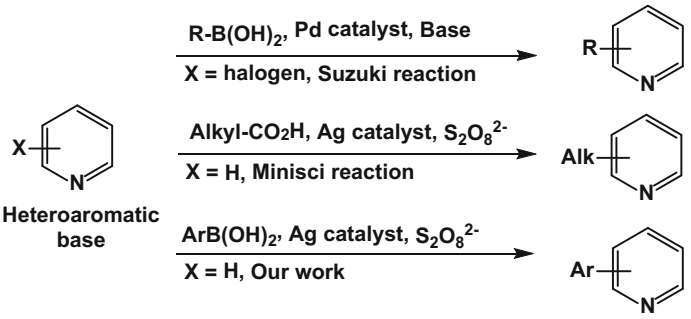

Fig. 1 Overview of the synthesis of arylated electron-deficient heteroaromatics

displayed a broad scope with respect to both heteroaromatics and arylboronic acids and functional group tolerance, although the regioselectivities and yields are insufficient. The most notable example of this reaction is the direct C–H arylation of complex druggable molecules (Scheme 2b). These results display the utility of this reaction in the LSF, because multisteps, which involve prefunctionalization, such as halogenation, are generally required for the synthesis of these products.

The proposed mechanism can be explained in a manner similar to the Minisci reaction (Fig. 2). In the presence of a silver (I) salt, the persulfate anion is cleaved into the sulfate dianion and sulfate radical anion. This radical can react with boronic

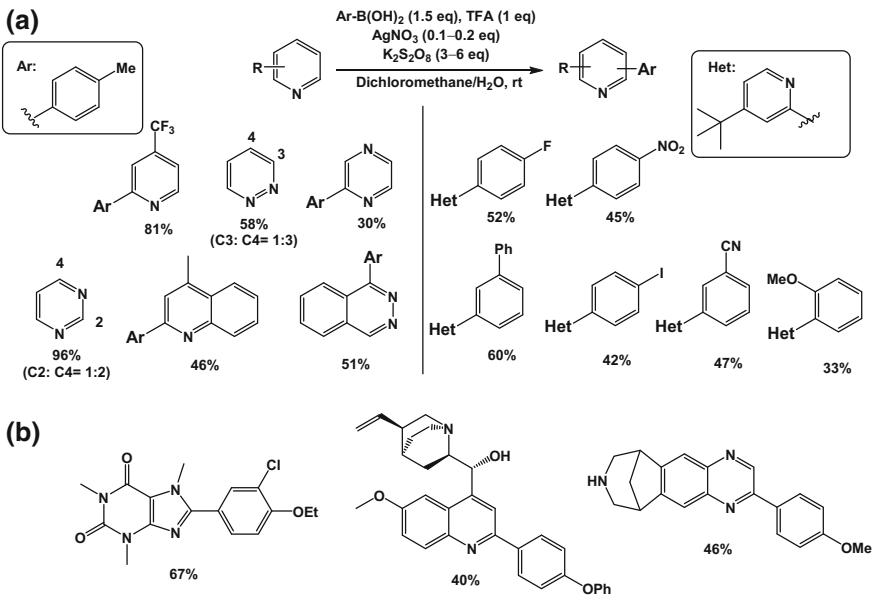

Scheme 2 Scope of the coupling of arylboronic acids to heteroaromatics

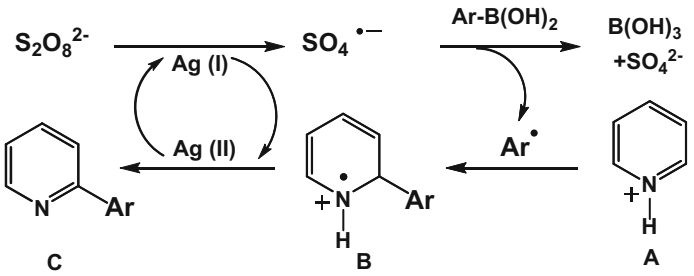

Fig. 2 Proposed mechanism for the direct C–H arylation

acid and provide the aryl radical [11, 12]. It is probable that this aryl radical reacts with protonated heterocycles **A** to form the radical cation **B**, which is reoxidized by silver (II), producing the desired product **C** and regenerating the silver (I) catalyst. This hypothesis led us to investigate new substrates which have a high capacity to receive radicals.

2.2 C–H Functionalization of Quinones with Aryl/Alkylboronic Acids

The quinone moiety, which possesses electron and proton transfer properties, is found in various chemicals, such as natural products and medicines [13, 14]. Among them, arylated quinones are useful in photosynthesis and the dye industry due to their unique visual and electronic properties [15, 16]. However, the electronic properties make their synthesis difficult in the case of the addition of organometallics, Heck coupling and prehalogenation followed by a palladium-catalyzed cross coupling. In the case of the radical-based C–H functionalization, conventional methods require unstable and explosive aryldiazonium salts, which are difficult to prepare. Therefore, a practical method for the direct access to arylated quinones is in demand.

Based on the proposed mechanism for the radical-based C–H arylation of heteroaromatics using arylboronic acids and the inherent reactivity of quinones to radicals, it was assumed that our method could be applicable to the direct arylation of quinones. This prediction was verified when quinones were exposed to arylboronic acids (1.5 eq) with the combination of $AgNO_3$ (0.2 eq) and $K_2S_2O_8$ (3 eq) in a DCM/H_2O solvent system (the use of α,α,α-trifluorotoluene as an organic solvent significantly improved the efficiency when multi-functionalized quinones were employed as the substrate). Almost all the reactions were completed within 24 h at rt without bis-arylation and O-arylation, and the arylated quinones were obtained with good yields after purification (Scheme 3a) [17].

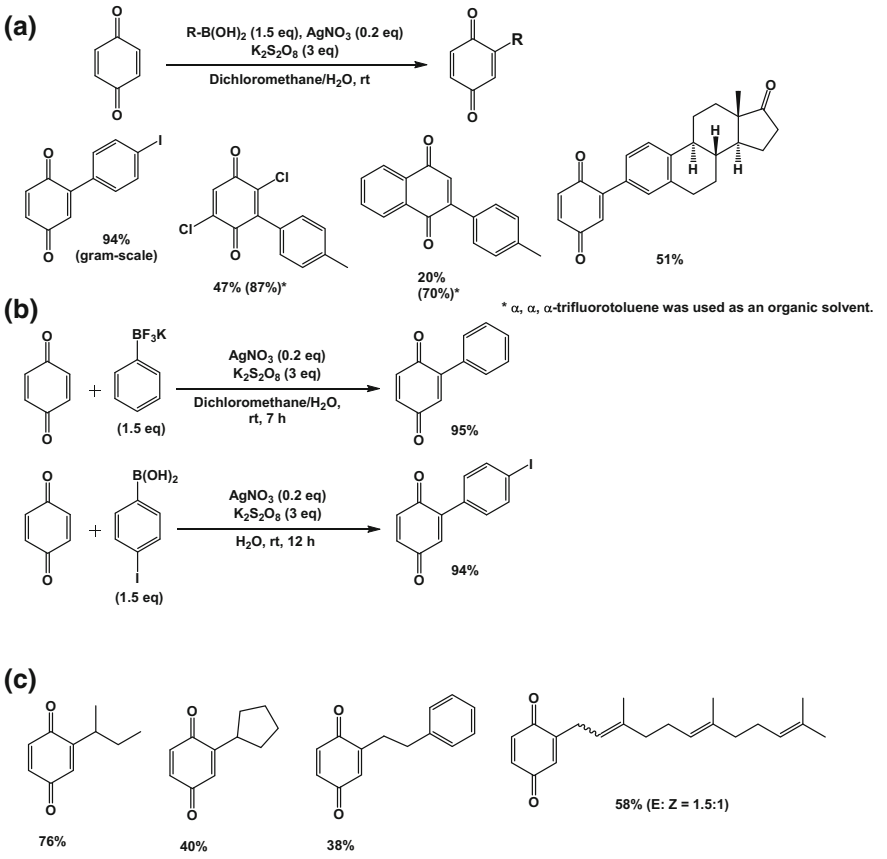

Scheme 3 C–H arylation/alkylation of quinones using boronic acids

In addition, this reaction displayed several features which were different from the C–H arylation of heteroaromatics. First, the trifluoroborates (Molandar salts) are applicable as a radical precursor. Second, the organic solvent of the biphasic solvent system can be omitted. The desired products were obtained in quantitative yield in both cases (Scheme 3b). The most notable feature is shown in Scheme 3c. Several alkylboronic acids and the trifluoroborate of farnesol provided the desired products in decent to fair yields. Unfortunately, the benzyl, vinyl and *tert*-butyl boronic acids failed to give the desired products. These results led us to design the divergent synthesis of natural products which have a quinone or hydroquinone unit in their structure.

2.3 *Divergent Synthesis of Meroterpenoids Using Radical Based C–H Alkylation*

Quinone or hydroquinone units are found in many terpenoids [18–20]. These natural products have attracted much attention because of their structural diversity and biological activity for anti-fungal, anti-cancer and anti-HIV [21–23]. Despite these important biological activities, traditional synthesis requires more than 12 steps due to the use of protecting groups and subsequent redox manipulations. Therefore, a quick approach to these natural products is in demand. As shown in Scheme 4a, it was proposed that the direct coupling of a terpenoid donor with a non-terpenoid donor could minimize the reliance on concession steps. Based on the results of the C–H alkylation of quinones, the non-terpenoid donor would be derived from 1,4-benzoquinone, and the terpenoid donor would be derived from the alkyl radical precursor.

Based on this hypothesis, the radical-based C–H alkylation using 1,4-benzoquinone and various radical precursors was investigated. Our first approaches using a variety of radical precursor, such as carboxylic acids, iodides, and trifluoroborates which were derived from (+)-sclareolide, failed. However, it was found that the use of only trifluoroborates as a radical precursor gave the interesting byproduct, (+)-yahazunone, in 10–20% yield. Furthermore, the use of borono-sclareolide, 5 eq of an oxidant and degassing of the reaction gave (+)-chromazonarol in an improved 60% yield on a gram-scale (Scheme 4b).

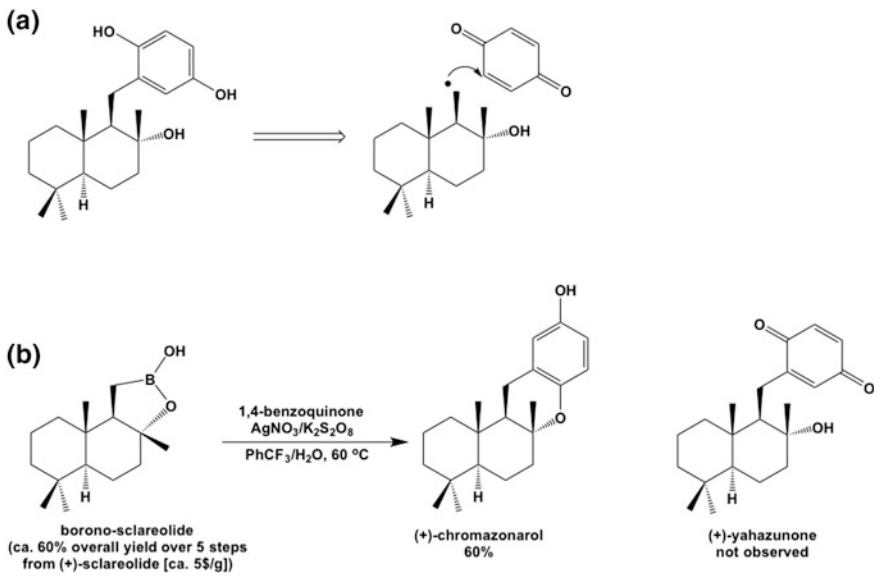

Scheme 4 A global approach to meroterpenoids utilizing borono-sclareolide

This radical precursor was prepared in an ca. 60% overall yield from (+)-sclareolide (ca. $5/g) in 5 steps. Including the above transformation, borono-sclareolide displayed the ability as a divergent intermediate to rapidly access 10 meroterpenoids: (+)-chromazonarol (6 steps, 34% overall yield), (−)-isozonarol and (−)-zonarol (7 steps, 25% overall yield), (−)-yahazunone (7 steps, 29% overall yield), (+)-yahazunol (8 steps, 26% overall yield), (−)-zonarone and (−)-isozonarone (8 steps, 24% overall yield), (+)-8-*epi*-puupehedione (9 steps, 8% overall yield), the formal synthesis of (−)-pelorol (11 steps, 8.5% overall yield), and synthesis of (+)-dictyvaric acid (7 steps, 33% overall yield); (Scheme 5) [24].

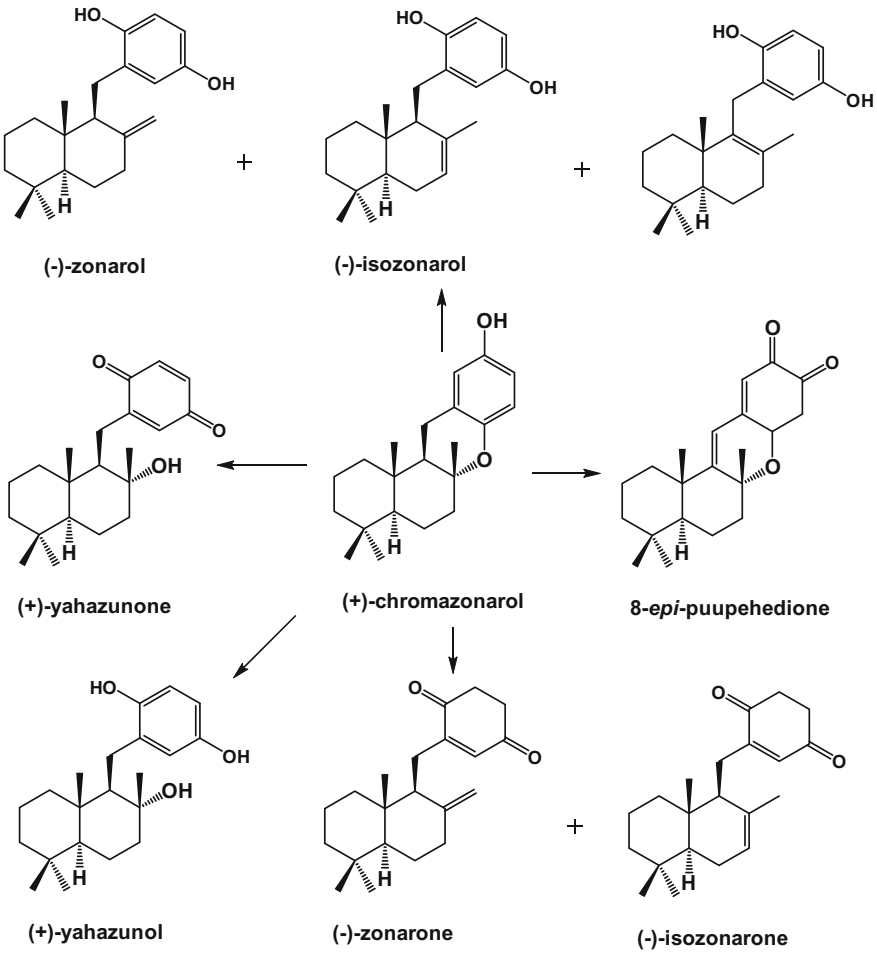

Scheme 5 Divergent synthesis of meroterpenoids via (+)-chromazonarol

3 C–H Functionalization with Sodium/Zinc Alkyl Sulfinates

3.1 Radical-Based C–H Trifluoromethylation of Heteroaromatics

The introduction of the trifluoromethyl group to heteroaromatics is becoming a powerful tool in the development of pharmaceuticals, agrochemicals, liquid crystals, dyes, and polymers, because it can easily modify the chemical space, molecular weight, lipid solubility, electron density, etc. [25–30]. Due to these drawbacks, a practical and rapid introduction of the trifluoromethyl group is desirable and some elegant methodologies have been reported [31–38]. Among them, the direct C–H trifluoromethylation of heteroaromatics is an undeveloped area in spite of their high potential for drug development. These drawbacks and radical-based C–H alkylation and arylation using boronic acids led our attention on the radical based C–H trifluoromethylation of heteroaromatics. Unfortunately, the reaction with $KF_3B–CF_3$ or $K(OMe)_3B–CF_3$ as a radical source failed for the trifluoromethylation of pyridine derivatives although the use of boronic acids or trifluoroborates was supposed to be important as the trifluoromethyl radical source. Over 500 reactions using various trifluoromethylation reagents, oxidants, Lewis acids and solvents, revealed that only the use of trifluoromethanesulfinate (Langlois salt) gave desired the trifluoromethylated product. This result was surprising to us because Langlois's pioneering studies covered the trifluoromethylation of electron rich substrates, such as anisole, anilines and enol, due to their electrophilic nature [39, 40]. Further investigation revealed that the use of Langlois salt, an aqueous solution of *t*BuOOH (TBHP), and the two-phase solvent system of CH_2Cl_2 and H_2O gave the desired product with an acceptable yield. Using these standard conditions, various heterocycles were directly trifluoromethylated at room temperature (Scheme 6) [41]. A second addition of the Langlois salt and TBHP drove the reaction toward completion when the conversion was exceptionally low. In contrast, the reaction for a highly reactive substrate, such as caffeine and uracil, could even be carried out under purely aqueous conditions without an organic workup. Solvent effects play a significant role in not only the conversion, but also the regioselectivity. In the case of 4-acetyl pyridine, a complete reversal in regioselectivity was observed by substituting dimethysulfoxide (DMSO) for DCM [42].

The combination of previous studies with our experimental results allowed for a putative mechanism to be proposed (Fig. 3). The *tert*-butoxy radical, presumably generated from trace metals, which contaminate the Langlois salt (in the Langlois salt, many kinds of metals, such as Fe and Zn, were detected by a trace metal analysis), reacts with $CF_3SO_2^-$ to provide $CF_3SO_2\cdot$. This transient intermediate disproportionates, releasing SO_2 and $CF_3\cdot$ (CF_3 radical was detected in situ EPR studies of Langlois salt and TBHP in aqueous solution). The fate of the inherently reactive CF_3 radical after its generation can follow many pathways. The productive pathway involves capture of the CF_3 radical with Ar–H, followed by reoxidation to

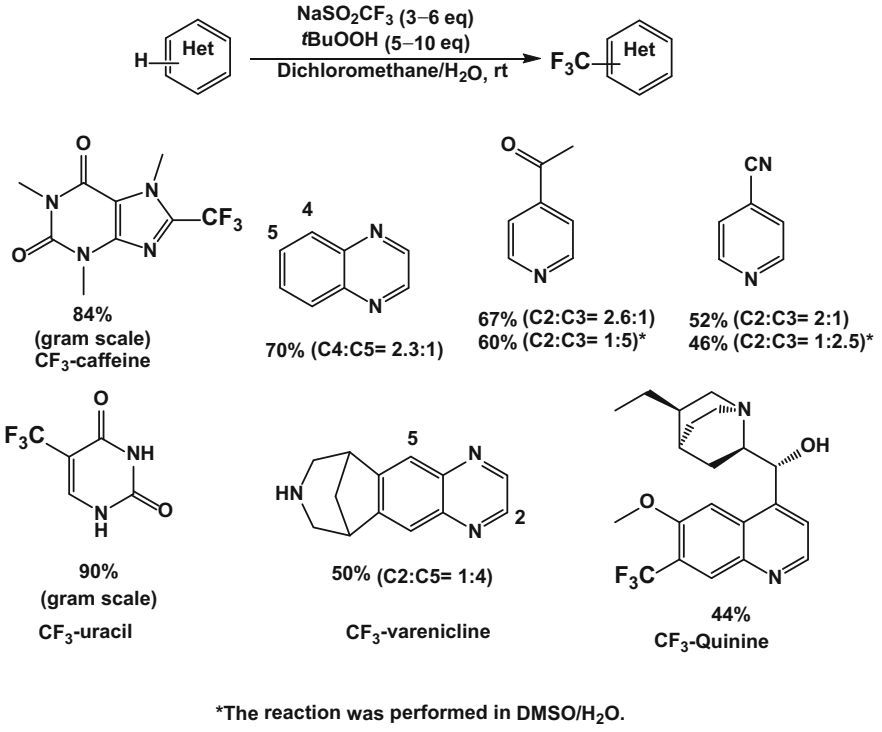

Scheme 6 C–H trifluoromethylation of heteroaromatics using Langlois salt

Ar–CF_3, concomitantly generating another molecule of the *tert*-butoxy radical. Two competitive pathways give two undesired byproducts. Abstraction of a hydrogen atom yields CF_3H (observed by ^{19}F-NMR). Alternatively, the reaction with isobutene, which is generated from TBHP followed by the reaction with an arene, leads to an alkyltrifluoromethyl byproduct, such as **A** in Fig. 3 (confirmed by ^{1}H-NMR and MS).

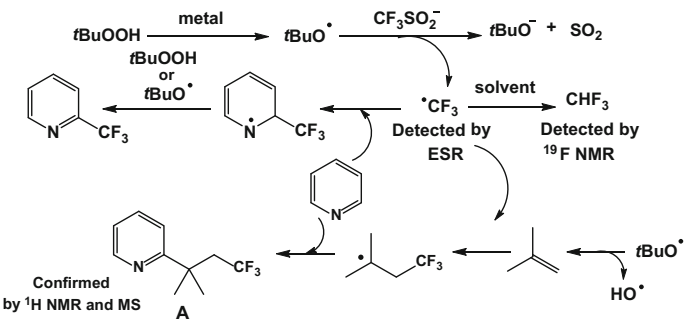

Fig. 3 Proposed mechanism for the C–H trifluoromethylation

These surprising reactivities of the Langlois salt and the proposed mechanism encouraged us to investigate the utility of sulfinates on the C–H functionalization of heteroaromatics. Fortunately, no paper had been published about the sulfinate-mediated C–H functionalization except for Langlois's report when we started this project.

3.2 *Direct and Practical C–H Difluoromethylation Using $Zn(SO_2CF_2H)_2$*

Heteroaromatics are found in a large number of pharmaceuticals, natural products, agrochemicals, etc. Direct introduction of a small functional group, such as CF_3 [25–30] or the Me [43] group, to them can extremely simplify their synthesis or modification because traditional access to functionalized heteroaromatics requires pre-functionalization. Due to these drawbacks and the proposed mechanism of the C–H trifluoromethylation, we designed new C–H functionalization methods with various sulfinate salts. Our idea begins with the estimation of the radical precursors based on the bond dissociation energy (BDE) (Fig. 4).

In contrast to their more widely available relatives, carboxylic acids, sulfinates have a significantly weaker energy barrier for homolysis leading to radicals. This relatively weak C–S bond in sulfinates makes them ideal radical precursors as compared to carboxylic acids, which often require strong oxidants, heat, light and specialized transition-metal catalysis. Actually, trifluoroacetic acid or its salt did not act as the CF_3 radical precursor under mild reaction conditions, while the use of the Langlois salt enabled the radical-based C–H trifluoromethylation.

As a starting point to demonstrate our hypothesis for the invention of a new toolkit for the C–H functionalization of heteroaromatics, the sulfinate-mediated C–H difluoromethylation was chosen because the seemingly simple extension of the C–H trifluoromethylation using the Langlois salt allows us to smoothly carry out the research.

Our approach started from the synthesis of various difluoromethane sulfinates, because it was assumed that the metal counteraction could make a difference in the reactivity. After several strategies to prepare them, difluoromethane sulfonyl chloride was recognized as a convenient and commercially available starting point

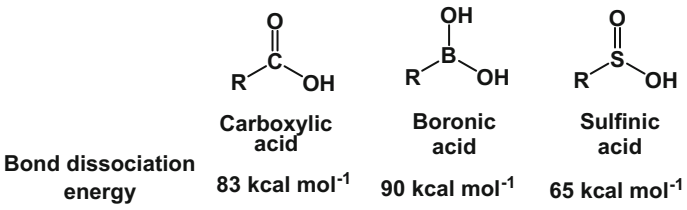

Fig. 4 Bond dissociation energy of various radical precursors

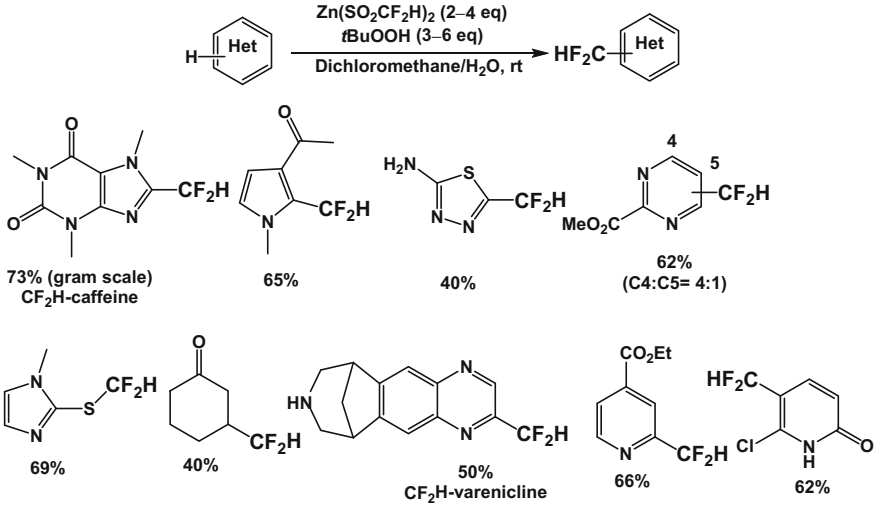

Scheme 7 C–H difluoromethylation using DFMS

for the synthesis of various difluoromethane sulfinates. Among the prepared salts, $Zn(SO_2CF_2H)_2$ (DFMS) gave 100% conversion and good yield of the C–H difluoromethylation of caffeine. In addition, many heteroaromatics displayed a good reactivity toward DFMS under standard conditions using TBHP in a DCM/H_2O solvent system (Scheme 7) [44]. In a manner similar to the C–H trifluoromethylation with the Langlois salt, a second addition of DFMS and TBHP drove the reaction toward completion, and substituting DMSO for DCM as the organic solvent gave a significant reversal in regioselectivity. However, this reaction has two different properties regarding the regioselectivity and the substrate scope from the C–H trifluoromethylation. First, the reaction takes place at an electron deficient position. In the case of varenicline and dihydroquinine, the C–H trifluoromethylation mainly takes place at the electron rich position, while the C–H difluoromethylation occurs at an electron deficient position with high selectivity. These results suggest that the difluoromethyl radical can act as nucleophilic radical. Regarding the substrate scope, not only heteroaromatics, but also the S–H bond of an aromatic thiol and double bond of α,β-unsaturated enones are reactive.

3.3 *Direct and Practical C–H Alkylation Using Various Zinc Sulfinates*

The sulfinate-mediated C–H trifluoromethylation and difluoromethylation aroused interest in the direct introduction of other medicinally-important functionalities. In a manner similar to DFMS, alkylsulfonyl chlorides are a convenient starting point of

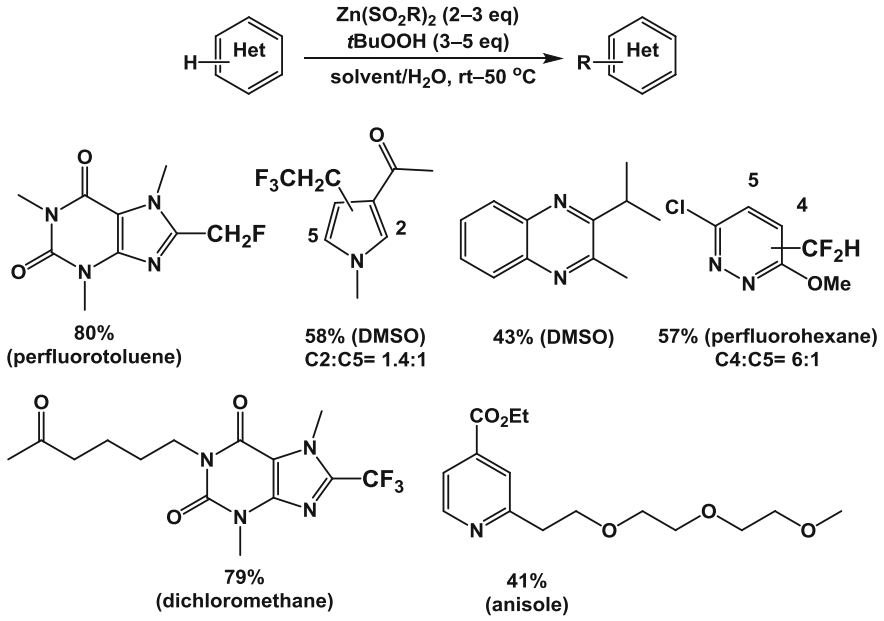

Scheme 8 C–H alkylation of heteroaromatics using zinc sulfinates

various alkylsulfinates. They were easily prepared by only the zinc-mediated reduction in water, and the C–H alkylation and C–H fluoroalkylation of heteroaromatics using them are then performed. The desired functionalization proceeded in various solvents under mild conditions although the yields depended on the solvents (Scheme 8) [45].

These results demonstrated the power of our sulfinate reagents on the C–H functionalization, and the increasing commercial demand for alkylsulfinates led us to establish new synthetic methods of the sulfinates [46–49]. As shown in Scheme 9, various alkylsulfinates have been prepared by several methods. They are usually free flowing and bench-stable powder. Additionally, the stability at room temperature and in air allows us to run the reactions in air and an aqueous solvent

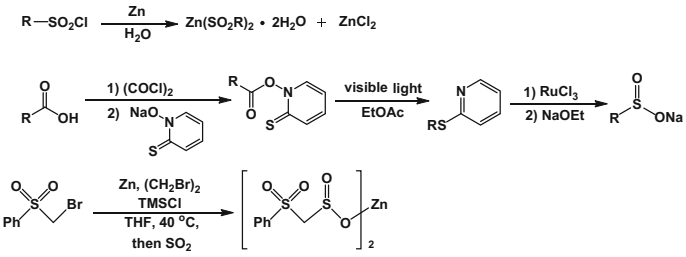

Scheme 9 General procedures to prepare sulfinates

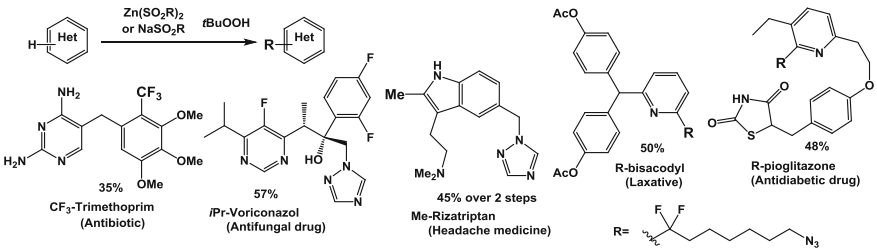

Scheme 10 Direct C–H functionalization of pharmaceuticals using sulfinates

system with extreme operational ease (No special tools, such as a glove box, and no dehydrated/deoxidized solvents are required). Twenty sulfinates are now commercially available from Aldrich.

Diversification of the sulfinates enabled us to expand this sulfinate chemistry into other scientific studies such as the prediction of drug metabolism [50], the preparation of drug-antibody conjugates [51] and electrochemistry [52].

3.4 *Power of Alkylsulfinates-Mediated C–H Functionalization in Drug Discovery*

From the view point of drug discovery, perhaps this topic covers the most intriguing applications of our methods. First, to demonstrate the power of our method as the

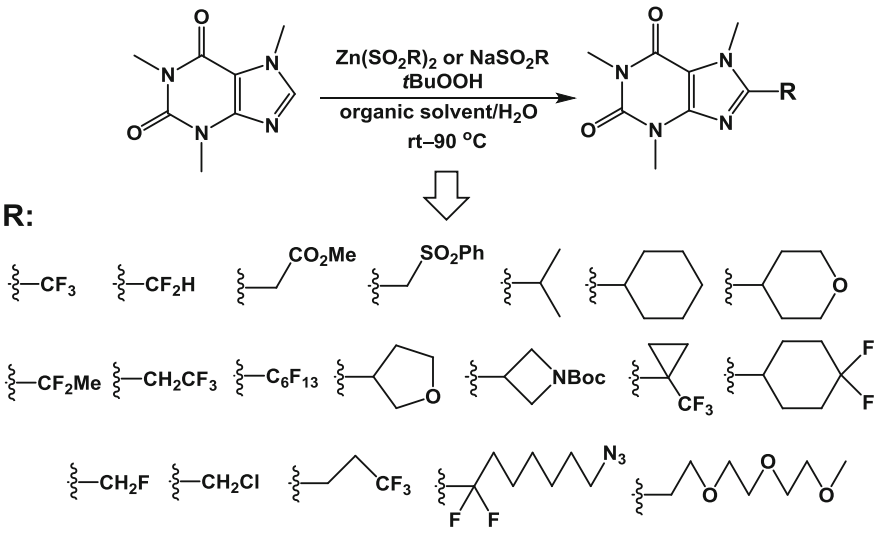

Scheme 11 Diversification of caffeine using sulfinates

LSF strategy, the C–H functionalization of complex molecules was performed (Scheme 10). With one-step and a simple procedure, various natural products and pharmaceuticals were functionalized under ambient conditions, although the yield and regioselectivity should be improved [41, 44, 45, 47–49].

In addition, the diversification of commercially-available sulfinates enables us to quickly collect information about SAR, SPR, ADME, etc. In the case of caffeine, our methods can provide over nineteen derivatives within several days (Scheme 11).

These results demonstrate that our methods can accelerate drug discovery for both the lead identification and the lead optimization.

Features of our methods about reducing the pre-functionalization step, the simple protocol and inexpensive reagents (starting material, radical source, oxidant and solvent) will likely render them useful tools in process chemistry [53, 54]. As shown in Scheme 12, the conventional routes to **A**, **B**, **C** and **D** involve 6-step, 5-step, 3-step and 5-step sequences, respectively [55–57]. Additionally, they sometimes require the use of a hazardous reagent, such as DAST, KCN and diazomethane, which should be avoided in process chemistry, and result in a low

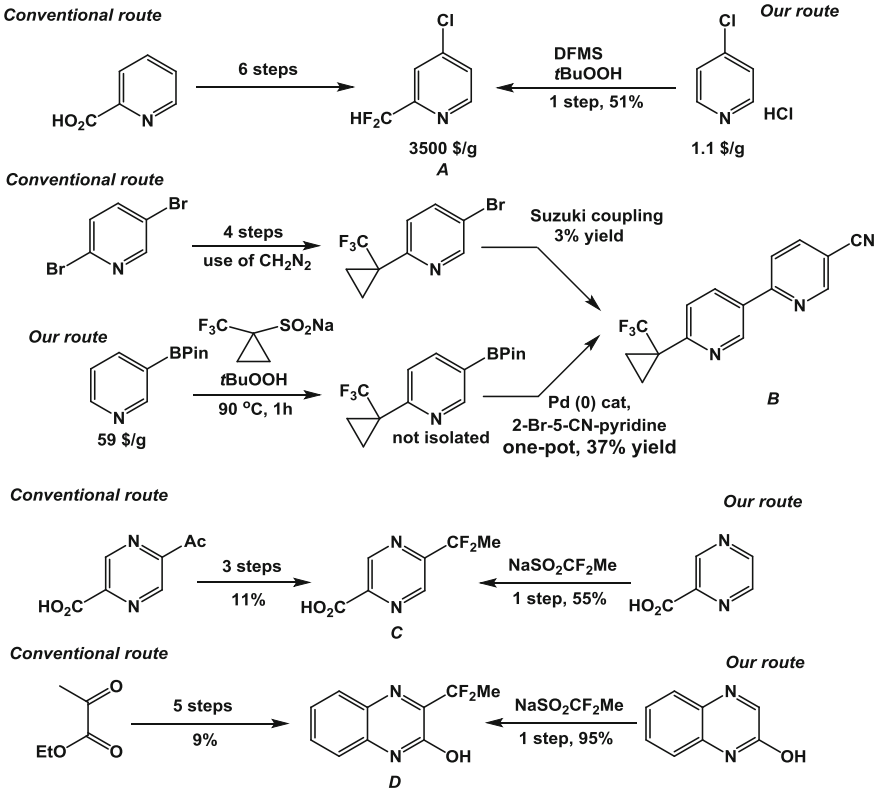

Scheme 12 Comparison of conventional and C–H functionalization route

overall yield. In contrast, our methods directly provide **A**, **B**, **C** and **D** from commercially-available inexpensive starting materials with significant improvement in the overall yields (51, 37, 55, and 95%, respectively) [45, 47, 49], and represent ideal syntheses [58].

4 Summary

In summary, new methods and reagents, which enable the C–H functionalization of medicinally-relevant heteroaromatics, have been invented. Our methods can directly introduce medicinally-important functionalities, such as Me and CF_3, under ambient conditions, and displays a broad scope of substrates and high functional group tolerance. Additionally, the simple protocol and inexpensive reagents make them powerful tools for the LSF of druggable molecules in drug discovery. In fact, our strategies have already been utilized at Pfizer and many alkylsulfinates are commercially available from Sigma-Aldrich. With growing interest in the LSF strategy for drug discovery, we anticipate their widespread application in the near future.

References

1. For a review on LSF of druggable molecules for medicinal chemistry, see; Cernak, T.; Dykstra, K. D.; Tyagarajan, S.; Vachal, P.; Krska, S. W. *Chem. Soc. Rev.*, **2016**, *45*, 546.
2. Sawada, S.; Okijima, S.; Aiyama, R.; Nokata, K.; Furuta, T.; Yokokura, T.; Sugino, E.; Yamaguchi, K.; Miyasaka, T. *Chem. Pharm. Bull.,* **1991**, *39*, 1446.
3. Nagib, D. A.; MacMillan, D. W. C. *Nature*, **2011**, *480*, 224.
4. DiRocco, D. A.; Dykstra, K.; Krska, S.; Vachal, P.; Conway, D. V.; Tudge, M. *Angew. Chem. Int. Ed.,* **2014**, *53*, 4802.
5. Jin, J.; MacMillan, D. W. C. *Nature*, **2015**, *525*, 87.
6. Suzuki, A.; Brown, H. C. *Organic Synthesis via Boranes*, Vol. 3; Aldrich: Milwaukee, WI, 2003.
7. For a review on direct aryl-aryl bond formation, see; Allberico, D.; Scott, M. E.; Lautens, M.; *Chem. Rev.* **2007**, *107*, 174.
8. For a review on minisci reaction for medicinal chemistry, see; Duncton, M. A. J. *Med. Chem. Commun.*, **2011**, *2*, 1135.
9. Demir, A. S.; Reis, Ö.; Emrullahoglu, M. *J. Org. Chem.* **2003**, *68,* 578.
10. Seiple, I. B.; Su, S.; Rodriguez, R. A.; Gianatassio, R.; Fujiwara, Y.; Sobel, A. L.; Baran, P.S. *J. Am. Chem. Soc.* **2010**, *132*, 13194.
11. For a detailed mechanism study, see; Patel, N. R.; Flowers, R. A. II. *J. Am. Chem. Soc.* **2013**, *135*, 4672.
12. For a detailed study to figure out a role of biphasic solvent system, see; Baxter, R. D.; Liang, Y.; Hong, X.; Brown, T. A.; Zare, R. N.; Houk, K. N.; Baran, P. S.; Blackmond, D. G. *ACS Cent. Sci.* **2015**, *1*, 456.
13. *The Chemistry of the Quinonoid Compounds,* Vol 2.; Patai, S., Rappoport, Z., Eds.; Wiley: New York, 1988; Parts 1 and 2.
14. Thomson, R. H. *Naturally Occurring Quinones IV*; Blackie Academic: London, 1997.

15. Cramer, W. A.; Crofts, A. R. . In *Photosynthesis*, Vol. 1; Govindjee, Ed.; Academic Press: New York, 1982; pp 387.
16. Bechtold, T. . In *Handbook of Natural Colorants*; Bechtold, T., Mussak, R., Eds.; Wiley: New York, 2009; pp 151.
17. Fujiwara, Y.; Domingo, V.; Seiple, I. B.; Gianatassio, R.; Bel, M. D.; Baran, P. S. *J. Am. Chem. Soc.* **2011**, *133*, 3292.
18. Geris, R.; Simpson, T. *J. Nat. Prod. Rep*. **2009**, *26*, 1063.
19. Marcos, I. S.; Conde, A.; Moro, R. F.; Basabe, P.; Diez, D.; Urones, J. G. *Mini-Rev. Org. Chem.* **2010**, *7*, 230.
20. Yong, K. W. L.; Jankam, A.; Hooper, J. N. A.; Suksamrarn, A.; Garson, M. J. *Tetrahedron* **2008**, *64*, 6341.
21. Hamann, M. T. *Curr. Pharm. Des.* **2003**, *9*, 879.
22. Piña, I. C.; Sanders, M. L.; Crews, P. *J. Nat. Prod*. **2003**, *66*, 2.
23. Takamatsu, S.; Hodges, T. W.; Rajbhandari, I.; Gerwick, W. H.; Hamann, M. T.; Nagle, D. G. *J. Nat. Prod.* **2003**, *66*, 605.
24. Dixon, D. D.; Lockner, J. W.; Zhou, Q.; Baran, P. S. *J. Am. Chem. Soc.* **2012**, *134*, 8432.
25. Smart, B. E. *Chem. Rev.* **1996**, *96*, 1555.
26. Filler, R.; Kobayashi, Y.; Yagupolskii, L. M. *Organofluorine Compounds in Medicinal Chemistry and Biomedical Applications*; Elsevier: Amsterdam, 1993.
27. Welch, J. T. *Tetrahedron* **1987**, *43*, 3123.
28. Ma, J-A.; Cahard, D. *J. Fluorine. Chem.* **2007**, *128*, 975.
29. Meanwell, N. A. *J. Med. Chem.* **2011**, *54*, 2529.
30. Furuya, T.; Kamlet, A. S.; Ritter, T. *Nature*, **2011**, *473*, 470.
31. Wu. X.-F.; Neumann, H.; Beller, M. *Chem. Eur. J.* **2012**, *7*, 1744.
32. Garcia-Monforte, M. A.; Martinez-Salvador, S.; Menjon, B. *Eur. J. Inorg. Chem.* **2012**, 4945.
33. Liu, T.; Shen, Q. *Eur. J. Org. Chem.* **2012**, *34*, 6679.
34. Furuya, T.; Kamlet, A. S.; Ritter, T. *Nature* **2011**, 473, 470.
35. Tomashenko, O. A.; Grushin, V. V. *Chem. Rev.* **2011**, *111*, 4475.
36. Cho, E. J.; Senecal, T. D.; Kinzel, T.; Zhang, Y.; Watson, D. A.; Buchwald, S. L. *Science* **2010**, *328*, 1679.
37. Fier, P. S.; Hartwig, J. F. *J. Am. Chem. Soc.* **2012**, *134*, 5524.
38. Wang, X.; Truesdale, L.; Yu, J-Q. *J. Am. Chem. Soc.* **2010**, *132*, 3648.
39. Langlois, B. R.; Laurent, E.; Roidot, N. *Tetrahedron Lett.* **1991**, *32*, 7525.
40. Langlois, B. R.; Laurent, E.; Roidot, N. *Tetrahedron Lett.* **1992**, *33*, 1291.
41. Ji, Y.; Brueckl, T.; Baxter, R. D.; Fujiwara, Y.; Seiple, I. B.; Su, S.; Blackmond, D. G.; Baran, P. S. *Proc. Natl. Acad. Sci. U. S. A.* **2011**, *108*, 14411.
42. For the detail of the regioselectivity on sulfinates-mediated C-H functionalization, see; O'Hara, F.; Blackmond, D. G.; Baran. P. S. *J. Am. Chem. Soc*. **2013**, *135*, 12122.
43. Schönherr, H.; Cernak, T. *Angew. Chem. Int. Ed.* **2013**, *52*, 12256.
44. Fujiwara, Y.; Dixon, J. A.; Rodriguez, R. A.; Baxter, R. D.; Dixon, D. D.; Collins, M. R.; Blackmond, D. G.; Baran, P. S. *J. Am. Chem. Soc*. **2012**, *134*, 1494.
45. Fujiwara, Y.; Dixon, J. A.; O'Hara, F.; Funder, E. D.; Dixon, D. D.; Rodriguez, R. A.; Baxter, R. D.; Herlé, B.; Sach, N.; Collins, M. R.; Ishihara, Y.; Baran, P. S. *Nature* **2012**, *492*, 95.
46. O'Hara, F.; Baxter, R. D.; O'Brien, A. G.; Collins, M. R.; Dixon, J. A.; Fujiwara, Y.; Ishihara, Y.; Baran, P. S. *Nat. Protoc*. **2013**, *8*, 1042.
47. Zhou, Q.; Ruffoni, A.; Gianatassio, R.; Fujiwara, Y.; Sella, E.; Shabat, D.; Baran, P. S. *Angew. Chem. Int. Ed.* **2013**, *52*, 3949.
48. Gui, J.; Zhou, Q.; Pan, C.-M.; Yabe, Y.; Burns, A. C.; Collins, M. R.; Ornelas, M. A.; Ishihara, Y.; Baran, P. S. *J. Am. Chem. Soc*. **2014**, *136*, 4853.
49. Gianatassio, R.; Kawamura, S.; Eprile, C. L.; Foo, K.; Ge, J.; Burns, A. C.; Collins, M. R.; Baran, P. S. *Angew. Chem. Int. Ed.* **2014**, *53*, 9851.
50. O'Hara, F.; Burns, A. C.; Collins, M. R.; Dalvie, D.; Ornelas, M. A.; Vaz, A. D. N.; Fujiwara, Y.; Baran, P. S. *J. Med. Chem.* **2014**, *57*, 1616.

51. Zhou, Q.; Gui, J.; Pan, C.-M.; Albone, E.; Cheng, X.; Suh, E. M.; Grasso, L.; Ishihara, Y.; Baran, P. S. *J. Am. Chem. Soc*. **2013**, *135*, 12994.
52. O'Brien, A. G.; Maruyama, A.; Inokuma, Y.; Fujita, M.; Baran, P. S. *Angew. Chem. Int. Ed.* **2014**, *53*, 11868.
53. Ouellet, S. G.; Roy, A.; Molinaro, C.; Angelaud, R.; Marcoux, J.-F.; O'Shea, P. D.; Davies, I. W. *J. Org. Chem.* **2011**, *76*, 1436.
54. Mitchell, D.; Cole, K. P.; Pollock, P. M.; Coppert, D. M.; Burkholder, T. P.; Clayton, J. R. *Org. Process. Res. Dev*. **2012**, *16*, 70.
55. Oballa, R. WO2006/133559, **2006**.
56. Ellard, J. M; Farthing, C. N.; Hall, A. WO 2011/09898, **2011**.
57. Chen, H.; Mcdaniel, K. F.; Green, B. E.; Shanley, J. P.; Kruger, A. W.; Gandarilla, J.; Welch, D. S.; Cink, R. D.; Gai, Y.; Wang, G.; Yat, S. WO 2011/156337, **2011**.
58. Gaich, T.; Baran, P. S. *J. Org. Chem.* **2010**, *75*, 4657.

Magnetic Nanoparticle-Supported Iodoarene Oxidative Catalysts and Its Application to Phenol Oxidation

Hisanori Nambu, Ikumi Shimokawa, Tomoya Fujiwara and Takayuki Yakura

Abstract Iodoarene oxidative catalysts immobilized on magnetite (Fe_3O_4) were developed. The catalysts showed reactivities similar to that of 4-iodophenoxyacetic acid for the oxidation of 4-alkoxyphenols in the presence of Oxone® as a co-oxidant. In addition, they were easily recovered by the use of an external magnet and could be recycled up to eight times. The oxidation of various 4-alkoxyphenols with the catalyst proceeded smoothly at room temperature to give the corresponding *p*-quinones in good to high yields. This is the first example of a magnetic nanoparticle-supported iodoarene catalyst.

Keywords Hypervalent compounds · Magnetic properties · Nanoparticles · Oxidation · Quinones

1 Introduction

Environmentally benign procedures are required for the production of pharmaceuticals, flavors and fragrances, and agrochemicals. Hypervalent iodine compounds, trivalent iodine reagents such as phenyliodine(III) diacetate (PIDA) and phenyliodine(III) bis(trifluoroacetate) (PIFA), and pentavalent iodine reagents such as Dess–Martin periodinane (DMP) and *o*-iodoxybenzoic acid (IBX), have recently received significant attention as efficient, useful, and non-metallic oxidants in organic synthesis owing to their low toxicity, ready availability, and ease of handling (Fig. 1) [1–3]. With respect to the principles of green chemistry, hypervalent iodines are not ideal because stoichiometric amounts of iodine reagents are necessary during oxidation to produce equimolar amounts of iodine waste. Accordingly, many researchers have made efforts to overcome these disadvantages by two approaches: (1) use of easily recoverable and recyclable iodine reagents,

H. Nambu · I. Shimokawa · T. Fujiwara · T. Yakura (✉)
Graduate School of Medicine and Pharmaceutical Sciences, University of Toyama, Sugitani 930-0194, Toyama, Japan
e-mail: yakura@pha.u-toyama.ac.jp

K. Tomioka et al. (eds.), *New Horizons of Process Chemistry*,
DOI 10.1007/978-981-10-3421-3_9

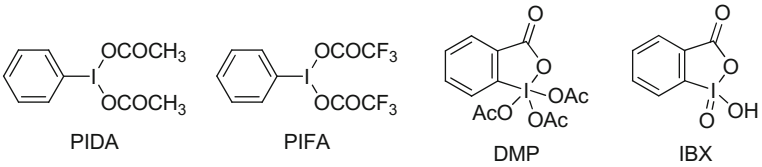

Fig. 1 Structures of hypervalent iodoarene reagents

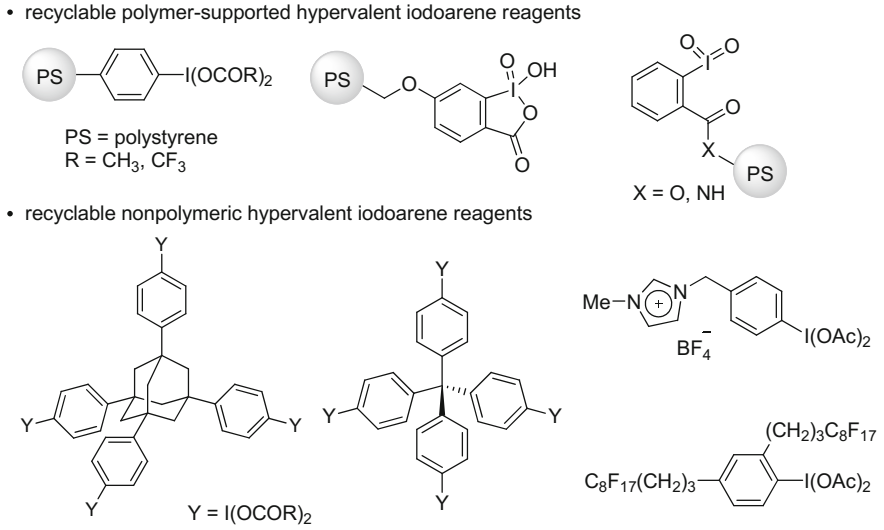

Fig. 2 Structures of recyclable hypervalent iodoarene reagents

(2) developing catalytic versions of hypervalent iodine oxidation. (1) Two types of recyclable stoichiometric iodine reagents were reported, polymer-supported reagents [3, 4] and nonpolymer ones such as 1,3,5,7-tetraphenyladamantane-derived, [5] tetraphenylmethane-derived [6], ion-supported [7, 8], and fluorous [9, 10] compounds (Fig. 2). Although the polymer-supported reagents can be easily recovered, they show much less reactive than the corresponding monomeric forms owing to steric hindrance of the reactive sites. On the other hand, nonpolymeric reagents show high reactivity, but they require solvent-choice. (2) Several iodoarenes in combination with the appropriate co-oxidant were used in a catalytic system based on in situ generation of hypervalent iodine species (Scheme 1) [11, 12]. *m*-Chloroperbenzoic acid (*m*CPBA) [13, 14], Oxone® ($2KHSO_5 \cdot KHSO_4 \cdot K_2SO_4$) [15, 16], hydrogen peroxide [17], and peracetic acid [18] have been utilized as a co-oxidant. Moreover, recoverable iodoarenes such as 1,3,5-triazine-derived [19], ion-supported [20], and fluorous [21] compounds have been applied to catalytic reactions (Fig. 3). We have also reported catalytic hypervalent iodine oxidation of 4-alkoxyphenols **1** to *p*-quinones **2** using a catalytic amount of

Scheme 1 Catalytic oxidation with iodoarenes and co-oxidants

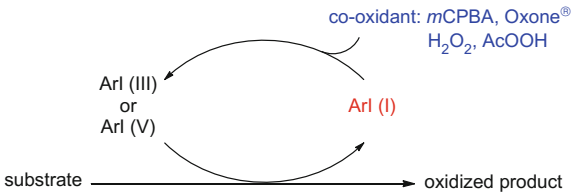

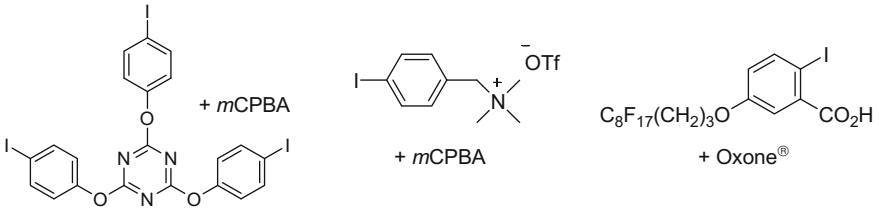

Fig. 3 Combination of recyclable iodoarene catalysts and co-oxidants

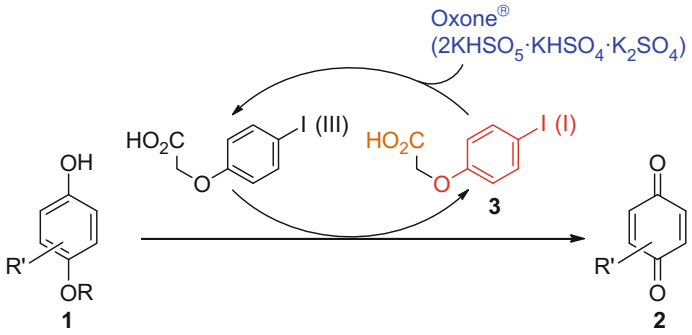

Scheme 2 A catalytic hypervalent iodine oxidation of 4-alkoxyphenols **1** to *p*-quinones **2** using 4-iodophenoxyacetic acid (**3**) with Oxone®

4-iodophenoxyacetic acid (**3**) with Oxone® (Scheme 2) [22, 23]. This system needs easier procedure to separate **3** from the reaction than that in other iodoarene catalyst systems because of the high solubility of **3** in an alkaline solution. However, several treatments of acid–base liquid separation are required to recover **3**.

Magnetic nanoparticles have recently shown their efficiency as a core for catalyst support [24, 25]. The catalytic reactivity of these supported catalysts is higher than that of usual polymer-supported heterogeneous catalysts, and they show the comparable reactivity to homogeneous catalysts owing to a large surface area to volume ratio. Therefore, they are often called "quasi-homogeneous catalysts". Moreover, they can be easily separated from the reaction by application of an external magnetic field, allowing simple separation of the catalysts without liquid separation and

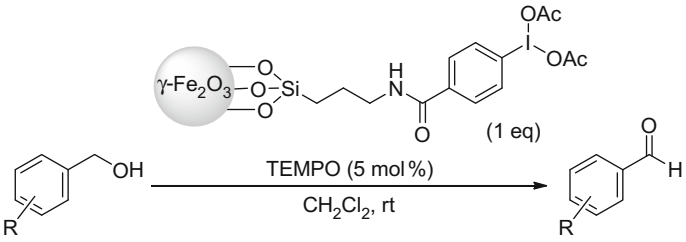

Scheme 3 Magnetite-supported hypervalent iodine reagent for alcohol oxidation reported by Zhu and Wei

filtration. In 2012, Zhu and Wei introduced magnetite-supported reagent to hypervalent iodine chemistry. They prepared magnetite-PIDA, which worked as a co-oxidant in TEMPO oxidation of alcohols (Scheme 3) [26]. However, the catalytic use of the reagent has not yet been accomplished. Very recently, we applied a magnetic nanoparticle-supported catalyst system to hypervalent iodine oxidation to develop easily recoverable and recyclable iodoarene catalysts for oxidation of 4-alkoxyphenols to *p*-quinones [27]. Here, we describe the details of the development of magnetite-supported iodoarene catalysts.

2 Silica-Coated Magnetic Nanoparticle-Supported Iodoarene Catalyst

We initially prepared a silica-coated iodoarene catalyst **4a** as shown in Scheme 4. The known silica-coated magnetite **5** [28] was obtained by coupling magnetite with 3-aminopropyltriethoxysilane, which acts as the linker to catalyst. Acylation of **5** with acid chloride **6** derived from **3** was used to combine the magnetic nanoparticles and catalyst. Amidation of **5** with **6** was conducted in the presence of triethylamine and 4-(*N*,*N*-dimethylamino)pyridine (DMAP) in dichloromethane to give **4a**. The organic loading of **4a** was very low (0.087 mmol/g) as determined by elemental analysis of iodine.

Catalyst **4a** was evaluated for the oxidation of 4-methoxy-2-pivaloyloxy methylphenol (**1a**) to *p*-quinone **2a** by using our reported procedure [22, 23] for

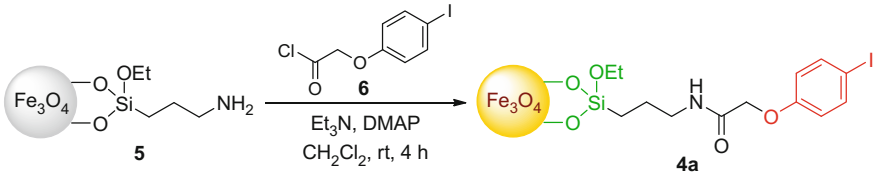

Scheme 4 Synthesis of magnetic nanoparticle-supported iodoarene catalyst **4a**

Table 1 Recyclability of **4a** for the oxidation of **1a**

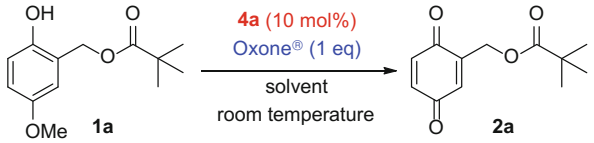

Cycle	Solvent	Time (h)	Yield (%)	Recovery of **4a** (%)
1	CF_3CH_2OH/H_2O (1:2)	1.5	84	93
2	CF_3CH_2OH/H_2O (1:2)	4.5	82	96
3	CF_3CH_2OH/H_2O (1:2)	8	68[b]	97
1	CF_3CH_2OH/buffer[a] (1:2)	2	91	98
2	CF_3CH_2OH/buffer[a] (1:2)	4	91	100
3	CF_3CH_2OH/buffer[a] (1:2)	8	91	100
4	CF_3CH_2OH/buffer[a] (1:2)	24	80	100

[a]Buffer: 0.1 M phosphate buffer solution
[b]Unknown by-product was isolated

3 (Table 1). When **1a** was treated with 10 mol% of catalyst **4a** in the presence of Oxone® (1 eq) in CF_3CH_2OH–H_2O (1:2) at room temperature, the reaction was completed within 1.5 h to give the corresponding *p*-quinones **2a** in 84% yield. The magnetic catalyst **4a** was rapidly collected in 93% yield by application of an external magnet, washed with EtOAc, H_2O, acetone and Et_2O, and dried to recover and reuse. The recovered **4a** was used again to oxidize **1a** under the same conditions to give **2a** in 82% yield with recovery of **4a** in 96% yield, although the reaction required a longer time of 4.5 h for completion. The catalytic reactivity of **4a** in the third use was poor and gave 68% yield of **2a** with a significant amount of unknown by-product after 8.0 h. These results indicate that **4a** decomposes under these conditions and that pure **4a** could not be recovered by our hands. Next, we investigated the use of 0.1 M phosphate buffer instead of H_2O to avoid the strong acidic conditions caused by the presence of Oxone®. The oxidation of **1a** with **4a** in CF_3CH_2OH–0.1 M phosphate buffer (1:2) also proceeded smoothly at room temperature to afford **2a** in 91% yield after 2 h and recovery of **4a** in 98% yield [29]. The reusability of **4a** in CF_3CH_2OH–0.1 M phosphate buffer was examined again. The reactivity of **4a** gradually lowered, resulting in an increase in the reaction time. The fourth use of **4a** needed 24 h to complete the reaction.

3 Phosphonic Acid-Coated Magnetic Nanoparticle-Supported Iodoarene Catalyst

Since Tucker-Schwartz and Garrell demonstrated that the phosphonic acid-coated particles remain stable under the highly acidic oxidizing conditions [30], we synthesized the phosphonic acid-anchored catalyst **4b** as shown in Scheme 5.

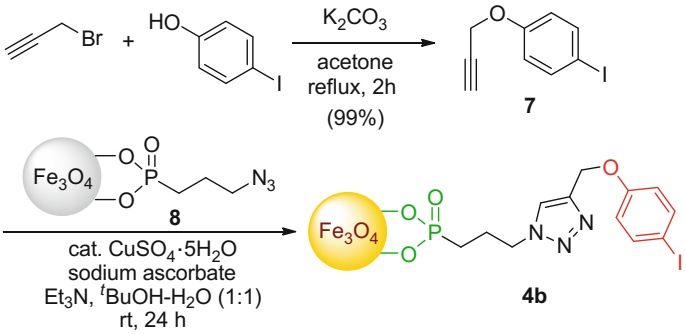

Scheme 5 Synthesis of magnetic nanoparticle-supported iodoarene catalyst **4b**

Table 2 Recyclability of **4b** for the oxidation of **1a** in CF_3CH_2OH/buffer[a] (1:2)

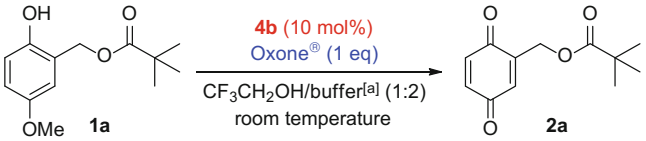

Cycle	Time (h)	Yield (%)	Recovery of **4b** (%)
1	4	80	98
2	4	81	97
3	5.5	80	98
4	7.5	82	96
5	8	82	96
6	11	81	99
7	15	78	96
8	24	71[b]	96

[a]Buffer: 0.1 M phosphate buffer solution
[b]Starting material **1a** was recovered in 3% yield

1-Iodo-4-(prop-2-ynyloxy)benzene (**7**) [31] was prepared by propargylation of 4-iodophenol. Coupling of iodoarene **7** and known magnetite-supported 3-azidopropylphosphonate (**8**) [30], prepared by a three-step sequence from the commercially available diethyl 3-bromopropylphosphonate, was accomplished by treatment with $CuSO_4$ via the "click" reaction to afford phosphonic acid-coated catalyst **4b**, whose organic loading (0.33 mmol/g) was much higher than that of **4a**.

The reactivity of the catalyst **4b** was tested for the oxidation of **1a** to **2a** in CF_3CH_2OH–0.1 M phosphate buffer (1:2) (Table 2). The reaction with **4b** was completed within 4 h to give **2a** in 80% yield. The catalyst **4b** was also rapidly collected by an external magnet and washed with EtOAc, H_2O, acetone, and Et_2O. No signs of iodoarene catalyst could be detected in the crude reaction mixture, obtained by concentration of the EtOAc solution, and the residues (<1 mg), obtained

Table 3 Oxidation of 4-alkoxyphenols **1** using catalyst **4b**[a]

Entry	Substrate	Product	Time (h)	Yield (%)
1	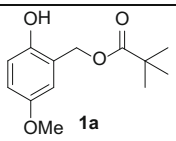 **1a**	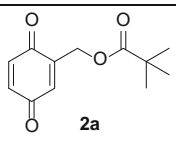 **2a**	4	80 (98)[b]
2	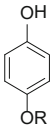 **1b**: R = H	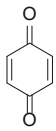 **2b**	0.5	81 (96)[b]
3	**1c**: R = Me		2	95 (93)[b]
4	**1d**: R = Et		3	93 (99)[b]
5	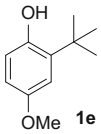 **1e**	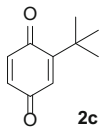 **2c**	2.5	73 (98)[b]
6	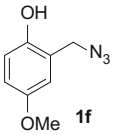 **1f**	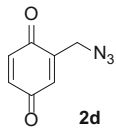 **2d**	2.5	68 (92)[b]
7[c]	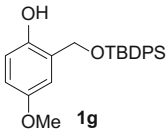 **1g**	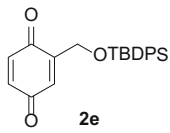 **2e**	4	79 (86)[b]
8	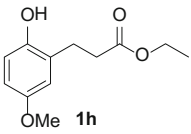 **1h**	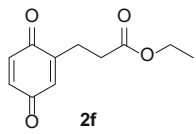 **2f**	3	75 (98)[b]
9	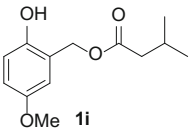 **1i**	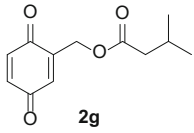 **2g**	4	76 (92)[b]

[a]Reactions were conducted in CF_3CH_2OH/0.1 M phosphate buffer solution (1:2) at room temperature

[b]Yields in parentheses were that of recovered catalyst **4b**

[c]CF_3CH_2OH/0.1 M phosphate buffer solution (3:1) was used as a solvent

by concentration of acetone and Et_2O solutions, by ^1H NMR spectroscopy. The recovered catalyst **4b** could be efficiently recycled up to eight times, although the reaction times gradually increased [32, 33]. In all cases, **4b** was recovered in over 96% yields. These results suggest that the phosphonic acid-coated catalyst **4b** is more stable than the silica-coated catalyst **4a** under acidic conditions [34].

With the optimal conditions in Table 2, we next investigated the ability of our synthesized catalyst **4b** to oxidize other 4-alkoxyphenols bearing several substituents (Table 3). Simple hydroquinone (**1b**), 4-methoxyphenol (**1c**), and 4-ethoxyphenol (**1d**) were oxidized to *p*-benzoquinone (**2b**) in excellent yields (entries 2–4). The reaction of the phenol **1e**, possessing a bulky *tert*-butyl group at the C2 position, proceeded smoothly to give the corresponding quinone **2c** in 73% yield (entry 5). Azido and *tert*-butyldiphenylsilyloxy (TBDPSO) groups were tolerated under the oxidation conditions (entries 6 and 7), although the reaction of **1g** required changing the solvent to a 3:1 mixture of CF_3CH_2OH–0.1 M phosphate buffer owing to its solubility (entry 7). The use of an ethyl ester **1h** [35] led to good product yield (75%, entry 8). This oxidation could be applied to the synthesis of blattellaquinone (**2g**) [36], the sex pheromone of the German cockroach, *Blattella germanica*, isolated in 2005 (entry 9). Oxidation of **1i** under the standard conditions afforded **2g** in 76% yield. In all cases, the magnetic catalyst **4b** could be recovered by an external magnet in 86–99% yields.

4 Conclusion

Magnetic nanoparticle-supported catalysts **4a** and **4b** were easily synthesized as magnetic iodoarene nanocatalysts and were evaluated for the oxidation of 4-alkoxyphenols **1** to *p*-quinones **2**. Catalyst **4b** could be recycled up to eight times by simple magnetic separation. The oxidation of various 4-alkoxyphenols **1a**–**i** with **4b** proceeded smoothly at room temperature to give the corresponding *p*-quinones **2a**–**g** in good to high yields.

5 Experimental Procedure

Typical procedure for the oxidation of *p*-alkoxyphenols **1** using magnetic nanoparticle-supported iodoarene catalyst **4b**.

Magnetic nanoparticle-supported iodoarene catalyst **4b** (121 mg, 0.04 mmol, 10 mol%) was added to a solution of *p*-alkoxyphenol **1** (0.40 mmol) and Oxone® (246 mg, 0.40 mmol) in CF_3CH_2OH–0.1 M phosphate buffer (2.0 mL, 1:2). After completion of the reaction (checked by TLC), the catalyst **4b** was collected at the bottom of the flask using an external magnet, and the supernatant carefully decanted. The catalyst **4b** was washed three times with EtOAc, three times with H_2O, three times with acetone, two times with Et_2O, and dried in vacuo. Then, the recovered catalyst **4b** was reused in the next reaction cycle. The organic layer was washed with H_2O and brine, dried over Na_2SO_4, and concentrated in vacuo. The residue was purified by column chromatography (silica gel, 10% EtOAc in hexane) to provide *p*-quinone **2**.

References and Notes

1. *Hypervalent Iodine Chemistry: Modern Developments in Organic Synthesis*, (Ed.: Wirth, T.), *Top. Curr. Chem.* Vol: 224, Springer, Berlin, **2003**.
2. Zhdankin, V. V., *Hypervalent Iodine Chemistry: Preparation, Structure, and Synthetic Applications of Polyvalent Iodine Compounds*, Wiley, Chichester, UK, **2013**.
3. For a review, see: Yoshimura, A.; Zhdankin, V. V. *Chem. Rev.* **2016**, *116*, 3328.
4. For a review, see: Yusubov, M. S.; Zhdankin, V. V. *Mendeleev Commun.* **2010**, *20*, 185.
5. Tohma, H.; Maruyama, A.; Maeda, A.; Maegawa, T.; Dohi T.; Shiro, M.; Morita, T.; Kita, Y. *Angew. Chem. Int. Ed.* **2004**, *43*, 3595.
6. Dohi, T.; Maruyama, A.; Yoshimura, M.; Morimoto, K.; Tohma, H.; Shiro, M.; Kita, Y. *Chem. Commun.* **2005**, 2205.
7. Qian, W.; Jin, E.; Bao, W.; Zhang, Y. *Angew. Chem. Int. Ed.* **2005**, *44*, 952.
8. Handy, S. T.; Okello, M. *J. Org. Chem.* **2005**, *70*, 2874.
9. Rocaboy, C.; Gladysz, J. A. *Chem. Eur. J.* **2003**, *9*, 88.
10. Tesevic, V.; Gladysz, J. A. *J. Org. Chem.* **2006**, *71*, 7433.
11. For a review, see: T. Dohi, Y. Kita, *Chem. Commun.* **2009**, 2073.
12. For a review, see: M. Uyanik, K. Ishihara, *Chem. Commun.* **2009**, 2086.
13. Dohi, T.; Maruyama, A.; Yoshimura, M.; Morimoto, K.; Tohma, H.; Kita, Y. *Angew. Chem. Int. Ed.* **2005**, *44*, 6193.
14. Ochiai, M.; Takeuchi, Y.; Katayama, T.; Sueda, T.; Miyamoto, K. *J. Am. Chem. Soc.* **2005**, *127*, 12244.
15. Thottumkara, A. P.; Bowsher, M. S.; Vinod, T. K. *Org. Lett.* **2005**, *7*, 2933.
16. Uyanik, M.; Akakura, M.; Ishihara, K. *J. Am. Chem. Soc.* **2009**, *131*, 251.
17. Dohi, T.; Minamitsuji, Y.; Maruyama, A.; Hirose, S.; Kita, Y. *Org. Lett.* **2008**, *10*, 3559.
18. Minamitsuji, Y.; Kato, D.; Fujioka, H.; Dohi, T.; Kita, Y. *Aust. J. Chem.* **2009**, *62*, 648.
19. Thorat, P. B.; Bhong, B. Y.; Shelke, A. V.; Karade, N. N. *Tetrahedron Lett.* **2014**, *55*, 3332.
20. Ishiwata, Y.; Togo, H. *Tetrahedron Lett.* **2009**, *50*, 5354.
21. Miura, T.; Nakashima, K.; Tada, N.; Itoh, A. *Chem. Commun.* **2011**, *47*, 1875.
22. Yakura, T.; Tian, Y.; Yamauchi, Y.; Omoto, M.; Konishi, T. *Chem. Pharm. Bull.* **2009**, *57*, 252.
23. Yakura, T.; Omoto, M.; Yamauchi, Y.; Tian, Y.; Ozono, A. *Tetrahedron* **2010**, *66*, 5833.
24. For a review, see: Nasir Baig, R. B.; Varma, R. S. *Chem. Commun.* **2013**, *49*, 752.
25. For a review, see: Wang, D.; Astruc, D. *Chem. Rev.* **2014**, *114*, 6949.
26. Zhu, C.; Wei, Y. *Adv. Synth. Catal.* **2012**, *354*, 313.
27. Nambu, H.; Shimokawa, I.; Fujiwara, T.; Yakura, T. *Asian J. Org. Chem.* **2016**, *5*, 486.
28. Fujita, K.; Umeki, S.; Yasuda, H. *Synlett* **2013**, *24*, 94.
29. Oxidation of **1a** with 4-iodophenoxyacetic acid (**3**) in CF_3CH_2OH–0.1 M phosphate buffer (1:2) at room temperature proceeded to completion within 1.5 h, giving **2a** in 88% yield.
30. Tucker-Schwartz, A. K.; Garrell, R. L. *Chem. Eur. J.* **2010**, *16*, 12718.
31. Pal, M.; Parasuraman, K.; Yeleswarapu, K. R. *Org. Lett.* **2003**, *5*, 349.
32. The catalyst loading **4b** after eight cycles was very low (0.043 mmol/g) as determined by elemental analysis of nitrogen and IR spectroscopy.
33. The reactivity of the recovered catalyst **4b** with a reductive treatment using sat. $Na_2S_2O_3$ solution was almost the same as that of **4b** without a reductive treatment. Therefore, a reductive treatment after the reaction is not necessary.
34. The IR spectrum of the recovered catalyst **4b** after treatment with Oxone® in the absence of substrate **1a** for 4 h was almost the same as that of the original catalyst **4b**. This result indicated that the structure of the catalyst **4b** was almost unchanged by using Oxone®.
35. Gutsche, C. D.; Oude-Alink, B. A. M. *J. Am. Chem. Soc.* **1968**, *90*, 5855.
36. Nojima, S.; Schal, C.; Webster, F. X.; Santangelo, R. G.; Roelofs, W. L. *Science* **2005**, *307*, 1104.

Recent Development of Diphenyl Phosphorazidate (DPPA) as a Synthetic Reagent

Takayuki Shioiri

Abstract Recent development of the synthetic use of diphenyl phosphorazidate (DPPA, $(PhO)_2P(O)N_3$) is described. DPPA can be used for the peptide bond formation, macrolactamization, the modified Curtius reaction, conversion of hydroxyl groups to azides, azidation of pyridine *N*-oxides, *N*-alkylation, 1,3-dipolar cycloaddition, phosphoramidation, carbamate synthesis and the activation of carbamate anions.

Keywords Diphenyl phosphorazidate · Peptide bond formation · Macrolactamization · The modified Curtius reaction · Azidation · *N*-Alkylation · 1,3-Dipolar cycloaddition · Phosphoramidation · Carbamate

1 Introduction

In 1972, we revealed the efficient use of diphenyl phosphorazidate (DPPA, $(PhO)_2P(O)N_3$) for the peptide synthesis and the Curtius reaction [1]. Since then, More than 4 decades have elapsed and DPPA proved to be a versatile synthetic reagent. As of today many manufacturers produce DPPA commercially. Since the development of the synthetic use of DPPA was summarized in 2007 [2], this mini-review will mainly focus the development of the synthetic use of DPPA after that time, but some of the interesting works before 2007 will be referred. The topics described here are not comprehensive but limited on the interesting ones.

T. Shioiri (✉)
Faculty of Agriculture, Meijo University,
1-501, Shiogamaguchi, Tempaku, Nagoya 468-8502, Japan
e-mail: shioiri@mb.ccnw.ne.jp

K. Tomioka et al. (eds.), *New Horizons of Process Chemistry*,
DOI 10.1007/978-981-10-3421-3_10

2 Peptide and Amide Bonds Formation

DPPA proved to be a suitable reagent for the amide bond formation. It is especially useful for the peptide bond formation with little epimerization in the fragment coupling [1–3].

The tuftsin derivatives **1** were prepared by stepwise addition of proline, lysine, and threonine derivatives to nitroarginine benzyl ester using DPPA-triethylamine, as shown in Scheme 1 [4]. The method affords **1** with high chiral purity and little impurities in a good yield of 75–80% in each step, which was higher than those reported using DCC (*N,N′*-dicyclohexylcarbodiimide) or *N*-ethoxycarbonyl-2-ethoxy-1,2-dihydroquinoline (EEDQ). Acylation of the threonine amino group in the protected tuftsin derivatives **1** with the isoglutamine carboxyl group of muramyl dipeptide or nor-muramyl dipeptide **2** was accomplished using the DPPA coupling procedure to give several conjugates **3**.

Coupling of the imidazole carboxylic acid **4** with the imidazole amine **5** was reported to be fruitless when 1-(3-dimethylaminopropyl)-3-ethylcarbodiimide (EDC) or benzotriazol-1-yloxytris(pyrrolidino)phosphonium hexafluorophosphate (PyBOP) was used. However, the use of DPPA in the presence of *N,N*-diisopropylethylamine (Hünig's base) in acetonitrile provided the coupling product **6** in 70% yield [5], as shown in Scheme 2. The compound **6** is a precursor of imidazole analogues of *Lissoclinum* cyclopeptides.

Screening of the reaction conditions for the coupling of the amine **7** with the carboxylic acid **8** giving the amide **9** revealed that efficiency of EDC

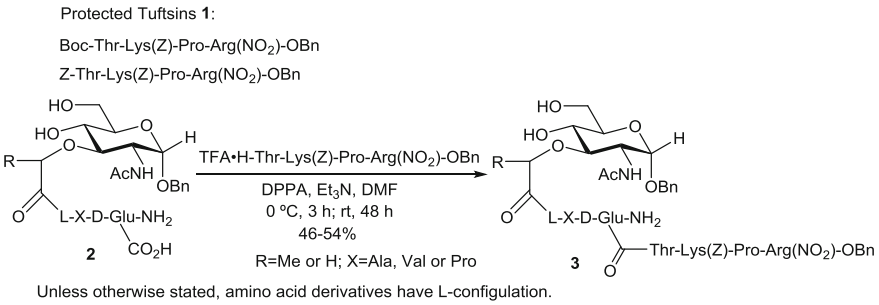

Scheme 1 Synthesis of Tuftsin derivatives

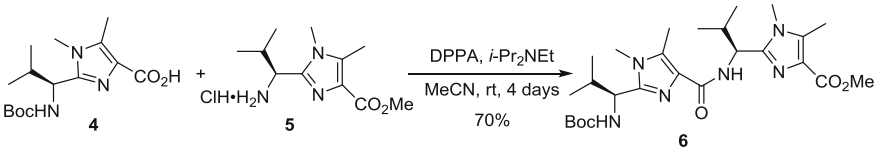

Scheme 2 Synthesis of diimidazole amide derivatives

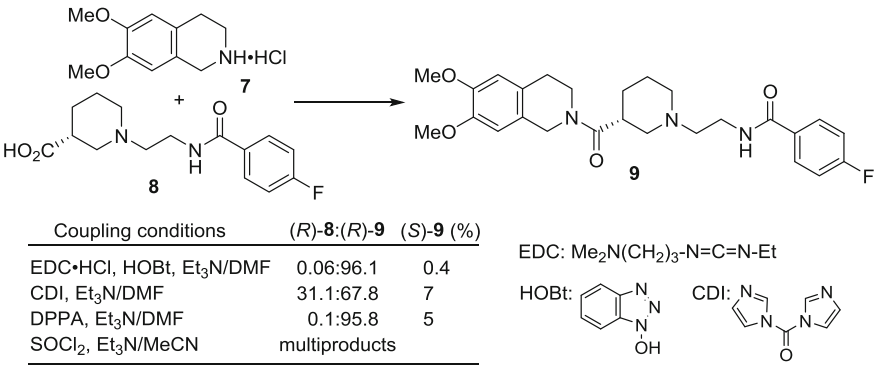

Coupling conditions	(*R*)-**8**:(*R*)-**9**	(*S*)-**9** (%)
EDC•HCl, HOBt, Et_3N/DMF	0.06:96.1	0.4
CDI, Et_3N/DMF	31.1:67.8	7
DPPA, Et_3N/DMF	0.1:95.8	5
$SOCl_2$, Et_3N/MeCN	multiproducts	

Scheme 3 Comparison of coupling efficiency in the synthesis of amide derivatives **9**

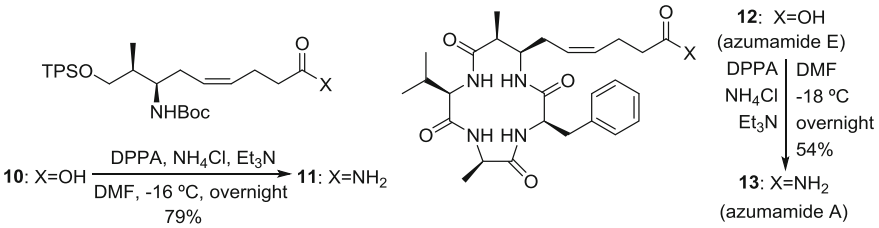

Scheme 4 Primary amide synthesis using DPPA

hydrochloride-HOBt (1-hydroxybenzotriazole) and DPPA was comparable but DPPA caused slightly more racemization [6], as shown in Scheme 3. In contrast, 1,1′-carbonyldiimidazole (CDI) and thionyl chloride activation gave a poor reaction profile.

As shown in Scheme 4, primary amides can also be constructed by using DPPA-NH_4Cl-triethylamine in DMF. The primary amide **11** was obtained from the carboxylic acid **10** while azumamide E (**12**) of marine origin afforded azumamide A (**13**) through amidation [7].

3 Macrolactamization

DPPA is quite effective for intramolecular macrolactamization of linear peptides [2]. The macrolactamization is usually carried out under high dilution conditions to avoid the intermolecular condensation. In many cases, the yields are not high (more than 50% yield will be acceptable), and excesses of coupling reagents and bases will be required in longer reaction times (more than one day) to increase the yields. Scheme 5 shows examples of macrolactamization and cyclotrimerization. 13-Membered cyclic largazole analogue **14** was prepared by use of DPPA-Hünig's

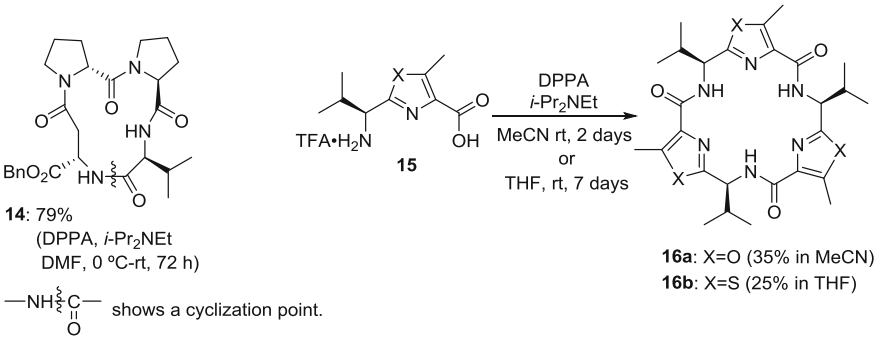

Scheme 5 Macrolactamization and cyclotrimerization using DPPA

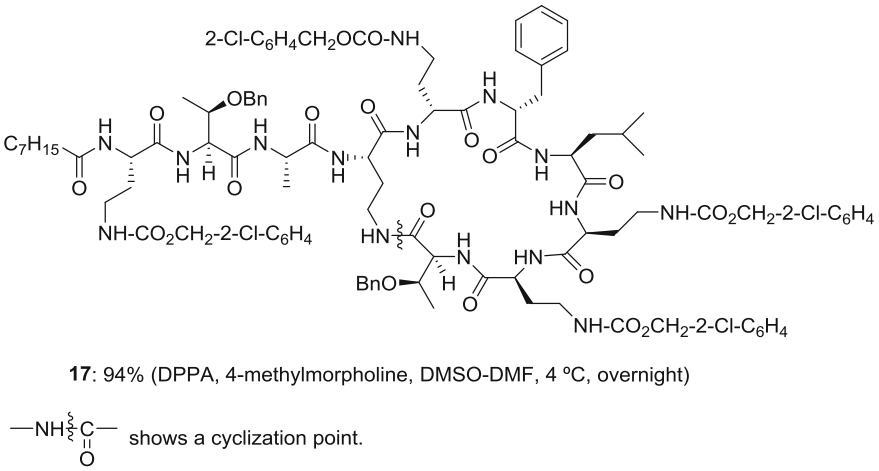

Scheme 6 Synthesis of polymyxin B analogues

base in 79% yield [8]. DPPA can also be used for cyclotrimerization, as shown in Scheme 5. The oxazole and thiazole amino acids **15** underwent the cyclotrimerization to give the 18-membered cyclic trimers **16** [9]. After a search of several methods for a one-pot process, DPPA was found to be the most advantageous for the cyclotrimerization in this case.

More than 20 analogues of polymyxin B were prepared in excellent yields by the DPPA method among which the construction of 23-membered cyclic polymyxin analogue **17** was depicted in Scheme 6 [10].

4 The Modified Curtius Reaction

One of the most used reactions utilizing DPPA is the modified Curtius reaction. While the amide and peptide bond formation reaction using DPPA is carried out at or below room temperature, the Curtius reaction requires a thermal process since the acid azides first formed from carboxylic acids and DPPA rearrange accompanied with nitrogen evolution under thermal conditions, giving the corresponding isocyanates. Some representative examples of the DPPA Curtius reactions are shown in Schemes 7 and 8 [11–16].

The carbamate **19** is the early intermediate for the synthesis of candesartan cilexetil, an antihypertensive drug [11]. The synthesis of **19** was first carried out by the method A which was the usual Curtius reaction of the carboxylic acid **18** in 3 steps. At present, the method B which is the modified Curtius reaction using DPPA in 1 step is employed. Tomioka and co-workers utilized the DPPA method for the conversion of the carboxylic acid **20** to the carbamate **21**, which was ultimately

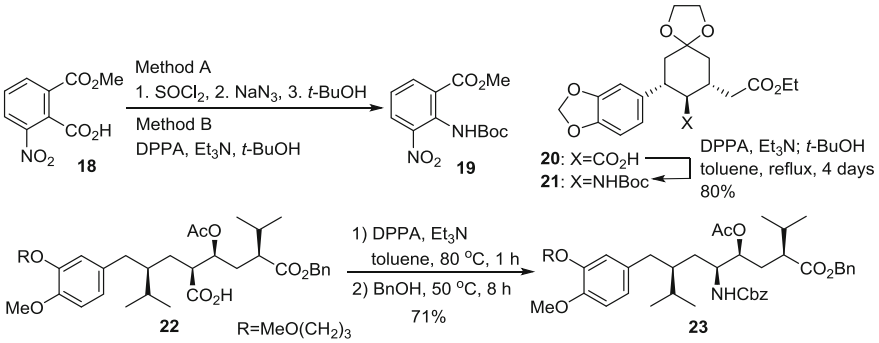

Scheme 7 The modified Curtius reaction using DPPA

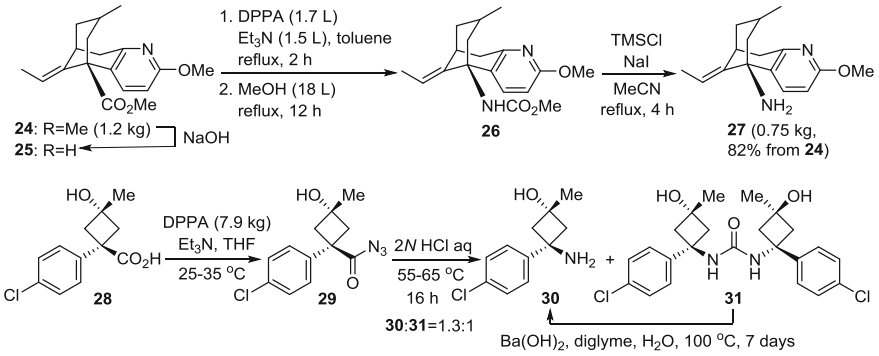

Scheme 8 Large scale use of DPPA for the modified Curtius reactions

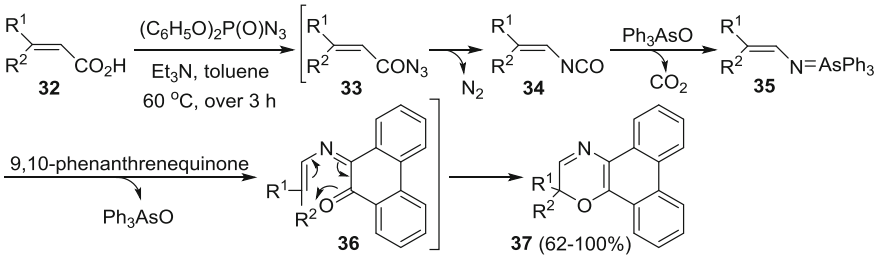

Scheme 9 Synthesis of novel photochromic oxazine compounds using DPPA

transformed to lycorine, one of the representative Amaryllidaceae alkaloids [12]. Another interesting modified Curtius reaction using DPPA is the synthesis of the benzyl carbamate **23** from the carboxylic acid **22**, an intermediate for the synthesis of the renin inhibitor aliskiren [13]. In this particular case, the reaction did not proceed in *tert*-butanol [Scheme 7].

Large scale use of DPPA (1.7 L) was accomplished in the modified Curtius reaction of **25** obtained from the ester **24** [14], and the product **26** was finally converted to (−)-huperzine (**27**) effective for Alzheimer's disease, as shown in Scheme 8. Conversion from the ester **24** to (−)-huperzine (**27**) was conducted without isolation of the intermediates. In the kilogram synthesis of an Akt kinase inhibitor, treatment of the carboxylic acid **28** with DPPA at room temperature immediately afforded the acid azide **29**, which underwent the Curtius rearrangement with hot hydrochloric acid to give a mixture of the required amine **30** and the urea **31** in a ratio of 1.3:1 [15]. The urea **31** gave the amine **30** by forcing alkaline conditions.

Novel photochromic oxazine compounds **37** were prepared in a single step from the acrylic acids **32** and 9,10-phenanthrenequinone by treatment of DPPA, triethylamine, and a catalytic amount of triphenylarsine oxide in hot toluene [16]. As shown in Scheme 9, the azide **33** formed from the acid **32** by the action of DPPA-base yields the isocyanate **34** through the Curtius rearrangement. Trapping of **34** with triphenylarsine oxide forms the arsonium ylide **35** which undergoes the aza-Wittig reaction with 9,10-phenanthrenequinone to generate the quinone imine **36** that cyclizes to the oxazine **37**.

Continuous flow chemical processes are also applied to the modified Curtius reaction using DPPA [17–19].

5 Conversion of Hydroxyl Groups to Azides

In 1977, Bose and co-workers reported the use of stable DPPA in place of hazardous hydrogen azide for the Mitsunobu conversion of alcohols to the corresponding azides [20]. Furthermore, the Merck chemists used a combination of

DPPA and DBU (1,8-diazabicyclo[5.4.0]undec-7-ene) for the same one-pot conversion in 1993 [21, 22]. Since then both methods have been utilized by many researchers for the effective azidation. Some recent typical examples will be reviewed here.

5.1 The Bose-Mitsunobu Azidation

The intermediate **38** for the synthesis of harmonine, the toxic principle of the Asian lady beetle *Harmonia axyridis*, has primary and secondary alcohol functions, both of which underwent the azidation under the Bose-Mitsunobu conditions (DPPA, triphenylphosphine, and diisopropyl azodicarboxylate (DIAD) in THF at room temperature) to give the azide **39** [23]. Since the reaction proceeds through an S_N2 manner, the chiral center at the *sec*-alcohol position is inverted in the azide, as shown in Scheme 10. In the 5- and 6-membered ring compounds, **40** and **42**, having *sec*-hydroxyl functions, the Bose-Mitsunobu reaction afforded the azides, **41** and **43**, respectively, with complete inversion of the configuration [24, 25].

Multikilogram synthesis of a HCV polymerase inhibitor was carried out by the use of Bose-Mitsunobu inversion of the secondary alcohol **44** with DPPA [26]. As shown in Scheme 11, the alcohol **44** was first activated with diisopropyl azodicarboxylate (DIAD) (1.2 equiv.) and triphenylphosphine (1.2 equiv.) in THF. DPPA (1.2 equiv.) was added after the triphenylphosphine had fully reacted with DIAD since triphenylphosphine reacts with DPPA to form the corresponding iminophosphorane with release of nitrogen. Hünig's base (1.0 equiv.) was also added at the reaction outset to ensure the pH of the system remained basic to avoid the release of toxic and highly explosive hydrazoic acid (HN_3) in the reactor headspace. Smooth conversion to the azide **45** took place at room temperature (20–25 °C) and with typical assay yields of 95%. Without handling of the azide **45**, the Staudinger reduction of **45** to the iminophosphorane followed by hydrolysis with water afforded the primary amine, which was isolated as the hydrochloride salt **46** in an overall yield of 84% with minimal erosion of enantiopurity. In this case, the Merck azidation of the alcohol **44** with DPPA-DBU did not give the desired azide **45**.

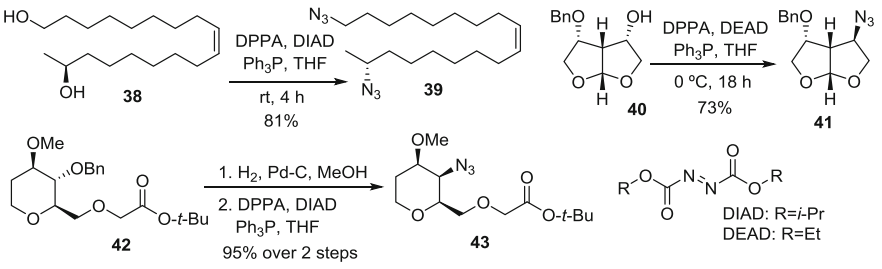

Scheme 10 The Bose-Mitsunobu azidation using DPPA

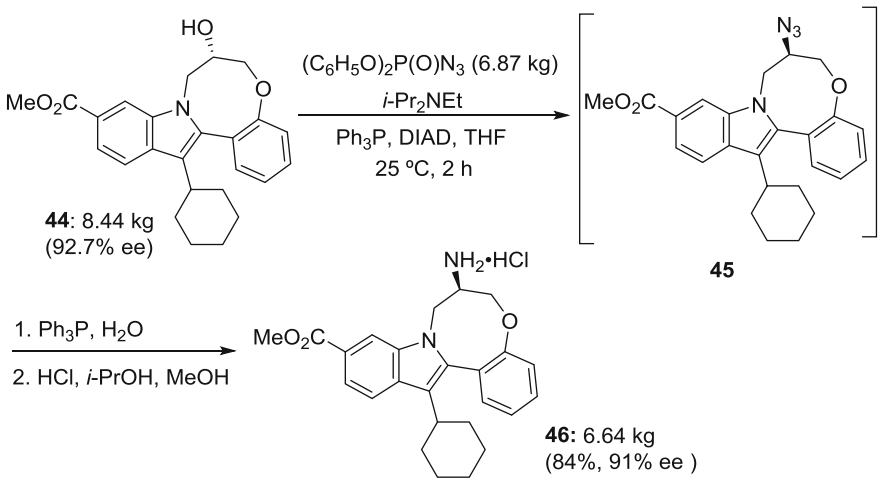

Scheme 11 Large scale use of DPPA for the Bose-Mitsunobu azidation

5.2 *The Merck Azidation*

Although the Bose-Mitsunobu azidation is an excellent method for the conversion of alcohols to azides, treatment and removal of the by-products, triphenylphosphine oxide and 1,2-dialkoxycarbonylhydrazine, poses a problem. The Merck azidation using DPPA-DBU allows treatment and removal of the by-products much easier. Some recent examples are shown in Scheme 12 [27–30]. An efficient conversion of the alcohol **47** to the azide **48** was achieved by the Merck procedure by the use of DPPA-DBU [27, 28]. The primary alcohol **49** smoothly afforded the azide **50** under the reaction conditions of the Merck azidation [29]. The mechanism of the Merck azidation is shown in the conversion of the nucleosides **51a** and **51b** to **53a** and **53b**, respectively [30]. Treatment of **51a** and **51b** with DPPA in conjunction with DBU afforded the phosphates **52** as an intermediate, which underwent an S_NAr reaction with azide anion to yield **53a** and **53b**, respectively.

The Merck azidation also offers an efficient method for a smooth conversion of alcohols to azides, but alcohols should be active ones in most cases. We found that bis(*p*-nitrophenyl) phosphorazidate (*p*-NO_2DPPA, $(p\text{-}NO_2C_6H_4O)_2P(O)N_3$) was much more effective than DPPA (31,32). As shown in Scheme 13, decan-2-ol (**54**) was smoothly converted to the corresponding azide **55** using *p*-NO_2DPPA-DBU in toluene while the use of DPPA-DBU sluggishly proceeded to give **55** in low yield. Highly stereoselective inversion was observed in the conversion of the optically active alcohols **56** and **58** to the azides **57** and **59**, respectively [31]. In the synthesis of α,α-disubstituted α-azido esters from the corresponding hydroxy esters, an

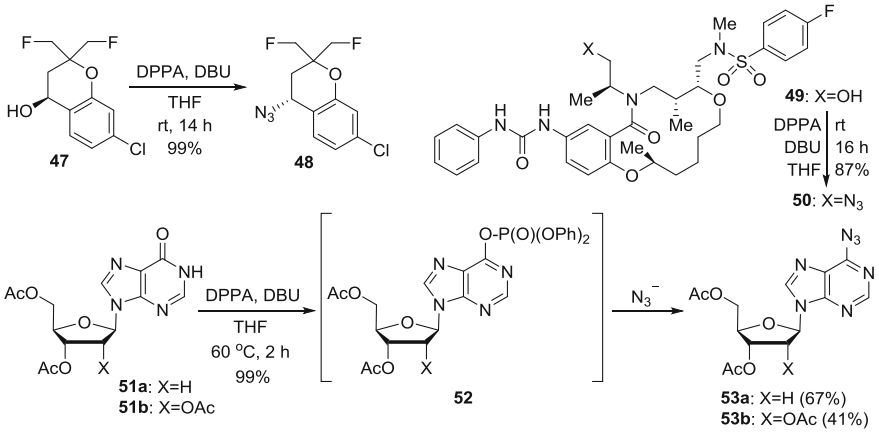

Scheme 12 The Merck azidation using DPPA

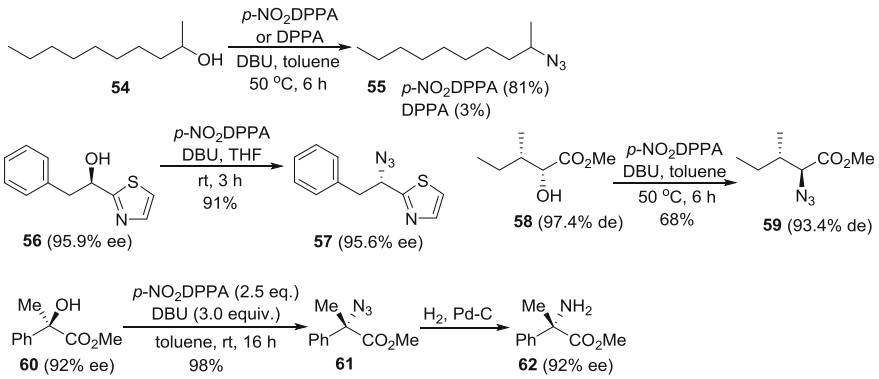

Scheme 13 Conversion of alcohols to azides using *p*-NO_2DPPA

excess of *p*-NO_2DPPA (2.5 equiv.) and DBU (3 equiv.) in toluene proved to be a best choice [32]. Again DPPA was less efficient. Various hydroxy esters could be converted to the azide esters in good yields with complete inversion without loss of stereochemical integrity, and the latter were conveniently transformed into α,α-disubstituted α-amino acid esters by catalytic hydrogenation. One example (conversion of **60** to **62** via **61**) is shown in Scheme 13. It will be worthy of note that this azide synthesis proceeds through an S_N2 inversion mechanism while an S_N1 reaction or elimination will usually occur in tertiary alcohols.

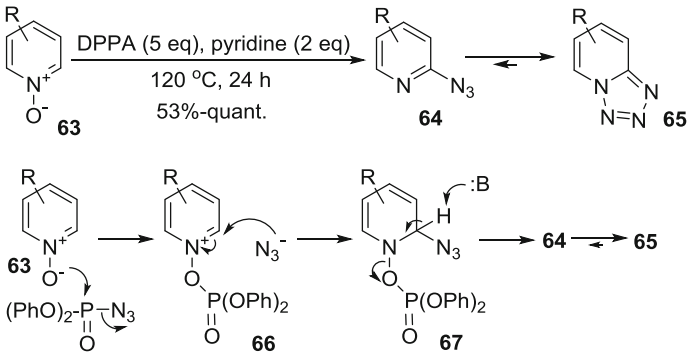

Scheme 14 Azidation of pyridine *N*-oxides using DPPA

Scheme 15 *N*-Alkylation with DPPA

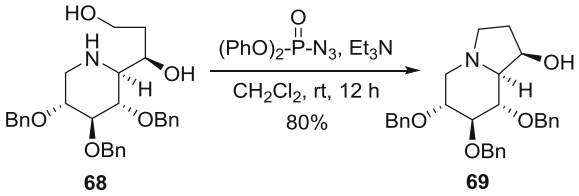

6 Azidation of Pyridine *N*-Oxides Using DPPA

Pyridine *N*-oxides **63** were converted to tetrazolo[1,5-a]pyridines **65** in good to excellent yields by heating in the presence of phosphoryl or sulfonyl azides and pyridine under solvent free conditions. DPPA proved to be the most convenient reagent and gave high yields [33]. Pyridine *N*-oxides **63** will first attack the phosphorus atom of DPPA to give the phosphate **66** with liberation of an azide ion. Nucleophilic attack of the azide ion to the 2-position of pyridine nucleus will give the azide **67**, from which diphenyl phosphate will be removed to afford 2-azidopyridines **64**, as shown in Scheme 14. The azide **64** will be in equilibrium with tetrazolo[1,5-a]pyridines **65**, but the equilibrium will be shifted to **65**.

7 *N*-Alkylation with DPPA

N-Alkyaltion occurs with DPPA as shown in Scheme 15. Treatment of the piperidine derivative **68** having primary and secondary alcohols with DPPA in the presence triethylamine afforded the cyclized product **69** [34]. Obviously, the primary alcohol function of **68** preferentially reacts with DPPA to give the corresponding phosphate and/or azide, which will intramolecularly react with piperidinyl amine to produce the *N*-alkylated compound **69**.

8 [3+2] Dipolar Cycloadditions of DPPA

The azide group of DPPA also works as a 1,3-dipole [35–39]. Benzylic alcohols **70** reacted with active ketones (**71**, EWG = electron withdrawing groups) in the presence of DPPA and DBU to give the 1,2,3-triazoles **72**, as shown in Scheme 16 [35]. Benzylic alcohols **70** will first produce the corresponding azides just like the Merck azidation, and then the [3+2] cycloaddition of the azides with the enolates from the active ketones **71** accompanied with expulsion of water yields the triazoles **72**. The amides **73** afforded the tetrazoles **74** by treatment with DPPA, DIAD, and diphenyl-2-pyridylphosphine just like the Bose-Mitsunobu azidation [36].

DPPA was employed as an efficient partner in the Cu-catalyzed three component reaction with 1-alkynes and amines to produce the corresponding phosphoryl amidines **75**, as shown in Scheme 17 [37]. The Cu acetylide **76** first formed will undergo the [3+2] cycloaddition with DPPA to give the 1,2,3 triazole intermediate **77**, which will undergo a ring opening rearrangement with expulsion of nitrogen to yield the ketenimine intermediate **78**. Subsequent addition of amines will afford the phosphoryl amidines **75** [38].

The direct synthesis of sulfur-containing triazoles **79** was achieved by Cu-catalyzed transformation of alkynes with DPPA and dimethyl sulfoxide (DMSO), as shown in Scheme 18. Alkenes also underwent the reaction but yields were moderate [39]. Initially, DPPA will react with DMSO to give thionium ion **81** via intermediate **80** with releasing an azide ion just like the Pummerer reaction. The azide ion will attack **81** to give the Pummerer product **82**, which will undergo 1,3-dipolar cycloaddition to alkynes to produce the triazoles **79** under copper catalytic conditions.

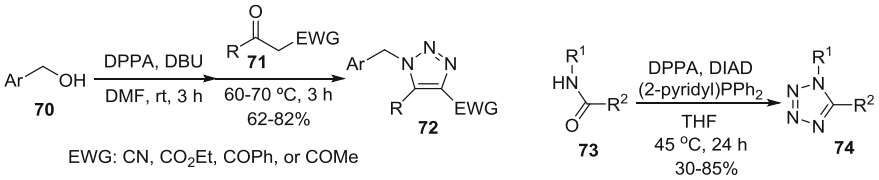

Scheme 16 [3+2] Dipolar cycloadditions of DPPA

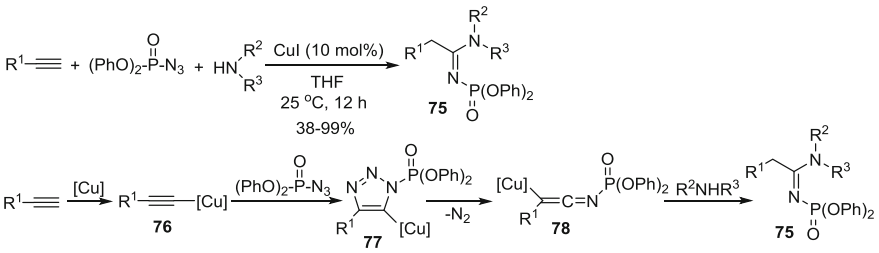

Scheme 17 Cu-catalyzed three component reactions

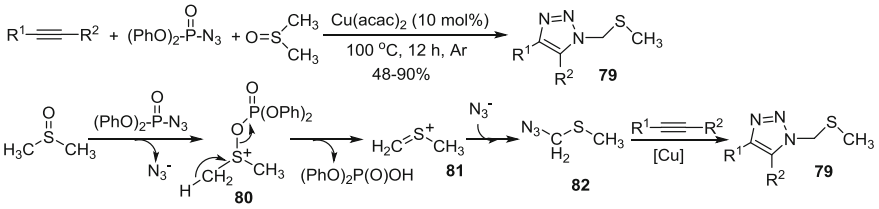

Scheme 18 Cu-catalyzed transformation of alkynes and alkenes with DPPA and DMSO

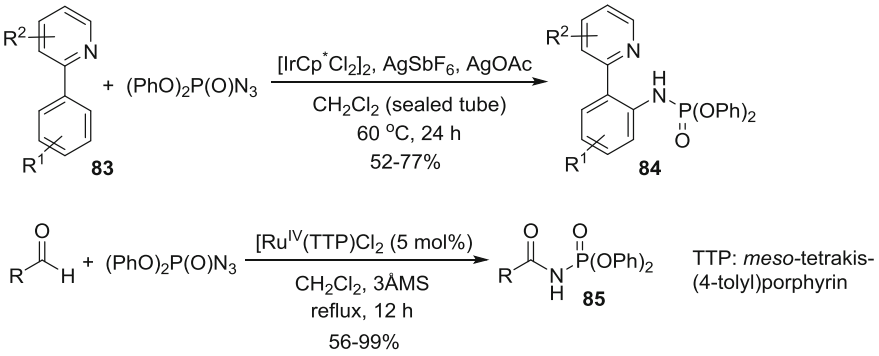

Scheme 19 Phosphoramidation with DPPA

9 Synthesis of Phosphoramidates and Carbamate Using DPPA

The C–N bond formation (phosphoramidation and carbamate synthesis) was achieved with DPPA in various ways as shown in Schemes 19 and 20 [40–42]. An iridium-catalyzed phosphoramidation of arene C–H bonds with DPPA as the amino source was realized to give *N*-aryl phosphoramidates [40]. The arenes bearing pyridinyl, pyrazoyl and quinolinyl as the directing group smoothly afforded *N*-aryl phosphoramidates using DPPA [40]. Conversion of the pyridinyl compounds **83** to the corresponding phosphoramidate **84** is shown in Scheme 19 as a typical example. Phosphoramidation of aldehydes was carried out by using DPPA as a nitrene source and [Ru^{II}(TTP)(CO)] as a catalyst to give *N*-acylphosphoramidates **85** in good yields [41].

Furthermore, treatment of the compound **86** with lithium diisopropylamide (LDA) followed by DPPA and then di-*tert*-butyl dicarbonate (Boc_2O) afforded the carbamate **87** in 85% yield as a mixture of diastereomers [42], shown in Scheme 20.

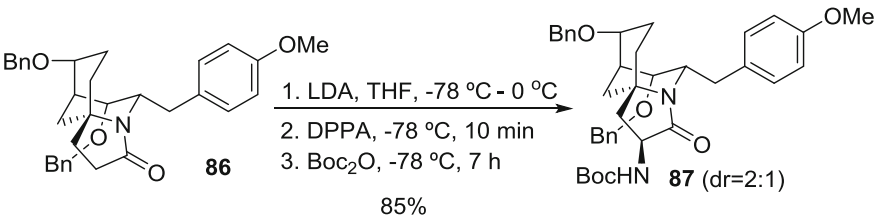

Scheme 20 Synthesis of the carbamate **87** Using DPPA

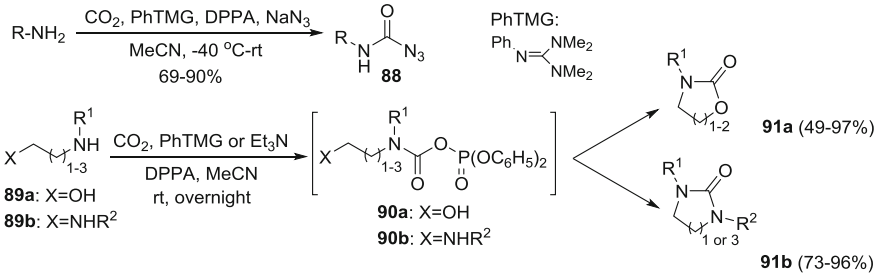

Scheme 21 Reactions of carbamate anions with DPPA

10 Reactions of Carbamate Anions with DPPA

Treatment of various primary amines with DPPA, sodium azide and tetramethylphenylguanidine (PhTMG) under carbon dioxide atmosphere in acetonitrile yielded carbamoyl azides **88**, as shown in Scheme 21 [43]. Amines react with carbon dioxide under basic conditions to give transient carbamate anions, which react with DPPA just like amide bond formation and subsequently afford carbamoyl azides **88**. Addition of sodium azide facilitates the azidation and suppresses the formation of ureas. This carbamate anion method was extended to 1,2- and 1,3-amino-alcohols **89a** and diamines **89b** to give the activated intermediates **90a** and **90b**, respectively [44]. The intramolecular cyclization of **90a** and **90b** produces the cyclized products **91a** (2-oxazolidinones and 2-oxazinones) and **91b** (cyclic ureas). In this case, PhTMG could be replaced with triethylamine and no sodium azide is required.

11 Conclusion

Recent various aspects of DPPA in organic synthesis have been summarized. It will have other possibilities which will be found and developed further in near future.

References

1. Shioiri, T.; Ninomiya, K.; Yamada, S. *J. Am. Chem. Soc.* **1972**, *94*, 6203–6205.
2. Shioiri, T. *TCIMAIL* **2007**, No. 134, 2-19.
3. Takuma, S.; Hamada, Y.; Shioiri, T. *Chem. Pharm. Bull.* **1982**, *30*, 3147–3153.
4. Dzierzbicka, K.; Trzonkowski, P.; Sewerynek, P.; Kolodziejczyk, A. M.; Myśliwski, A. *J. Peptide Sci*. **2005**, *11*, 123–135.
5. Haberhauer, G.; Rominger, F. *Eur. J. Org. Chem.* **2003**, 3209–3218.
6. Yoshida, S.; Marumo, K.; Takeguchi, K.; Takahashi, T.; Mase, T. *Org. Process Res. Dev.* **2014**, *18*, 1721–1727.
7. Izzo, I.; Maulucci, N.; Bifulco, G.; Riccardis, F. D. *Angew. Chem. Int. Ed.* **2006**, *45*, 7557–7560.
8. Reddy, D. N.; Ballante, F.; Chuang, T.; Pirolli, A.; Marrocco, B.; Marshall, G. R. *J. Med. Chem.* **2016**, *59*, 1613–1633.
9. Haberhauer, G.; Drosdow, E.; Oeser, T.; Rominger, F. *Tetrahedron*, **2008**, *64*, 1853–1859.
10. Kanazawa, K.; Sato, Y.; Ohki, K.; Okimura, K.; Uchida, Y.; Shindo, M.; Sakura, N. *Chem. Pharm. Bull.* **2009**, *57*, 240–244.
11. Kubo, K.; Kohara, Y.; Imamiya, E.; Sugiura, Y.; Inada, Y.; Furukawa, Y.; Nishikawa, K.; Naka, T. *J. Med. Chem.* **1993**, *36*, 2182–2195.
12. Yamada, K.; Yamashita, M.; Sumiyoshi, T.; Nishimura, K.; Tomioka, K. *Org. Lett.* **2009**, *11*, 1631–1633.
13. Cini, E.; Banfi, L.; Barreca, G.; Carcone, L.; Malpezzi, L.; Manetti, F.; Marras, G.; Rasparini, M.; Riva, R.; Roseblade, S.; Russo, A.; Taddei, M.; Vitale, R.; Zanotti-Gerosa, A. *Org. Process Res. Dev.* **2016**, *20*, 270–283.
14. Tudhope, S. R.; Bellamy, J. A.; Ball, A.; Rajasekar, D.; Azadi-Ardakani, M.; Meera, H. S.; Gnanadeepam, J. M.; Saiganesh, R.; Gibson, F.; He, L.; Behrens, C. H.; Underiner, G.; Marfurt, J.; Favre, N. *Org. Process Res. Dev.* **2012**, *16*, 635–642.
15. Grongsaard, P.; Bulger, P. G.; Wallace, D. J.; Tan, L.; Chen, Q.; Dolman, S. J.; Nyrop, J.; Scott Hoerrner, R.; Weisel, M.; Arredondo, J.; Itoh, T.; Xie, C.; Wen, X.; Zhao, D.; Muzzio, D. J.; Bassan, E. M.; Scott Shultz, C. *Org. Process Res. Dev.* **2012**, *16*, 1069–1081.
16. Zhao, W.; Carreira, E. M. *Org. Lett.* **2011**, *13*, 5084–5087.
17. Carter, C. F.; Lange, H.; Ley, S. V.; Baxendale, I. R.; Wittkamp, B.; Goode, J. G.; Gaunt. N. L. *Org. Process Res. Dev.* **2010**, *14*, 393–404.
18. Filipponi, P.; Ostacolo, C.; Novellino, E.; Pellicciari, R.; Gioiello, A. *Org. Process Res. Dev.* **2014**, *18*, 1345–1353.
19. Park, J.-K. *Abstracts of The 3rd International Symposium on Process Chemistry*, **2015**, p. 80.
20. Lal, B.; Pramanik, B. N.; Manhas, M. S,; Bose, A. K. *Tetrahedron Lett.* **1977**, *18*, 1977–1980.
21. Thompson, A. S.; Humphrey, G. R.; DeMarco, D. J.; Mathre, D. J.; Grabowski, E. J. J. *J. Org. Chem.* **1993**, *58*, 5886–5888.
22. Thompson, A. S.; Hartner, Jr., F. W.; Grabowski, E. J. J. *Org. Synth.* **2004**, *Coll. Vol. 10*, 382–384.
23. Nagel, N. C.; Masic, A.; Schurigt, U.; Boland, W. *Org. Biomol. Chem.* **2015**, *13*, 5139–5146.
24. Ghosh, A. K.; Martyr, C. D.; Osswald, H. L.; Sheri, V. R.; Kassekert, L. K.; Chen, S.; Agniswamy, J.; Wang, Y.-F.; Hayashi, H.; Aoki, M.; Weber, I. T.; Mitsuya, H. *J. Med. Chem.* **2015**, *58*, 6994–7006.
25. Feher-Voelger, A.; Borges-González, J.; Carrillo, R.; Morales, E. Q.; González-Platas, J.; Martín, T. *Chem. Eur. J.* **2014**, *20*, 4007–4022.
26. Scott, J. P.; Alam, M.; Bremeyer, N.; Goodyear, A.; Lam, T.; Wilson, R. D.; Zhou, G. *Org. Process Res. Dev.* **2011**, *15*, 1116–1123.
27. Voight, E. A.; Daanen, J. F.; Hannick, S. M.; Shelat, B. H.; Kerdesky, F. A.; Plata, D. J.; Kort, M. E. *Tetrahedron Lett.* **2010**, *51*, 5904–5907.
28. Bellizzi, M. E.; Bhatia, A. V.; Cullen, S. C.; Gandarilla, J.; Kruger, A. W.; Welch, D. S. *Org. Process Res. Dev.* **2014**, *18*, 303–309.

29. Heidebrecht Jr., R. W.; Mulrooney, C.; Austin, C. P.; Barker Jr., R. H.; Beaudoin, J. A.; Cheng, K. C.; Comer, E.; Dandapani, S.; Dick, J.; Duvall, J. R.; Ekland, E. H.; Fidock, D. A.; Fitzgerald, M. E.; Foley, M.; Guha, R.; Hinkson, P.; Kramer, M.; Lukens, A. K.; Masi, D.; Marcaurelle, L. A.; Su, X.-Z.; Thomas, C. J.; Weïwer, M.; Wiegand, R. C.; Wirth, D.; Xia, M.; Yuan, J.; Zhao, J.; Palmer, M.; Munoz, B.; Schreiber, S. *ACS Med. Chem. Lett.* **2012**, *3*, 112–117.
30. Lakshman, M. K.; Singh, M. K.; Parrish, D.; Balachandran, R.; Day, B. W. *J. Org. Chem.* **2010**, *75*, 2461–2473.
31. Mizuno, M.; Shioiri, T. *Chem. Commun.* **1997**, 2165–2166.
32. Ishihara, K.; Hamamoto, H.; Matsugi, M.; Shioiri, T. *Tetrahedron Lett.* **2015**, *56*, 3169–3171.
33. Keith, J. M. *J. Org. Chem.* **2006**, *71*, 9540–9543.
34. Malil, M.; Witkowski, G.; Jarosz, S. *Org. Lett.* **2014**, *16*, 3816–3819.
35. González-Calderón, D.; Santillán-Iniesta, I.; González-González, C. A.; Fuentes-Benítes, A.; González-Romero, C. *Tetrahedron Lett.* **2015**, *56*, 514–516.
36. Schroeder, G. M.; Marshall, S.; Wan, H.; Purandare, A. V. *Tetrahedron Lett.* **2010**, *51*, 1404–1406.
37. Kim, S. H.; Jung, D. Y.; Chang, S. *J. Org. Chem.* **2007**, *72*, 9769–9771.
38. Kim, S. H.; Park, S. H.; Choi, J. H.; Chang, S. *Chem. Asian J.* **2011**, *6*, 2618–2634.
39. Shen, T.; Huang, X.; Liang, Y.-F.; Jiao, N. *Org. Lett.* **2015**, *17*, 6186–6189.
40. Pan, C.; Jin, N.; Zhang, H.; Han, J.; Zhu, C. *J. Org. Chem.* **2014**, *79*, 9427–9432.
41. Xiao, W.; Zhou, C.-Y.; Che, C.-M. *Chem. Commun.* **2012**, *48*, 5871–5873.
42. Ma, A.-J.; Tu, Y.-Q.; Peng, J.-B.; Dou, Q.-Y.; Hou, S.-H.; Zhang, F.-M.; Wang, S.-H. *Org. Lett.* **2012**, *14*, 3604–3607.
43. García-Egido, E.; Fernández-Suárez, M.; Muñoz, L. *J. Org. Chem.* **2008**, *73*, 2909–2911.
44. Paz, J.; Pérez-Balado, C.; Iglesias, B.; Muñoz, L. *J. Org. Chem.* **2010**, *75*, 3037–3046.

Methylenation Reaction of Carbonyl Compounds Using Julia-Kocienski Reagents

Kaori Ando

Abstract Methylenation of carbonyl compounds is an important reaction in organic synthesis. In this mini-review, typical and most often used methylenation reactions are summarized briefly. The new Julia-Kocienski type methylenation reagents are fully summarized together with its reaction mechanism and applications to the total synthesis of natural products.

Keywords Methylenation reagents · Julia-Kocienski reaction · Olefination · Carbonyl compounds · Heteroaryl sulfones

1 Introduction

The synthesis of alkenes from carbonyl compounds is one of the most fundamental reactions in organic synthesis. Since terminal alkene structures are not only found in many natural products but also used as substrates for many synthetic reactions such as olefin metathesis and sigmatropic reactions, their preparation has been studied intensively and many methylenation reagents have been developed [1]. The Wittig reaction [2], discovered by Georg Wittig in 1953, is one of the most often used reactions for this transformation. The reaction involves treatment of an aldehyde or a ketone with a phosphonium ylide **1**, yielding an alkene with the concomitant generation of phosphine oxide (Scheme 1). The methylenation reagent, $CH_3P(C_6H_5)_3Br$ is commercially available, inexpensive and used widely after the treatment with base such as *n*-BuLi. Although this reaction has been used extensively in organic synthesis, it includes some drawbacks. (1) The separation of the product akene from the byproduct, $Ph_3P{=}O$, is not always easy. (2) Since the Wittig reagents are strongly basic, the formation of enolates from carbonyl compounds is problematic. (3) The Wittig reaction with sterically hindered ketones often gives

K. Ando (✉)
Department of Chemistry and Biomolecular Science, Faculty of Engineering,
Gifu University, Yanagido 1-1, Gifu 501-1193, Japan
e-mail: ando@gifu-u.ac.jp

K. Tomioka et al. (eds.), *New Horizons of Process Chemistry*,
DOI 10.1007/978-981-10-3421-3_11

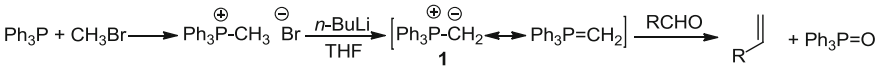

Scheme 1 Methylenation using the Wittig reaction

low yields or fails. To overcome these problems, many methodologies were developed. For examples, polymer-bound or fluorus-tagged phosphines, and water soluble phosphines have been invented for the separation of the byproduct phosphine oxides. Salt-free conditions were used for the reaction of an enolizable α-chiral ketone to give the corresponding methylene in good yield and high epimeric purity [3].

Peterson reported that trimethylsilyl-substituted organometallic compounds, $(CH_3)_3SiCHMR$, were effective intermediates in the conversion of carbonyl compounds to the corresponding alkenes [4]. Both $(CH_3)_3SiCH_2MgCl$ and $(CH_3)_3SiCH_2Li$ are commercially available. When either an aldehyde or a ketone is treated with $(CH_3)_3SiCH_2M$ (M = MgCl, Li), an addition product such as **3** forms (Scheme 2). Treatment of **3** with either K-base or Lewis acid causes the elimination of trimethylsilanol to give the corresponding methylene compound. Relatively speaking, the reagent **2** can react even with sterically hindered ketones and the by-product is easily removable hexamethyldisiloxane, $Me_3SiOSiMe_3$. Although their high basicity is sometimes problematic, it was reported that the reagent derived from Me_3SiCH_2Li and anhydrous $CeCl_3$ gave better yields of addition products from enolizable aldehydes and ketones than Me_3SiCH_2M (M = MgX, Li) [5].

The *gem*-dimetallic reagents have been studied extensively for methylenation reagents for carbonyl compounds. Tebbe reported the reagent **4** prepared from Cp_2TiCl_2 and $AlMe_3$ can react with carbonyl compounds, not only aldehydes and ketones but also esters and amides, to give the corresponding methylene products (Scheme 3) [6]. The active species is believed to be $Cp_2Ti{=}CH_2$, which is also the active species of the Petasis reagent **5** [7]. The Petasis reagent, Cp_2TiMe_2, is easily prepared from Cp_2TiCl_2 with either MeMgCl or MeLi and can be isolated as a relatively stable solid. It undergoes thermal α-elimination at 60–65 °C to afford

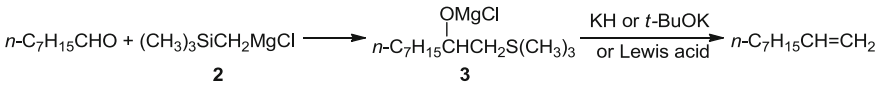

Scheme 2 Methylenation using the Peterson reaction

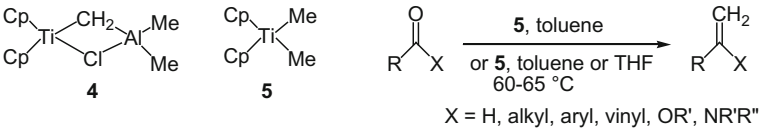

Scheme 3 Methylenation with Tebbe reagent **4** and Petasis reagent **5**

$Cp_2Ti{=}CH_2$ and reacts with carbonyl compounds including both esters and amides to give the corresponding methylene compounds in good yields. Since **5** does not contain strongly Lewis acidic aluminum compounds, the reaction of **5** is milder than that of Tebbe reagent **4** and the methylenation reaction is more reproducible. Although both reagents **4** and **5** are commercially available, the cost of these reagents as well as sensitivity and functional compatibility calls for alternative procedures.

Nozaki/Oshima/Takai and Lombardo reported the methylenation of aldehydes and ketones with a CH_2X_2–$TiCl_4$–Zn (X = Br, I) system [8, 9] and Takai/Utimoto later discovered that the effective lots of zinc contained 0.04–0.07 mol% of lead on the basis of zinc and the less effective zinc sample was free of lead [10]. From their study, a catalytic amount of lead promotes the formation of a geminal dizinc compound, $CH_2(ZnX)_2$, which is a key intermediate of the methylenation reaction [11]. In the improved procedure, $PbCl_2$ (1 mol% based on zinc) is added to zinc from the beginning (Scheme 4). Generally, the CH_2Br_2–$TiCl_4$–Zn–$PbCl_2$ system is useful for the methylenation of aldehydes and ketones especially when the substrates cannot tolerate basic conditions. Commercially available Nysted reagent **7** is also used for the methylenation of aldehydes and ketones in the presence of Lewis acid such as $BF_3{\cdot}OEt$, $BF_3{\cdot}OEt/TiCl_2$, and $TiCl_4$ [12, 13].

Transition metal-catalyzed methylenation reactions using $TMSCHN_2$ have also been reported. Not only Rhodium catalyst [14] (Scheme 5) but also Copper-carbene complexes [15] can be used as a catalyst.

The methods mentioned above are all useful methylenation reactions and often used in the synthesis of natural products. However, the methylenation reactions sometimes failed or gave only disappointing yields. For example, attempted methylenation of **8** by employing either a Wittig reaction or a Peterson olefination of the corresponding silyl ether proved unsuccessful or met with only limited success (Scheme 6) [16]. This transformation of **8** was accomplished by application of the method of Nozaki/Oshima/Takai and Lombardo to give the corresponding methylene in 48% yield [8, 9]. Various attempted methylenation of **9**, including

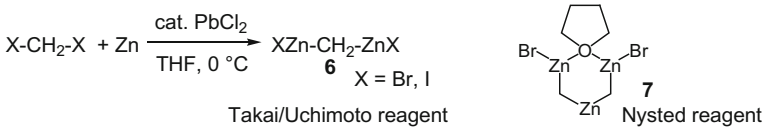

Scheme 4 Takai/Uchimoto reagent **6** and Nysted reagent **7**

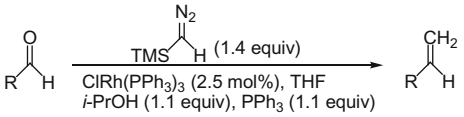

Scheme 5 Rhodium-catalyzed methylenation

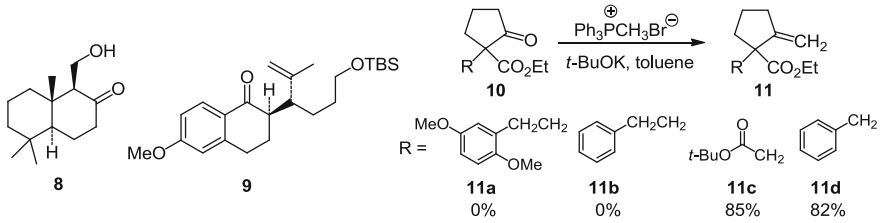

Scheme 6 Examples of methylenation reactions

Peterson, Wittig, Lombardo, and Tebbe olefinations, failed or gave only disappointing yields of the methylene product [17]. The best results were achieved by using the Petasis method [7] to give the desired alkene in 90% yield. Attempted methylenation of **10a** to give **11a** with either the Wittig reagent or the Takai/Uhimoto reagent [10] resulted in complete recovery of **10a** at room temperature and decomposition at elevated temperature [18]. Interestingly, both **11c** and **11d** were obtained at high yields by the Wittig reaction, while **11b** was not obtained at all. Thus, the results of the methylenation reactions depend on only a slight difference of the substrate structures and the methods used. Therefore, there is still a need to develop a new and practical route to the methylenation reaction.

2 Methylenation Reaction with Benzothiazol-2-yl (BT) Methyl Sulfone

The Julia-Kocienski reaction (one-pot Julia olefination) is a very efficient tool for direct alkene synthesis from carbonyl compounds and used extensively in the last decade for the construction of C=C bonds present in many natural products [19, 20]. In 1991, Sylvestre A. Julia and co-workers described a direct olefine synthesis from the reaction of carbanions of benzothiazol-2-yl sulfones (BT-sulfones) **12** with ketones and aldehydes [21, 22]. When **12** was treated with LDA in the presence of carbonyl compounds at −78 °C and then the temperature was allowed to rise to room temperature, alkenes were obtained in reasonable yields (Scheme 7). This Barbier-type procedure (a reagent is treated with base in the presence of a carbonyl compound) gave better yields than the procedure that a reagent is treated with base before the addition of a carbonyl compound. A plausible reaction mechanism is also shown in Scheme 7. The reaction of alkyl BT-sulfones with aliphatic aldehydes gave a mixture of *E* and *Z*-alkenes (generally $E/Z \approx 50/50$). *E*-alkenes were obtained from the reaction of either alkyl BT-sulfones with aromatic aldehydes, or benzyl BT-sulfones with branched aldehydes, α,β-unsaturated aldehydes, or aromatic aldehydes. *Z*-alkenes were obtained from the reaction of propargylic BT-sulfones. Although this reaction is useful for not only alkene synthesis but also fragment linkage, it has some limitations. That is, high stereoselectivities are only

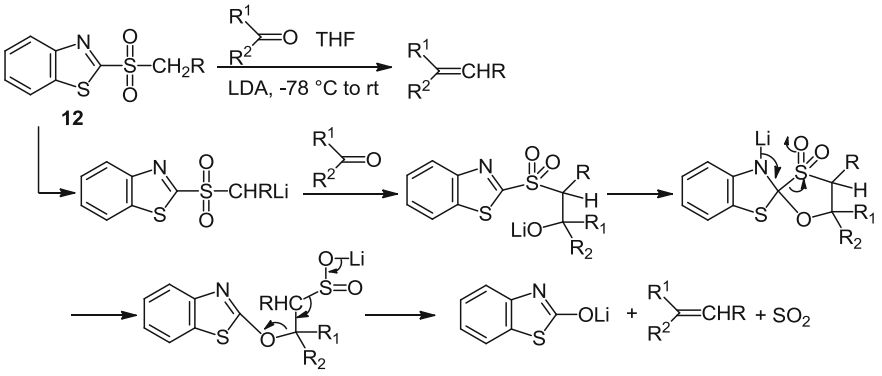

Scheme 7 One-pot Julia olefination with the BT sulfone **12**

Scheme 8 Methylenation with the BT methyl sulfone **12a**

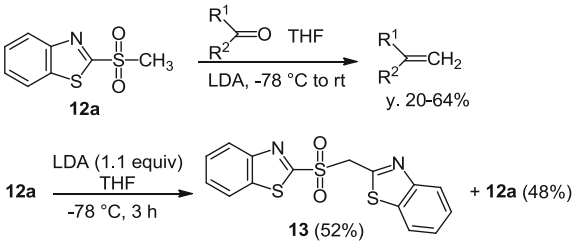

obtained in special cases and many lithiated BT-sulfones are unstable and undergo self-condensation even at low temperature as shown in Scheme 8. In addition, the Barbier conditions are likely to be incompatible with complex aldehyde substrates.

Julia and co-workers also studied the methylenation reaction of ketones and aldehydes briefly with benzothiazol-2-yl (BT) methyl sulfone **12a** [21, 22]. When a THF solution of **12a** and carbonyl compound was treated with LDA at −78 °C under the Barbier conditions, terminal alkenes were obtained in 20–21% yields from an aliphatic aldehyde and ketone, and in 44–64% yields from aromatic aldehydes and ketones (Scheme 8). The lithiated carbanion derived from **12a** proved to be unstable. Treatment of **12a** with 1.1 equiv of LDA at −78 °C for 3 h gave compound **13** (52%) resulting from the nucleophilic attack of the lithiated carbanion at the *ipso* position of itself or **12a**. Since **12a** are susceptible to nucleophilic attack at the *ipso* position, deprotonation of **12a** should be performed with non-nucleophilic bases. For the methylenation reaction, the reagent **12a** is only useful for the reactive carbonyl compounds such as aromatic aldehydes and ketones.

Methylenation of sugar-derived lactones using the reagent **12a** was reported by Gueyard et al. [23]. Although the standard modified Julia procedure gave low yields of the corresponding methylene exoglycals, a two-step sequence worked. The first step consists of the addition of $(Me_3Si)_2NLi$ (LiHMDS) to a THF solution of **12a**

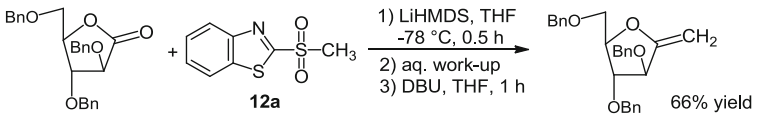

Scheme 9 Methylenation of sugar-derived lactones with **12a**

and lactone at −78 °C to provide the hemiketal intermediate. After aqueous work-up, treatment of the crude intermediate with DBU in THF led to the methylene exoglycals in 46–74% yields (7 examples) (Scheme 9). Both pyranose and furanose rings were successfully employed.

3 Methylenation Reaction with Methyl 1-Phenyl-1*H*-tetrazol-5-yl (PT) Sulfone

In order to improve carbanion stability and stereoselectivity, Kocienski and co-workers examined many heterocyclic sulfones and found 1-phenyl-1*H*-tetrazol-5-yl (PT) sulfones **14** gave much better yields and stereoselectivity compared with its BT counterpart **12** [24]. The PT-sulfone anions are less prone to self-condensation and the reactions of **14** with aldehydes can be performed via premetallated carbanions (non-Barbier conditions). Simple *E*-alkenes were obtained from the reaction of the alkyl PT-sulfones with aldehydes highly selectively, while the BT-sulfones gave a mixture of *E*- and *Z*-alkenes (1:1). For examples, the reaction of *n*-pentyl PT-sulfone **14a** with *n*-hexanal gave 5*E*-undecene in 71% yield with *E*:*Z* = 94:6 selectivity and a similar reaction of **12b** gave a nearly 1:1 mixture (Scheme 10). Generally, a combination of potassium hexamethyldisilazide (KHMDS) as base and 1,2-dimethoxyethane (DME) as solvent results in high *E*-selectivity with a sacrifice in yield compared with LiHMDS and NaHMDS as base. When the yield is unacceptable, the use of NaHMDS in DME provides optimum yield and stereoselectivity. The BT-sulfones and the PT-sulfones were prepared from the commercially available benzothiazole-2-thiol and 1-phenyl-1*H*-tetrazole-5-thiol, respectively, by alkylation and the following oxidation.

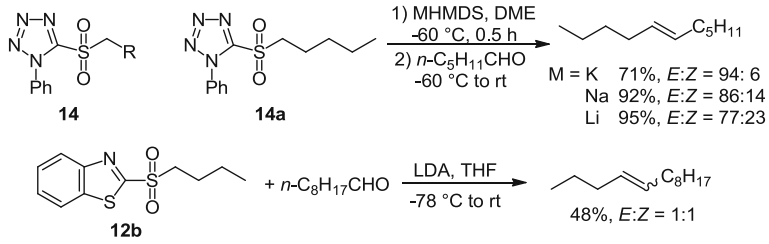

Scheme 10 Julia-Kocienski reactions with **14a** and **12b**

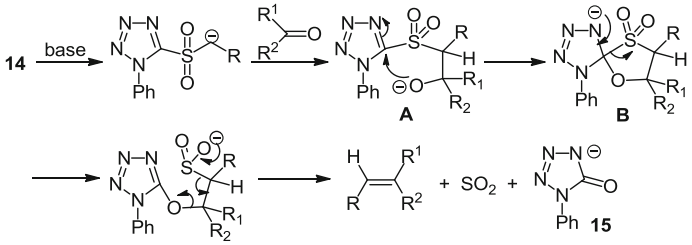

Scheme 11 A plausible reaction mechanism of olefination with the PT sulfone **14**

The reactions of **14** with carbonyl compounds are believed to occur in a similar way as the reactions of the BT-sulfones in Scheme 7. The anions derived from **14** and base react with carbonyl compounds to give the alkoxide **A**, from which nucleophilic addition to the tetrazole ring occurs to give **B** (Scheme 11). Alkene products would be formed by Smiles rearrangement along with **15** and SO_2.

The methylenation reaction using methyl PT-sufone **14b** was first reported by Hale and co-workers [25]. In their formal total synthesis of (−)-Agelastatin A, the Wittig methylenation of **16** with $Ph_3P{=}CH_2$ was unsuccessful under all the conditions that they studied. Tebbe and Peterson olefination with $Cp_2Ti{=}CH_2$ and Me_3SiCH_2MgCl, respectively, also failed to give **17**. Finally, they prepared the Kocienski's Me reagent **14b** and a THF solution of **14b** and **16** was treated with a toluene solution of KHMDS (3.6 equiv) at −20 °C to give **17** (Barbier conditions) contaminated with tetrazole by-product. After ring-closing metathesis and then heating with K_2CO_3 in MeOH at reflux, **18** was obtained in 36% overall yield from **16** (Scheme 12). The same procedure was applied for the methylenation of **19** with **14b** by Davis and co-workers in the synthesis of piperidine (2S,3S)-(+)-CP-99,994

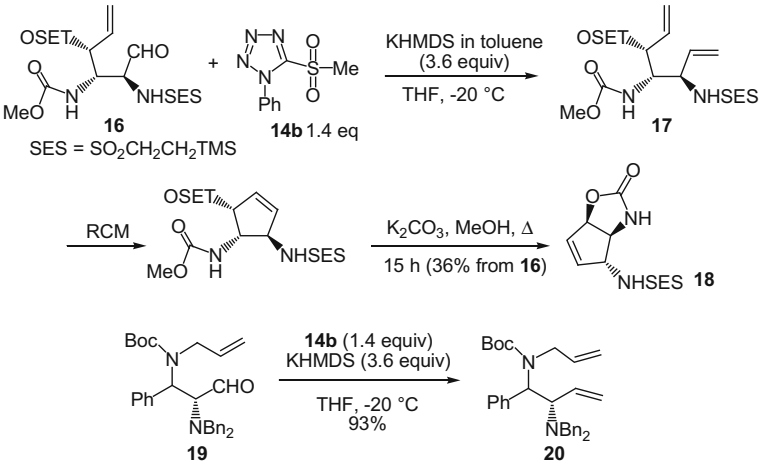

Scheme 12 Methylenation with the PT methyl sulfone **14b**

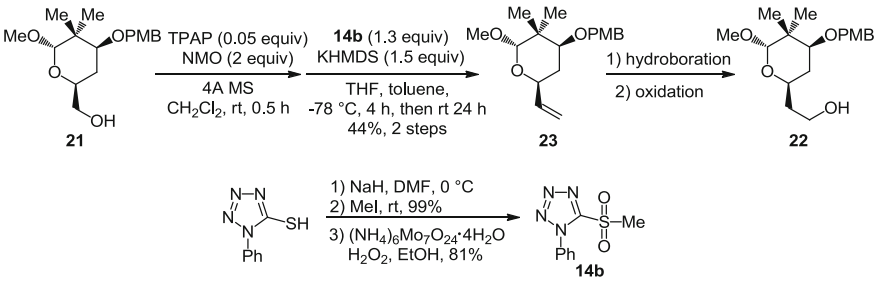

Scheme 13 Preparation of **14b** and its use in synthesis

[26]. Termianl alkene **20** was obtained in 93% yield. Attempted Wittig reaction of **19** using $Ph_3PCH_3^+Br^-$/*t*-BuOK resulted in decomposition.

Hale and co-workers also reported the methylenation using the reagent **14b** under the Barbier conditions in the formal total synthesis of Bryostatin 7 [27]. Several unsuccessful methods were explored for homologation of **21** to prepare **22** (Scheme 13). This could be achieved by sequential TPAP oxidation of **21** and the Julia-Kocienski methylenation with **14b** to give **23** in 44% overall yield. The Wittig reaction of the same aldehyde with $Ph_3P{=}CH_2$ gave totally unsatisfactory results. The terminal alkene **23** was transformed to the alcohol **22** by Evans' rhodium-catalyzed hydroboration and oxidative workup. Thus, the methyleneation reaction can be used for the homologation of alcohols. The reagent **14b** was prepared from commercially available 1-phenyl-1*H*-tetrazole-5-thiol by methylation using NaH and MeI in DMF and the following oxidation by 30% H_2O_2 catalyzed by ammonium molybdate in ethanol [28, 29].

Rychnovsky and co-workers reported the methylenation of **24** using **14b** in the total synthesis of SCH 351448 and the terminal alkene **25** was obtained in 93% yield (Scheme 14) [30]. They used NaHMDS as base in THF and the premetallated sulfone was treated with aldehyde **24** at −78 °C followed by warming to room temperature. Zhu and Panek also performed the same methylenation of **24** according to the procedure of Rychnovsky and got a similar high yield of **25** [31]. Krishna et al. [32] used similar conditions for the methylenation of **26** to give **27** in 74% yield in the formal synthesis of amphidinin B. In the synthesis of aglycone of Mandelalide A, alcohol **28** was oxidized with Dess-Martin periodinane (DMP) to give an aldehyde which was subjected to the Julia-Kocienski methylenation using Rychnovsky's procedure by Ghosh et al. [33]. The terminal alkene **29** was obtained in 80% yield from **28**. They used the same procedure for the methylenation of α-chiral aldehyde in the total synthesis of (−)-bitungolide B & E [34]. The desired alkene was obtained in 78% yield from the corresponding alcohol over two steps. Smith and co-workers also reported methylenation of a similar system to **28** using the same procedure and got a terminal alkene in high yield [35].

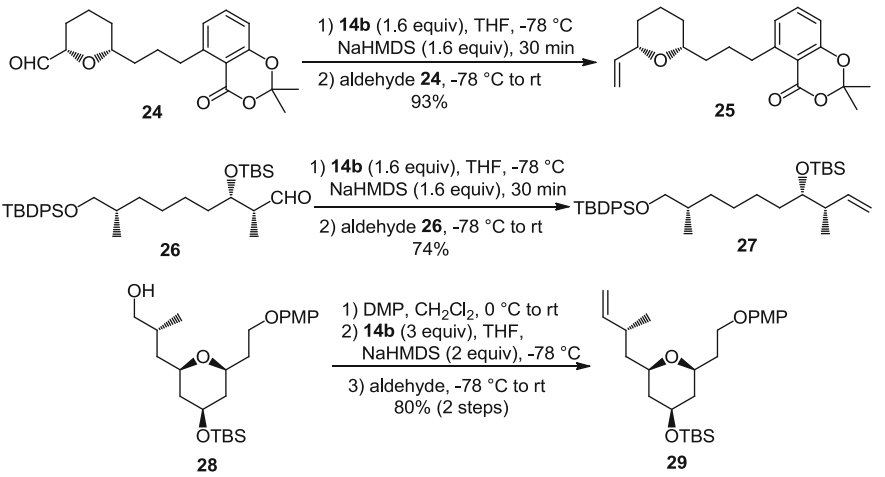

Scheme 14 Examples of methylenation reaction with **14b**

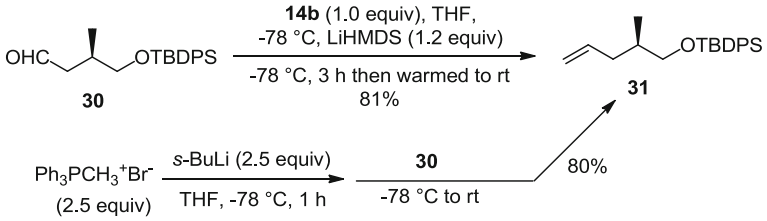

Scheme 15 Methylenation with **14b** and the Wittig reagent

Li, Piccirilli and co-workers reported methylenation of aldehyde **30** in the total synthesis of β-D-mannosyl phosphomycoketide [36]. The Julia-Kocienski methylenation was performed by treating a THF solution of **14b** and **30** with LiHMDS (1.2 equiv) at −78 °C, and then the mixture was allowed to warm to room temperature (Barbier conditions) (Scheme 15). The alkene **31** was obtained in 81% yield. The Wittig reaction of **30** using $Ph_3PCH_3^+Br^-$ (2.5 equiv) and *s*-BuLi (2.5 equiv) in THF was also performed and **31** was obtained in 80% yield.

4 Methylenation Reaction with 1-*Tert*-Butyl-1*H*-tetrazol-5-yl (TBT) Methyl Sulfone

Although the PT-sulfones **14** are more stable than the BT-sulfones **12**, they too decompose, especially when KHMDS is used as base. Kocienski and co-workers reasoned that by simply increasing the steric bulk of the substituent on the tetrazole

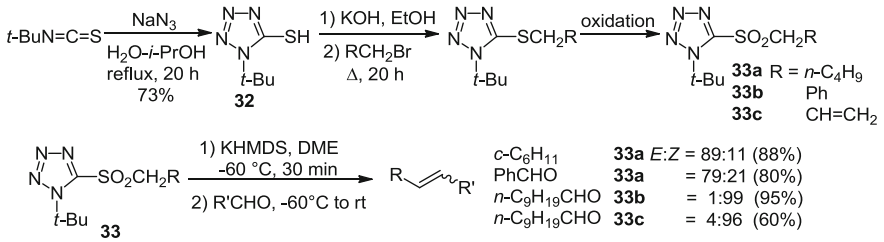

Scheme 16 The preparation of the TBT sulfones **33** and their olefination reaction

ring, the stability of the corresponding metallated sulfones should be enhanced. They prepared 1-*tert*-butyl-1*H*-tetrazol-5-yl sulfones which is in fact more stable than the PT-sulfones under the basic conditions. The thiol **32** is readily prepared in 73% yield by the reaction of commercial *tert*-butyl isothiocynate with sodium azide (1 equiv) in refluxing aqueous 2-propanol for 20 h (Scheme 16) [37]. Alkylation of **32** with alkyl halide followed by oxidation gave 1-*tert*-butyl-1*H*-tetrazol-5-yl (TBT) sulfones **33**. The oxidation was accomplished by three different procedures. The *n*-pentyl sulfone **33a** was prepared by oxidation with oxone in MeOH (81%) or MCPBA in CH_2Cl_2 in the presence of 2.5 equiv of $NaHCO_3$ (73%). The allyl sulfone **33c** was prepared in 49% yield by oxidation with ammonium molybdate and H_2O_2. By contrast, oxidation of the benzyl sulfide was poor by any method and the best yield of **33b** was 12% using oxone in MeOH. The olefination reaction of aldehydes with **33** using KHMDS in DME was briefly studied (only 4 examples) (Scheme 16) [38]. Although the yields of alkenes are higher with **33a**, the *E*-selectivity is lower compared with the reaction with the PT-analogue **14**. The *Z*-alkenes were obtained highly selectively from the reaction of both **33b** and **33c** with *n*-decanal.

The methylenation reaction using the TBT-sulfone was reported by Aïssa [39]. Since the TBT-sulfones are more stable than the PT- and BT-sulfones, methyl TBT-sulfone **33d** is supposed to be useful for methylenation. The reagent **33d** was prepared from **32** by methylation with NaH and MeI in THF followed by oxidation with H_2O_2 and $Mo_7O_{24}(NH_4)_6$ in EtOH in 91% yield (Scheme 17). It became clear that a Barbier-type procedure was convenient and the generation of the premetalled sulfone led only to low conversion to the terminal alkene and degradation.

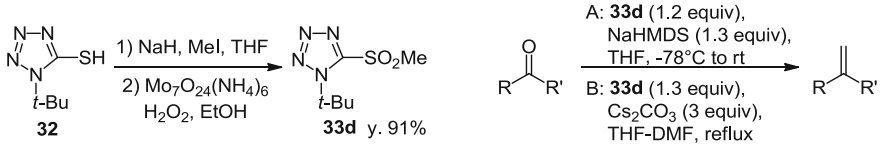

Scheme 17 Methylenation with the TBT methyl sulfone **33d**

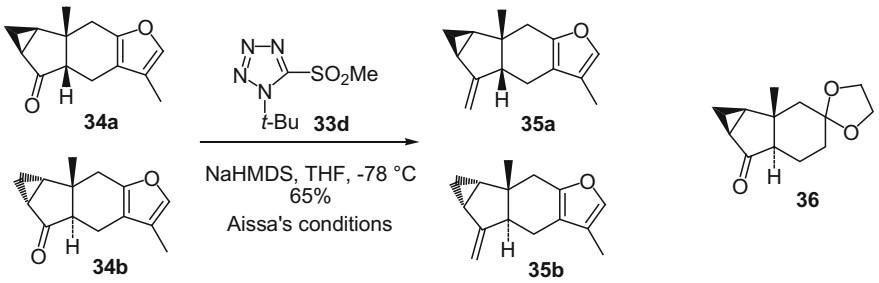

Scheme 18 Examples of methylenation with **33d**

Two different sets of conditions were found to be best. With conditions A, NaHMDS (1.3 equiv) was added to a THF solution of **33d** and an aldehyde or a ketone at −78 °C, and the mixture was slowly warmed to room temperature. With conditions B, a suspension of Cs_2CO_3 (3 equiv), **33d**, an aldehyde or a ketone in THF-DMF (3:1) was heated at 70 °C. Both aldehydes and ketones reacted smoothly to furnish the desired terminal alkenes in good to excellent yields (A: 59–99% yields, 10 examples, B: 45–96% yields, 11 examples). The reaction displayed a good functional group compatibility as esters, lactones, carbamates, acetals, silyl, and *p*-methoxybenzyl ethers were tolerated.

During the synthetic study of Lindenene, the ketone groups of compounds **34a** and **34b** were transformed to exo-methylene groups by Baldwin and co-workers (Scheme 18) [40]. This seemingly trivial functional group modification turned out to be more difficult than expected. Mixture **34a** and **34b** was found to be completely inert toward $Ph_3P{=}CH_2$, presumably due to steric factors. When Nysted reagent **7** and $TiCl_4$ was used, substantial decomposition of compounds **34a** and **34b** occurred, presumably due to the acid-sensitive nature of the furan ring and the strong Lewis acidity of $TiCl_4$. Finally, a mixture of **34a** and **34b** was transformed to *epi*-lindenene **35a** and *iso*-lindenene **35b** in 65% combined yield by using **33d** and NaHMDS at −78 °C according to Aïssa's procedure. A similar ketone **36** was also methylenated using the same procedure to give the corresponding terminal alkene in 72% yield [41].

Methylenation of **37** using **33d** (10 equiv) and NaHMDS (10 equiv) under the Barbier conditions was reported by Sasaki and co-workers during the synthetic study of (−)-Exiguolide analogues to give **38** in 100% yield (Scheme 19) [42]. On the other hand, methylenation of the ketone prepared from **39** by oxidation with Dess-Martin periodinane in the presence of $NaHCO_3$ was performed via premetallated sulfone from **33d** by Zhao and Qian. The terminal alkene **40** was obtained in 99% yield from **39** over two steps in the total synthesis of (+)-chloranthalactone F [43].

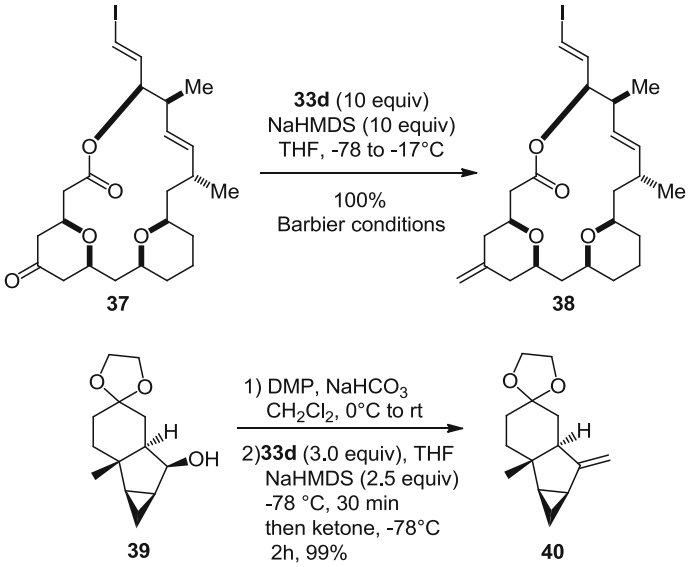

Scheme 19 Examples of methylenation with **33d**

5 Methylenation Reaction with 3,5-Bis(trifluoromethyl) phenyl Methyl Sulfone

Nájera and co-workers studied the reaction of 3,5-bis(trifluoromethyl)phenyl methyl sulfone **41** with various aldehydes and ketones (Scheme 20) [44]. The reaction proved to be much more efficient when Barbier-type conditions were used and employing P4-*t*-Bu as base. The terminal alkenes were obtained in 30–82% yields (9 examples). Since both 3,5-bis(trifluoromethyl)thiophenol and P4-*t*-Bu are very expensive and the yields are just moderate, no application for the total synthesis has been reported so far.

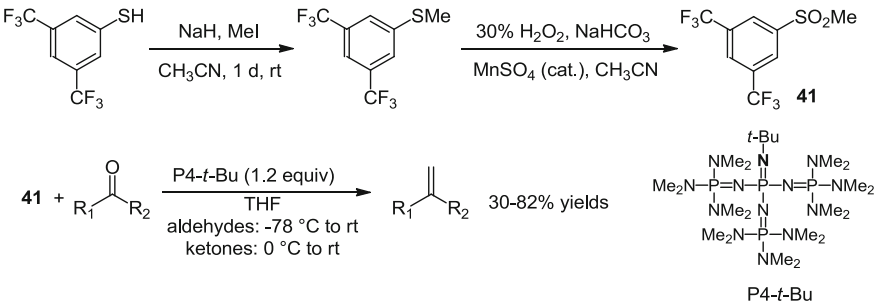

Scheme 20 Methylenation with 3,5-bis(trifluoromethyl)phenyl methyl sulfone **41**

6 Methylenation Reaction with 1-Methylbenzimidazoly (MBI) Methyl Sulfone

Since Kocienski and co-workers demonstrated that the anions derived from TBT alkyl sulfones are more stable than the PT and BT counterparts [35], **33d** seems to be the best methylenation reagent. However, the starting material for the preparation of **33d** is expensive, the metalation reaction requires rather expensive bases such as NaHMDS or Cs_2CO_3, and there is some room for improvement of the yields. Kende and Mendoza reported that the imidazolyl sulfones **42** react with aldehydes to give β-hydroxy imidazolyl sulfones, which can be transformed to alkenes using SmI_2 [45]. We had a working hypothesis that the benzo-fused imidazolyl sulfone **43** can react with carbonyl compounds to afford alkenes directly. New methylenation reagent **43a** was prepared from cheap 2-mercaptobenzimidazole by dimethylation and oxidation in 92% yield. A DMF solution of **43a** and a ketone was treated with NaHMDS (1.7 equiv) at −55 °C and the mixture was slowly warmed to room temperature. After aqueous work-up with aq. NH_4Cl, the corresponding terminal alkenes were directly obtained in 86–95% yields along with **44** (Scheme 21) [46]. Although the reactions with aldehydes proceeded efficiently in the same procedure, it is better to use 1.3 equiv of base instead of 1.7 equiv.

The methylenation reaction of ketones and aldehydes with **43a** was also performed using *t*-BuOK (2.6–4.0 equiv) in DMF at room temperature (Scheme 22) [46]. Excess amount of *t*-BuOK is needed in order to get higher yields especially for the reaction of ketones. Generally, the reaction completed within 1 h to give the terminal alkenes in high yields. α-Tetralone **45g** is known to be easily deprotonated to give a stable enolate ion and it was reported that treatment of **45g** with $Ph_3P{=}CH_2$ gave its enolate instead of leading to any alkene product. On the other hand, the reaction of **45g** with **43a** gave the terminal alkene in 71% yield. The yield

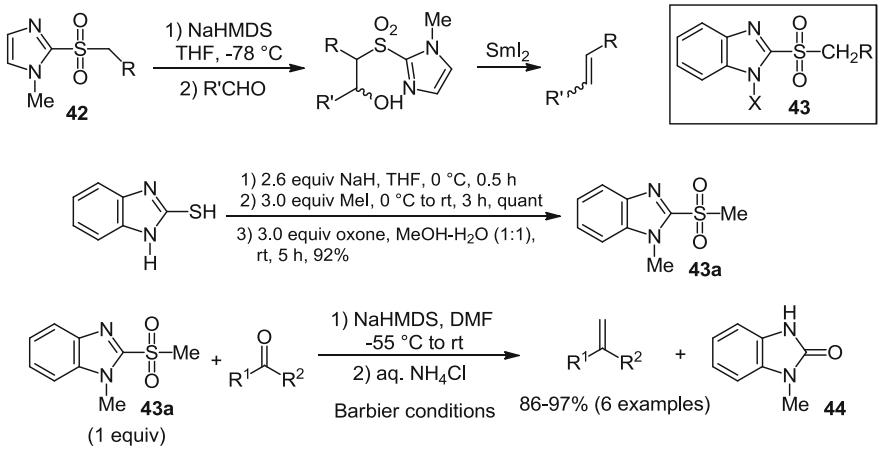

Scheme 21 Methylenation with 1-methylbenzimidazoly methyl sulfone **43a**

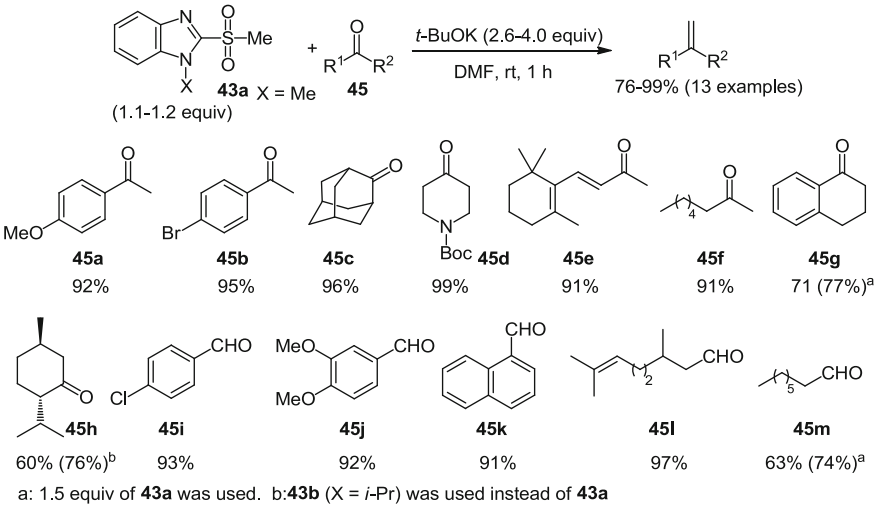

Scheme 22 Methylenation with **43a** using *t*-BuOK at room temperature

of the alkene was improved to 77% along with the recovered **45g** (23%) by using 1.5 equiv of **43a**. The reaction of sterically hindered (−)-menthone **45 h** with **43a** gave the terminal alkene in 60% yield along with the recovered **45h** (39%) and trace amount of **43a**. The results show that **43a** decomposes slowly in the presence of *t*-BuOK in DMF at room temperature, and the yield of the alkene was just moderate because of the low reactivity of sterically hindered **45h**. The yield was increased to 76% by using the more stable reagent **43b** (X = *i*-Pr). The combined yields of the product alkenes and the recovered carbonyl compounds **45** in Scheme 22 were nearly equal to 100% except for the reaction with *n*-octanal **45m**, where **45m** was not left at all after 1 h. Since simple aldehyde **45m** is not stable under basic conditions, the yield of the alkene is moderate (74%).

For comparison, the PT-sulfone reagent **14b** was reacted with ketone **45d** using *t*-BuOK (3.0 equiv) in DMF at room temperature for 1 h. The alkene was obtained in 72% yield along with the recovered **45d** (14%). The sulfone **14b** was not recovered at all. Since **43a** is much more stable than **14b** in the presence of base, this seems to be the reason that **43a** gave much higher yield (99%).

A plausible reaction mechanism is shown in Scheme 23. The anion derived from **43a** and base reacts with carbonyl compound to give the adduct **A**, from which nucleophilic addition to the benzimidazole part occurs to give **B**. The terminal alkene would be formed by Smiles rearrangement along with **44** and SO_2. Since we could not detect any gas bubble even in a 5 mmol scale reaction, SO_2 probably reacts with *t*-BuOK to form *t*-$BuOSO_2K$. After aqueou workup with aq NH_4Cl, the alkene and **44** were obtained. The byproduct **44** can be removed from the reaction mixture by either filtration or column chromatography. When the reaction mixture was diluted with hexane and washed with 1 M NaOH in order to remove the anion

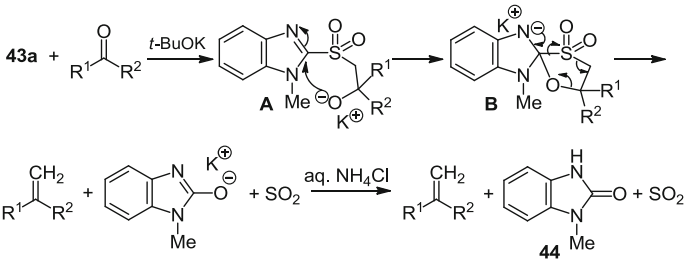

Scheme 23 A plausible reaction mechanism of methylation with **43a**

of **44**, the usual workup gave almost pure alkenes. At least, in some cases, higher yields were obtained after basic workup rather than neutral workup.

7 Conclusions

In this mini-review, the Julia-Kocienski type methyenation reagents were fully summarized. At present, five Julia-Kocienski type methylenation reagents were invented. Both their reactivity and stability under basic conditions is dependent on the heteroaryl group of these reagents. For comparison, classical methylenation reaction of carbonyl compounds, the Wittig reaction, the Peterson reaction, the reaction with *gem*-dimetallic reagents such as Tebbe reagent, Petasis reagent, $CH_2(ZnX)_2$ reagents, and Nysted reagent, and transition metal-catalyzed methylenation reaction are also summarized briefly. Although these methods may be still the first choice of the methylenation reaction, the Julia-Kocienski reaction is becoming one of the most reliable methylenation methods. I believe some of the Julia-Kocienski type reagents are useful complements to the classical methods and have wide applicability for the synthesis of bioactive active molecules and materials.

Acknowledgements This work was partially supported financially by the JSPS KAKENHI Grant Number 25410111.

References

1. For a review: see Muller, C.; Cokoja, M.; Kuhn, F. E. "Modern variants of Wittig, Peterson, and Tebbe protocols" from Science of Synthesis, C-1 Building Blocks in Organic Synthesis, **2014**, *2*, 1–19.
2. Wittig, G.; Geissler, G. *Liebigs Ann. Chem.* **1953**, *580*, 44.
3. Liapis, M.; Ragoussis, V.; Ragoussis, N. *J. Chem. Soc., Perkin Trans. 1* **1985**, 815.
4. Peterson, D. J. *J. Org. Chem.* **1968**, *33*, 780.
5. Johnson, C. R.; Tait, B. D. *J. Org. Chem.* **1987**, *52*, 281.

6. Tebbe, F. N.; Parshall, G. W.; Reddy, G. S. *J. Am. Chem. Soc.* **1978**, *100*, 3611.
7. Petasis, N. A.; Bzowej. E. *J. Am. Chem. Soc.* **1990**, *112*, 6392.
8. Takai, K.; Hotta, Y.; Oshima, K.; Nozaki, H. *Tetrahedron Lett.* **1978**, *19*, 2417.
9. Lombardo, L. *Tetrahedron Lett.* **1982**, *23*, 4293.
10. Takai, K.; Kakiuchi, T.; Kataoka, Y.; Utimoto, K. *J. Org. Chem.* **1994**, *59*, 2668.
11. Sada, M.; Komagawa, S.; Uchiyama, M.; Kobata, M.; Mizuno, T.; Utimoto, K.; Oshima, K.; Matsubara, S. *J. Am. Chem. Soc.* **2010**, *132*, 17452.
12. Matsubara, S.; Sugihara, M.; Utimoto, K. *Synlett* **1998**, 313.
13. Chausset-Boissarie, L.; Àrvai, R.; Cumming, G. R.; Guénée, L.; Kündig, E. P. *Org. Biomol. Chem.* **2012**, *10*, 6473.
14. Lebel, H.; Paquet, V. *J. Am. Chem. Soc.* **2004**, *126*, 320.
15. Lebel, H.; Davi, M.; Díez-González, S.; Nolan, S. P. *J. Org. Chem.* **2007**, *72*, 144.
16. Shishido, K.; Tokunaga, Y.; Omachi, N.; Hiroya, K.; Fukumoto, K.; Kametani, T. *J. Chem. Soc., Perkin Trans. I* **1990**, 2481.
17. Kaluza, N. M.; Schollmeyer, D.; Nubbemeyer, U. *Eur. J. Org. Chem.* **2016**, 357.
18. Chen, D.; Liu, H.-M.; Li, M.-M.; Yan, Y.-M.; Xu, W.-D.; Li, X.-N.; Cheng, Y.-X.; Qin, H.-B. *Chem. Commun.* **2015**, *51*, 14594.
19. For a review: Blakemore, P. R. *J. Chem. Soc., Perkin Trans. 1* **2002**, 2563.
20. For a review: Aïssa, C. *Eur. J. Org. Chem.* **2009**, 1831.
21. Baudin, J. B.; Hareau, G.; Julia, S. A.; Ruel, O. *Tetrahedron Lett.* **1991**, *32*, 1175.
22. Baudin, J. B.; Hareau, G.; Julia, S. A.; Lorne, R.; Ruel, O. *Bull. Soc. Chim. Fr.* **1993**, *130*, 856.
23. Gueyrard, D.; Haddoub, R.; Salem, A.; Bacar, N. S.; Goekjian, P. G. *Synlett* **2005**, 520.
24. Blakemore, P. R.; Cole, W. J.; Kocienski, P. J.; Morley, A. *Synlett* **1998**, 26.
25. Hale, K. J.; Domostoj, M. M.; Tocher, D. A.; Irving, E.; Scheinmann, F. *Org. Lett.* **2003**, *5*, 2927.
26. Davis, F. A.; Zhang, Y.; Li, D. *Tetrahedron Lett.* **2007**, *48*, 7838.
27. Manaviazar, S.; Frigerio, M.; Bhatia, G. S.; Hummersone, M. G.; Aliev, A. E.; Hale, K. J. *Org. Lett.* **2006**, *8*, 4477.
28. Lebrun, M.-E.; Marquand, P. L.; Berthelette, C. *J. Org. Chem.* **2006**, *71*, 2009.
29. Kauer, J. C.; Sheppard, W. A. *J. Org. Chem.* **1967**, *32*, 3580.
30. Cheung, L. L.; Marumoto, S.; Anderson, C. D.; Rychnovsky, S. D. *Org. Lett.* **2008**, *10*, 3101.
31. Zhu, K.; Panek, J. S. *Org. Lett.* **2011**, *13*, 4652.
32. Krishna, P. R.; Anitha, K.; Raju, G. *Tetrahedron* **2013**, *69*, 1649.
33. Ghosh, S. ; Reddy, K. M.; Yamini, V.; Singarapu, K. K. *Org. Lett.* **2014**, *16*, 2658.
34. Reddy, K. M.; Shashidhar, J.; Ghosh, S. *Org. Biomol. Chem.* **2014**, *12*, 4002.
35. Nguyen, M. H.; Imanishi, M.; Kurogi, T.; Smith, III, A. B. *J. Am. Chem. Soc.* **2016**, *138*, 3675.
36. Li, N.-S.; Scharf, L.; Adams, E. J.; Piccirilli, J. A. *J. Org. Chem.* **2013**, *78*, 5970.
37. Quast, H.; Bieber, L. *Chem. Ber.* **1981**, *114*, 3253.
38. Kocienski, P. J.; Bell. A.; Blakemore, P. R. *Synlett* **2000**, 365.
39. Aïssa, C. *J. Org. Chem.* **2006**, *71*, 360.
40. Fenlon, T. W.; Schwaebisch, D.; Mayweg, A. V. W.; Lee, V.; Adlington, R. M.; Baldwin, J. E. *Synlett* **2007**, 2679.
41. Fenlon, T. W.; Jones, M. W.; Adlington, R. M.; Lee, V. *Org. Biomol. Chem.* **2013**, *11*, 8026.
42. Fuwa, H.; Suzuki, T.; Kubo, H.; Yamori, T.; Sasaki, M. *Chem. Eur. J.* **2011**, *17*, 2678.
43. Qian, S.; Zhao, G. *Chem. Commun.* **2012**, *48*, 3530.
44. Alonso, D. A.; Fuensanta, M.; Nájera, C.; Varea, M. *J. Org. Chem.* **2005**, *70*, 6404.
45. Kende, A. S.; Mendoza, J. S. *Tetrahedron Lett.* **1990**, *31*, 7105.
46. Ando, K.; Kobayashi, T.; Uchida, N. *Org. Lett.* **2015**, *17*, 2554.

Development of Shelf-Stable Reagents for Electrophilic Trifluoromethylthiolation Reaction

Zhongyan Huang and Norio Shibata

Abstract Pharmaceutical and agrochemical companies are interested in fluorinated compounds as a promising source of drug candidates. About 25% of marketed pharmaceuticals and 40% of agrochemicals contain fluorine atom(s) in their chemical structures. Therefore, the development of efficient synthetic methodology for organofluorine compounds is an important task for synthetic chemists in the field of medicinal chemistry. Among a variety of fluorinated compounds, we discuss herein trifluoromethylthio (SCF_3) compounds. The SCF_3 group is one of the most lipophilic functional groups in organic chemistry. The electron-withdrawing effect of the SCF_3 group is similar to that of the popular trifluoromethyl (CF_3) group. Hence, the replacement of the CF_3 moiety in market drugs and drug candidates by a SCF_3 group is a potential strategy to control bioavailability and cell-membrane permeability of original compounds. In recent decades, a large number of reports for the synthesis of SCF_3 compounds have been appeared. Among them, direct trifluoromethylthiolation reaction using shelf-stable reagents is obviously attractive since this functionalization can be performed at a late stage of the multistep synthesis of target molecules. Currently, several shelf-stable reagents for electrophilic trifluoromethylthiolation have been developed. We herein introduce our recent contributions for the development of efficient, shelf-stable reagents for electrophilic trifluoromethylthiolation reaction. Design, synthesis and reactivity of two novel shelf-stable reagents, trifluoromethanesulfonyl hypervalent iodonium ylide and its diazo-derivative are discussed.

Keywords Trifluoromethylthio · Electrophilic · Fluorine · Sulfur · Trifluoromethyl · Ylide

Z. Huang · N. Shibata (✉)
Department of Frontier Materials, Department of Nanopharmaceutical Sciences, Life Science and Applied Chemistry, Nagoya Institute of Technology, Gokiso, Showa-ku, Nagoya 466-8555, Japan
e-mail: nozshiba@nitech.ac.jp

K. Tomioka et al. (eds.), *New Horizons of Process Chemistry*,
DOI 10.1007/978-981-10-3421-3_12

1 Introduction

Organofluorine compounds are of great importance in the field of agrochemicals and pharmaceuticals. About 25% of marketed pharmaceuticals and 40% of agrochemicals contain fluorine atom(s) in their chemical structures. In the development of pharmaceuticals, natural products have played an important role over the past half century. However, new drug discovery is going to be increasingly difficult based on a natural product strategy, thus pharmaceutical companies will be interested in fluorinated compounds as a promising source of drug candidates. In contrast to natural products, fluorinated pharmaceuticals are completely man-made. Only a handful of organofluorine compounds have been found in nature [1] and it is thus unrealistic to use natural fluorinated compounds as starting materials for drug synthesis. Therefore, the development of practical ways to introduce fluorine or a fluorinated functional group into organic compounds has caught the attention of more and more chemists. In particular, fluorination and trifluoromethylation are two of the most important reactions for the synthesis of biologically attractive organofluorine compounds as evidenced by a large number of fluorinated and trifluoromethylated pharmaceuticals that are available on the market.

Although there are a variety of fluorinated compounds, we discuss herein trifluoromethylthio (SCF_3) compounds. The SCF_3 group is one of the most lipophilic functional groups in organic chemistry. The electron-withdrawing effect of the SCF_3 group is similar to that of the popular trifluoromethyl (CF_3) group. Hence, the replacement of the CF_3 moiety in market drugs and drug candidates by a SCF_3 group is a potential strategy to control bioavailability and cell-membrane permeability of original compounds [2]. Indeed, the SCF_3 group is frequently found in many pharmaceutical products, such as Toltrazuril [3], Tiflorex [4], and Cefazaflur [5], among others. In the last few decades, a large number of effective methodologies have been reported for the synthesis of SCF_3-containing molecules [6]. Fundamental methods for the preparation of the SCF_3 functional group can be divided into three categories: (1) halogen-fluorine exchange [7, 8]; (2) trifluoromethylation of sulfur-containing compounds [9–11]; and (3) direct introduction of the SCF_3 unit into targets by the trifluoromethylthiolation reaction. Obviously, direct trifluoromethylthiolation is ideal and practical since this functionalization can be performed at a late stage of the multistep synthesis of target molecules. However, the reagents for direct trifluoromethylthiolation generally include liable trifluoromethylthiolate salts or toxic, gaseous reagents such as $Hg(SCF_3)_2$, $HSCF_3$, $ClSCF_3$ or F_3CSSCF_3 [12–18]. Therefore, in recent years, much effort has focused on the development of shelf-stable reagents for this purpose. Currently, several shelf-stable reagents for electrophilic trifluoromethylthiolation have been developed by Munavalli, Billard and Shen (**a**–**f**, Fig. 1) [19–25]. These reagents can be prepared by trifluoromethylthiolation or related trifluoromethylation reactions.

In addition to the SCF_3 unit, we are interested in the trifluoromethanesulfonyl (SO_2CF_3) unit. SO_2CF_3 is stable and the strongest electron-withdrawing functional

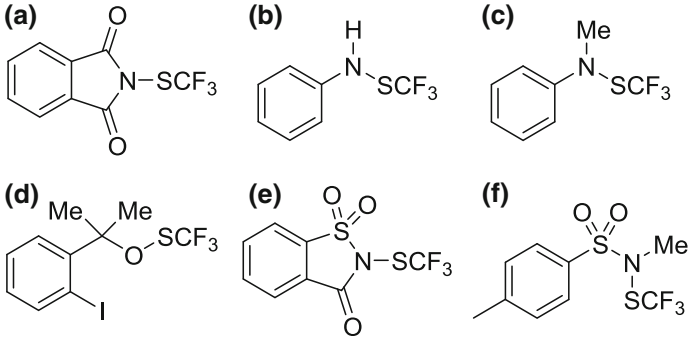

Fig. 1 Shelf-stable reagents for electrophilic trifluoromethylthiolation

group. The lipophilicity of SO_2CF_3 is less than that of the CF_3 group. Hence, replacement of the CF_3 group in biologically active molecules by SO_2CF_3 is also an attractive strategy for drug development. During our research on the synthesis of SO_2CF_3 compounds (triflones), the idea to use SO_2CF_3 compounds as trifluoromethylthiolation reagents emerged. SO_2CF_3 compounds are ubiquitous and commercially available general reagents such as CF_3SO_2Cl, CF_3SO_2Na, CF_3SO_2H and $(CF_3SO_2)_2O$. We envisaged that these SO_2CF_3 compounds could be used as sources for introducing the CF_3S moiety while combining reductive conditions. In order to realize this idea, we focused on iodonium ylides, which are attractive progenitors for carbene-generation and react with a variety of substrates under thermal or catalytic conditions [26–28]. They are easily synthesized by the use of hypervalent iodine compounds such as phenyliodine diacetate (PIDA) and can be stabilized by two strong electron-withdrawing groups. Two very unique reports showed that the phenyl thio group is generated in situ from phenyliodonium bis (phenylsulfonyl) methylide under light or thermal conditions with copper catalysis (Scheme 1) [29, 30].

Encouraged by these reports, we assumed that a reactive, electrophilic SCF_3 species might be produced from steady SO_2CF_3 compounds by carbene-mediated

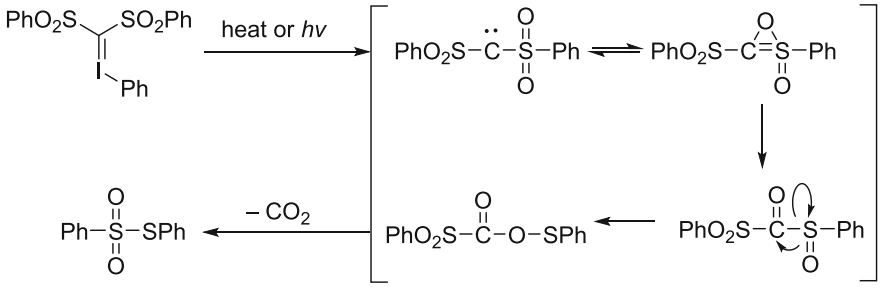

Scheme 1 Reduction of phenyliodonium bis(phenylsulfonyl) methylide

in situ reduction under copper catalysis. Therefore, we designed a novel SO_2CF_3 iodonium ylide compound as an electrophilic trifluoromethylthiolation reagent based on the CF_3SO_2 analogue of phenyliodonium bis(phenylsulfonyl) methylide.

2 Trifluoromethanesulfonyl Hypervalent Iodonium Ylide: Preparation and Reactivity

2.1 *Synthesis of Trifluoromethanesulfonyl Hypervalent Iodonium Ylide 1*

A trifluoromethanesulfonyl hypervalent iodonium ylide **1** was synthesized as follows [31]. We first synthesized 2-bromo-1-phenylethanone by bromination of acetophenone with *N*-bromosuccinimide (NBS) in the catalysis of *p*-toluenesulfonic acid. The bromide obtained was transformed to the corresponding triflone by reaction with $NaSO_2CF_3$ in DMF. Finally, compound **1** was synthesized by the treatment of triflone with PIDA in CH_3CN at 0 °C for 2 h simply by filtration of the precipitate and a wash with water and ether (Scheme 2). Reagent **1** is stable at room temperature for more than one week, and for more than one year in a refrigerator, without showing any signs of decomposition.

2.2 *Reaction of Reagent 1 with Enamines*

Enamines are multipurpose intermediates for many types of organic synthesis [32–34]. We first examined the electrophilic trifluoromethylthiolation of enamines. The reaction of variety enamines with hypervalent iodonium ylide reagent **1** in the presence of 20 mol% CuCl in 1,4-dioxane at room temperature proceeded very rapidly to afford the corresponding SCF_3 compounds in high to excellent yields in 5 min (Scheme 3). Various substitutions on the amino groups such as aromatic and

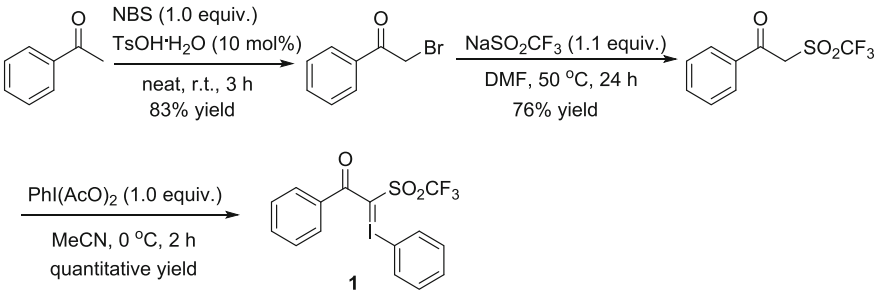

Scheme 2 Synthesis of trifluoromethanesulfonyl hypervalent iodonium ylide **1**

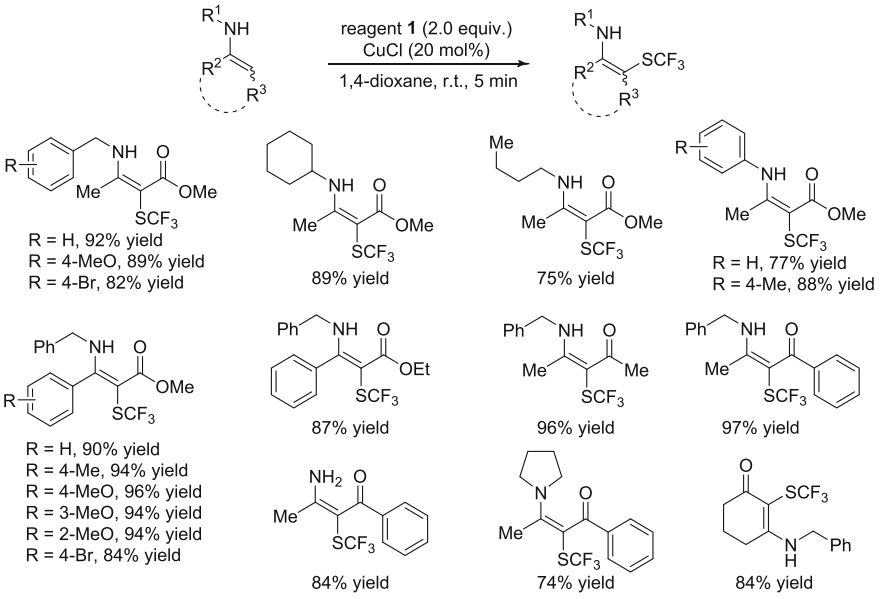

Scheme 3 Trifluoromethylthiolation of enamines with reagent **1**

aliphatic substituents gave high yields of SCF_3-enamines under copper catalysis conditions. Not only β-enaminoesters, but also β-enaminoketones were efficiently trifluoromethylthiolated under standard conditions by reagent **1**. Unprotected enamine also reacted with **1** to give SCF_3-enamine in 84% yield [31].

2.3 *Reaction of Reagent 1 with Indoles and β-Keto Esters*

Indole derivatives are vital structural units in biologically active natural compounds in pharmaceuticals and agrochemicals [35]. Direct electrophilic trifluoromethylthiolation of indoles by **1** was next examined. Trifluoromethylthiolation of indole with **1** under standard conditions for enamines only resulted in low yield. Fortunately, the addition of a catalytic amount of *N*,*N*-dimethylaniline sharply increased the reactivity and afforded the desired trifluoromethylthiolated product in good yield. With a slight change in reaction conditions, a series of indoles were smoothly transformed to the corresponding trifluoromethylthiolated products in moderate to high yields within 2 h at room temperature (Scheme 4). 1-Indanone-2-carboxylate with a tetrasubstituted sp^3 carbon center and ethyl 3-phenylpropanoate were trifluoromethylthiolated with **1** in the presence of 10 mol% CuCl and 20 mol% 2,4,6-collidine (Scheme 4) [31].

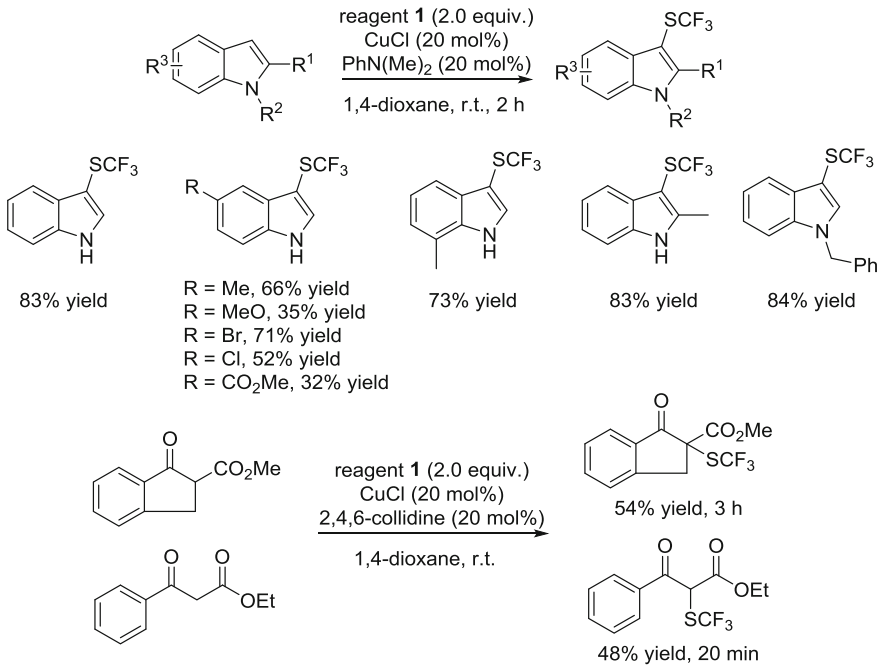

Scheme 4 Trifluoromethylthiolation of indoles and β-keto esters with reagent **1**

2.4 Reaction of Reagent 1 with Pyrroles

Pyrroles are five membered nitrogen-containing heterocyclic compounds which are often encountered in natural products, as exemplified by porphyrins. Pyrroles are also popular as a unit of man-made biologically active molecules and dyes for solar cells [36]. Thus, the development of synthetic methods that provide fluoro-functionalized pyrrole derivatives is of great importance in the fields of medicinal chemistry and material sciences. Pyrroles are highly sensitive towards oxidation and polymerization, and mild and neutral conditions are required for their transformation. Trifluoromethylthiolation of pyrroles was originally examined using gaseous and toxic $ClSCF_3$, but the scope of substrates was narrow and conversion yields were not satisfactory [37]. In 2012, Billard and co-workers attempted the trifluoromethylthiolation of pyrroles by shelf-stable reagents, trifluoromethanesulfanylamides, and $ArNRSCF_3$ (Billard–Langlois reagents), but failed, resulting in polymerization [38]. We thus attempted the direct trifluoromethylthiolation of pyrroles with reagent **1** under copper catalysis. After optimization of the reaction conditions using 2-phenyl pyrrole and reagent **1**, catalyst of 20 mol% CuF_2 in *N*-methyl-2-pyrrolidinone (NMP) afforded the best yield of the desired product, i.e., 94% yield. Under these optimized reaction conditions, a broad set of pyrroles were nicely transformed to their corresponding

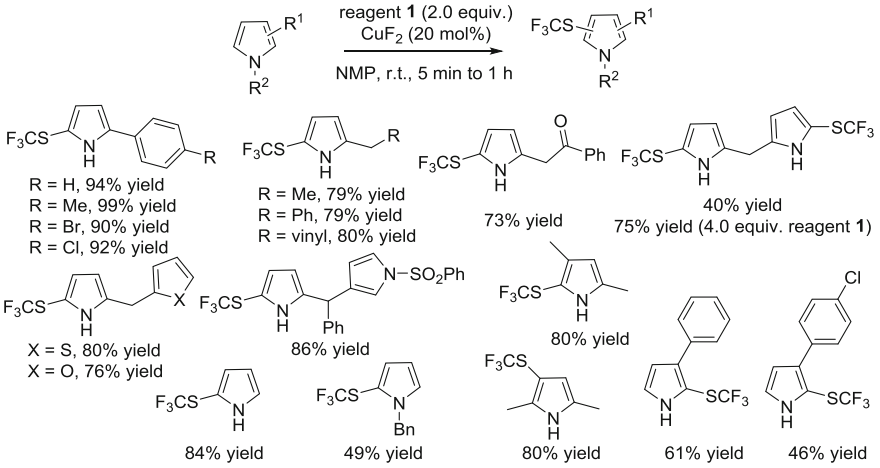

Scheme 5 Trifluoromethylthiolation of pyrroles with reagent **1**

trifluoromethylthiolated pyrroles in moderate to excellent yields (Scheme 5) [39]. Most of the reactions were completed within 1 h and the desired products were obtained smoothly, independent of the substitution of pyrroles. Regioselective trifluoromethylthiolation was achieved with substrates having multiple reaction centers.

2.5 *Reaction of Reagent 1 with Arylamines*

Billard–Langlois reagents, $ArNRSCF_3$, are very attractive electrophilic trifluoromethylthiolation reagents. Many kinds of trifluoromethylthio-functionalization reactions have been achieved with $ArNRSCF_3$ including of alkenes, alkynes, indoles, alkylamines, boronic acids, Grignard reagents, lithium reagents, and allylsilanes [40]. The Billard–Langlois reagents are prepared in several steps from diethylaminosulfur trifluoride, trifluoromethyltrimethylsilane, and anilines. In addition to the wide utility of Billard–Langlois reagents for trifluoromethylthiolation, aryl $NSCF_3$ compounds have potential bioactivity. Reagent **1** was next examined in the one-step synthesis of aryl $NSCF_3$ compounds. Fortunately, a standard set of conditions was found to be effective for the direct trifluoromethylthiolation of arylamines using 20 mol% CuF_2 as the catalyst in NMP at room temperature. A wide range of arylamines were converted into the corresponding SCF_3-products in high yields under these standard conditions in 3 h. As shown in Scheme 6, Billard–Langlois reagents $PhNHSCF_3$ and $PhN(Me)SCF_3$ were obtained in 83 and 81% yield in a single step. Hydrazinephthaloimide derivative was also transformed into the $NHNSCF_3$ compound in 77% yield (Scheme 6) [41].

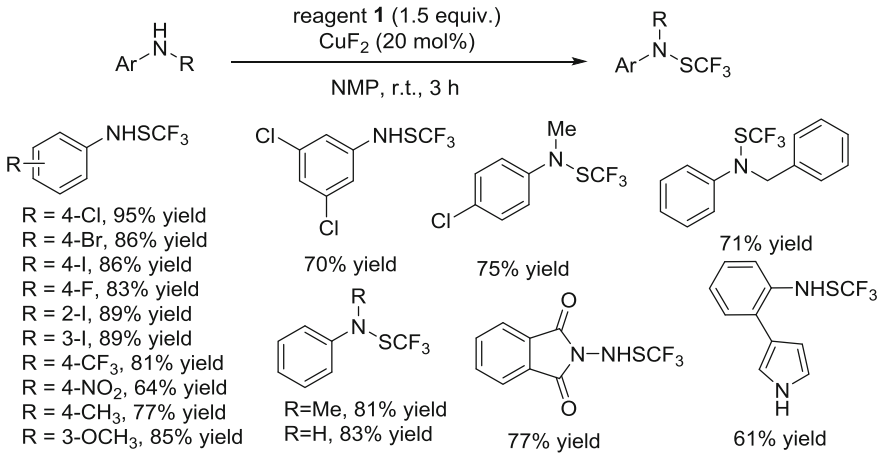

Scheme 6 Trifluoromethylthiolation of arylamines with reagent **1**

2.6 *Reaction of Reagent 1 with Allylsilanes and Silyl Enol Esters*

The trifluoromethylthiolation of allylsilanes and silyl enol esters were examined by Qing and Billard, but a different reagent with different conditions were required [25, 42]. Moreover, the trifluoromethylthiolation of silyl enol esters tends to give a mixture of mono- and bis-SCF_3 products. We next examined the trifluoromethylthiolation of allylsilanes and silyl enol esters with reagent **1**. The combination of catalyst and solvent was very important after screening the optimization of reaction conditions, and 20 mol% CuF_2 as catalyst in NMP or *N*,*N*-dimethylacetamide (DMAc) at room temperature for 10 h were found to be the best reaction conditions. Under these optimized conditions, diverse allylsilanes and a series of silyl enol esters were smoothly transformed to the corresponding SCF_3 compounds in satisfactory to good yields (Scheme 7) [43]. Both cyclic and acyclic substrates were accepted under the same conditions to provide SCF_3 compounds.

2.7 *Reaction of Reagent 1 with Boronic Acids*

Aromatic compounds having fluorinated functional groups such as F and CF_3 are also important raw materials for the synthesis of more complex fluorine-containing functional materials and drugs. Hence, trifluoromethylthiolated aromatics were targeted next. The cross-coupling reaction of boronic acids with reagent **1** is the most straightforward way to obtain the desired targets. We thus turned our attention to examine the direct trifluoromethylthiolation of boronic acids. After optimization

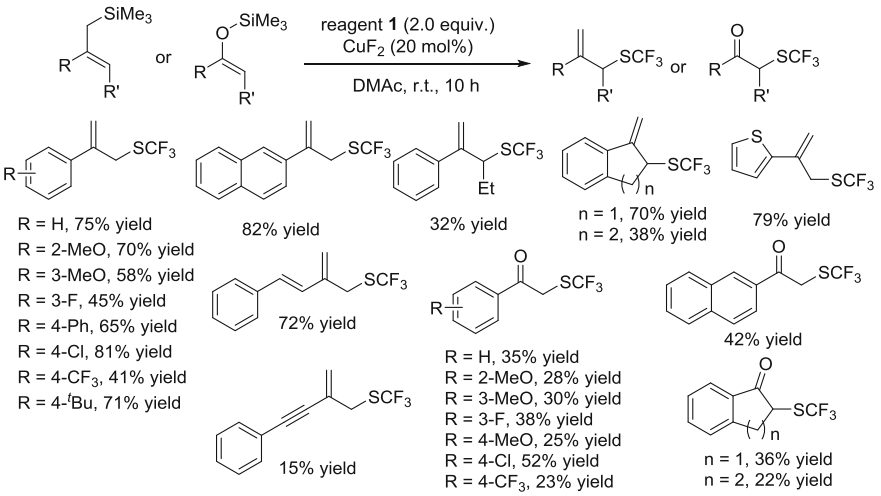

Scheme 7 Trifluoromethylthiolation of allylsilanes and silyl enol esters with reagent **1**

of the reaction conditions, the coupling reaction of arylboronic acids with reagent **1** afforded the desired products in satisfactory to moderate yields with 1.2 equivalents of $Cu(OAc)_2$ in DMAc at 80 °C for 10 h [44]. Vinyl boronic acids were also converted to vinyl-SCF_3 compounds under the same reaction conditions in moderate yields (Scheme 8).

2.8 Reaction of Reagent 1 with Allylic Alcohols

The trifluoromethyl sulfinyl ($S(O)CF_3$) group is found in Fipronil, which is a widely used phenylpyrazole insecticide [45]. The compounds that contain the $S(O)CF_3$ group may be a new class of drugs and agrochemical candidates. However, the methods to synthesize $S(O)CF_3$ compounds have lagged behind those of SCF_3 and

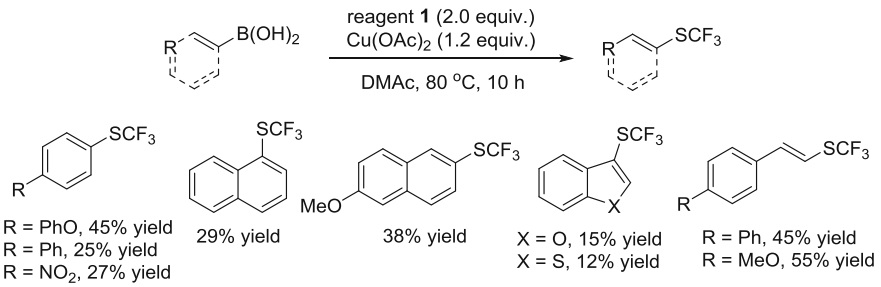

Scheme 8 Trifluoromethylthiolation of boronic acids with reagent **1**

SO_2CF_3 moieties. The traditional method is oxidation of SCF_3 compounds. Direct trifluoromethylsulfinylation uses triflinate salts CF_3SO_2M (M = Na, K) or N–S(O)CF_3 succinimide [6]. Unfortunately, only few references have been reported for these methods. Thus, the development of alternative routes to enrich this chemistry is of current interest [46]. We thus attempted the reaction of allylic alcohols with reagent **1**, which afforded trifluoromethyl sulfoxide products via a [2,3]-sigmatropic rearrangement of sulfenates that were generated in situ by direct trifluoromethylthiolation of allylic alcohols. (Scheme 9). The reaction of allylic alcohols with reagent **1** in the presence of a catalytic amount of CuF_2 in DMAc at room temperature for 10 h furnished trifluoromethylsulfinyl compounds in good yields [44].

2.9 *Proposed Reaction Mechanism for Copper-Catalyzed Trifluoromethylthiolation by Reagent 1*

The reaction mechanism was proposed based on experimental results, ^{19}F NMR analysis, and mass spectral data. First, carbene **A** should be generated in situ via a copper carbenoid **A′** or copper catalysis. Next, oxathiirene **B**, which is in equilibrium with carbene **A** via path I, would rearrange to sulfoxide **C**. The subsequent intramolecular nucleophilic collapse of **C** would then form the reactive species, thioperoxoate **D**. Trifluoromethylthiolation from **D** to the nucleophile (Nu) via an electrophilic pathway III would yield the desired products Nu–SCF_3. In the absence of a nucleophile, thioperoxoate **D** collapsed into CF_3SSCF_3 via radical path II, although path III was more rapid than path II. The friable signals at −56.4 and

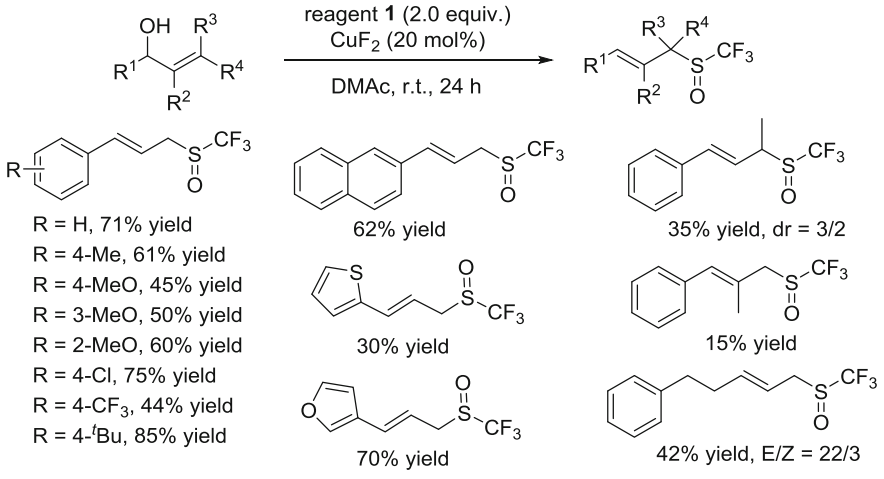

Scheme 9 Trifluoromethylthiolation of allylic alcohols with reagent **1**

−76.6 ppm were assigned to **D** and **C** by comparison of the reported data of R–S(O)CF_3 and R–O–SCF_3 compounds [31, 39]. Although the role of cupper salts, CuX_2, is explained by the generation of carbine **A** or carbenoide **A′**, the exact role of the X group cannot be explained. Deeper DFT calculation should be required for more discussion [47].

3 2-Diazo-1-Phenyl-2-((Trifluoromethyl)Sulfonyl) Ethan-1-One: Preparation and Reactivity

3.1 Synthesis of 2-Diazo-1-Phenyl-2-((Trifluoromethyl) Sulfonyl)Ethan-1-One

We have discussed the wide utility of the trifluoromethanesulfonyl hypervalent iodonium ylide **1** for the electrophilic trifluoromethylthiolation reaction, including the coupling reaction. Reagent **1** is stable and easily activated under copper catalysis to generate a carbene intermediate (Scheme 10). We noticed that the same carbene intermediate should be generated from a conventional diazo-precursor **2** instead of hypervalent iodonium ylide **1**. The diazo-precursor, 2-diazo-1-phenyl-2-((trifluoromethyl)sulfonyl)ethan-1-one **2** was reported by Zhu and co-authors [48]. It was prepared using polyfluoroalkanesulfonyl azide ($I(CF_2)_2O(CF_2)_2SO_2N_3$) as the diazo transfer reagent. However, we found an alternative protocol using $CF_3SO_2N_3$ as the diazo transfer reagent. Our method is easy to conduct in laboratory conditions. First, the diazo transfer reagent $CF_3SO_2N_3$ was prepared fresh from sodium azide (NaN_3) with trifluoromethanesulfonic anhydride (Tf_2O), then the $CF_3SO_2N_3$/DCM solution was directly added to a mixture of 1-phenyl-2-((trifluoromethyl)sulfonyl)ethan-1-one in MeCN. After pyridine was added and stirred at room temperature for 14 h, the diazo reagent **2** was obtained in 85% yield (Scheme 11) [49].

3.2 Trifluoromethylthiolation of Nucleophiles with Reagent 2

With reagent **2** in hand, enamines were first examined in the electrophilic trifluoromethylthiolation reaction. The corresponding trifluoromethylthiolated compounds were obtained in moderate to good yields in the presence of a catalytic amount of CuCl in 1,4-dioxane at 50 °C for 12 h (Scheme 12a). Other nucleophiles, such as indoles, pyrrole, β-keto esters, and anilines were smoothly transformed to the trifluoromethylthiolated products after a slight change in the reaction conditions. For example, the addition of 0.2 equivalents of $PhNMe_2$ in 1,4-dioxane with CuCl catalysis gave moderate yields of trifluoromethylated indoles, while 0.2

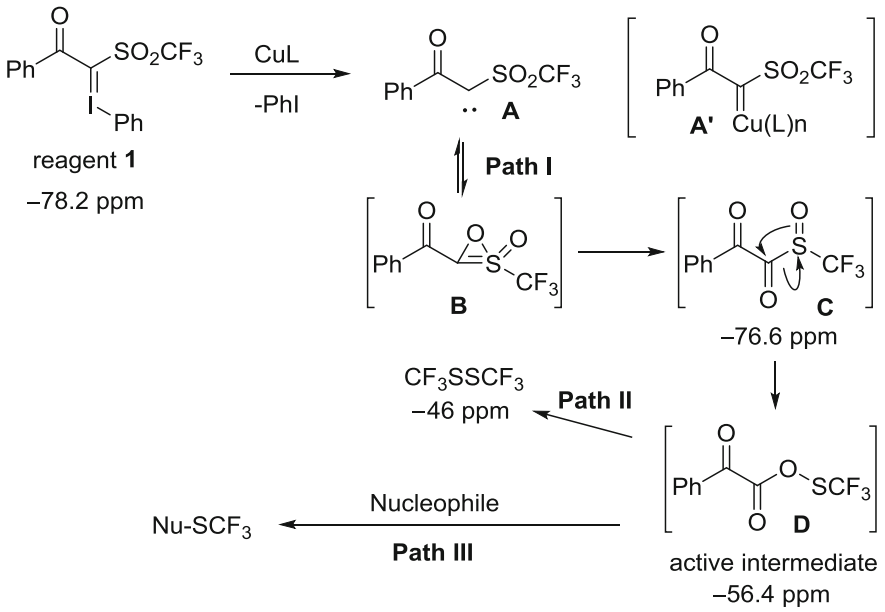

Scheme 10 Proposed mechanism for copper-catalyzed trifluoromethylthiolation with reagent **1**

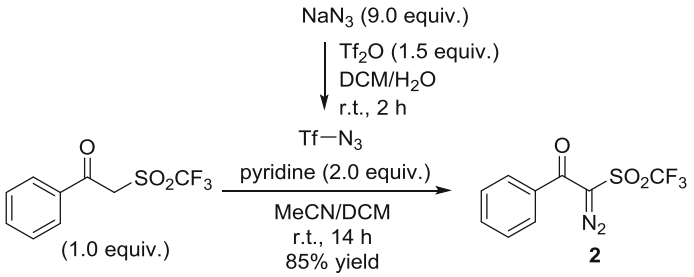

Scheme 11 Synthesis of diazo-triflone reagent **2**

equivalents of 2,4,6-collidine helped to obtain trifluoromethylated β-keto ester in 58% yield. Trifluoromethylthiolation of pyrrole and aniline were achieved in NMP in the presence of 20 mol% CuF_2 (Scheme 12b) [50].

3.3 Trifluoromethylthiolation of Aryl Iodides with Reagent 2

Encouraged by the success of direct trifluoromethylthiolation of nucleophiles using **2**, we next examined the trifluoromethylthiolation of aromatic compounds under a

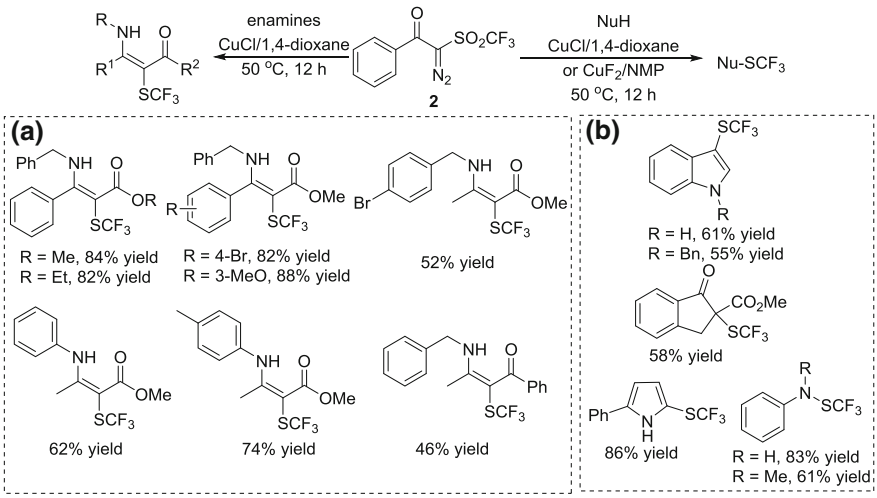

Scheme 12 Trifluoromethylthiolation with reagent **2**

cross-coupling type of trifluoromethylthiolation reaction. A two-step heating condition in the presence of 5.0 equivalents of copper in DMF was useful for the trifluoromethylthiolation of aryl iodides, independent of whether they bear electron-donating or electron-withdrawing groups, to yield the desired products in 34–56% (Scheme 13). The two-step heating is necessary to get the higher yields of the products, since the first heating for the generation of reactive species of $CuSCF_3$ and the next heating for the cross coupling reaction [50].

3.4 *Reagent 2 as a Building Block for the Synthesis of β-Lactam Triflones*

We are currently interested in extending the applications of our reagents. Reagent **2** was found to be an alternative reagent for the trifluoromethylthiolation reaction.

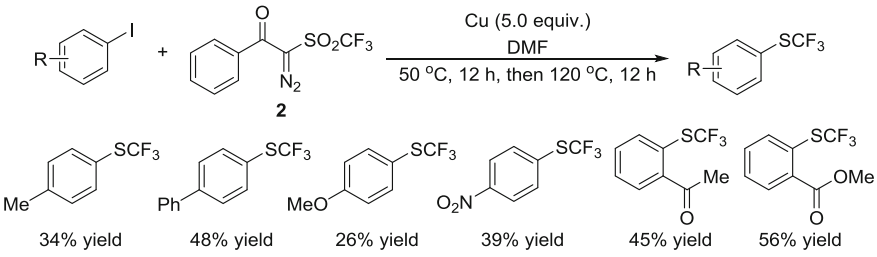

Scheme 13 Trifluoromethylthiolation of aryl iodides with reagent **1**

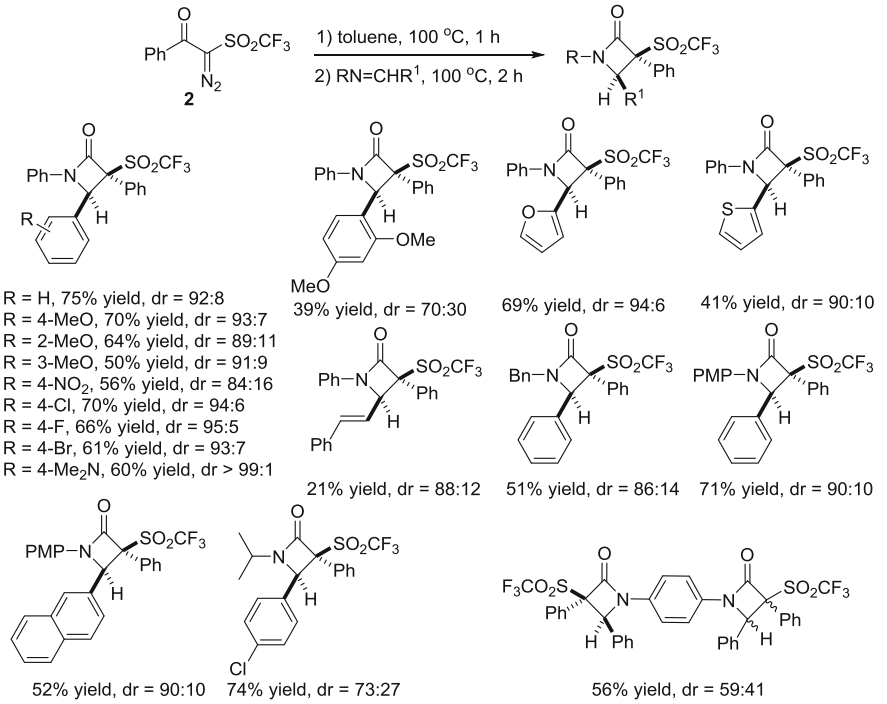

Scheme 14 Stereoselective synthesis of β-lactam triflones

We next attempted to discover other utilities of reagent **2**. We hypothesized that reagent **2** should undergo a Wolff-rearrangement under thermolysis conditions. So we attempted to heat reagent **2** to generate a carbene intermediate without using copper catalysis. After heating reagent **2** at 120 °C in a solvent-free under N_2 atmosphere for 30 min, IR spectroscopy showed the production of ketene triflone at 2150 cm^{-1}, while the original reagent **2** formed a peak at 2131 cm^{-1}. The ^{19}F NMR peak of reagent **2** also shifted from −77.401 to −77.671 ppm [49]. With this evidence of ketene species, we attempted the reaction of ketene with imines towards Staudinger [2 + 2] cycloaddition to afford β-lactams. β-Lactams are a biologically important class of heterocyclic compounds that play a crucial role in pharmaceutical chemistry and life sciences [51]. Ketenes bearing strong electron-withdrawing moieties have difficulty in bringing the ring closer in the Staudinger [2 + 2] cycloaddition reaction. Fortunately, the reaction proceeded smoothly to provide 3,3-aryltriflyl multisubstituted β-lactams from diazo-triflones with imines. A broad scope of products was synthesized by our method in good yields (Scheme 14). That protocol is the first report on the introduction of a triflyl group into the 3-position of a β-lactam [49].

4 Conclusions

We have developed two reagents for the electrophilic trifluoromethylthiolation reaction, trifluoromethanesulfonyl hypervalent iodonium ylide **1** and 2-diazo-1-phenyl-2-((trifluoromethyl)sulfonyl)ethan-1-one **2**. Both **1** and **2** are easily prepared and shelf-stable in the atmosphere. In contrast to other shelf-stable electrophilic trifluoromethylthiolation reagents, our reagents have a CF_3SO_2 unit rather than SCF_3, which can generate electrophilic SCF_3 species in situ during the reaction via carbene and thioperoxoate. Both **1** and **2** are highly reactive with a broad range of nucleophilic substrates like enamines, indoles, pyrroles, β-keto esters and amines under copper catalysis. The utility of **1** was greatly expanded to the functionalization of allylsilanes, silyl enol esters, boronic acids and allylic alcohols, while **2** was used to direct the trifluoromethylthiolation of aryl iodides under a cross-coupling reaction. Reagent **2** is not only a reagent for electrophilic trifluoromethylthiolation but also a trifluoromethanesulfonyl building block for the synthesis of 3,3-aryltriflyl multisubstituted β-lactams under thermal conditions via a Wolff rearrangement and a Staudinger [2 + 2] cycloaddition. Although these two reagents are easily synthesized and shelf-stable, their application in process chemistry is still a matter of debate [52]. We are now researching possibilities to expand their practical use.

Acknowledgements The author would like to thank all our collaborators and coauthors listed in the original papers. These studies were financially supported in part by the Platform for Drug Discovery, Informatics, and Structural Life Science from the Ministry of Education, Culture, Sports, Science and Technology (MEXT) Japan, the Japan Agency for Medical Research and Development (AMED), the Advanced Catalytic Transformation (ACT-C) from the Japan Science and Technology (JST) Agency, the Hoansha Foundation, and the Kobayashi International Scholarship Foundation. Mr. Zhongyan Huang thanks the Hori Sciences & Arts Foundation (Japan) for support.

References

1. O'Hagan D, Harper DB, J Fluorine Chem. 1999;100:127–133.
2. Barata-Vallejo S, Bonesi S. Postigo A. Org. Biomol. Chem. 2016;14, 7150–7182.
3. Laczay P, Vörös G, Semjén G. Int J Parasitol. 1995;25:753–756.
4. Silverstone T, Fincham J, Plumley J. Br J Clin Pharmacol. 1979;7:353–356.
5. Aswapokee N, Neu HC. Antimicrob Agents Chemother. 1979;15:444–446.
6. Xu XH, Matsuzaki K, Shibata N. Chem Rev. 2015;115:731–764.
7. Scherer O. Angew Chem. 1939;52:457–459.
8. Nodiff EA, Lipschutz S, Craig PN, Gordon M. J Org Chem. 1960;25:60–65.
9. Wakselman C, Tordeux M. J Chem Soc Commun. 1984;793–794.
10. Kieltsch I, Eisenberger P, Togni A. Angew Chem Int Ed. 2007;46:754–757.
11. Yasui H, Yamamoto T, Tokunaga E, Shibata N. J Fluorine Chem. 2011;132:186–189.
12. Man EH, Coffman DD, Muetterties EL. J Am Chem Soc. 1959;81:3575–3577.
13. Andreades S, Harris JF Jr, Sheppard WA. J Org Chem. 1964;29:898–900.
14. Hanack M, Kìhnle A, Tetrahedron Lett. 1981;22:3047–3048.

15. Kolasa A. J Fluorine Chem. 1987;36:29–40.
16. Popov VI, Haas A, Lieb M. J Fluorine Chem. 1990;47:131–136.
17. Adams DJ, Clark JH. J Org Chem. 2000;65:1456–1460.
18. Kremsner JM, Rack M, Pilger C, Kappe CO. Tetrahedron Lett. 2009;50:3665–3668.
19. Munavalli S, Rohrbaugh DK, Rossman DI, Berg FJ, Wagner GW, Durst HD. Syn Commun. 2000;30:2847–2854.
20. Ferry AL, Billard T, Langlois BR, Bacque E. J Org Chem. 2008;73:9362–9365.
21. Bootwicha T, Liu X, Pluta R, Atodiresei I, Rueping M. Angew Chem Int Ed. 2013;52: 12856–12859.
22. Shao X, Wang X, Yang T, Lu L, Shen Q, Angew Chem Int Ed. 2013;52:3457–3460.
23. Xu C, Shen Q, Org Lett. 2014;16:2046–2049.
24. Xu C, Ma B, Shen Q. Angew Chem Int Ed. 2014;53:9316–9320.
25. Alazet S, Zimmer L, Billard T, Chem Eur J. 2014;20:8589–8593.
26. Hayashi Y, Okada T, Kawanisi M. Bull Chem Soc Jpn. 1970;43:2506–2511.
27. Camacho MB, Clark AE, Liebrecht TA, Deluca JP. J Am Chem Soc. 2000;122:5210–5211.
28. Müller P. Acc Chem Res. 2004;37:243–251.
29. Hadjiarapoglou L, Spyroudis S, Varvoglis A. J Am Chem Soc. 1985;107:7178–7179.
30. Sander W, Strehl A, Winkler M. Eur J Org Chem. 2001;3771.
31. Yang YD, Azuma A, Tokunaga E, Yamasaki M, Shiro M, Shibata N. J Am Chem Soc. 2013;135:8782–8785.
32. Rappoport Z, editor. The chemistry of enamines (Parts 1 & 2). New York: Wiley; 1994.
33. Xie JH, Zhu SF, Zhou QL, Chem Soc Rev. 2012;41:4126–4139.
34. Abdel-Magid AF, Cohen JH, Maryanoff CA. Curr Med Chem. 1999;6:955–970.
35. Gribble GW, Editor. Heterocyclic scaffolds II: reactions and applications of indoles, Berlin: Springer-Verlag; 2010.
36. d'Ischia M, Napolitano A, Pezzella A. Pyrroles and their benzo derivatives: applications. In: Katritzky AR, Ramsden C A, Scriven EFV, Taylor RJK, editors. Comprehensive Heterocyclic Chemistry III. Amsterdam: Elsevier; 2008. Vol. 3. p. 353–388.
37. Haas A, Niemann U. Chem Ber. 1977;110:67–77.
38. Ferry A, Billard T, Bacqué E, Langlois BR. J Fluorine Chem. 2012;134:160–163.
39. Huang Z, Yang YD, Tokunaga E, Shibata N. Org Lett. 2015;17:1094–1097.
40. Toulgoat F, Alazet S, Billard T. Eur J Org Chem. 2014;2415.
41. Huang Z, Yang YD, Tokunaga E, Shibata N. Asian J Org Chem. 2015;4:525–527.
42. Liu J, Chu L, Qing FL. Org Lett. 2013;15:894–897.
43. Arimori A, Takada M, Shibata N. Org Lett. 2015;17:1063–1065.
44. Arimori A, Takada M, Shibata N. Dalton Trans. 2015;44:19456–19459.
45. Aajoud A, Raveton M, Azrou-Isghi D, Tissut M, Ravanel P. J Agric Food Chem. 2008;56:3732–3737.
46. Chachignon H, Maeno M, Kondo H, Shibata N, Cahard D. Org Lett. 2016;18:2468–2470.
47. Miyamoto K, Iwasaki S, Doi R, Ota T, Kawano Y, Yamashita J, Sakai Y, Tada N, Ochiai M, Hayashi S, Nakanishi W, Uchiyama M, J. Org. Chem., 2016; 81:3188–3198.
48. Pang W, Zhu S, Xing C, Luo N, Jiang H, Zhu S. J Fluorine Chem. 2008;129:343–348.
49. Huang Z, Wang C, Tokunaga E, Sumii Y, Shibata N. Org Lett. 2015;17:5610–5613.
50. Huang Z, Okuyama K, Wang C, Tokunaga E, Li X, Shibata N. ChemistryOpen. 2016; 5:188–191.
51. Morin RB, Gorman M. editors. Chemistry and biology of β-lactam antibiotics. New York: Academic Press, New York: 1982. Vols. 1−3.
52. The reagent **1** is commercially available. See the websites, "Shibata trifluoromethylthiolation reagent" from SyQuest Laboratories, http://synquestlabs.com/product/id/98242.html, and "Shibata Reagent II", from TCI America, http://www.tcichemicals.com/eshop/en/us/commodity/P2143/.

Practical and Environmentally Friendly Transformation of Tetrahydrofuran-2-Methanols to γ-Lactones via Oxidative Cleavage

Tomoya Fujiwara, Yuto Horiuchi, Akihiro Yamada, Hisanori Nambu and Takayuki Yakura

Abstract Transformation of oxacycle-2-methanols to the corresponding lactones is often applied to total synthesis of natural products. It is accomplished by either direct oxidative cleavage reaction using a heavy metal oxidant or multistep conversion. As a practical and environmentally friendly procedure, a direct oxidative cleavage reaction of tetrahydrofuran-2-methanols to the corresponding γ-lactones was developed. This new catalytic reaction proceeds with a catalytic amount of 2-iodobenzamide and stoichiometric Oxone ($2KHSO_5 \cdot KHSO_4 \cdot K_2SO_4$) at room temperature.

Keywords Catalysis · Green chemistry · Hypervalent iodine · Oxidative cleavage · Oxone

1 Introduction

Lactones are ubiquitously present as a key structural skeleton in natural product and are utilized as versatile synthetic intermediates. Among many methods for the preparation of lactones, transformation of oxacycle-2-methanols to the corresponding lactones is often used in total synthesis of natural products. This transformation is classified into two categories. One is the direct oxidative cleavage reaction and the other is the multistep conversion. The direct transformation clearly has advantages over the multistep approach, however, all the previously reported direct reactions require an excess amount of hexavalent chromium oxidant and harsh conditions. In larger scale synthesis, use of toxic Cr(VI) oxidants should be avoided. And in the synthesis of chemically labile and structurally complex compounds, mild reaction conditions are preferred. Therefore, development of a direct oxidative cleavage reaction with non-toxic oxidant at low temperature is strongly

T. Fujiwara · Y. Horiuchi · A. Yamada · H. Nambu · T. Yakura (✉)
Graduate School of Medicine and Pharmaceutical Sciences, University of Toyama, Toyama, Japan
e-mail: yakura@pha.u-toyama.ac.jp

K. Tomioka et al. (eds.), *New Horizons of Process Chemistry*,
DOI 10.1007/978-981-10-3421-3_13

required. Very recently, we have succeeded in developing a practical and environmentally friendly reaction of tetrahydrofuran-2-methanols to the corresponding γ-lactones, which employs a 2-iodobenzamide catalyst and Oxone ($2KHSO_5 \cdot KHSO_4 \cdot K_2SO_4$) at room temperature. Here we describe a brief review of the precedent transformations and the approach to the new catalytic system.

2 Direct Oxidative Cleavage Reactions

Direct oxidative cleavage reactions of tetrahydrofuran-2-methanols to γ-lactones have been developed since early 1990s. In 1990, Borchardt and colleagues reported the first oxidative cleavage of tetrahydrofuran-2-methanol **1** (Scheme 1a) [1]. When **1** was treated with 4 eq. of pyridinium chlorochromate (PCC) in benzene with a Dean-Stark apparatus under reflux conditions, the corresponding lactone **2** was obtained in 56% yield. This conversion was applied to the synthesis of a transfer-RNA nucleoside [2] and antiplatelet drug metabolites [3] by the groups of Carell and Shaw, respectively. Similar reaction of the 3,4-epimer of **1** gave lower yield of the product [4]. At almost the same time as Borchardt, Chandrasekaran and colleagues reported the oxidative cleavage of **3** to **4** with PCC in the presence of molecular sieves 3A (MS3A) in CH_2Cl_2 at reflux temperature (Scheme 1b) [5]. Singh, Kumar, and coworkers examined the PCC oxidation of **5** at room temperature for their synthesis of a selective cyclooxygenase(COX)-2 inhibitor in 2006 (Scheme 1c) [6]. However, the yield of lactone **6** was very low (15%) and a substantial amount (31%) of carboxylic acid **7** was formed.

Use of pyridinium dichromate (PDC) as an oxidant was reported by Papaioannou et al. in 1990 (Scheme 2a) [7]. Compound **8** was treated with 1.5 eq. of PDC in the presence of MS4A in CH_2Cl_2 at room temperature to generate lactone **2** in 12% yield accompanied with 16% of ester **9** and 7% of aldehyde **10**. In 1992, Ryu and colleagues found that a combination of PDC and acetic anhydride (Ac_2O) was effective for oxidation of ribonucleoside derivative **11a** (Scheme 2b) [8]. When uridine derivative **11a** was allowed to react with 4 eq. of PDC in the presence of 12 eq. of Ac_2O in a mixture of CH_2Cl_2 and *N*,*N*-dimethylformamide (DMF) at room temperature for 0.5 h, the corresponding lactone **12a** was obtained in 50% yield. However, the oxidation of adenosine derivative **11b** resulted in decomposition. The PDC-Ac_2O system was applied to the preparation of lactone **12c** and **12d** for the syntheses of hydrindene derivatives and diterpenoid lactone, respectively, by Taber and colleagues [9, 10]. We also applied the PDC-Ac_2O system to the synthesis of an analogue of natural phospholipase A_2 inhibitor (Scheme 2c) [11]. However, the reaction of **13** to **14** required extremely large amounts of PDC (16 eq.) and very high temperature (150 °C) were required to complete the reaction.

Direct oxidative cleavage reactions are simple and useful transformations for synthesizing γ-lactones from the corresponding tetrahydrofuran-2-methanols. However, these reactions have several drawbacks; an excess amount (up to 16 eq.

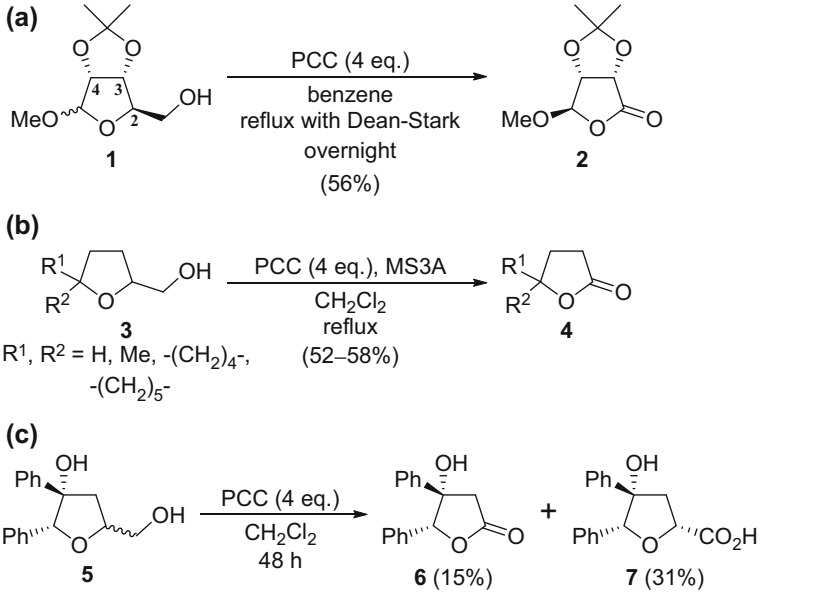

Scheme 1 Oxidative cleavages with PCC

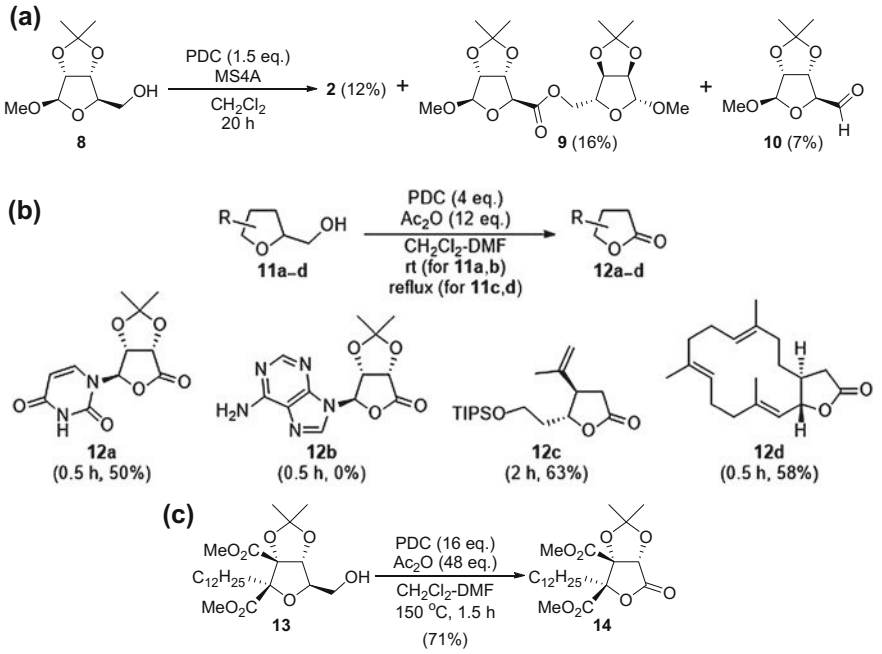

Scheme 2 Oxidative cleavages with PDC

to the substrate) of toxic hexavalent chromium oxidant was required, most are performed at high temperature, and the yields of γ-lactones are often low.

3 Multistep Conversion

Lactones are also prepared from tetrahydrofuran-2-methanols in several steps. Tomooka and coworkers reported the synthesis of γ-lactone **17** from **15** by using sequential two different type oxidations via aldehyde **16** in their total synthesis of a squalene synthase inhibitor (Scheme 3a) [12]. Oxidation of **15** with a catalytic amount of tetrapropylammonium perruthenate (TPAP) in the presence of *N*-methylmorpholine *N*-oxide (NMO) as a co-oxidant and MS4A gave the corresponding aldehyde **16** in 98% yield, which was allowed to react with a catalytic amount of copper(II) acetate [$Cu(OAc)_2$] and 2,2′-bipyridyl in the presence of 1,4-diazabicyclo [2.2.2]octane (DABCO) under oxygen bubbling to afford lactone **17** in 72% yield. Four step conversion from **18** into lactone **22** was accomplished in high yield by Hatakeyama group in the total synthesis of a phospholipase A_2 inhibitor (Scheme 3b) [13]. Oxidation of **18** with Dess-Martin periodinane [14] produced aldehyde **19**, which was subjected to Baeyer-Villiger oxidation to furnish formate **20**. Methanolysis of **20** followed by TPAP oxidation of the resultant lactol **21** afforded **22** in 68% yield from **18**. An interesting procedure was reported for the synthesis of δ-lactone **27** from **23** in 2010 (Scheme 3c) [15]. The conversion of **23** to iodide **25** was carried out by tosylation and following iodination. Elimination reaction of **25** generated *exo*-olefin **26**, whose ozonolysis gave lactone **27**.

These multistep conversions successfully produced the desired γ-lactones in good overall yields. However, considering the application of such conversions to large-scale synthesis, the direct conversion is better in terms of handling, material use, energy consumption, and environmental pollution.

4 Development of a Practical and Environmentally Friendly Oxidative Cleavage of Tetrahydrofuran-2-Methanols into γ-Lactones by 2-Iodobenzamide Catalyst in Combination with Oxone

Hypervalent iodine compounds have been used extensively in recent organic synthesis as alternative oxidants of heavy metals because of their low toxicity and easy handling [16–18]. They usually require stoichiometric amounts and produce equimolar amounts of organic iodine waste. Moreover, they are very expensive and some of them are potentially explosive. An excellent solution to these problems can be a catalytic version of hypervalent iodine oxidation [16–23]. Some iodoarenes

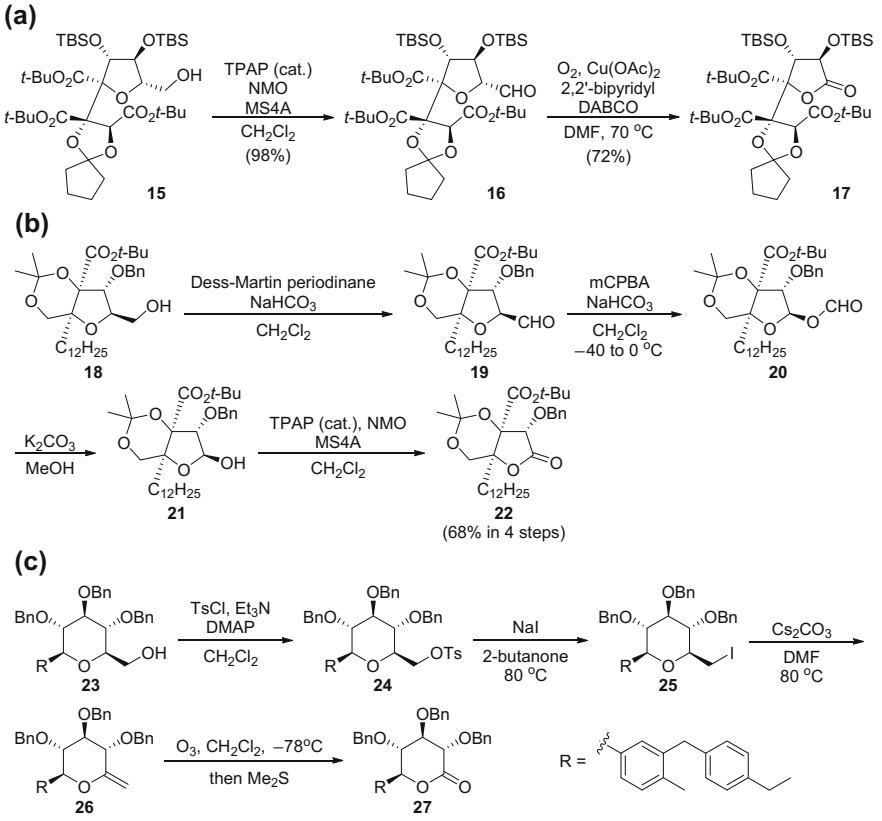

Scheme 3 Multistep conversions

such as 2-iodobenzoic acid (**28**) [24, 25], 2-iodobenzenesulfonic acid (**29**), [26–29] and their derivatives [30–32] have been employed as a catalyst with Oxone as a co-oxidant in alcohol oxidation (Fig. 1). These catalytic reactions require the heating conditions (**70 °C**) to generate the potentially explosive iodine(V) species which work to oxidize the substrates. We recently found a novel catalytic oxidation of alcohols **at room temperature**, which include a catalytic *N*-isopropyl-2-iodobenzamide (**30**) and Oxone (Scheme 4) [33]. Oxone is well-known as an environmentally safe oxidant, because Oxone is an inorganic and water-soluble oxidant with a low order of toxicity, and moreover it is commercially available and inexpensive [34, 35]. In comparison with other catalytic hypervalent iodine oxidations and stoichiometric pentavalent iodine oxidations, this catalytic system converts primary alcohols into the corresponding carboxylic acids not aldehydes. This result suggested us that tetrahydrofuran-2-methanols might be led to γ-lactones via aldehydes and carboxylic acids.

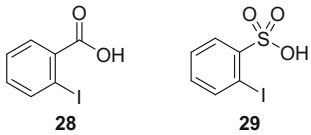

Fig. 1 Structures of 2-iodobenzoic acid (**28**) and 2-iodobenzenesulfonic acid (**29**)

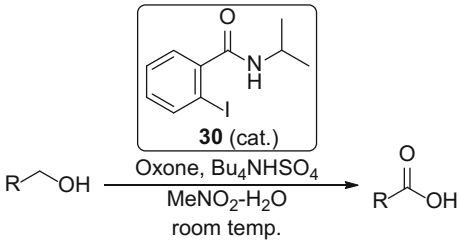

Scheme 4 Oxidation of primary alcohols to the corresponding carboxylic acids using a catalytic amount of *N*-isopropyl-2-iodobenzamide (**30**) and Oxone

First, the reaction of tetrahydrofuran-2-methanol **31a** with several oxidizing reagents was examined (Table 1). Reaction of **31a** with 4 eq. of PCC in the presence of MS3A in CH_2Cl_2 under reflux conditions [5] afforded a complex mixture (entry 1). Oxidation of **31a** with either Dess-Martin periodinane (**34**) [14] or 2-iodoxybenzoic acid (IBX, **35**) [36] gave the corresponding aldehyde **33** in 55 and 38% yields, respectively (entries 2 and 3). On the basis of the previously reported conditions [33], **31a** was treated with 1 eq. of **30** in the presence of 2.5 eq. of Oxone and 1 eq. of tetrabutylammonium hydrogen sulfate (Bu_4NHSO_4) in an 8:3 mixture of $MeNO_2$ and water at room temperature. Fortunately, the desired oxidative cleavage of **31a** successfully proceeded to provide the corresponding γ-lactone **32a** in 71% yield after 60 h (entry 4). On the other hand, similar oxidation with **28** [24, 25] instead of **30** was very slow and produced only a 17% yield of **32a** after 60 h (entry 5). We examined the oxidation of **31a** without any iodine reagent to confirm the role of iodine compound, resulting in no detectable product formation (entry 6). To shorten the reaction time, the effects of Oxone, Bu_4NHSO_4, and solvent on the reaction were then investigated. When **31a** was reacted with 1 eq. of **30** in the presence of 5 eq. of Oxone, the reaction time (33 h) was much shorter than that with 2.5 eq. of Oxone (entry 7). The use of 10 eq. of Oxone, however, was not as effective for shortening the reaction time (entry 8). The oxidation without Bu_4NHSO_4 afforded the best result, with **32a** obtained in 73% yield after 26 h (entry 9). Changing the ratio of $MeNO_2$ and water did not affect the result (entry 10). The reaction in water resulted in a very low yield of **32a** (entry 11) whereas $MeNO_2$ as a sole solvent led to a high yield of **32a** (entry 12). Use of MeCN, 2,2,2-trifluoroethanol, and toluene gave unsuccessful results (entries 13–15). The reaction in dimethylsulfoxide (DMSO) also did not proceed (entry 16) [37–39]. Interestingly, DMF [40] and *N*,*N*-dimethylacetamide (DMA) drastically accelerated the reaction, which was complete within just 9 and 10 h, respectively (entries 17 and 18). From these results, we have confidence that the reaction would work well even with a catalytic amount of **30**. When the reaction was performed

Table 1 Oxidation of **31a** to **32a** with various oxidizing reagents at room temperature[a]

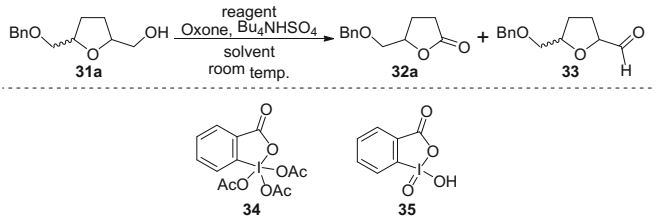

Entry	Reagent (eq.)	Oxone (eq.)	Bu_4NHSO_4 (eq.)	Solvent	Time (h)	Product [yield (%)]
1[b]	PCC (4)	None	None	CH_2Cl_2	24	Complex mixture
2	**34** (2.5)	None	None	$MeNO_2$	24	**33** [55]
3	**35** (2.5)	None	None	$MeNO_2$	24	**33** [38][c]
4	**30** (1)	2.5	1	$MeNO_2$–H_2O (8:3)	60	**32a** [71]
5	**28** (1)	2.5	1	$MeNO_2$–H_2O (8:3)	60	**32a** [17][c]
6	None	2.5	1	$MeNO_2$–H_2O (8:3)	60	no reaction[c]
7	**30** (1)	5	1	$MeNO_2$–H_2O (8:3)	33	**32a** [60]
8	**30** (1)	10	1	$MeNO_2$–H_2O (8:3)	27	**32a** [67]
9	**30** (1)	5	None	$MeNO_2$–H_2O (8:3)	26	**32a** [73]
10	**30** (1)	5	None	$MeNO_2$–H_2O (3:8)	28	**32a** [73]
11	**30** (1)	5	None	H_2O	28	**32a** [35]
12	**30** (1)	5	None	$MeNO_2$	24	**32a** [81]
13	**30** (1)	5	None	MeCN	25	**32a** [69]
14	**30** (1)	5	None	CF_3CH_2OH	25	**32a** [54]
15	**30** (1)	5	None	Toluene	48	**32a** [29][c)]
16	**30** (1)	5	None	DMSO	48	No reaction[c]
17	**30** (1)	5	None	DMF	9	**32a** [73]
18	**30** (1)	5	None	DMA	10	**32a** [67]
19	**30** (0.3)	5	None	DMF	15	**32a** [67]
20	**30** (0.1)	5	None	DMF	25	**32a** [63]
21[d]	**30** (0.3)	5	None	DMF	21	**32a** [73]

[a]All reactions were performed using 0.25 mmol of **31a** unless otherwise specified
[b]The reaction was performed using 0.40 mmol of **31a**
[c]The starting **31a** was recovered
[d]The reaction was performed using 1.00 mmol of **31a**

using 0.3 eq. of **30** in DMF, **32a** was obtained in 67% yield after 15 h (entry 19). Even with 0.1 eq. of **30**, the reaction was complete within 25 h and afforded **32a** in 63% yield (entry 20). When 1 mmol of **31a** was reacted with 0.3 eq. of **30**, the longer reaction time (21 h) was required to give **32a** in slightly increased yield (entry 21). These results strongly indicate that the oxidative cleavage with **30** and Oxone becomes a catalytic reaction.

Various tetrahydrofuran-2-methanols **31b–l** were oxidized using 0.3 eq. of **30** in the presence of 5 eq. of Oxone in DMF at room temperature (Table 2). When **31b** and **31c** bearing an acyloxymethyl group at the 5-position were allowed to react with **30** and Oxone for 22 and 24 h, respectively, the corresponding lactones **32b** and **32c** were each obtained in 73% yield (entries 1 and 2). Oxidation of phthalimide **31d** gave **32d** in high yield (entry 3), although tosyloxy derivative **31e** required 0.5 eq. of **30** to complete the reaction (entry 4). Alkylated **31f** and **31g** were smoothly converted to the corresponding lactones **32f** and **32g** (entries 5 and 6). Reactions of 4-substituted 2-methanols **31h** and **31i**, bicyclic **31j**, and 5,5-disubstituted methanol **31k** were oxidized to lactones **32h–k** in high yields (entries 7–10). However, the reaction of **31l** bearing a *tert*-butyldiphenylsilyl (TBDPS) group afforded a complex mixture without the formation of the desired product **32l** (entry 11), presumably due to removal of the silyl group under the reaction conditions. Catalyst **30** was recovered in high yields after reductive treatment in all cases.

Next, the focus shifted to understanding the reaction mechanism. Considering the mechanism of alcohol oxidation with **30** [33], aldehyde **33** and/or carboxylic acid **36** were proposed as possible reaction intermediates in the present oxidative cleavage reaction of **31a**. Then, **33** and **36** were reacted with 1 eq. of **30** in the presence of 5 eq. of Oxone in DMF at room temperature (Table 3). While the reaction of **33** afforded **32a** in 77% yield only after 1 h (entry 1), the reaction of **36** did not proceed (entry 2). Interestingly, the reaction of **33** in the absence of **30** was also complete within 1 h and afforded **32a** in 75% yield (entry 3). The reaction of **31a** with 1.2 eq. of 2-iodylbenzamide **37**, prepared from **30** according to Zhdankin's procedure [41], at room temperature for 8 h successfully produced the corresponding aldehyde **33** in 51% yield (Scheme 5). Based on the above results, a possible mechanism for the oxidative cleavage of **31** using **30** and Oxone was proposed (Scheme 6). Iodobenzamide **30** is oxidized by Oxone to iodine(V) species **37**, which reacts with **31** to generate aldehyde **39** as a key intermediate. Compound **39** would be then reacted with Oxone to generate not carboxylic acid **41** [40] but formate **40** [13], which is further oxidized to lactone **32**. The iodine(III) species **38** derived during the reaction of **31** and **37** is re-oxidized by Oxone to reform **37**.

The direct oxidative cleavage of **31** to **32** using **30** and Oxone [42] is accomplished at room temperature without the use of any toxic heavy metals, and the desired lactones are obtained in good to high yields. It provides a practical and environmentally friendly transformation to lactones.

Table 2 Oxidative cleavage of **31b–l** to **32b–l** using **30** and Oxone

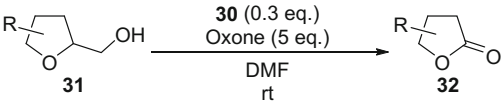

Entry	**31**	**32**	Time (h)	Yield (%)
1	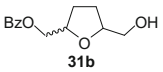 **31b**	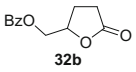 **32b**	22	73
2	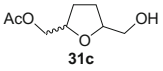 **31c**	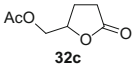 **32c**	24	73
3	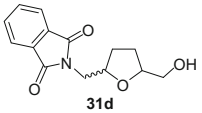 **31d**	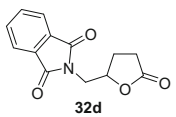 **32d**	22	71
4	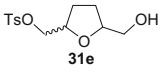 **31e**	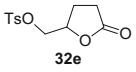 **32e**	14	46[a]
5	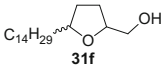 **31f**	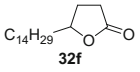 **32f**	24	66
6	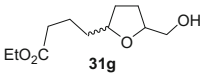 **31g**	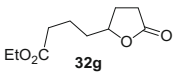 **32g**	23	51
7	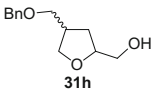 **31h**	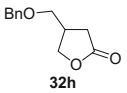 **32h**	20	67
8	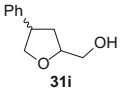 **31i**	 **32i**	22	70
9	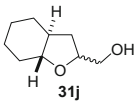 **31j**	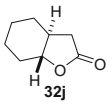 **32j**	24	60
10	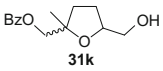 **31k**	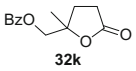 **32k**	22	68
11	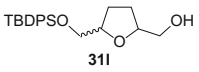 **31l**	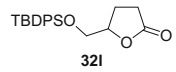 **32l**	24	–[b]

[a]0.5 eq. of **30** was used
[b]Complex mixture was obtained

Table 3 Oxidative cleavage of **33** and **36** using **30** and Oxone

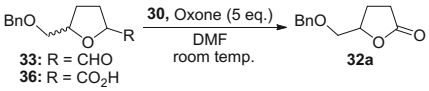

Entry	Substrate	**30** (eq.)	Time (h)	Yield (%)
1	**33**	1	1	77
2	**36**	1	24	No reaction
3	**33**	None	1	75

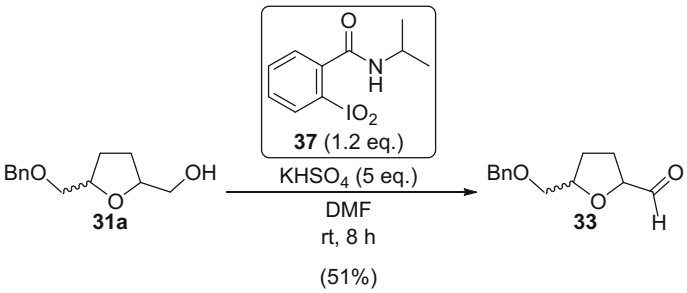

Scheme 5 Oxidation of **31a** with 2-iodylamide **37**

Scheme 6 Proposed mechanism for the oxidative cleavage of **31** to **32** using **30** and Oxone

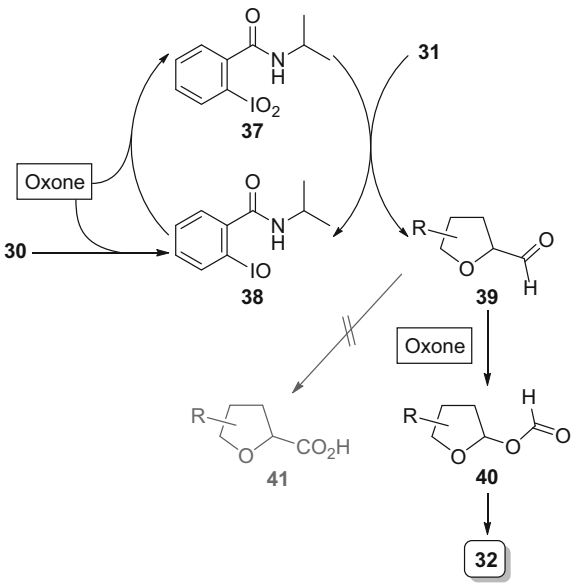

5 Summary

Transformation of oxacycle-2-methanols to the corresponding lactones is usually accomplished by either direct oxidative cleavage reaction or multistep conversion. We have developed a mild and efficient oxidative cleavage reaction for the conversion of tetrahydrofuran-2-methanols to γ-lactones using 2-iodobenzamide catalyst and Oxone. In this reaction, the conversion is accomplished at room temperature without the use of any toxic heavy metals, and γ-lactones are obtained in good to high yields. This method provides a new, practical, and environmentally friendly procedure for the synthesis of γ-lactones with various functionalities.

References

1. S. M. Ali, K. Ramesh, R. T. Borchardt, *Tetrahedron Lett.* **1990**, *31*, 1509–1512.
2. F. Klepper, E.-M. Jahn, V. Hickmann, T. Carell, *Angew. Chem. Int. Ed.* **2007**, *46*, 2325–2327.
3. S. A. Shaw, B. Balasubramanian, S. Bonacorsi, J. C. Cortes, K. Cao, B.-C. Chen, J. Dai, C. Decicco, A. Goswami, Z. Guo, R. Hanson, W. G. Humphreys, P. Y. S. Lam, W. Li, A. Mathur, B. D. Maxwell, Q. Michaudel, L. Peng, A. Pudzianowski, F. Qiu, S. Su, D. Sun, A. A. Tymiak, B. P. Vokits, B. Wang, R. Wexler, D.-R. Wu, Y. Zhang, R. Zhao, P. S. Baran, *J. Org. Chem.* **2015**, *80*, 7019–7032.
4. L. G. Dickson, E. Leroy, J.-L. Reymond, *Org. Biomol. Chem.* **2004**, *2*, 1217–1226.
5. S. Baskaran, S. Chandrasekaran, *Tetrahedron Lett.* **1990**, *31*, 2775–2778.
6. P. Singh, A. Mittal, S. Kaur, S. Kumar, *Bioorg. Med. Chem.* **2006**, *14*, 7910–7916.
7. D. Papaioannou, G. W. Francis, D. W. Aksnes, T. Brekke, K. Maartmann-Moe, *Acta Chem. Scand.* **1990**, *44*, 90–95.
8. J. N. Kim, E. K Ryu, *Tetrahedron Lett.* **1992**, *33*, 3141–3144.
9. D. F. Taber, Y. Song, *J. Org. Chem.* **1996**, *61*, 7508–7512.
10. D. F. Taber, Y. Song, *J. Org. Chem.* **1997**, *62*, 6603–6607.
11. T. Yakura, A. Ozono, K. Matsui, M. Yamashita, T. Fujiwara, *Synlett* **2013**, *24*, 65–68.
12. K. Tomooka, M. Kikuchi, K. Igawa, M. Suzuki, P.-H. Keong, T. Nakai, *Angew. Chem. Int. Ed.* **2000**, *39*, 4502–4505.
13. F. Urabe, S. Nagashima, K. Takahashi, J. Ishihara, S. Hatakeyama, *J. Org. Chem.* **2013**, *78*, 3847–3857.
14. D. B. Dess, J. C. Martin, *J. Org. Chem.* **1983**, *48*, 4155–4156.
15. R. P. Robinson, V. Mascitti, C. M. Boustany-Kari, C. L. Carr, P. M. Foley, E. Kimoto, M. T. Leininger, A. Lowe, M. K. Klenotic, J. I. MacDonald, R. J. Maguire, V. M. Masterson, T. S. Maurer, Z. Miao, J. D. Patel, C. Préville, M. R. Reese, L. She, C. M. Steppan, B. A. Thuma, T. Zhu, *Bioorg. Med. Chem. Lett.* **2010**, *20*, 1569–1572.
16. V. V. Zhdankin, *Hypervalent Iodine Chemistry: Preparation, Structure, and Synthetic Applications of Polyvalent Iodine Compounds*, John Wiley & Sons, Ltd, **2013**.
17. *Iodine Chemistry and Applications* (ed.: T. Kaiho), John Wiley & Sons, Ltd, **2014**.
18. A. Yoshimura, V. V. Zhdankin, *Chem. Rev.* **2016**, *116*, 3328–3435.
19. T. Dohi, Y. Kita, *Chem. Commun.* **2009**, 2073–2085.
20. M. Uyanik, K. Ishihara, *Chem. Commun.* **2009**, 2086–2099.
21. T. Dohi, *Chem. Pharm. Bull.* **2010**, *58*, 135–142.
22. F. V. Singh, T. Wirth, *Chem. Asian J.* **2014**, *9*, 950–971.
23. F. Berthiol, *Synthesis* **2015**, *47*, 587–603.
24. A. P. Thottumkara, M. S. Bowsher, T. K. Vinod, *Org. Lett.* **2005**, *7*, 2933–2936.

25. A. Schulze, A. Giannis, *Synthesis* **2006**, 257–260.
26. M. Uyanik, M. Akakura, K. Ishihara, *J. Am. Chem. Soc.* **2009**, *131*, 251–262.
27. M. Uyanik, R. Fukatsu, K. Ishihara, *Org. Lett.* **2009**, *11*, 3470–3473.
28. M. Uyanik, K. Ishihara, *Aldrichimica Acta* **2010**, *43*, 83–91.
29. M. Uyanik, T. Mutsuga, K. Ishihara, *Molecules* **2012**, *17*, 8604–8616.
30. T. Miura, K. Nakashima, N. Tada, A. Itoh, *Chem. Commun.* **2011**, *47*, 1875–1877.
31. J. N. Moorthy, K. Senapati, K. N. Parida, S. Jhulki, K. Sooraj, N. N. Nair, *J. Org. Chem.* **2011**, *76*, 9593–9601.
32. J. N. Moorthy, K. N. Parida, *J. Org. Chem.* **2014**, *79*, 11431–11439.
33. T. Yakura, A. Yamada, N. Noda, T. Fujiwara, H. Nambu, *Asian J. Org. Chem.* **2014**, *3*, 421–424.
34. M. C. Marcotullio, F. Epifano, M. Curini, *Trends Org. Chem.* **2003**, 10, 21–34.
35. H. Hussain, I. R. Green, I. Ahmed, *Chem. Rev.* **2013**, *113*, 3329–3371.
36. C. Hartmann, V. Mayer, *Chem. Ber.* **1893**, *26*, 1727–1732.
37. R. J. Kennedy, A. M. Stock, *J. Org. Chem.* **1960**, *25*, 1901–1906.
38. T. Pandurengan, P. Maruthamuthu, *Bull. Chem. Soc. Jpn.* **1981**, *54*, 3551–3555.
39. J. R. McCarthy, D. P. Matthews, J. P. Paolini, *Org. Synth.* **1995**, *72*, 209–212.
40. B. R. Travis, M. Sivakumar, G. O. Hollist, B. Borhan, *Org. Lett.* **2003**, *5*, 1031–1034.
41. V. V. Zhdankin, A. Y. Koposov, B. C. Netzel, N. V. Yashin, B. P. Rempel, M. J. Ferguson, R. R. Tykwinski, *Angew. Chem. Int. Ed.* **2003**, *42*, 2194–2196.
42. T. Yakura, Y. Horiuchi, Y. Nishimura, A. Yamada, H. Nambu, T. Fujiwara, *Adv. Synth. Catal.* **2016**, *358*, 869–873.

Five Step Asymmetric Total Synthesis of β-Lycorane Employing Chiral Diether Ligand-Controlled Conjugate Addition-Michael Reaction Cascade

Kiyoshi Tomioka

Abstract Really useful and indispensable tools for the organic synthesis of complex molecules as well as practical manufacturing are reagents and catalysts based on concept. However, the nature of synthetic schemes towards target molecules essentially determines the born of these tools. Synthetic scheme is highly desirable to be as short as possible and operation should be as simple as possible, desirably in one-pot or in one slide scheme. Described herein the asymmetric construction of a skeleton of representative Amaryllidaceae alkaloids, optically pure β-lycorane, in 5 steps as we say "asymmetric total synthesis of complex molecule in one slide" (Nishimura et al. in Synthesis 47:2256–2264, 2015 [1], Nishimura et al. in Tetrahedron 71:7222–7226, 2015 [2]).

Keywords Short-step-synthesis · Cascade reaction · Amaryllidaceae alkaloid · One-slide synthesis

1 Introduction

Amaryllidaceae alkaloids have attracted much attention due to their rich bioactivities, especially anti-Alzheimer activities as has been known as clinically useful galantamine [3–6] Among these alkaloids, lycorine (**1**) [7, 8] and its deoxygenated derivative β-lycorane (**2**) [9] possess characteristic pyrrolophenanthridine skeleton (Fig. 1). We have previously reported the asymmetric total synthesis of (–)-lycorine (**1**) using chiral ligand-controlled asymmetric conjugate addition cascade [10]. As a continuous study to show the utility of this cascade reaction as well as mechanistic pathway, here we report a five-steps asymmetric total synthesis of (+)-β-lycorane (**2**) [11–17].

K. Tomioka (✉)
Faculty of Pharmaceutical Sciences, Doshisha Women's College of Liberal Arts, Kodo, Kyotanabe, Kyoto 610-0395, Japan
e-mail: tomioka@pharm.kyoto-u.ac.jp

K. Tomioka et al. (eds.), *New Horizons of Process Chemistry*,
DOI 10.1007/978-981-10-3421-3_14

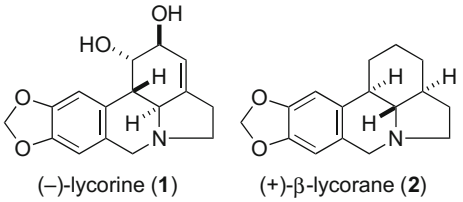

Fig. 1 Structures of lycorine and β-lycorane

2 Asymmetric Conjugate Addition-Michael Reaction Cascade

The most attractive and powerful methods for the asymmetric construction of skeletons of complex molecules **1** and **2** are the asymmetric conjugate addition of carbonucleophiles to electron-deficient olefins activated by an electron withdrawing group [18–27]. A chiral lithium enolate is produced by an asymmetric conjugate addition of an organolithium to an α,β-unsaturated carbonyl compound and this enolate can further react with an electrophile to form the second bond in one-pot. In the case of intramolecular electrophile, the carbocycles or heterocyles are constructed as has been shown in the asymmetric total synthesis of lycorane (**2**), the topic of this tutorial presentation. The conformation of the α,β-unsaturated carbonyl compound, i.e., s-*cis* or s-*trans*, is responsible to the facial selectivity of the conjugate addition and also to the *E,Z*-geometry of the resulting lithium enolate, which should then governs the diastereoselectivity of the subsequent reaction with other electrophiles. Accordingly, a central interest is the reactive conformation of α,β-unsaturated carbonyl compounds in which conjugate addition occurs [28–38].

The initial step toward asymmetric total synthesis of β-lycorane **2** starts from the conjugate addition of aryllithium **4** to bis-enoate **3** giving cyclohexane derivative **7** with three contiguous stereogenic centers through intramolecular Michael reaction of a lithium enolate **6** (Scheme 1). In these three decades we have been engaged in an external chiral dieter ligand **5**-controlled asymmetric conjugate addition reaction

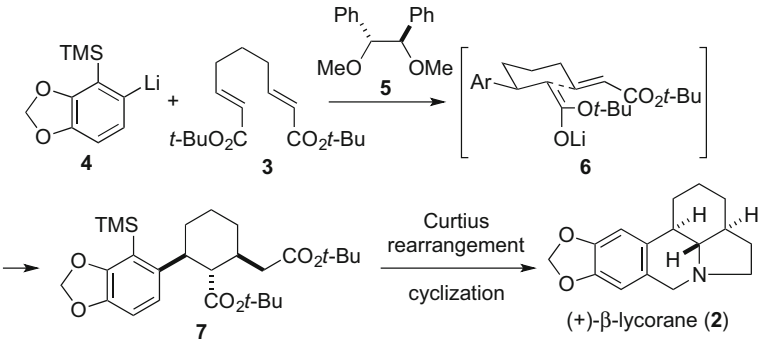

Scheme 1 Synthetic strategy for (+)-β-lycorane (**2**)

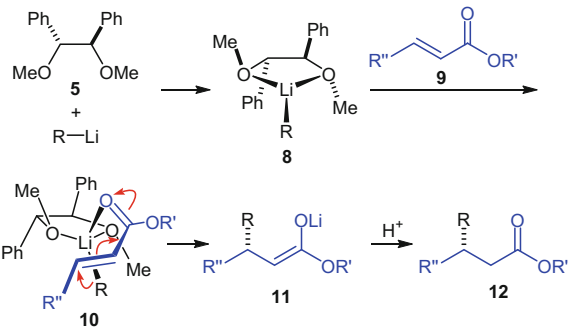

Scheme 2 Our proposal for chiral diether ligand **5**-mediated asymmetric conjugate addition of lithium reagents to α,β-unsaturated carbonyl compounds

of a variety of lithiated nucleophiles such as organolithium, lithium ester enolate, lithium thiolate, and lithium amide to linear α,β-unsaturated imine [39, 40], enoate [41–46] and nitroolefin [47, 48]. Recent our NMR studies revealed that chiral diether ligand **5** and a lithium reagent form C_2-symmetric-like [49] five-membered chelate complex **8** by coordination of the two ethereal oxygen atoms of **5** to the lithium atom. It is important to know that the methyl groups on the oxygen atoms are fixed to situate up and down faces of the chelation **8,** probably by avoiding steric repulsion by the phenyl groups on the chiral carbon centers [50, 51]. The reaction of complex **8** with enoate **9** afforded conjugate addition product **12** with high enantioselectivity. The relationship between the newly created stereogenic center in **12** and chiral chelate complex **8** lead us to the proposal of cyclic reaction model **10**, in which the lithium atom is coordinated by the carbonyl oxygen atom of s-*cis*-enoate on the olefin side. The olefin moiety is placed in the less crowded space avoiding the steric repulsion by the two methyl groups of **8** (Scheme 2) [39, 40, 44, 52]. Then, organolithium R group attacks the olefin moiety from underneath to afford lithium enolate **11**, providing after protonation **12** with the observed absolute configuration [39–48]. If *s-trans*-enoate were involved in the reaction, *Z*-enolate with the opposite absolute configuration would result.

Although the similar cyclic reaction models were proposed by other groups for the conjugate addition of lithium amide to s-*cis*-enoate [28, 37, 38], lithium-involved models with s-*trans*-enoate were also proposed for the conjugate addition of lithium enolate [53] and methyllithium [54]. Thus, determination of the reactive conformation of an α,β-unsaturated carbonyl compound in the conjugate addition of lithium reagent is still a formidable challenging target. Instead of direct identification of enolate geometry, conjugate addition and following Michael cyclization of the resulting enolate with intramolecular enoate were designed to identify the enolate geometry as shown in Scheme 5.

To a toluene solution of chiral diether **5** (2 equiv) at −78 °C, were added cyclohexane–diethyl ether solution of phenyllithium (1.5 equiv) and then toluene solution of bis-enoate **13a** having quite bulky BHA (2,6-di-*tert*-butyl-4-methoxyphenyl) ester 20 min apart [41]. After 30 min stirring at −78 °C, simple conjugate addition product **14a** with 87% ee was obtained in 56% yield along

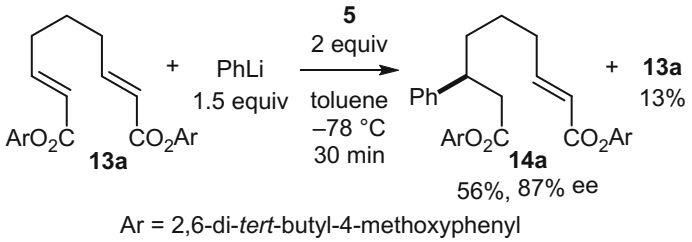

Scheme 3 Monophenylation of **13a**

with recovered **13a** in 13% yield. Desired cascade products **15** was not obtained (Scheme 3).

To our delight, the reaction of bis-*tert*-butyl ester **13b** (=**3**) of decreased steric hindrance and phenyllithium (3 equiv) complexed with **5** (4.2 equiv) was completed within 0.5 h to give desired cascade products *trans*,*trans*-cyclohexane ***tt*-15a** with 71% ee in 50% yield and *trans*,*cis*-cyclohexane ***tc*-15a** with 3% ee in 9% yield (Table 1, entry 1) [55]. The relative and absolute configuration of ***tt*-15a** was unambiguously determined by derivatization. The other diastereomers ***ct*-15** and ***cc*-15** were not obtained. It is noteworthy that **13b** mainly reacted with only one equivalent of phenyllithium. Even though **13b** was added into the solution of the excess amount of phenyllithium and **5**, only slight amount of double phenylated product **16a** (Scheme 4) was produced (<10%). In contrast, when the reaction was conducted in THF as a solvent under the absence of **5**, **16a** was mainly produced (79% yield), and only tiny amount of ***tt*-15a** and ***tc*-15a** were obtained (9 and 4% yields, respectively). These results clearly indicate that chiral ligand **5** significantly accelerates the intramolecular Michael addition of resulting lithium enolate with intramolecular enoate moiety in toluene.

Table 1 Asymmetric conjugate addition-Michael addition cascade

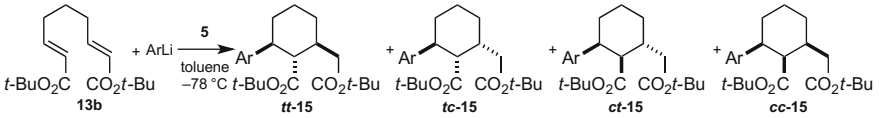

Entry	Ar	15	*tt*-15		*tc*-15		*ct*-15	*cc*-15
			Yield (%)	ee (%)	Yield (%)	ee (%)	Yield (%)	Yield (%)
1	Ph	**15a**	50	71	9	3	0	0
2		**15c**	40	74	10	72	0	0
3		**15d** (**7**)	68	99	18	88	0	0

All reactions were carried out using ArLi (3 equiv) and **5** (4.2 equiv) in toluene

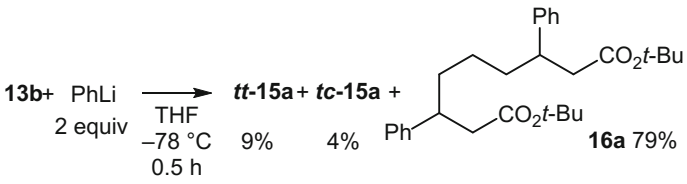

Scheme 4 Double phenylation in THF

Aryllithium bearing a removable and bulky TMS substituent at the *ortho*-position was effective to enhance the enantioselectivity to give **15d** (=**7**) with 99% ee (entry 3). Importantly, chiral ligand **5** was quantitatively recovered without any loss of optical purity, and was reusable.

3 Stereochemical Insight in Cascade Reaction

The production of ***tt*-15**, having *trans*,*trans*-configuration, as the major product suggests two possibilities: (1) the first conjugate addition proceeded with s-*cis*-**13** to give *E*-enolate, which underwent the intramolecular Michael addition with the enoate moiety of s-*cis* conformation, or (2) the first conjugate addition proceeded with s-*trans*-**13**, and the resulting *Z*-enolate undergoes the Michael addition in s-*trans* conformation (Scheme 5). Our studies then went to solve this problem.

As shown in Scheme 6 intramolecular Michael reaction of monophenyl adduct di-*tert*-butyl ester **14b** with LDA (1.2 equiv) in THF at −78 °C gave mainly ***tt*-15a**, which is also the main product of the conjugate arylation-Michael cascade reaction of **13b**, in 66% yield along with ***tc*-15a** in 28% yield. In contrast, diastereoselectivity of the corresponding methyl ester **14c** was opposite to give ***tc*-15e** as a major product in 75% yield along with ***tt*-15e** as a minor product in 17% yield. The observed impressive difference in diastereoselectivity certainly reflects the difference in the geometry of the lithium enolates that formed from **14b** and **14c**. Interestingly, the cascade reaction of dimethyl bis-enoate **13c** (R′ = Me) with phenyllithium in THF at −78 °C gave *trans,trans*-product ***tt*-15e** in 19% yield as a major product and ***tc*-15e** in 3% yield, showing the same stereochemical tendency as that of di-*tert*-butyl bis(enoate) **13b**. These results clearly indicate that the *E*-geometry of the lithium enolate that formed by the deprotonation of **14b** should be the same as that formed by the conjugate addition of **13b**, whereas those should be different between dimethyl esters **14c** and **13c**.

The deprotonation of methyl ester **14c** probably proceeded via 6-membered transition state **C** according to the Ireland model [56, 57], where the 1,3-diaxial interaction between the α-substituent of the ester and the isopropyl group of LDA was avoided, to give enolates with *Z*-geometry. Hence, ***tc*-15e** was obtained as a major product via the Michael addition through s-*cis* transition state **D** (Scheme 6).

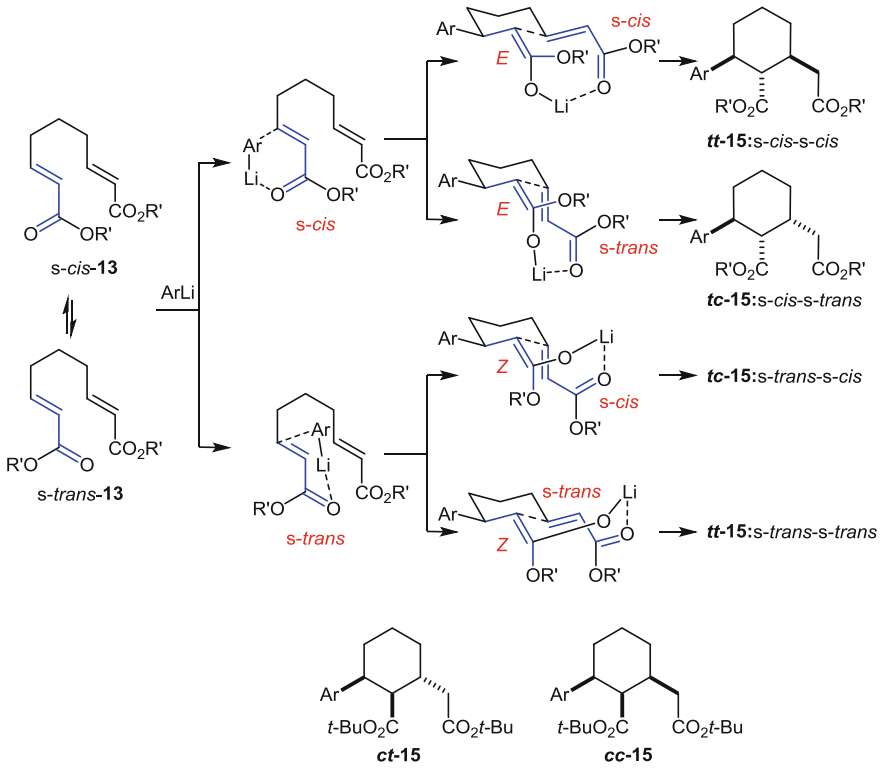

Scheme 5 Products of conjugate addition-Michael cyclization cascade

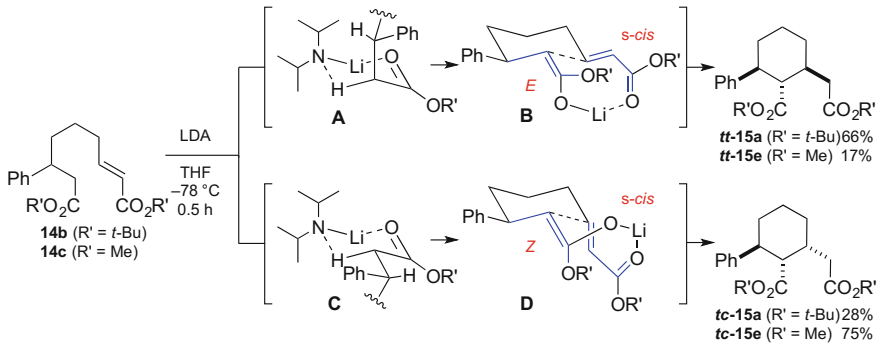

Scheme 6 Michael cyclization of monophenyl adducts **14b** and **14c** with LDA

Indeed, deprotonation of **14c** with LDA in 23% HMPA–THF [56, 57], under which an *E*-enolate should formed via an open transition state, led to the opposite diastereoselectivity, giving ***tt*-15e** as a major product in 21% yield along with ***tc*-15e**

in 9% yield. The low yields were due to competitive γ-deprotonation of the alkenoate moiety giving rise to the corresponding deconjugated *Z*- and *E*-alkenoates in 28 and 6% yield, respectively.

Deprotonation of ketones by LDA preferentially gives *E*-enolate via analogous transition states to **A** to avoid steric repulsion between the two substituents on the carbonyl carbons [56, 57]. Therefore, it is highly probable that the deprotonation of *tert*-butyl ester **14b** mainly proceeded via transition state **A** due to the bulkiness of the α-substituent and the *tert*-butoxy moiety, giving *E*-enolate. As a consequence, ***tt*-15a** was produced as a major product by subsequent intramolecular conjugate addition via s-*cis* transition state **B**. All these results lead to the conclusion that the lithium enolate intermediate should undergo the intramolecular conjugate addition in s-*cis* conformation, and consequently, that the both conjugate addition should proceed with the alkenoate moieties in s-*cis* conformation as proposed in the possibility (1) above.

4 Asymmetric Total Synthesis of (+)-β-Lycorane in Five Steps

The completion of asymmetric total synthesis of (+)-β-lycorane (**2**) was carried out by starting from ***tt*-15d** (=**7**) as shown in Scheme 7. Treatment of ***tt*-15d** with HCl for 0.5 h in refluxing ethanol gave protodesilylated half ester **17** in 98% yield. Interestingly, the carboxylic acid at the C-2 position was not esterificated, probably due to steric hindrance [58]. Curtius rearrangement using diphenylphosphoryl azide (DPPA) [59] followed by Bischler–Napieralski-type cyclization with polyphosphoric acid (PPA) [60, 61] converted **17** into lactam **18** via an isocyanate intermediate in 70% yield. Finally, treatment of **18** with borane–dimethyl sulfide complex [62] in refluxing THF induced in one pot three manipulation: reduction of

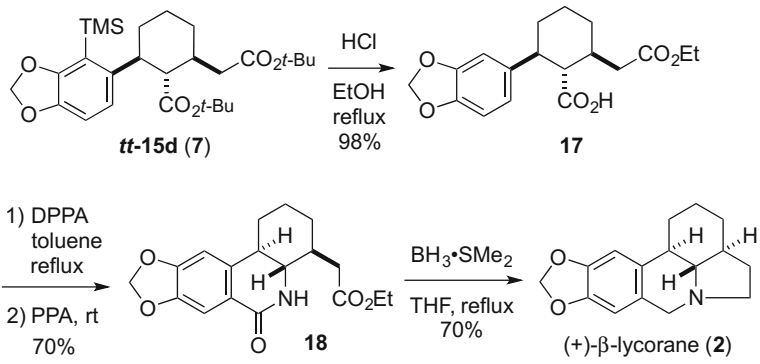

Scheme 7 Asymmetric total synthesis of (+)-β-lycorane (**2**)

the lactam, lactam formation between the resulting amine and the ester moiety, and finally reduction of the resulting lactam to give (+)-β-lycorane (**2**) in 70% yield.

^{1}H and ^{13}C NMR [13, 14], and the specific rotation [14] were in good agreement with those reported. Notably, the asymmetric total synthesis was accomplished through only five steps from **3** in high overall yield (33%).

5 Conclusion

This study revealed that the bulky TMS group at the *ortho*-position of aryllithium is effective to improve the enantioselectivity of the chiral ligand-mediated asymmetric conjugate addition cascade of bis-enoate. Cyclohexanes bearing three contiguous stereogenic centers with *trans,trans*-configuration were obtained in high optical purity. It was suggested that the 1,3-diaxial interaction would play an important role in determining the diastereoselectivity. This methodology enables the formation of two C–C bonds and three stereogenic centers in one pot to give synthetically useful chiral cyclohexane derivatives. The utility of this methodology was clearly demonstrated by the achievement of the shortest asymmetric total synthesis of (+)-β-lycorane. Importantly, the chiral ligand could be recycled, and the one-pot reactions are economically and ecologically beneficial.

References

1. Parts of this contents have been published: Nishimura, K.; Fukuyama, N.; Yamashita, M.; Sumiyoshi, T.; Yamamoto, Y.; Yamada, K.; Tomioka, K. *Synthesis* **2015**, *47*, 2256–2264.
2. Parts of this contents have been published: Nishimura, K.; Fukuyama, N.; Yasuhara, T.; Yamashita, M.; Sumiyoshi, T.; Yamamoto, Y.; Yamada, K.; Tomioka, K. *Tetrahedron* **2015**, *71*, 7222–7226.
3. Jin, Z. *Nat. Prod. Rep.* **2011**, *28*, 1126–1142.
4. Jin, Z. *Nat. Prod. Rep.* **2009**, *26*, 363–381.
5. Zarotsky, V.; Sramek, J. J.; Cutler, N. R. *Am. J. Health-Syst. Pharm.* **2003**, *60*, 446–452.
6. *WHO Drug Info.* **1998**, *12*, 205.
7. Cook, J. W.; Loudon, J. D. In *The Alkaloids*; Manske, R. H. F., Holmes, H. L., Eds; Academic Press: New York, 1952; Vol. 2, p 331.
8. Kondo, H.; Uyeo, S. *Chem. Ber.* **1935**, *68*, 1756.
9. Kotera, K. *Tetrahedron* **1961**, *12*, 240–247.
10. Yamada, K.; Yamashita, M.; Sumiyoshi, T.; Nishimura, K.; Tomioka, K. *Org. Lett.* **2009**, *11*, 1631–1633.
11. Racemic syntheses: Hill, R. K.; Joule, J. A.; Loeffler, L. J. *J. Am. Chem. Soc.* **1962**, *84*, 4951–4956.
12. Racemic syntheses: Martin, S. F.; Tu, C.-y. *J. Org. Chem.* **1981**, *46*, 3763–3764.
13. Racemic syntheses: Martin, S. F.; Tu, C.-y.; Kimura, M.; Simonsen, S. H. *J. Org. Chem.* **1982**, *47*, 3634–3643.
14. Asymmetric syntheses: Dong, L.; Xu, Y.-J.; Yuan, W.-C.; Cui, X.; Cun, L.-F.; Gong, L.-Z. *Eur. J. Org. Chem.* **2006**, 4093–4105.

15. Asymmetric syntheses: Hong, B.-C.; Nimje, R. Y.; Wu, M.-F.; Sadani, A. A. *Eur. J. Org. Chem.* **2008**, 1449–1457.
16. Our other approaches for lycoranes: Yasuhara, T.; Nishimura, K.; Yamashita, M.; Fukuyama, N.; Yamada, K.; Muraoka, O.; Tomioka, K. *Org. Lett.* **2003**, *5*, 1123–1126.
17. Our other approaches for lycoranes: Yasuhara, T.; Osafune, E.; Nishimura, K.; Yamashita, M.; Yamada, K.; Muraoka, O.; Tomioka, K. *Tetrahedron Lett*. **2004**, *45*, 3043–3045.
18. Tomioka, K. *Synthesis* **1990**, 541–549.
19. Kanai, M.; Shibasaki, M. In *Catalytic Asymmetric Synthesis*; Ojima, I., ed: VCH: Weinheim, 2000, p. 569.
20. Sibi, M. P.; Manyem, S. *Tetrahedron* **2000**, *56*, 8033–8061.
21. Krause, N.; Hoffmann-Röder, A. *Synthesis* **2001**, 171–196.
22. Feringa, B. L.; Naasz, R.; Imbos, R.; Arnold, L. A. In *Modern Organocopper Chemistry;* Krause, N., ed.; Wiley-VCH: Weinheim, 2002, chapter 7.
23. Hayashi, T.; Yamasaki, K. *Chem. Rev.* **2003**, *103*, 2829–2844.
24. Tomioka, K. In *Comprehensive Asymmetric Catalysis, Supplement*; Jacobsen, E. N., Pfaltz, A., Yamamoto, H., Eds.; Springer, 2004; Chapter 31.1, pp 109–124.
25. Yamataka, H.; Yamada, K.; Tomioka, K. In *The Chemistry of Organolithium Compounds*; Rappoport, Z., Marek, I., Eds; Wiley, 2004; Part 1, Chapter 14.
26. Christoffers, J.; Koripelly, G.; Rosiak, A.; Rössle, M. *Synthesis* **2007**, 1279–1300.
27. Tomioka, K.; Yamamoto, Y.; Yamada, K. In *Comprehensive Chirality*; Carreira, E. M., Yamamoto, H., Eds.; Elsevier, 2012; Vol. 4, pp 122–131.
28. Asao, N.; Uyehara, T.; Yamamoto, Y. *Tetrahedron* **1990**, *46*, 4563–4572.
29. Suzuki, I.; Kin, H.; Yamamoto, Y. *J. Am. Chem. Soc.* **1993**, *115,* 10139–10146.
30. Shida, N.; Kabuto, C.; Niwa, T.; Ebata, T.; Yamamoto, Y. *J. Org. Chem.* **1994**, *59*, 4068–4075.
31. Börner, C.; König, W. A.; Woodward, S. *Tetrahedron Lett.* **2001**, *42*, 327–329.
32. Cardillo, G.; Gentilucci, L.; Gianotti, M.; Tolomelli, A. *Org. Lett.* **2001**, *3*, 1165–1167.
33. Börner, C.; Dennis, M. R.; Sinn, E.; Woodward, S. *Eur. J. Org. Chem.* **2001**, 2435–2446.
34. Nishimura, K.; Tomioka, K. *J. Org. Chem.* **2002**, *67*, 431–434.
35. Dambacher, J.; Anness, R.; Pollock, P.; Bergdahl, M. *Tetrahedron* **2004**, *60*, 2097–2110.
36. Davies, S. G.; Hermann, G. J.; Sweet, M. J; Smith, A. D. *Chem. Commun.* **2004**, 1128–1129.
37. Beddow, J. E.; Davies, S. G.; Ling, K. B.; Roberts, P. M.; Russell, A. J.; Smith, A. D.; Thomson, J. E. *Org. Biomol. Chem.* **2007**, *5*, 2812–2825.
38. Davies, S. G.; Foster, E. M.; McIntosh, C. R.; Roberts, P. M.; Rosser, T. E.; Smith, A. D.; Thomson, J. E. *Tetrahedron: Asymmetry* **2011**, *22*, 1035–1050.
39. Tomioka, K.; Shindo, M.; Koga, K. *J. Am. Chem. Soc.* **1989**, *111*, 8266–8268.
40. Tomioka, K.; Shioya, Y.; Nagaoka, Y.; Yamada, K. *J. Org. Chem*. **2001**, *66*, 7051–7054, and references therein.
41. C-nucleophiles: Asano, Y.; Iida, A.; Tomioka, K. *Tetrahedron Lett.* **1997**, *38*, 8973–8976.
42. C-nucleophiles: Asano, Y.; Yamashita, M.; Nagai, K.; Kuriyama, M.; Yamada, K.; Tomioka, K. *Tetrahedron Lett.* **2001**, *42*, 8493–8495, and references therein.
43. N-nucleophiles: Doi, H.; Sakai, T.; Iguchi, M.; Yamada, k.; Tomioka, K. *J. Am. Chem. Soc.*, **2003**, *125*, 2886–2887.
44. N-nucleophiles: Sakai, T.; Doi, H.; Tomioka, K. *Tetrahedron* **2006**, *62*, 8351–8359, and references therein.
45. S-nucleophiles: Nishimura, K.; Ono, M.; Nagaoka, Y.; Tomioka, K. *J. Am. Chem. Soc.* **1997**, *119*, 12974–12975.
46. S-nucleophiles: Nishimura, K.; Ono, M.; Nagaoka, Y.; Tomioka, K. *Angew. Chem., Int. Ed.* **2001**, *40*, 440–442.
47. Yamashita, M.; Yamada, K.; Tomioka, K. *J. Am. Chem. Soc.* **2004**, *126*, 1954–1955.
48. Valleix, F.; Nagai, K.; Soeta, T.; Kuriyama, M.; Yamada, K.; Tomioka, K. *Tetrahedron* **2005**, *61*, 7420–7424, and references therein.
49. Of course sp3 character of lithium and Li-R bond constitute a destroying factor of perfect *C2*-symmetry.

50. Yamamoto, Y.; Yasuda, Y.; Oulyadi, H.; Maddaluno, J.; Tomioka, K. *Tetrahedron* **2010**, *66*, 2470–2473.
51. Yamamoto, Y.; Nasu, H.; Tomioka, K. *Tetrahedron* **2013**, *69*, 3836–3840.
52. Ester substituent R' of enoate affects the stereoselectivity. In the asymmetric conjugate addition of lithium amide (R = N(Bn)TMS), the ee of the reaction of *tert*-butyl crotonate was 97%, whereas that of methyl crotonate was 85%. These results indicated that an enoate with bulky ester substituent preferred the coordination to lithium as shown in **10**.
53. Corey, E. J.; Peterson, R. T. *Tetrahedron Lett.* **1985**, *26*, 5025–5028.
54. Uchiyama, M.; Nakamura, S.; Furuyama, T.; Nakamura, E.; Morokuma, K. *J. Am. Chem. Soc.* **2007**, *129*, 13360–13361.
55. The inverse addition (adding phenyllithium to a solution of **13b**) significantly prevented the formation of **16a** (8%) and improved the yield of ***tt*-15a** and ***tc*-15a** to 52% and 5% yields, respectively.
56. Ireland, R. E.; Mueller, R. H.; Willard, A. K. *J. Am. Chem. Soc.* **1976**, *98*, 2868–2877.
57. Heathcock, C. H.; Buse, C. T.; Kleschick, W. A.; Pirrung, M. C.; Sohn, J. E.; Lampe, J. *J. Org. Chem*. **1980**, *45,* 1066–1081.
58. Also in the LiAlH4 reduction of ***tt*-15b**, the ester group at the C-2 remained unchanged.
59. Ninomiya, K.; Shioiri, T.; Yamada, S. *Tetrahedron* **1974**, *30*, 2151–2157.
60. Sánchez I. H.; Mendoza M. T. *Tetrahedron Lett.* **1980**, *21*, 3651–3654.
61. Taylor, E. C., Jr.; Kalenda, N. W. *J. Am. Chem. Soc.* **1954**, *76*, 1699–1700.
62. Venuti, M. C.; Ort, O. *Synthesis* **1988**, 985–988.

Concise Synthesis of Peptide Analogs Using a Fluorous-Fmoc Protection Strategy

Masato Matsugi

Abstract The syntheses of fluorous-Fmoc reagents and their application to peptide synthesis are described. Fluorous-Fmoc reagents bearing C_3F_7, C_4F_9, and C_6F_{13} chains were prepared at a multigram scale and used as fluorous encoding tags for amino acids. Using the fluorous-Fmoc reagents, a liquid-phase fluorous mixture synthesis of various peptides, some of which are analogs of angiotensin-converting-enzyme inhibitors, was achieved. Similarly, a concise liquid-phase fluorous mixture synthesis of all stereoisomers of dendroamide A was also achieved by encoding each asymmetric center of the amino acid starting material. The stereoisomers were synthesized individually in fewer steps compared with their corresponding linear synthetic routes.

Keywords Peptide · Fluorous mixture synthesis · f-Fmoc reagent · Natural product · Stereoisomers

1 Introduction

Since the introduction of fluorous solid-phase extraction (FSPE) as a separation technique for light-fluorous-tagged molecules (fluorine content is under ca. 30%) in 1997 [1], it has proven to be widely applicable for separating light-fluorous molecules [2] from organic molecules. This separation technique has the advantage of enabling an efficient separation of molecules that are not heavily fluorinated [3]. The efficient separation reduces the costs involved in rendering compounds fluorous and allows for the application of reaction conditions used in analogous standard reaction protocols.

To date, a variety of light-fluorous protecting groups have been reported, such as fluorous-*t*-butoxycarbonyl [4], fluorous-benzyloxycarbonyl [5], fluorous-methoxymethyl [6], fluorous-triisopropylsilyl [7], and fluorous-phosphates [8], some of which are now commercially available [9]. The structures of these fluorous protecting groups

M. Matsugi (✉)
Faculty of Agriculture, Meijo University, Nagoya, Japan
e-mail: matsugi@meijo-u.ac.jp

K. Tomioka et al. (eds.), *New Horizons of Process Chemistry*,
DOI 10.1007/978-981-10-3421-3_15

are very similar to those of the original non-fluorous protecting groups, which allows the protection and deprotection of the fluorous protecting groups under nearly identical conditions. Furthermore, molecules bearing light-fluorous tags readily dissolve in organic solvents, allowing the reactions to be monitored by thin-layer chromatography, high-performance liquid chromatography (HPLC), and liquid chromatography–mass spectrometry. In the last decade, these fluorous protecting groups have been used in peptide and oligosaccharide syntheses [10] as well as the stereoisomer library synthesis of natural products by fluorous mixture synthesis (FMS) [11].

In peptide synthesis, fluorous *t*-butoxycarbonyl [4] and fluorous benzyloxycarbonyl [5] are currently available as amino acid protecting groups. Meanwhile, 9-fluorenylmethoxycarbonyl (Fmoc) [12] is an important *N*-terminal protecting group for amino acids because it is easy to introduce, acid-stable, and can be easily removed under basic conditions (e.g., piperidine) [13]. The FMS of various peptides would be possible if a variety of fluorous-Fmoc (f-Fmoc) reagents bearing homologous fluorous tags were available. In this chapter, we describe the multigram syntheses of f-Fmoc reagents and their application to the FMS of biologically active peptides, including natural products.

2 Multigram Syntheses of f-Fmoc Reagents

Scheme 15.1 shows the multigram scale applicable synthetic route to access f-Fmoc reagents [14] bearing each C_3F_7 or C_4F_9 or C_6F_{13} fluorous chain. After exploring a variety of conditions to introduce the perfluoroalkyl chain, we found that the

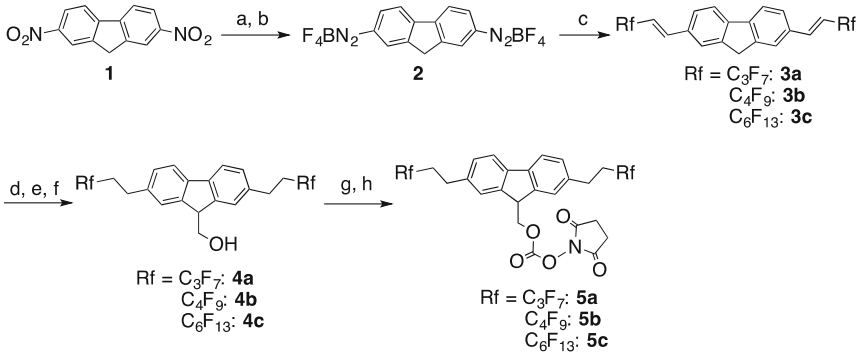

Reagents and conditions: (a) H_2, 5 mol% of Pd/C, MeOH/THF, rt, quant.; (b) 3 equiv of $NaNO_2$, 48% aq HBF_4, 0 °C -rt, quant.; (c) 1.0 equiv of $RfCH{=}CH_2$, 5 mol% of $Pd(OAc)_2$, MeOH, 40 °C or 4 °C, 84% (C_3F_7), 83% (C_4F_9), 99% (C_6F_{13}); (d) 5-20 mol% of Pd/C, H_2, MeOH/THF, rt, quant. (C_3F_7), quant. (C_4F_9), quant. (C_6F_{13}); (e) 10 equiv of NaH, HCO_2Et (excess), diethylether, reflux (f) 5 equiv of $NaBH_4$, MeOH/THF, 0 °C-rt, 87% (C_3F_7), 72% (C_4F_9), 93% (C_6F_{13}) (2steps); (g) 3 equiv of phosgene, 1.5 equiv of *N,N*-dimethylaniline, CH_2Cl_2, rt; (h) NaOSu, CH_2Cl_2, rt, quant. (C_3F_7), 99% (C_4F_9), 98% (C_6F_{13}) (2steps).

Scheme 15.1 A multigram scale synthetic route to access the f-Fmoc reagents

Heck-type reaction of a bis-diazonium salt with fluorous olefin was the most effective [15]. Therefore, the reaction was used for the introduction of fluorous tags to the fluorene core structure in the multigram synthesis. First, the hydrogenation of dinitrofluorene **1** provided the corresponding diaminofluorene. After derivation to the corresponding bis-diazonium salt **2a–c**, a Heck-type reaction was conducted with the corresponding fluorous olefin to yield the fluorous fluorenes **3a–c** in the range of 83–99% yield. Interestingly, when 1.1 equiv of fluorous-olefin bearing C_6F_{13} (Rf = C_6F_{13}) was used as the substrate, the corresponding product **3c** was obtained at 50% yield, corresponding to a 95% yield with regards to the alkene used. During the reaction, we observed that the bis-diazonium salt did not dissolve in MeOH; however, the Heck products **3a–c** were soluble in the reaction solvent. We thus believe that either the mono-diazonium salt resulting from the first Heck reaction may be much more soluble than the bis-diazonium salt or the second Heck reaction occurs quickly. Further hydrogenation, hydroxymethylation [16], chlorocarbonylation, and condensation with the sodium salt of *N*-hydroxysuccinimide (NaOSu) provided the target f-Fmoc reagents **5a–c**. The f-Fmoc were obtained on a multi-gram scale (Rf = C_3F_7: 20.1 g, Rf = C_4F_9: 30 g, Rf = C_6F_{13}: 2.9 g) when the diazonium salts were used as the starting materials in quantities of 20.1, 30, and 2.9 g, respectively [17].

3 FMS of Simple Peptides Employing f-Fmoc Reagents

3.1 FMS of Tripeptide Derivatives

Here, we describe the first example of the FMS of a variety of tripeptides, angiotensin-converting enzyme (ACE) inhibitors, encoded by f-Fmoc tags with three different type of fluorine (F14, F18, F26). First, as shown in Scheme 15.2, L-alanine, L-phenylalanine, and L-leucine were each protected with f-Fmoc reagents bearing different fluorine contents. The yields of the protected amino acids (89–98%) were about the same as that for the non-fluorous standard Fmoc reagent. A mixture of the protected amino acids was then divided into two groups, and the

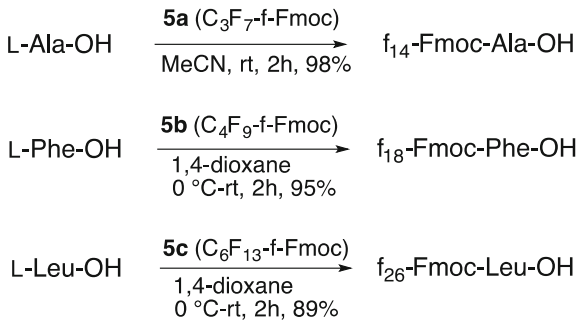

Scheme 15.2 f-Fmoc protection of L-alanine, L-phenylalanine, and L-leucine

condensation reaction for the dipeptide synthesis was accomplished using the 2-(1*H*-benzotriazol-1-yl)-1,1,3,3-tetramethyluronium hexafluorophosphate (HBTU)/1-hydroxy-benzotriazole (HOBt) method [18]. One group was reacted with L-alanine benzyl ester in 95% yield, whereas the other group was reacted with L-valine benzyl ester in 98% yield (conditions a and b in Scheme 15.3). Condensation reactions using Fmoc-protected amino acids proceeded successfully, similar to the case of conventional Fmoc group. After deprotection of the *C*-terminus by hydrogenolysis [19] of the mixture of the two groups in quantitative yields (conditions c and d in Scheme 15.3), each mixture was divided into three groups. The f-Fmoc groups were not affected at all by the reducing conditions. Each of the six groups was then allowed to react with four different *C*-protected amino acids (Ala-OBn, Val-OBn, Leu-OBn, and Met-OMe) using the same condensation method (conditions e–j in Scheme 15.3). The yields were satisfactory, ranging from 86 to 96%.

Next, we attempted to separate the pure *C*-protected tripeptides from each mixture of the 6 groups (Groups A–F). Figure 15.1 shows the analytical

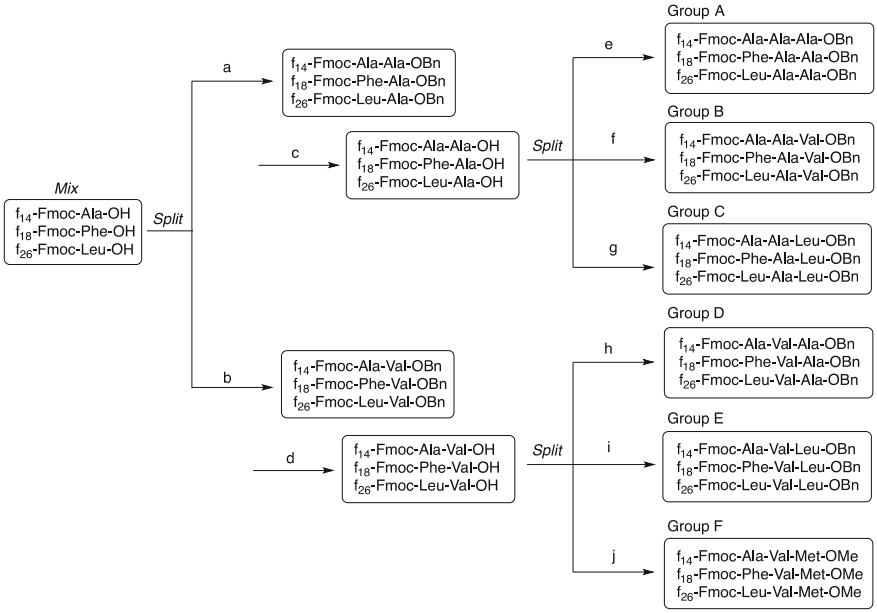

Reagents and conditions: a) 1.2 equiv Ala-OBn, 1.2 equiv HOBt, 1.2 equiv HBTU, 2.4 equiv DIEA, DMF, rt, 24 h, 95%; b) 1.2 equiv Val-OBn, 1.2 equiv HOBt, 1.2 equiv HBTU, 2.4 equiv DIEA, DMF, rt, 24 h, 98%; c) 5 mol% Pd/C, 1 atm H_2, MeOH/THF, rt, 3 h, quant.; d) 5 mol% Pd/C, 1 atm H_2, MeOH/THF, rt, 3 h, quant.; e) 1.2 equiv Ala-OBn, 1.2 equiv HOBt, 1.2 equiv HBTU, 2.4 equiv DIEA, DMF, rt, 24 h, 97%; f) 1.2 equiv Val-OBn, 1.2 equiv HOBt, 1.2 equiv HBTU, 2.4 equiv DIEA, DMF, rt, 24 h, 98%; g) 1.2 equiv Leu-OBn, 1.2 equiv HOBt, 1.2 equiv HBTU, 2.4 equiv DIEA, DMF, rt, 24 h, 92%; h) 1.2 equiv Ala-OBn, 1.2 equiv HOBt, 1.2 equiv HBTU, 2.4 equiv DIEA, DMF, rt, 24 h, 95%; i) 1.2 equiv Leu-OBn, 1.2 equiv HOBt, 1.2 equiv HBTU, 2.4 equiv DIEA, DMF, rt, 24 h, 98%; j) 1.2 equiv Met-OMe, 1.2 equiv HOBt, 1.2 equiv HBTU, 2.4 equiv DIEA, DMF, rt, 24 h, 86%; HOBt=1-hydroxybenzotriazole, HBTU= *O*-benzotriazole-*N*,*N*,*N*′,*N*′-tetramethyl-uronium-hexafluoro-phosphate, DIEA= *N*,*N*-diisopropylethylamine

Scheme 15.3 Fluorous mixture synthesis of *C*-protected tripeptides

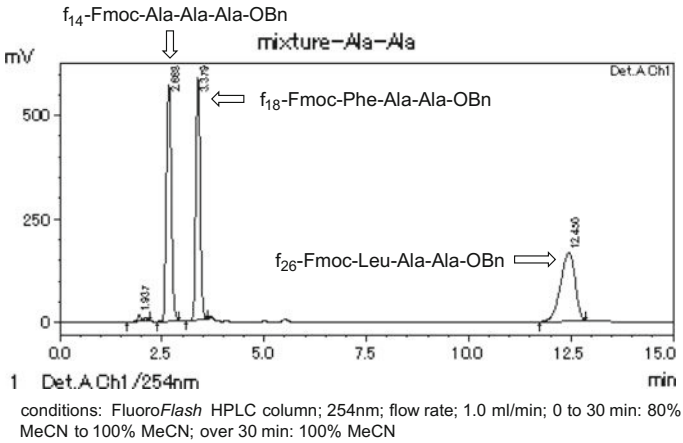

Fig. 15.1 Analytical fluorous HPLC chromatograph of the f_{14}-Fmoc-Ala-Ala-Ala-OBn, f_{18}-Fmoc-Phe-Ala-Ala-OBn, and f_{26}-Fmoc-Leu-Ala-Ala-OBn mixture

fluorous-HPLC (f-HPLC; Fluoro*Flash*® HPLC column, 4.6 mm i.d., 150 mm length) chromatograph [20] of the mixture of the tripeptide benzyl ester protected f-Fmoc compounds (f_{14}-Fmoc-Ala-Ala-Ala-OBn, f_{18}-Fmoc-Phe-Ala-Ala-OBn, and f_{26}-Fmoc-Leu-Ala-Ala-OBn; Group A). The peaks corresponding to f_{14}-Fmoc-Ala-Ala-Ala-OBn, f_{18}-Fmoc-Phe-Ala-Ala-OBn, and f_{26}-Fmoc-Leu-Ala-Ala-OBn appeared at 2.7, 3.4, and 12.5 min, respectively. With this remarkable difference in retention time, easy separation of the peptides should be possible. We separated each group of tripeptides by preparative f-HPLC (Fluoro*Flash*® HPLC column, 20 mm i.d., 250 mm length) using the same conditions used in the analytical f-HPLC. Using 200-mg-scale f-HPLC, the f-Fmoc-protected peptides f_{14}-Fmoc-Ala-Ala-Ala-OBn, f_{18}-Fmoc-Phe-Ala-Ala-OBn, and f_{26}-Fmoc-Leu-Ala-Ala-OBn were isolated in 43 mg, 63 mg, and 86 mg, respectively, with minimal loss. Similarly, the other 5 groups (Groups B–F) were subjected to preparative f-HPLC, and each pure tripeptide compound was effectively separated with almost quantitative recovery. Finally, deprotection of the f-Fmoc was conducted.

Scheme 15.4 shows the yield of each f-Fmoc deprotection reaction using excess diethylamine in acetonitrile at room temperature [13]. Eighteen *N*-deprotected tripeptides were obtained in the range of 82% to quantitative yield. If the tripeptides had been synthesized individually using the linear synthetic route outlined in this work, 90 synthetic steps would have been required; however, we conducted the syntheses in a mere 31 steps including f-Fmoc protections [21]. This f-Fmoc encoding strategy provides a new method for synthesizing various peptides in one fell swoop. It is likely that this strategy will be one of the most useful methods for divergent polypeptide synthesis.

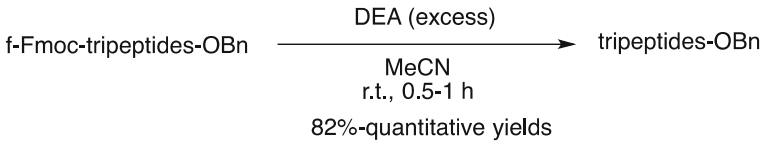

Ala-Ala-Ala-OBn	Phe-Ala-Ala-OBn	Leu-Ala-Ala-OBn
Ala-Ala-Val-OBn	Phe-Ala-Val-OBn	Leu-Ala-Val-OBn
Ala-Ala-Leu-OBn	Phe-Ala-Leu-OBn	Leu-Ala-Leu-OBn
Ala-Val-Ala-OBn	Phe-Val-Ala-OBn	Leu-Val-Ala-OBn
Ala-Val-Leu-OBn	Phe-Val-Leu-OBn	Leu-Val-Leu-OBn
Ala-Val-Met-OMe	Phe-Val-Met-OMe	Leu-Val-Met-OMe

Scheme 15.4 Individual yields of the f-Fmoc group deprotection process

3.2 ACE Inhibitory Assay of the Synthetic Tripeptides

Figure 15.2 shows the results of an ACE inhibitory assay of the eighteen synthetic *C*-protected tripeptides and the corresponding eighteen *C*-deprotected peptides [22]. The ACE inhibitory activities were measured by ACE Kit-WST (Dojindo Laboratories, Ltd.) at a concentration of 20 μM. The *C*-protected tripeptides were dissolved in 10% dimethyl sulfoxide and the *C*-deprotected peptides were dissolved in H_2O. The tripeptides indicated in bold-type are known ACE inhibitors, and the half maximal inhibitory concentration (IC_{50}, mmol/L) of each compound is listed in

Ala-Ala-Ala-OBn	88%	Phe-Ala-Ala-OBn		Leu-Ala-Ala-OBn	92%
(-OH)	92%	(-OH)	97%	**(-OH) [3]**	98%
Ala-Ala-Val-OBn	88%	Phe-Ala-Val-OBn	50%	Leu-Ala-Val-OBn	95%
(-OH) [25]	97%	(-OH)	98%	(-OH)	98%
Ala-Ala-Leu-OBn	94%	Phe-Ala-Leu-OBn	–	Leu-Ala-Leu-OBn	83%
(-OH) [93]	99%	(-OH)	96%	(-OH)	98%
Ala-Val-Ala-OBn	94%	Phe-Val-Ala-OBn	–	Leu-Val-Ala-OBn	–
(-OH)	98%	**(-OH) [6]**	98%	(-OH)	98%
Ala-Val-Leu-OBn	–	Phe-Val-Leu-OBn	71%	Leu-Val-Leu-OBn	74%
(-OH) [7]	99%	(-OH)	99%	(-OH)	99%
Ala-Val-Met-OMe	70%	Phe-Val-Met-OMe	96%	Leu-Val-Met-OMe	93%
(-OH) [8]	93%	(-OH)	97%	(-OH)	93%

Fig. 15.2 ACE inhibitory assay of the 36 synthetic *C*-protected and deprotected peptides

brackets. The results show that almost all the synthetic tripeptides in this work showed activity as ACE inhibitors.

4 FMS of Natural Product Isomers Employing f-Fmoc Reagents

4.1 Application of FMS for the Stereoisomer Synthesis of Natural Products

A particularly novel application of FMS is the determination of the stereochemical parameters required for a molecule to possess biological activity. In particular, the biological activity of peptides is governed by the configuration at the asymmetric center [23]. From a drug discovery perspective, it is interesting to study the biological activity of the non-natural configuration to ascertain whether the modification enhances the biological activity, diminishes it, or elicits an entirely different response. Synthetically, the task is daunting, especially in the case of polypeptides, where each additional center generates $2n$ possible stereoisomers. However, FMS is uniquely suited to address this challenge because the various isomers can be individually labeled with fluorous tags of different lengths and then mixed together. The mixture can then be carried through the synthesis and separated at the very end based purely on the fluorine content, thereby deconvoluting the entire mixture. This strategy saves significant effort because the synthetic steps between mixing and demixing need not be conducted on each individual isomer to obtain the entire family of desired stereoisomers isolated individually.

4.2 FMS of All Stereoisomers of Dendroamide A

We introduce an FMS for all stereoisomers of the biologically active compound dendroamide A **6a** to showcase f-Fmoc reagents as tools for effective peptide stereoisomer library synthesis. Dendroamide A isolated from the terrestrial blue-green alga (cyanobacterium) *Stigonema dendroideum Fremy* is a cyclic hexapeptide that exhibits multidrug-resistance reversing activity [24]. The first total synthesis of this compound was accomplished by Pattenden's group in 2000 [25]. Further total syntheses using pioneering strategies were reported by the groups of Smith [26], Kelly [27], and Shin [28]. A systematic conformational analysis of the linear precursors for the synthesis of **5a** was then reported by Shioiri's group [29]. The stereoisomers of **6a** can be expected to exhibit similar activity or other interesting biological activities.

The absolute configurations of the symmetric centers in the natural compound **6a** have an *R* absolute configuration, as shown in Fig. 15.3. This compound is

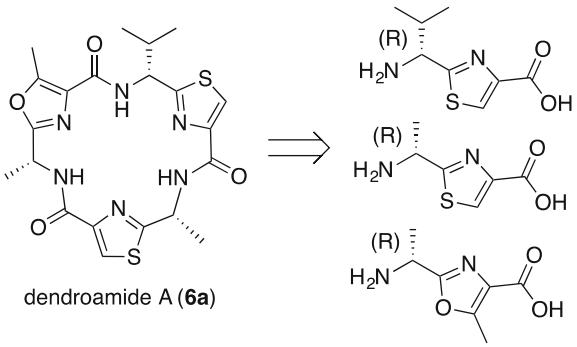

Fig. 15.3 Absolute configuration of dendroamide A **6a**

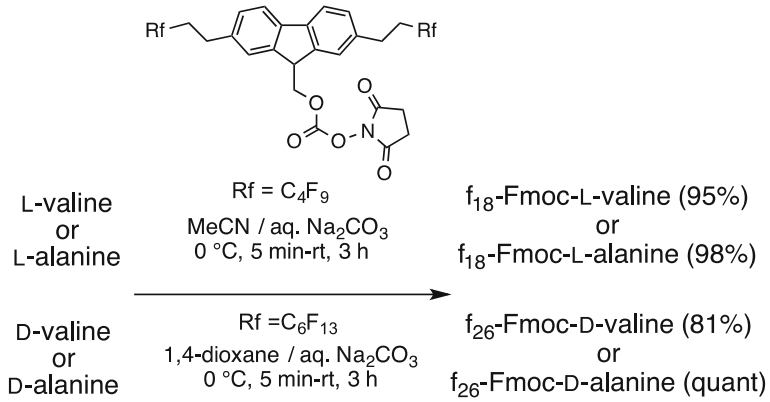

Scheme 15.5 *N*-terminal protection of starting amino acids by f-Fmoc

composed of three components: two thiazole units derived from D-alanine and D-valine and one methyloxazole unit derived from D-alanine. Our synthetic strategy is based on a split-type mixture synthesis using a mixture of the fluorous-tagged oxazole unit, which has different absolute configurations. The first step in the synthesis of the dendroamide family was to protect some amino acids using two different f-Fmoc reagents bearing C_4F_9 tags and C_6F_{13} tags. L-Alanine and L-valine were each protected using f-Fmoc reagents bearing C_4F_9 tags, while D-alanine and D-valine were protected using C_6F_{13} tags (Scheme 15.5). In all schemes, the f_{18}-Fmoc reagent is a bis-C_4F_9-tagged Fmoc, while the f_{26}-Fmoc reagent is a bis-C_6F_{13}-tagged Fmoc reagent.

Following the report of Kelly's group [30], we prepared a thiazole-ring unit (**9-mix**) derived from D-valine, L-valine, and L-cysteine as a mixture of enantiomers encoded with different f-Fmoc tags (Scheme 15.6). To remove the organic by-products and reagents after the reaction, FSPE [31] was conducted in steps c and d. For example, the condensation reaction in step c was accomplished using the HBTU/HOBt method. The reaction mixture was loaded onto fluorous silica gel with

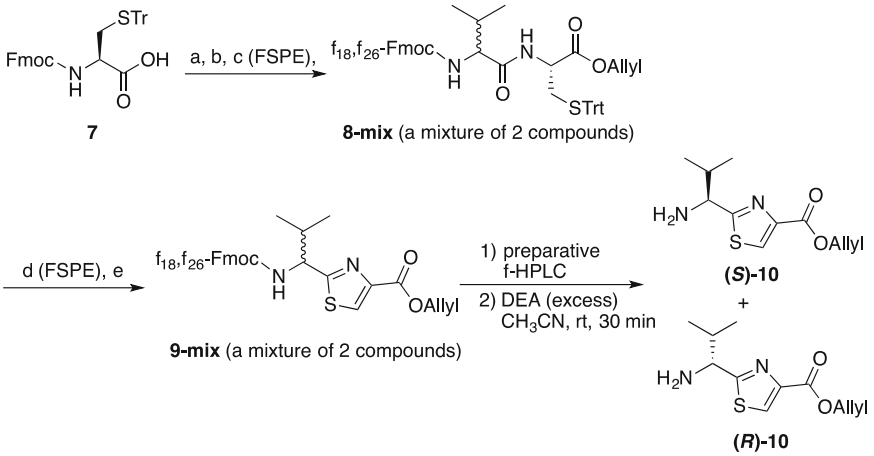

Reagents and conditions: (a) 2.0 equiv allyl alcohol, 1.1 equiv HOBT, 1.1 equiv HBTU, 2.1 equiv DIEA, DMF, rt, 24 h, quant.; (b) excess DEA, MeCN; (c) 1.0 equiv each f_{18}-Fmoc-L- and f_{26}-Fmoc-D-valine, 2.2 equiv HOBT, 2.2 equiv HBTU, 4.2 equiv DIEA, DMF, rt, 12 h; FSPE: 55% aq. THF on fluorous silicagel 95% (2 steps); (d) 18.0 equiv Ph_3PO, 9.0 equiv Tf_2O, CH_2Cl_2, 0 °C, 2 h, 77%; FSPE: 70% aq. MeOH on fluorous silicagel; (e) activated MnO_2, (10 w/w), $CHCl_3$, reflux, 30 min, 52%.

Scheme 15.6 Preparation of enantiomerically pure *O*-allylated thiazol units **(*S*)-10** and **(*R*)-10**

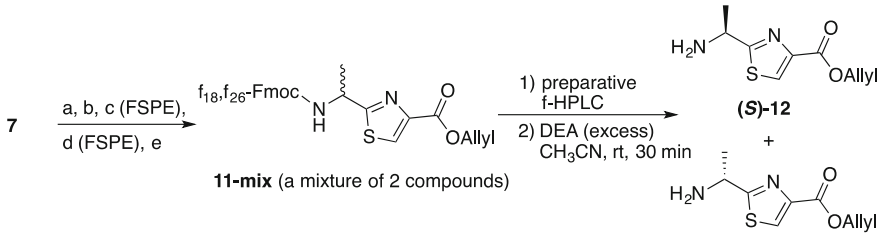

Reagents and conditions: (a) 2.0 equiv allyl alcohol, 1.1 equiv HOBT, 1.1 equiv HBTU, 2.1 equiv DIEA, DMF, rt, 24 h, quant.; (b) excess DEA, MeCN; (c) 1.0 equiv each f_{18}-Fmoc-L- and f_{26}-Fmoc-D-alanine, 2.2 equiv HOBT, 2.2 equiv HBTU, 4.2 equiv DIEA, DMF, rt, 12 h; FSPE: 55% aq. THF on fluorous silicagel 95% (2 steps); (d) 18.0 equiv Ph_3PO, 9.0 equiv Tf_2O, CH_2Cl_2, 0 °C, 2 h, 90%; FSPE: 70% aq. MeOH on fluorous silicagel; (e) activated MnO_2, (10 w/w), $CHCl_3$, reflux, 30 min, 75%.

Scheme 15.7 Preparation of enantiomerically pure *O*-allylated thiazol units **(*S*)-12** and **(*R*)-12**

tetrahydrofuran (THF), followed by a first elution with aqueous THF. During the first elution, the non-tagged organic compounds (reagents and reagent by-products) were washed from the column, while the fluorous-tagged compounds were retained. A second elution with THF washed the fluorous fraction off the column. In this way, the target f-Fmoc mixture compounds were isolated in 95% yield (yield after two steps including deprotection) without the use of a tedious purification procedure. Further separation of **9-mix** by preparative f-HPLC using an f-HPLC column [32] and the successive deprotection of the f-Fmoc group gave the enantiomerically pure thiazole-ring units **(*S*)-10** and **(*R*)-10**.

Similarly, a mixture of a thiazole-ring unit (**11-mix**) was prepared from the tagged mixture of L- and D-alanine. Scheme 15.7 shows the synthetic route for

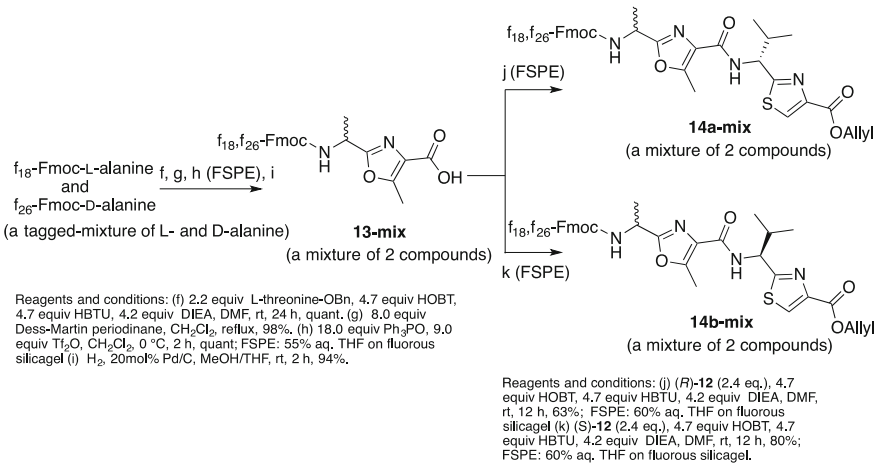

Scheme 15.8 Syntheses of **14a-mix** and **14b-mix** via a mixture of methyloxazol ring unit isomers **13-mix**

accessing **11-mix** as a mixture of two compounds bearing C_4F_9 or C_6F_{13} tags. For this case as well, FSPE was conducted in steps c and d to easily obtain **11-mix**. The separation of **11-mix** by preparative f-HPLC and the successive deprotection of the f-Fmoc group gave the enantiomerically pure thiazole-ring units **(*S*)-12** and **(*R*)-12**.

A mixture of the oxazole-ring unit (**13-mix**) was prepared from the tagged mixture of L- and D-alanine. Scheme 15.8 shows the synthetic route for accessing **14a-mix** and **14b-mix** as a mixture of two compounds bearing tags C_4F_9 or C_6F_{13}. FSPE was conducted in step h to obtain **13-mix** as the sole product. This oxazole-ring unit (**13-mix**), which is a fluorous-tagged mixture of enantiomers, was used as a starting material for the mixture synthesis. The mixture of two compounds (**13-mix**) was divided into two portions and then condensed with thiazole-ring units **(*R*)-10** and **(*S*)-10** to give **14a-mix** and **14b-mix**, respectively, each as a mixture of tagged compounds.

Next, **14a-mix** and **14b-mix** were each divided into two portions. The allyl group was deprotected, and each mixture was condensed with **(*S*)-12** and **(*R*)-12** separately. In this way, four pairs of compounds with different fluorine contents were obtained (Scheme 15.9): **15ab-mix**, **15cd-mix**, **15ef-mix**, and **15gh-mix**.

We conducted an f-HPLC analysis of **15ab-mix**, confirming that the C_4F_9-fmoc **15b** has a retention time of 16.3 min while the C_6F_{13}-fmoc **15a** has a retention time of 28.3 min, reflecting the fluorine content of each molecule (Fig. 15.4). Based on the large difference in retention times, each of the four pairs of **15ab-mix**, **15cd-mix**, **15ef-mix**, and **15gh-mix** were separated into the corresponding compounds **15a**–**h** in almost quantitative yield by preparative f-HPLC (Scheme 15.10).

After deprotection of both the allyl and the f-Fmoc protecting groups, each cyclization precursor **15a**–**h** was cyclized using medium-fluorous Mukaiyama reagent **16** [33] under high dilution using the syringe-pump technique. In this way,

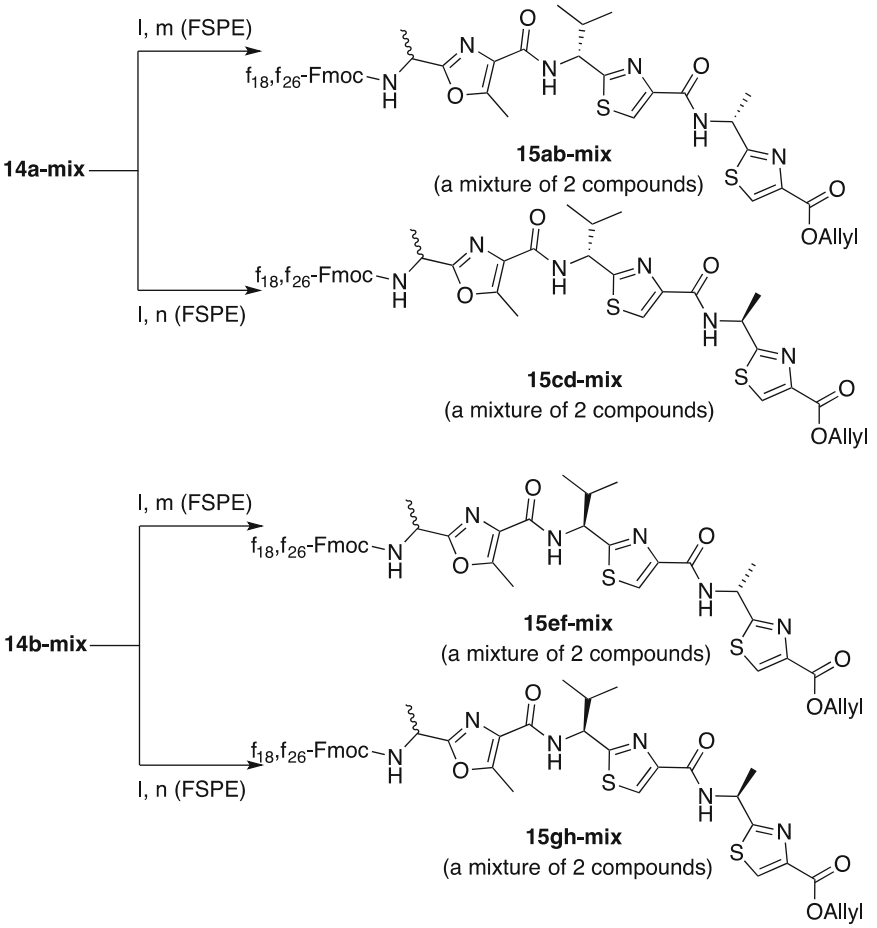

Reagents and conditions: (l) 20mol% $Pd(PPh_3)_4$, 2.0 equiv $PhSiH_3$, CH_2Cl_2, rt, 30 min. (m) (*R*)-**12** (2.4 eq.), 4.7 equiv HOBT, 4.7 equiv HBTU, 4.2 equiv DIEA, DMF, rt, 12 h; FSPE: 55% aq. THF, on fluorous silicagel; **15ef-mix**: 63%, **15ab-mix**: 54%, (2 steps) . (n) (*S*)-**12** (2.4 eq.), 4.7 equiv HOBT, 4.7 equiv HBTU, 4.2 equiv DIEA, DMF, rt, 12 h; FSPE: 55% aq. THF, on fluorous silicagel; **15cd-mix**: 54%, **15gh-mix**: 50% (2 steps).

Scheme 15.9 Synthesis of **15ab-mix**, **15cd-mix**, **15ef-mix**, and **15gh-mix**

all the target lactams (**6a**–**h**) were obtained in yields of 44–63% for each three-step process (Scheme 15.11) [34]. The ^{1}H NMR spectrum of dendroamide A **6a** obtained herein is consistent with the data for the natural dendroamide A reported by Smith's group [25]. In the spectra of the other stereoisomers, slightly different methyl and isopropyl chemical shifts were observed between the diastereomers. The ^{1}H NMR data for the pairs of diastereomers bearing enantiomeric relationships are consistent with each other.

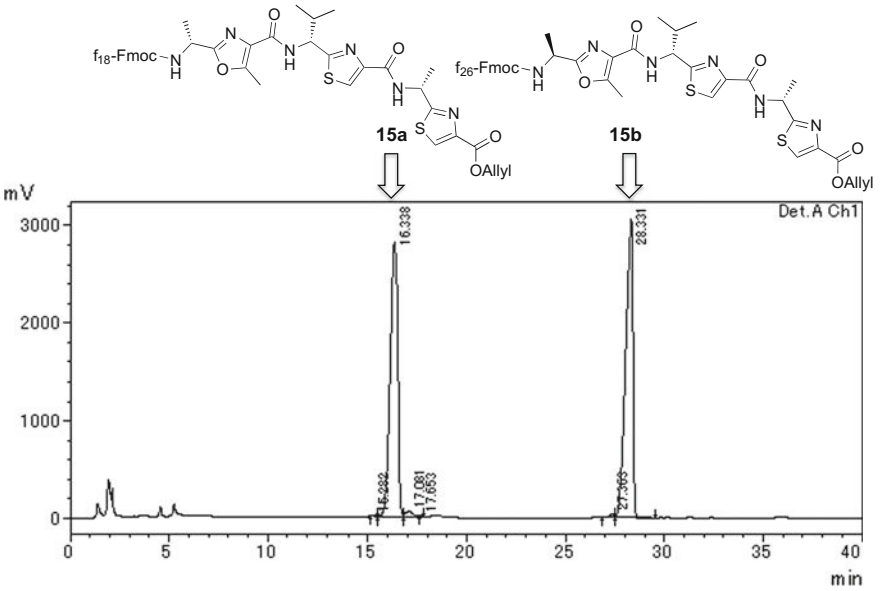

HPLC conditions: Fluoro*Flash*® HPLC column, 4.6 mm i.d., 150 mm length; 0 to 7.5 min 80% MeCN/H_2O up to 100% MeCN; Flow rate: 1.0mL/min; 254nm.

Fig. 15.4 Analytical f-HPLC of **15ab-mix**

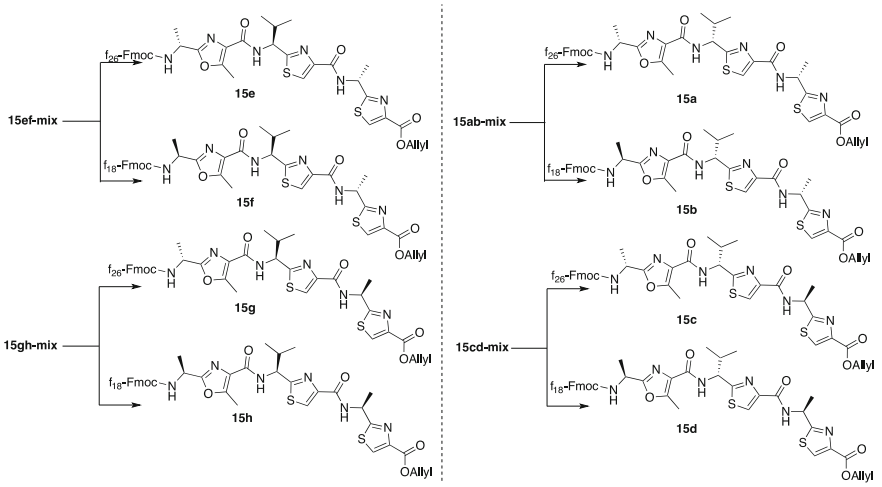

Preparative f-HPLC conditions: 0 to 7.5 min 80% MeCN /H2O up to 100% MeCN; Flow rate: 1.0mL/min; 254nm.

Scheme 15.10 Separation of **15ab-mix**, **15cd-mix**, **15ef-mix**, and **15gh-mix** by f-HPLC

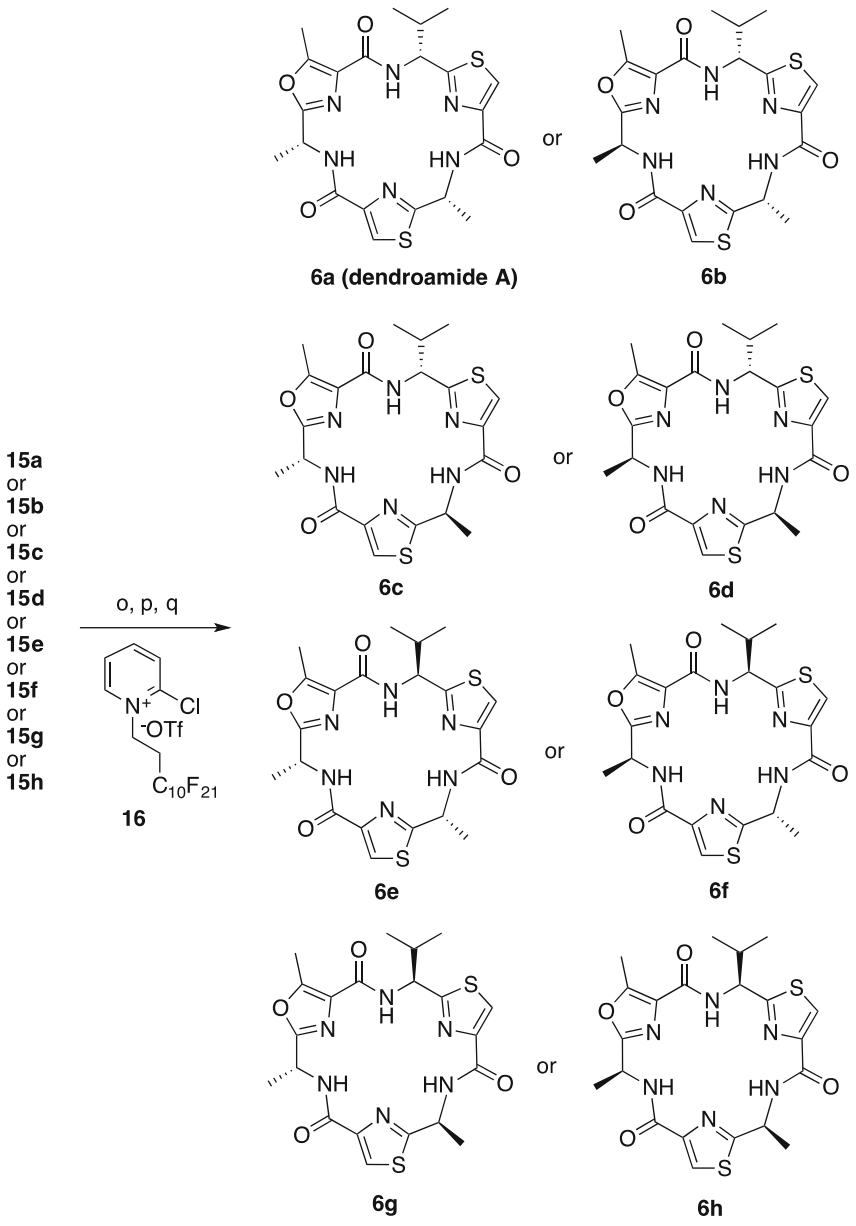

Reagents and conditions: (o) DEA (excess), MeCN, rt, 30 min; (p) 10 mol% $Pd(OAc)_2$, 2.0 equiv $PhSiH_3$, CH_2Cl_2, rt, 30 min; (q) 20.0 equiv medium fluorous-Mukaiyama reagent **16**, DMAP, DMF, 50 °C, 24 h, high dilution-conditions; **6a**: 63%, **6b**: 45%, **6c**: 59%, **6d**: 52%, **6e**: 44%, **6f**: 46%, **6g**: 52%, **6h**: 46% (3 steps). DMAP= *N,N*-dimethyl-4-aminopyridine.

Scheme 15.11 Macrolactamization of **15a–h** to **6a–h** employing medium-fluorous Mukaiyama reagent **16**

5 Summary

In summary, we have demonstrated a liquid-phase split-type synthesis of a large variety of tripeptides, ACE inhibitors, and a close synthesis of all stereoisomers of dendroamide A based on the encoding of the stereoisomers of amino acids by f-Fmoc reagents. If all stereoisomers of dendroamide A are to be synthesized using the same linear synthetic route, an 80-step reaction would be required; in comparison, our synthesis consisted only of 52 steps including the f-Fmoc protections. We believe that our f-Fmoc encoding strategy will be one of the most useful methods for the syntheses of divergent polypeptides and their analogs.

Acknowledgements This research was partially supported by JSPS KAKENHI Grant Number (C) 26450145, and Prof. Y. Uozumi's JST ACCEL program. We also thank Meiji Seika Pharma Co., Ltd. for funding this work.

References

1. D. P. Curran, S. Hadida, M. He, *J. Org. Chem.,* **1997**, *62*, 6714.
2. D. P. Curran, "A User's Guide to Light Fluorous Chemistry," in *The Handbook of Fluorous Chemistry*, J. Gladysz, I. Horváth, D. P. Curran, Wiley-VCH: Weinheim, **2004**, pp 128-155.
3. D. P. Curran, "Separations with Fluorous Silica Gel and Related Materials," in *The Handbook of Fluorous Chemistry*, Gladysz, J.; Horváth, I.; Curran, D. P., Wiley-VCH: Wienheim, **2004**, pp 101-127.
4. Z. Y. Luo, J. Williams, R. W. Read, D. P. Curran, *J. Org. Chem.,* **2001**, *66*, 4261.
5. D. P. Curran, M. Amatore, D. Guthrie, M. Campbell, E. Go, Z. Y. Luo, *J. Org. Chem.,* **2003**, *68*, 4643.
6. D. P. Curran, C. Ogoe, *QSAR Comb. Sci.*, **2006**, *25*, 732.
7. S. Rover, P. Wipf, *Tetrahedron Lett*., **1999**, *40*, 5667.
8. L. Liu, N. L. Pohl, *Org. Lett.*, **2011**, *13*, 1824.
9. f-Boc-ON, f-Cbz-OSu, and f-TIPS analog are commercially available from Aldrich: Product numbers: 55118, 14944, and 04537.
10. W. F. J. Hogendorf, L. N. Lameijer, T. J. M. Beenakker, H. S. Overkleeft, D. V. Filippov, J. D. C. Codée, G. A. Van der Marel, *Org. lett*., **2012**, *14*, 848.
11. Z. Luo, Q. Zhang, Y. Oderaotoshi, D. P. Curran, *Science,* **2001**, *291*, 1766.
12. Review see: C. Najera, *Synlett*, **2002**, 1388.
13. J. W. Perich, R. B. Johns, *Tetrahedron Lett*. **1988**, *29*, 2369.
14. M. Matsugi, K. Yamanaka, I. Inomata, N. Takekoshi, M. Hasegawa, D. P. Curran, *QSAR Comb. Sci.* **2006**, *25*, 713.
15. Selected example see: J. Masllorens, S. Bouquillon, A. Roglans, F. Henin, J. Muzart, *Organomet. Chem.,* **2005**, *690*, 3822.
16. L. A. Carpino, *J. Org. Chem.,* **1980**, *45*, 4250.
17. Y. Sugiyama, N. Endo, K. Ishihara, Y. Kobayashi, H. Hamamoto, T. Shioiri, M. Matsugi, *Tetrahedron,* **2015**, *71*, 4958.
18. R. Knorrl, A. Trzeciak, W. Bannwarth, D. Gillessen, *Tetrahedron Lett*., **1989**, *30*, 1927.
19. P. G. M. Wuts, in *Green's Protective groups in Organic Synthesis Fifth Edition* (ed: P. G. M. Wuts), John Wiley & Sons, Inc., Hoboken, New Jersy, 2014, pp 770–774.

20. Analytical and preparative f-HPLC were conducted by Fluoro*Flash*® columns purchased from Fluorous Technologies Inc. Fluorous columns (Wakopak® Fluofix-II 120E) having almost same separation ability are available from Wako Pure Chemical Industries, Ltd.
21. Y. Sugiyama, M. Hirose, J. Matsui, N. Endo, H. Hamamoto, T. Shioiri, M. Matsugi, *Synlett*, **2013**, *24*, 2701.
22. S. Miyoshi, H. Ishikawa, T. Kaneko, F. Fukui, H. Tanaka, S. Maruyama, *Agric. Biol. Chem.,* **1991**, *55*, 1313.
23. For representative examples, see: C. C. Thornburg, M. Thimmaiah, L. A. Shaala, A. M. Hau, J. M. Malmo, J. E. Ishmael, D. T. A. Youssef, K. L. McPhail, *J. Nat. Prod.* **2011**, *74*, 1677.
24. J. Ogino, R. E. Moore, G. M. L. Patterson, *J. Nat. Prod.*, **1996**, *59*, 581.
25. A. Bertram, G. Pattenden, *Synlett*, **2000**, 1519.
26. Z. Xia, C. D. Smith, *J. Org. Chem.*, **2001**, *66*, 3459.
27. S-L. You, J. W. Kelly, *J. Org. Chem.*, **2003**, *68*, 9506.
28. Y. Yonezawa, N. Tani, C-G. Shin, *Heterocycles*, **2005**, *65*, 95.
29. T. Matsumoto, E. Morishita, T. Shioiri, *Tetrahedron*, **2007**, *63*, 8571.
30. S. You, S. Deechongkit, J. W. Kelly, *Org. Lett.,* **2004**, *6*, 2627.
31. Fluorous silica gel (Fluoro*Flash*® Silica Gel, 40 μm), available from SIGMA-ALDRICH®, was used for all FSPE process.
32. D. P. Curran, Y. Oderaotoshi, *Tetrahedron,* **2001**, *57*, 5243.
33. M. Matsugi, S. Nakamura, Y. Kunda, Y. Sugiyama, T. Shioiri, *Terahedron Lett.,* **2010**, *51*, 133.
34. H. Takahashi, N. Endo, H. Takanose, Y. Sugiyama, F. Eguchi, K. Oguri, H. Hamamoto, T. Shioiri, M. Matsugi, *Eur. J. Org. Chem.* **2015**, 3971.

A Challenging Synthesis of the Highly Functionalized Echinocandin ASP9726: A Successor of Micafungin—How Can We Achieve the Large-Scale Synthesis?

Shinya Yoshida, Joji Hayashida, Yasuhiro Morinaga, Shoji Mizobata, Akihiro Okada, Kazumi Kawai, Shinjirou Tanoue, Tomohide Nakata, Minoru Kitayama, Atsushi Ohigashi, Mitsutaka Matsuura, Takumi Takahashi, Shigeru Ieda and Minoru Okada

Abstract Here, we describe a challenging scale-up synthesis of the highly functionalized echinocandin ASP9726 (**1**) starting from the natural product FR901379 (**3**), the same raw material of micafungin (**2**). The synthesis demanded various difficult chemoselective transformations due to the complexity and the unique property of the cyclic poly-peptide core. In the present study, we discovered an efficient, high-yielding route to ASP9726 (**1**) that is suitable for large-scale production. Namely, dehydration of carboxamide (**13**) to nitrile (**14**) was accomplished by the use of EDC・HCl with pyridine. Further, the sequential nitrile reduction and debenzylation was succeeded with Sponge Nickel- Pd/Ccatalyst mixed catalyst condition. Reductive amination between primary amine (**16**) with dihydroxyacetone (DHA) was accomplished using 2-picoline borane complex in MeOH, yielding 66.6 kg of peptide core unit (**17**). After the palmityl chain cleavage by bioconversion, the coupling between the core peptide unit (**18**) and side chain (**9**) was achieved by *tert*-butyl amine borane complex. Consequently, highly pure ASP9726 (**1**) was obtained in a practical manner without using silica gel or ODS column

S. Yoshida (✉) · J. Hayashida · Y. Morinaga · S. Mizobata · T. Nakata · A. Ohigashi · S. Ieda · M. Okada
Process Chemistry Labs., Astellas Pharma Inc., 160-2 Akahama, Takahagi-shi, Ibaraki 318-0001, Japan
e-mail: shinya.yoshida@astellas.com

A. Okada
Drug Discovery Research, Astellas Pharma Inc., 21, Miyukigaoka, Tsukuba-shi, Ibaraki 305-8585, Japan

K. Kawai · S. Tanoue · M. Kitayama · M. Matsuura
Fermentation and Biotechnology Labs., Astellas Pharma Inc., 5-2-3, Tokodai, Tsukuba-shi, Ibaraki 300-2698, Japan

T. Takahashi
Technology Product Management, Astellas Pharma Inc., 2-5-1, Nihonbashi-Honcho, Chuo-ku, Tokyo 103-8411, Japan

K. Tomioka et al. (eds.), *New Horizons of Process Chemistry*,
DOI 10.1007/978-981-10-3421-3_16

chromatography purification in any step. The number of step was reduced to 10-steps from 14-steps and the overall yield was drastically increased to 13.8% from 0.71% in comparison with the prior synthesis.

Keywords ASP9726 · Highly functionalized echinocandin · A successor of micafungin · Scale-up synthesis

1 Introduction

ASP9726 (**1**) is expected to be a successor of micafungin (**2**), which was launched by Astellas Pharma Inc. in 2002 (Fig. 1). ASP9726 (**1**) has shown the potent efficacy in the treatment of systemic candidiasis and aspergillosis without detectable concerns of the side effects [1]. Because of the highly functionalized peptide core unit of **1**, the preparation required the significant synthetic challenges, particularly in the chemoselectivity as well as the physical property. Chemical reactions with the natural product FR901379 (**3**) [1f, 2], a starting material of micafungin [1] and its derivatives, also present numerous processing issues related to the inherent nature of these lipopeptides (e.g. poor solubility in organic solvents, micellar and soap-like behavior, hygroscopicity in the solid state, and instability to both strong acid and strong base).

Under these difficult circumstances, medicinal chemists successfully synthesized a lab-scale of the target product **1** from **3** (Scheme 1). However, there were several drawbacks in the method for further scale-up manufacturing.

Drawbacks of the medicinal chemistry synthetic method

- Inefficient protection & deprotection steps
- Long sequence and poor yield: 14-steps, 0.71% yield
- Expensive ODS column chromatography: 14-times
- Toxic reagent use: $NaBH_3CN$

Therefore, the development of more efficient and practical approach was essential.

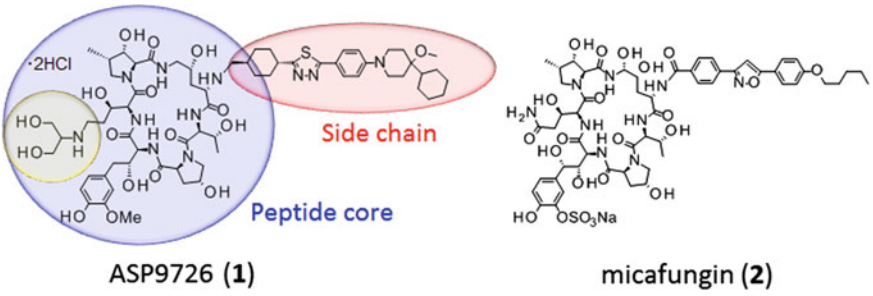

Fig. 1 Structure of ASP9726 (**1**) and micafungin (**2**)

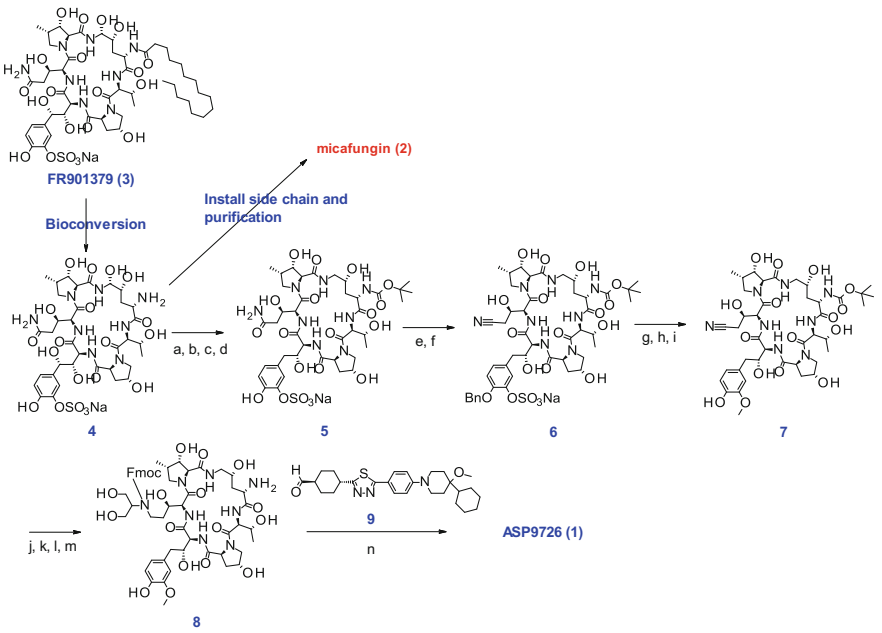

Scheme 1 Medicinal chemistry synthetic method for ASP9726 (**1**). Reagents and conditions: (a) benzyl chloroformate, THF, pH 6.86 standard buffer solution, ODS column chromatography, 68%; (b) Et_3SiH, TFA, CH_2Cl_2, ODS column chromatography, 45%; (c) H_2, Pd/C, H_2O, ODS column chromatography, 73%; (d) $(Boc)_2O$, NaOH, H_2O, 1,4-dioxane, ODS column chromatography, 88%; (e) BnBr, $LiOH{\cdot}H_2O$, DMF, ODS column chromatography, 85%; (f) MsCl, $NaHCO_3$, *i*-Pr_2NEt, zeolite, DMF, ODS column chromatography, 41%; (g) 10% HCl-MeOH, MeOH, ODS column chromatography; 86%; (h) MeI, $LiOH{\cdot}H_2O$, DMF, ODS column chromatography, 76%; (i) H_2, Pd/C, MeOH, ODS column chromatography, quant.; (j) $NaBH_4$, $CoCl_2$-$6H_2O$, MeOH, H_2O, ODS column chromatography, 85%; (k) dihydroxyacetone (DHA), $NaBH_3CN$, AcOH, ODS column chromatography, 73%; (l) Fmoc-Cl, *i*-Pr_2NEt, DMF, ODS column chromatography, 46%; (m) TFA, Et_3SiH, CH_2Cl_2, ODS column chromatography, 83%; (n) **10**, $NaBH_3CN$, AcOH, MeOH, DMF, $CHCl_3$, then piperidine, ODS column chromatography; 67%. Overall yield: 0.71%

2 Results and Discussion

2.1 New Synthetic Strategy

In order to overcome the issues in the medicinal method, we made a new synthetic strategy shown in Scheme 2 [3].

First, we aimed to utilize the $C_{15}H_{31}$ side chain of **3** as a useful protective group of the primary amine. This plan allowed us to avoid the inefficient protection/deprotection operations. In addition, the direct reduction of the carboxyamide **13** to the amine **15** would shorten one further step. However, we predicted that this chemoselective transformation would be highly ambitious due to the presences of numerous other amides. Therefore, we also prepared a back-up plan,

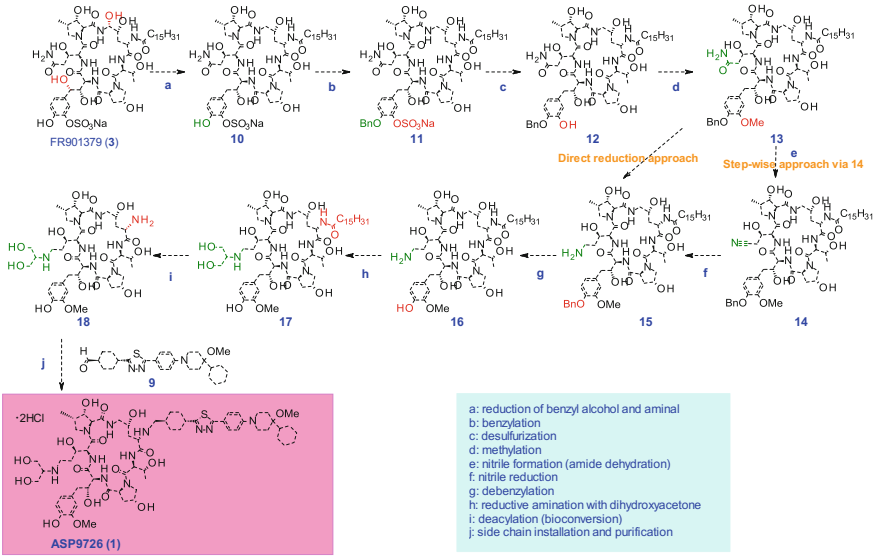

Scheme 2 New approach for the synthesis of ASP9726

which is a stepwise approach via nitrile **14**. Once the amine **15** is obtained, debenzylation and reductive amination with dihydroxyacetone (DHA) should afford the peptide core unit **17**. In the end of process, bioconversion would remove the palmityl group, and the coupling with a thiadiazole side chain **9** [4] should form the crude target compound. Finally, the purification and the hydrochloride salt formation would give the desired ASP9726 (**1**). With this strategy in our hands, we started the process development, so the details are described as follows.

2.2 *Challenging Direct Reduction of Amide to Primary Amine*

The synthesis of carboxyamide **13** was accomplished via reduction of benzyl alcohol and aminal moieties followed by benzylation, desulfurization and methylation using our previous process [1]. Next we attempted to reduce the carboxyamide **13** to access the amine **15** directly. The most common reducing agents such as borane complexes, ionic aluminums, and boron hydride described in the Table 1 afforded a little amount of the target amine **15**. Because of the detections of many unknown impurities, we tried to conduct the reactions at lower temperature as well as Leonard's BSTFA and $BH_3 \cdot THF$ combination method [5]. Unfortunately, all of our efforts did not give satisfactory results. Presumably, these were probably caused by the competitive reductions between the desired primary amide moiety and numerous others. Given these findings, we realized that this direct approach

Table 1 Direct reduction of amide to primary amine[a]

Entry	Conditions	HPLC yield of amine **15** (%)
1	Red-Al/THF-toluene	3
2	DIBAL-H/THF	5
3	$LiAlH_4$/THF	1
4	BH_3 • THF complex/THF	1
5	BH_3 • $S(CH_3)_2$ complex/THF	2
6	$CoCl_2/NaBH_4$/THF	16
7	BSTFA then BH_3 • THF/THF	14

[a]Reaction temp.: −30 to 25 °C

was not suitable for our system. Therefore, we decided to investigate our back-up plan, which is the formation of nitrile **14** followed by the reduction.

2.3 Stepwise Approach to Primary Amine

2.3.1 Nitrile Formation

In the medicinal method, the nitrile **6** was prepared in 41% yield by using MsCl, $NaHCO_3$ and *i*-Pr_2NEt. Applying this condition to amide **13** was found to be problematic for large-scale synthesis because of the decomposition of **13** and nitrile **14**. To optimize this transformation, the screening of dehydration reagents was conducted (Table 2). As a result, cyanuric chloride in DMF (Entry 2) [5], Vilsmeier reagent in DMF (Entry 5) or NMP (Entry 6) gave the moderate yield. However, utilizing these reaction conditions in a large-scale manufacturing has three critical concerns described below.

Table 2 Dehydration of amide **13** to nitrile **14**[a]

Entry	Reagents	HPLC area% amide/nitrile/others
1	MsCl (1.1 eq), $NaHCO_3$ (1.1 eq), *i*-Pr_2NEt (1.1 eq.), Zeolite/DMF	5/56[b]/39
2	Cyanuric chloride (2.5 eq)/DMF	2/67/31
3	Cyanuric chloride (2.5 eq)/DMF, water (250 mol%)	No reaction
4	Cyanuric chloride (2.5 eq)/NMP	No reaction
5	Vilsmeier reagent (2.5 eq)/DMF	2/65/33
6	Vilsmeier reagent (2.5 eq)/NMP	5/64/31
7	Dichlorotriazine (2.5 eq)/DMF	70/25/5
8	$(COCl)_2$(3.0 eq), pyridine (6.0 eq)/DMF	11/58/31

[a]Reaction temp.; −30 °C to rt
[b]Isolated yiled: 41%

Table 3 Screening of coupling agents[a]

Entry	Reagents	HPLC area% amide/nitrile/others
1	EDC·HCl	2/72/26
2	CIP	56/27/17
3	TFFH	31/10/59
4	DEPBT	73/2/25
5	HATU	No reaction
6	PyBop	No reaction
7	DPPA	No reaction
8	CMPI	No reaction
9	T3P®	No reaction
10	^{i}BuOC(= O)Cl	No reaction
11	CDMT	No reaction

[a]Reagent: (10 eq), Pyridine (×28 mol), NMP (×7 vol/wt.), rt to 50 °C, 24–27 h

- The requirement of very slow addition of reagent
- The avoidance of hot spot formation during slow addition
- The robustness of the reaction results.

Because the Vilsmeier type reagents seemed to be too reactive to control the reaction heat, we aimed to regulate it with milder dehydration conditions. Therefore, various kinds of peptide coupling reagents were screened (Table 3). As a result, we were pleased to find that the combination of EDC • HCl and Py afforded the desired nitrile **14** in 72% yield area with minimum amount of impurities (Entry 1). Interestingly, generally more reactive coupling reagents like PyBop and HATU were not effective for the reaction at all probably due to the steric hindrance of these reagents (Entries 5 and 6).

2.3.2 Catalytic Hydrogenation of Nitrile to Amine

Now that the primary amide **13** was successfully converted into the nitrile **14**, we attempted to transform it to the amine **15**. Originally, the reduction was performed in the catalytic Rh/Al_2O_3 hydrogenation condition [6] (Table 4, Entry 1). However, we noticed three obvious drawbacks for the scale-up synthesis.

- The use of expensive reagent: Rh/Al_2O_3
- The robustness of the reaction results
- The poorness of the yield: 45%

In order to solve these issues, the intensive catalyst screening was attempted (Table 4). The use of Pt/C and Raney Ni afforded the desired amine in the moderated yield (Entries 1 and 2). On the other hands, various types of Pd/C catalysts [7] gave only debenzylated undesired product with intact nitrile moiety (Entries 4 to 7). To our surprised, Sponge Nickel NDHT-90 [8] purchased from Kawaken

Table 4 Hydrogenation of nitrile to amine[a]

Entry	Catalysts	HPLC area% nitrile/amine
1	5% Rh/Al_2O_3	22/48, 45% yield (existing method)
2	Pt/C	Hydrolysis of nitrile occurred, 48% yield.
3	Raney Ni (Aldrich)	23/75
4	Pd/C (K-type)	Debenzylation occurred without touching nitrile
5	Pd/C (P-type)	↑
6	Pd/C (NX-type)	↑
7	Pd/C (STD-type)	↑
8	Sponge Cobalt ODHT-60	85/15
9	Sponge Nickel NDT-90	34/66
10	Sponge Nickel NDHT-90 (Kawaken Fine Chemicals)	4/96

[a]Solvent: EtOH/NH_3aq. = 10/1, hydrogen pressure: 43–58 psig, 40 °C, 8–9 h

Fine Chemicals allowed the remarkably clean conversion to the desired amine **15**. After optimizing the reaction conditions such as temperature, hydrogen pressure and the ammonia concentration in aqueous ethanol, the yield was improved over 90% (Entry 10).

Now that the problematic reduction step was solved, we decided to try more economical method. At the beginning of our study, the amine **15** was isolated as amorphous solid, and then exposed to the deprotection condition to form the phenol **16**. In order to raise the operation efficiency, we attempted the one-pot procedure, which is Sponge Nickel NDHT-90 mediated nitrile reduction followed by Pd/C catalyzed debenzylation without separating the metal catalysts. Fortunately, this sequential benzyl removal process cleanly completed within 1 h to give the desired phenol **16**. This highly practical and reproducible method was successfully demonstrated 63.0 kg scale synthesis of the intermediate **16** as a HCl salt.

2.3.3 Reductive Amination with Dihydroxyacetone

With the free amine **16** in our hand, the installation of the diethanolamine moiety was investigated.

In the medicinal chemistry synthetic method, reductive amination of the primary amine with dihydroxyacetone was conducted with $NaBH_3CN$. However, in the manufacturing scale, the use of this reagent should be avoided from the safety concern due to the notorious hydrogen cyanide generation. Furthermore, the crude diol **17** was purified by economic unfriendly ODS column chromatography. To solve these defects, we started optimizing the transition metals mediated hydrogenation conditions. After screening various catalysts including Pd/C, Pt/C, Raney Ni, Sponge Nickel NDHT-90, and Sponge Cobalt OFT-55, we found the reaction

with Pt/C afforded the desired diol **17** over 90% based on HPLC area. However, chemistry for scaling up is not as trivial as it sounds. In the large-scale trial batch, we faced to the unexpected troubles, the delay of the reaction as well as the decomposition of the product. Eventually we realized that this hydrogenation approach did not suit for our scale-up synthesis of **17**.

Does Hydride Reduction Work Well?

In order to overcome this crisis, we decided to revisit the hydride reduction conditions. Monitoring the reaction with $NaBH(OAc)_3$ in DMF revealed that the formation of desired diol **17** was competed with the degradation of it (Fig. 2).

Under the chaos situation, a hypothesis appeared in our brains as described below.

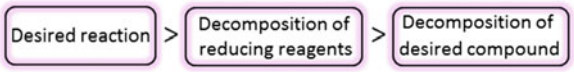

Desired reaction would proceed prior to decomposition of reducing reagents, and decomposition of reducing reagents would proceed prior to decomposition of

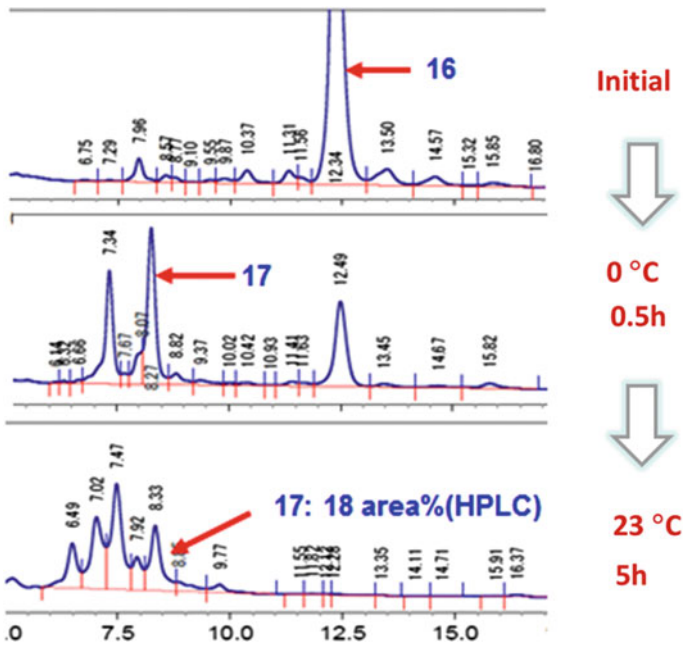

Fig. 2 HPLC chromatograms of reductive amination with $NaBH(OAc)_3$ in DMF

Table 5 Screening of reducing agents for reductive amination[a]

Entry	Reducing agent	**16/17**/others (HPLC area%)	Comments
1	$NaBH(OAc)_3$	ND/80/20	Excess of $NaBH(OAc)_3$ was necessary
2	Pyridine borane	ND/90/10	Unstable and safety operation issues
3	2-Picoline borane	ND/92/8	The best condition
4	5-ethyl-2-methylpyridine borane	10/67/23	Not completed and impurities were observed
5	Triethylamine borane	23/50/27	↑
6	*t*-$BuNH_2$ borane	33/41/26	↑

[a]MeOH solvent; reaction temp: −5 to 25 °C

product. If we could find the ideal reaction condition, the desired reaction would proceed cleanly.

With this hypothesis in our mind, we attempted a reaction with $NaBH(OAc)_3$ in MeOH (Table 5, Entry1) under the concise control of hydrogen generation, because an excessive amount of hydride would be quenched by MeOH. To our delight, the desired reaction cleanly proceeded to form the diethanolamine **17** in 80% yield. Now that we finally obtained a positive sign of breakthrough, the optimization of reducing reagents was conducted (Table 5). The borane complexes with aromatic amines such as pyridine [9] or 2-picoline [10] gave even the superior yields, 90 and 92% respectively (Entries 2 and 3). On the contrary, the ones with aliphatic amines such as trimethylamine or *t*-buthyl amine showed the inferior results (Entries 5 and 6). Interestingly, from the comparison between 2-picoline and 5-ethyl-2-methylpyridine [11], the fine tuning of electrical property of amine ligands is crucial for this reaction (Entries 3 and 4). At the end, we selected 2-picoline borane complex from safety point of view [10]. As a result, this reductive amination method achieved 66.6 kg synthesis of the diol **17** as a HCl salt.

2.4 End Game Process

Now that the modification of the peptide core unit of ASP9726 was completed, the remained transformation is to switch the palmityl group into a thiadiazole **9**, which was prepared with 9 steps sequence developed by our group [4]. First, the bioconversion applied to cleave the $C_{15}H_{31}$ side chain without any troubles [12]. Next, the reductive amination of the peptide core **18** and **9** with *t*-$BuNH_2 \cdot BH_3$ proceeded smoothly. Finally, the column purification followed by the hydrochloride salt formation afforded ASP9726 (**1**) with the applicable high quality.

3 Conclusion

A challenging synthesis of the highly functionalized echinocandin ASP9726 (**1**) was accomplished. **1** was prepared in an efficient and scalable method from fermentation product **3** in 10 steps and 13.8% overall yield. The production efficiency was dramatically improved in comparison with the initial medicinal chemistry procedure, 14 steps and 0.71% yield. The synthesis features that only proper reagents as well as finely tuned reaction conditions allowed to advance the sequence in chemoselective manner due to the complexity and instabilities of the intermediates. For instance, the formation of the primary amine **15** was achieved by the dehydration of nitrile with EDC•HCl in pyridine followed by hydrogenation with Sponge Ni NDHT-90 catalyst. The installation of the diethanolamine moiety was conducted under 2-picoline borane/MeOH condition. The coupling of the peptide core **18** and the thiadiazole side chain **9** succeeded under *t*-BuNH_2 borane mediated reductive amination. Finally, the practical purification and precipitation methods developed during the course of this study afforded pure ASP9726 (**1**).

Acknowledgements We would like to thank Dr. Masaki Tomishima, Dr. Natsuko Kayakiri and Mr. Hiroshi Morikawa for their helpful discussions about the medicinal synthetic method for **1**. We also appreciated Dr. Tatsuhiro Tokunaga for meaningful advice of NMR study.

References

1. (a) Tawara, S.; Ikeda, F.; Maki, K.; Morishita, Y.; Otomo, K.; Teratani, N.; Goto, T.; Tomishima, M.; Ohki, H.; Yamada, A.; Kawabata, K.; Takasugi, H.; Sakane, K.; Tanaka H.; Matsumoto, F.; Kuwahara, S. *Antimicrob. Agents Chemother.* **2000**, *44*, 57. (b) Ikeda F.; Wakai Y.; Matsumoto, S.; Maki K.; Watabe E.: Tawara, S.; Goto, T.; Watanabe Y.; Matsumoto, F.; Kuwahara, S. *Antimicrob. Agents Chemother*. **2000**, *44*, 614. (c) Matsumoto, S.; Wakai Y.; Nakai T.; Hatano, K.; Ushitani T.; Ikeda F.; Tawara, S.; Goto, T.; Matsumoto, F.; Kuwahara, S. *Antimicrob. Agents Chemother*. **2000**, *44*, 619. (d) Hatano, K.; Morishita, Y.; Nakai, T.; Ikeda, F. *J. Antibiot.* **2002**, *55*, 219. (e) Tomishima, M.; Ohki H.; Yamada A.; Takasugi H.; Maki K.; Tawara S.; Tanaka, H. *J. Antibiot*. **1999**, *52*, 674. (f) Morikawa, H.; Tomishima, M.; Kayakiri, N.; Araki, T.; Barrett, D.; Akamatsu, S.; Matsumoto, S.; Uchida, S.; Naka, T.; Takeda, S.; Maki, K. *Bioorganic and Medicinal Chem. Lett.*, **2014**, *24*, 1172.
2. (a) Boeck, L. D.; Fukuda, D. S.; Abbott, B. J.; Debono, M. *J. Antibiot.* **1989**, *42*, 382; (b) Debono, M.; Abbott, B. J.; Fukuda, D. S.; Barnhart, M.; Willard, . K. E.; Molloy, R. M.; Michel, K. H.; Turner, J. R.; Butler, T. F.; Hunt, A. H. *J. Antibiot.* **1989**, *42*, 389.
3. Yoshida, S.; Hayashida, J.; Morinaga, Y.; Mizobata, S.; Okada, A.; Kawai, K.; Tanoue, S.; Nakata, T.; Kitayama, M.; Ohigashi, A.; Matsuura, M.; Takahashi, T.; Ieda, S. and Okada M. *Org. Process Res. Dev.*, **2014**, *18*, 725.
4. Yoshida, S.; Ohigashi, A.; Morinaga, Y., Hashimoto, H.; Takahashi, Y.; Ieda, S.; Okada, M. *Org. Process Res. Dev.*, **2013**, *17*, 1252.
5. (a) Leonard, Jr., W. R; Belyk, K. M.; Conlon, S.A.; Bender, D. R.; DiMichele, L. M; Liu, J.; Hughes, D. L. *J, Org. Chem.*, **2007**, *72*, 2335. (b) Journet, M.; Cai, D.; DiMichele, L. M.; Hughes, D. L.; Larsen, R. D.; Verhoeven, T. R.; Reider, P. J. *J, Org. Chem.*, **1999**, *64*, 2411.

6. Kwang-Chung, L.; Yen-Shih, T.; Hao-Ling, F. *US20100168415A1*.
7. Pd catalysts (Kawaken Fine Chemicals Co., Ltd.) http://www.kawakenfc.co.jp/en/products/fine/index.php/search?list=1&cell003=+Precious+Metal+Catalysts&cell030=&keyword=.
8. Nickel catalysts (Kawaken Fine Chemicals Co., Ltd.) http://www.kawakenfc.co.jp/en/products/fine/index.php/search?list=1&cell003=Sponge+Nickel&cell030=&keyword=.
9. (a) Pelter, A.; Rosser, R.M. *J. Chem. Soc. Perkin Trans. I*, **1984**, 717. (b) Bomann, M. D.; Guch, I. C.; DiMare, M. *J. Org. Chem.*, **1995**, *60*, 5995. (c) Moormanna, A. E. *Synthetic Communications*, **1993**, *23*, 789.
10. (a) Cosenza, V. A.; Navarro, D. A.; Stortz, C. A. ARKIVOC 2011 (vii) 182. (b) Ruhaak, L. R.; Steenvoorden, E.; Koeleman, C. A. M.; Deelder, A. M.; Wuhrer, M. *Proteomics.* **2010** *10*, 2330. (c) Sato, S.; Sakamoto, T.; Miyazawa E.; Kikugawa, Y. *Tetrahedron*, **2004**, *60*, 7899. (d) Kawase, Y.; Yamagishi, T.; Kutsuma, T.; Ueda, K.; Iwakuma, T.; Nakata, T.; Yokomatsu, T. *Heterocycles*, **2009**, *78*, 463. (e) https://www.junsei.co.jp/upfile/topics/52/52-2.pdf.
11. Matos, K; Burkhardt, E. R. *Pharmaceutical process chemistry section 6, Direct Reductive Amination with Amine Boranes*, **2011**, 127.
12. Ueda S, Kinoshita M, Tanaka F, Tsuboi M, Shimizu S, Oohata N, Hino M, Yamada M, Isogai Y, Hashimoto S. *J. Biosci. Bioeng.* **2011**, 112, 409.

The Role of Silyl Protecting Group for the Synthesis of Procyanidins and Their Derivatives

Noriyuki Nakajima and Akiko Saito

Abstract The intramolecular [4–8] coupling of silyl-protected catechin and epicatechins is examined. Coupling reaction of silyl-protected epicatechin/catechin, epicatechin/epicatechin, catechin/catechin and catechin/epicatechin worked well to afford the corresponding dimers with excellent selectivity and yield. The series of procyanidin B analogues synthesis are achieved. We also carried out the synthesis of 3-*O*- and/or 5-*O*-acyl-catechin and epicatechin derivatives on a gram scale.

Keywords Condensed tannin · Oligomeric flavonoid · Synthesis · Protecting group

1 Introduction

Procyanidins are an important class of natural products [1, 2], and show interesting various biological activity [3–16]. Many synthetic research have been developed to obtain procyanidins and their derivatives in pure state [17–29]. In such research, phenolic hydroxyl group have been commonly protected by benzyl (Bn) groups. In 1968, Weinges reported benzyl protected catechin for the 3-glucosyl and 3-galloyl catechin synthesis [30]. Bn protection carried out with benzyl-halide (chloride, bromide) and base such as K_2CO_3, Na_2CO_3, Cs_2CO_3, $NaHCO_3$, DBU, NaH, Et_3N, and Hünig's base in various solvents such as DMF, acetone, EtOAc, water, and EtOAc/water with and without phase transfer catalyst (nBu_4NI) at room tempera-

N. Nakajima (✉)
Biotechnology Research Center and Department of Biotechnology, Toyama Prefectural University, 5180 Kurokawa, Imizu, Toyama 939-0398, Japan
e-mail: nori@pu-toyama.ac.jp

A. Saito
Graduate School of Engineering, Osaka Electro-communication University (OECU), 18-8 Hatsu-cho, Neyagawa-shi, Osaka 572-8530, Japan
e-mail: a-saito@isc.osakac.ac.jp

K. Tomioka et al. (eds.), *New Horizons of Process Chemistry*,
DOI 10.1007/978-981-10-3421-3_17

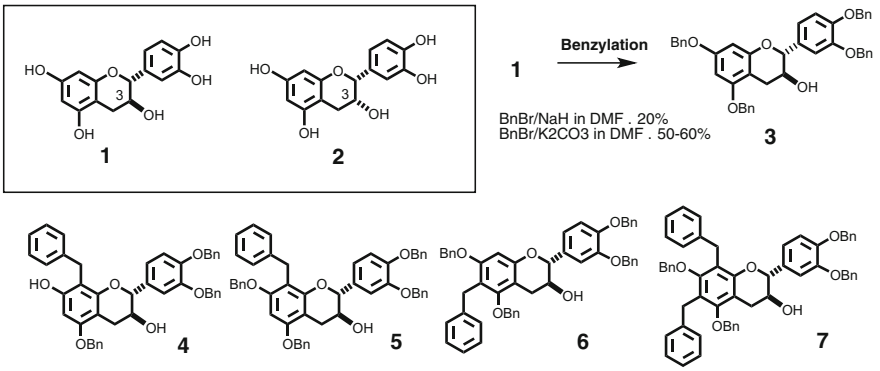

Fig. 1 Benzylation reaction of (+)-catechin (**1**) and obtained by-products (**4**-**7**)

ture, at moderate temperature (40–45 °C), or at reflux temperature. However, the benzyl protection process is low yield because of the by-products (**4**–**7**) formation as shown in Fig. 1 [31, 32]. We report here the synthesis of procyanidin derivatives to play a role of silyl-protecting group (*tert*-butyldimethylsilyl: TBS).

2 Procyanidins Synthesis Incorporating a TBS Protecting Group

2.1 Synthesis of 3-O-Acyl-Catechin [33]

TBS protection of (+)-catechin (**1**) and (−)-epicatechin (**2**) proceeded with TBS-Cl and imidazole in THF/CH_2C_{l2} afford 5,7,3′,4′-tetra-TBS (+)-catechin (**8**) and 5,7,3′,4′-tetra-TBS (−)-epicatechin (**10**) in 95 and 46% yields, respectively. TBS-protection was able to perform on hundred-gram scales within three hours. Purification of product was carried out by SiO_2 short column chromatography.

We first achieved the synthesis of 3-*O*-acyl-catechin (**9**) and 3-*O*-acyl-epicatechin derivatives (**11**) with unsaturated fatty acid esters on a gram scale (Scheme 1). The coupling of **1** and **2** with unsaturated fatty acid (oleic acid, linoleic acid, α-linoleic acid) were carried out with DCC, DMAP in CH_2Cl_2 at 0 °C. After stirring for 6–12 h at room temperature, desired pure esters were obtained in quantitative yield after silica gel column purification. Four TBS protecting groups were removed by tetra-*n*-butylammonium fluoride (TBAF, 4.8 eq.) in the presence of AcOH (6.0 eq.) in THF to give 3-*O*-acyl-catechin (**9a**–**9c**) in 65, 55, and 56%, respectively. 3-*O*-acyl-epicatechins (**11a**–**11c**) were also synthesized in 26–31% yield.

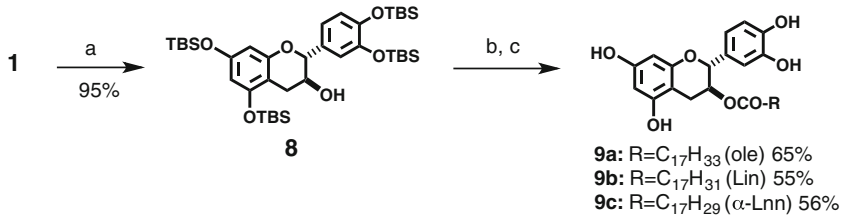

Reagents and Conditions: (a) TBSCl (4.4 eq), Imidazole (8.8 eq), THF/CH_2Cl_2 = 3/1 (b) Acid (2 eq), DCC (2 eq), DMAP (0.4 eq), CH_2Cl_2 (0.01 M) (c) TBAF (4.8 eq), AcOH (6 eq), THF.

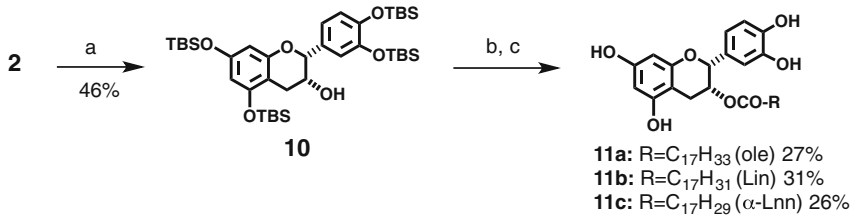

Reagents and Conditions: (a) TBSCl (4.4 eq), Imidazole (8.8 eq), THF/CH_2Cl_2 = 3/1 (b) Acid (2 eq), DCC (2 eq), DMAP (0.4 eq), CH_2Cl_2 (0.01 M) (c) TBAF (4.8 eq), AcOH (6 eq), THF.

Scheme 1 Synthesis of 3-*O*-acyl-catechins and 3-*O*-acyl-epicatechins

2.2 *Synthesis of Procyanidin Dimers [34]*

Dichloro-dicyano-benzoquinone (DDQ) oxidation at the C_4 position of **8** and **10** with ethoxyethanol (EE) in CH_2Cl_2 afforded electrophiles **12** and **14** in 65 and 64% yields, respectively. The electrophiles were acetylated to give acetates **13** and **15** in 100 and 78% yields, respectively (Scheme 2).

The intramolecular [4–8] coupling of epicatechin electrophile (**10**) and catechin nucleophile (**13**) is examined with $SnCl_4$ at 0 °C. Coupling reaction proceeded smoothly to give only 3,4-*trans* dimmer **16** in 98% yield. This finding encouraged us to investigate alternative combinations of nucleophile and electrophile. The

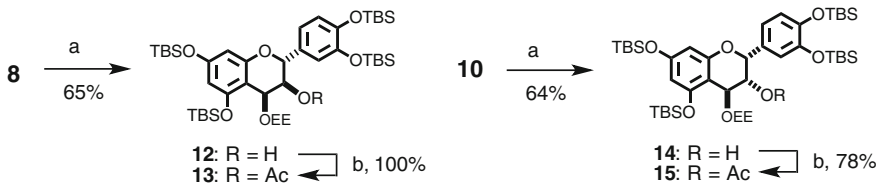

Reagents and Conditions: (a) 2-Ethoxyethanol (20 eq), DDQ (2 eq), CH_2Cl_2, rt, 18 h, (b) AcOH (2 eq), DCC (2 eq), DMAP (0.4 eq), CH_2Cl_2, rt.

Scheme 2 Synthesis of silyl-catechin and silyl-epicatechin electrophiles

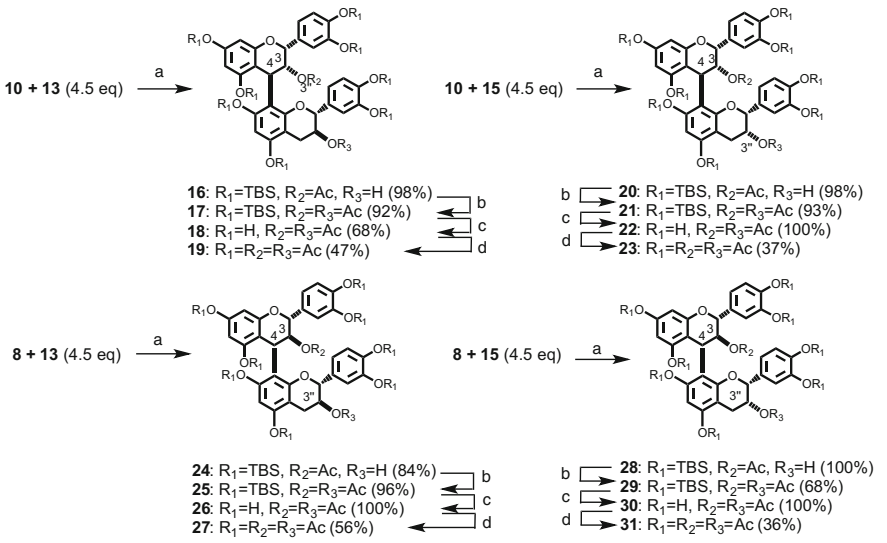

Scheme 3 Synthesis of procyanidin B analogues

intermolecular epicatechin-epicatechin, catechin-catechin, and catechin-epicatechin condensations using $SnCl_4$ worked well (Scheme 3). In all cases, the coupling reaction afforded the corresponding 3,4-*trans* products, **20**, **24**, and **28** in 98, 84, and 100% yields, respectively.

After acetylation of each C-3″ hydroxy group, the eight-TBS protecting groups of **17**, **21**, **25**, and **29** were removed with TBAF and AcOH in THF to give **18**, **22**, **26,** and **30** in 68–100% yields. All the spectral data [NMR, IR, MS] of the

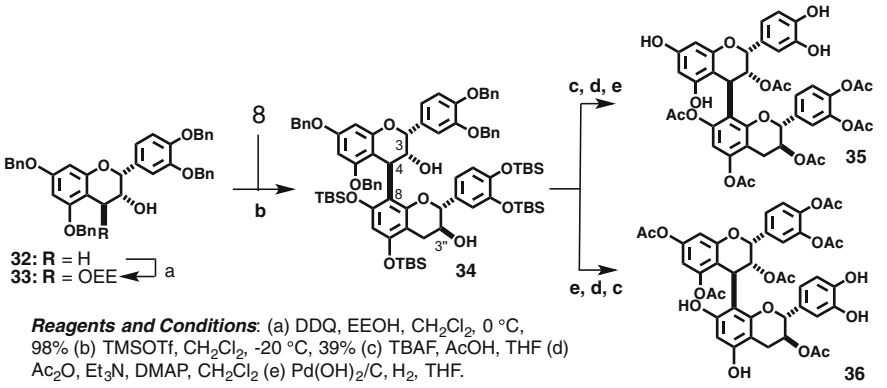

Scheme 4 Synthesis of acetylated procyanidin B1 analogs

corresponding decaacetyl-procyanidins (**19, 23**, **27,** and **31**), were identical to those of authenticated samples.

Demonstrated TBS-protection method is effective for the acetylated procyanidin analogs synthesis (**35** and **36**) as shown in Scheme 4. When the electrophile (**33**) derived from epicatechin (**2**) was condensed with the TBS protected nucleophile (**8**) in the presence of TMSOTf as a catalyst, the dimeric compound (**34**) was obtained in 39% yield. Deprotection of TBS groups first by TBAF followed by acetylation of phenolic groups and aliphatic hydroxyl groups and hydrogenation of benzyl group gave the lower-unit acetylated procyanidin B1 analog (**35**). On the other hand, deprotection of Bn groups by hydrogenation followed by acetylation of phenolic groups and aliphatic hydroxyl groups and TBAF treatment gave the upper-unit acetylated procyanidin B1 analog (**36**).

*2.3 Synthesis of 3- or 5-*O*-Galloyl (+)-Catechin and (−)-Epicatechin Derivatives [35]*

We next demonstrated the development of a regioselective deprotection of TBS protected flavan-3-ols, allowing for modification of the 5-position with various moieties, such as the galloyl group and the SAR studies of 3- or 5-*O*-galloyl-modified (+)-catechin (**37** and **39**) and (−)-epicatechin (**38** and **40**) (Fig. 2).

On the treatment of TFA with tetra-TBS products (**8**) and (**10**), the 5-*O*-TBS groups of **8** and **10** could be regioselectively removed to give **41** and **43** in 85 and 90% yield, respectively. Esterification of dihydroxyl compounds **41** and **43** using benzyl-protected gallic acid and DCC proceeded smoothly to provide digalloyl compounds **42** and **44**. The TBS groups of **42** and **44** were then removed with TBAF in the presence of AcOH and following hydrogenation of the six-benzyl groups, which protect the phenolic hydroxyl groups on the galloyl moiety, gave **37** and **38** in 60 and 18% yields (over 3 steps), respectively (Scheme 5).

5-*O*-Galloyl derivatives **38** and **40** were also synthesized. 5-Hydroxyl compounds (**41** and **43**) were esterified with tri-benzyl gallic acid using EDC as a condensation reagent to give **45** and **46** in 66 and 88% yields, respectively. Deprotection of the TBS groups gave **47** and **48** in 65 and 57% yields, respectively. Subsequent

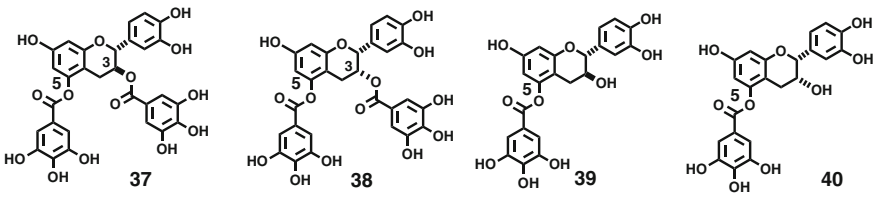

Fig. 2 Structure of 5-*O*-galloyl flavan-3-ols

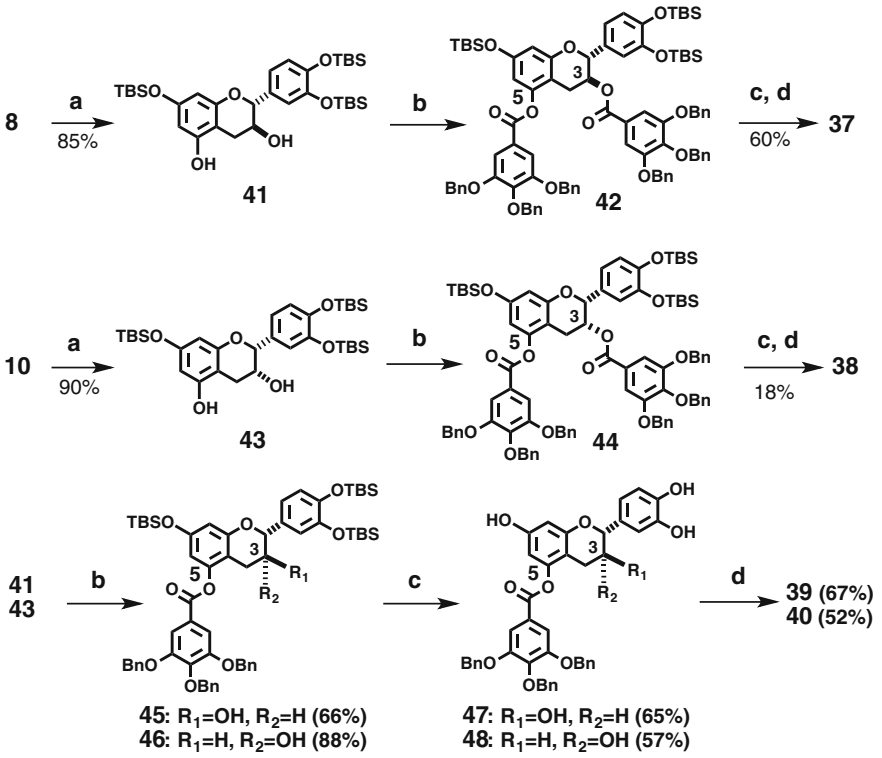

Scheme 5 Synthesis of 5-*O*-galloyl flavan-3-ols

hydrogenation afforded (+)-catechin-5-*O*-gallate (**39**) and (−)-epicatechin-5-*O*-gallate (**40**) in 67 and 52% yields, respectively.

3 Conclusions

In conclusion, we demonstrated the utility of TBS-protecting group for the series of procyanidin synthesis. These procedures offer a real advantage for the procyanidin synthesis over existing methods in this area. Several activities such as DPPH radical scavenging activity, antimicrobial activity, and inhibitory activity against cancer cell proliferation of synthesized compounds were investigated and reported in our papers [33, 35, 36].

References

1. J. B. Harborne, The Flavonoids: Advances in research from 1986; Chapman and Hall: London, 1993.
2. J. B. Harborne and H. Baxter, The Handbook of Natural Flavonoids; John Wiley & Sons: NY, 1999.
3. C. Hartisch, H. Von Kolodziej, and F. Bruchhausen, *Planta Med.* 1977, **63**, 106.
4. K. Kameda, T. Takau, H. Okuda, Y. Kimura, T. Okuda, T. Hatano, I. Agata, and S. Arichi, *J. Nat. Prod.* 1987, **50**, 680.
5. A. Scalbert, *Phytochemistry* 1991, **30**, 3875.
6. F. V. So, N. Guthrie, A. F. Chambers, and K. K. Carroll, *Cancer Lett.* 1997, **112**, 127.
7. H. Kolodziej, C. Haberland, H. Woerdenbag, and A. W. T. Konigs, *Phytotherapy Res.* 1995, **9**, 410.
8. D. Ramljak, L. J., Jr. Romanczyk, L. J. Metheny-Barlow, N. Thompson, V. Knezevic, M. Galaperin, A. Ramesh, and R. B. Dickson, *Mol. Cancer Ther.* 2005, **4**, 537.
9. L. Liviero, P. P. Puglisis, P. Morazzoni, and E. Bombardelli, *Fitoterapia* 1994, **65**, 203.
10. A. Constable, N. Varga, J. Richoz, and R. H. Stadler, *Mutagenesis* 1996, **11**, 189.
11. O. Inanami, Y. Watanabe, B. Syuto, M. Nakano, and M. Kuwabara, *Free Radical Res.* 1998, **29**, 359.
12. A. A. Shahat, S. I. Ismail, F. M. Hammouda, S. A. Azzam, G. Lemiere, T. De Bruyne, S. De Swaet, L. Piteters, and A. Vlietinck, *Phytomedicine* 1998, **5**, 133.
13. M. Saito, H. Hosoyama, T. Ariga, S. Kataoka, and M. Yamaji, *J. Agric. Food. Chem.* 1998, **46**, 1460.
14. O. Inanami, Y. Watanabe, B. Syuto, M. Nakano, and M. Kuwabara, *Free Radical Res.* 1998, **29**, 359.
15. M. Aviram and B. Fuhrman, *Artherosclerosis* 1998, **137**, S45.
16. J. Yamakoshi, S. Kataoka, T. Koga, and T. Ariga, T. *Artherosclerosis* 1999, **142**, 139.
17. H. Kawamoto, F. Nakatsubo, and K. Murakami, *J.* Wood. *Chem. Technol.* 1990, **10**, 59.
18. H. Kawamoto, F. Nakatsubo, and K. Murakami, *Mokuzai Gakkaishi* 1991, **37**, 488.
19. S. Yoneda, H. Kawamoto, and F. Nakatsubo, *J. Chem. Soc., Perkin Trans. 1* 1997, 1025.
20. W. Tückmantel, A. P. Kozikowski, and L. J. Jr. Romanczyk, *J. Am. Chem. Soc.* 1999, **121**, 12073.
21. A. P. Kozikowski, W. Tückmantel, and Y. Hu, *J. Org. Chem.* 2001, **66**, 1287.
22. W. Tückmantel, G. Böttcher, and L. J. Jr. Romanczyk, *J. Org. Chem.* 2003, **68**, 1641.
23. K. Ohomori, N. Ushimaru, and K. Suzuki, *Tetrahedron Lett.* 2002, **43**, 7753.
24. K. Ohomori, N. Ushimaru, and K. Suzuki, *PNAS* 2004, **101**, 12002.
25. Y. Mohri, M. Sagehashi, T. Yamada, Y. Hattori, K. Morimura, T. Kamo, M. Hirota, and H. Makabe, *Tetrahedron Lett.* 2007, **48**, 5891.
26. Y. Mohri, M. Sagehashi, T. Yamada, Y. Hattori, Y. Morimura, K. Hamauzu, T. Kamo, M. Hirota, and H. Makabe, *Heterocycles* 2009, **79**, 549.
27. I. Tarascou, K. Barathieu, Y. Andé, I. Pianet, E. J. Dufourc, and E. Fouquet, *Eur. J. Org. Chem.* 2006, 5367.
28. K. Oyama, M. Kuwano, M. Ito, K. Yoshida, and T. Kondo, *Tetrahedron Lett.* 2008, **49**, 3176.
29. R. D. Alharthy and C. J. Hayes, *Tetrahedron Lett*. 2010, **51**, 1193.
30. K. Weinges and D. Seiler, *Liebigs Ann. Chem.* 1968, 714, 193.
31. S. Nakayama, K. Oyama. T. Kondo, and K. Yoshida, *Heterocycles* 2007, **73**, 451.
32. P. K. Sharma, A. Kolchinski, H. A. Shea, J. J. Nair, Y. Gou, L. J. Jr. Romanczyk, and H. H. Schmitz, *Org. Process Res. Dev.* 2007, **11**, 422.
33. K. Matsubara, A. Saito. A. Tanaka, N. Nakajima, R. Akagi, M. Mori, and Y. Mizushina, *DNA & Cell Biol.* 2006, **25**, 95–103.
34. N. Nakajima, K. Horikawa, N. Takekawa, M. Hamada, and T. Kishimoto, *Heterocycles* 2012, **84**, 349–354.

35. K. Mori, Y. Ayano, Y. Hamada, T. Hojima, R. Tanaka, Y. Higashino, M. Izuno, T. Okamoto, T. Kawasaki, M. Hamada, N. Nakajima, and A. Saito, *Nat. Prod. Chem., Res.*, 2015, **3**, 172; doi:10.4172/2329-6836.1000172.
36. Y. Hamada, S. Takano, Y. Ayano, M. Tokunaga, T. Koashi, S. Okamoto, S. Doi, M. Ishida, T. Kawasaki, M. Hamada, N. Nakajima, and A. Saito, *Molecules* 2015, **20**(10), 18870–18885; doi:10.3390/molecules201018870.

Chemical Modification of the 3′-Dangling End of Small Interfering RNAs Such as siRNAs and miRNAs: The Development of miRNA Replacement Therapy

Yukio Kitade, Takashi Mori and Yukihiro Akao

Abstract The 3′-modified oligonucleotides using aromatic moieties, such as benzene(B)-pyridine(P) analogs (BP-type) and so on, showed prominent nuclease resistance, especially in vivo, and strong RNAi activity. One of non-coding RNAs ranging from 20 to 23 nucleotides in length is naturally occurring microRNAs (miRNAs) that are post-transcriptional regulators of gene expression. The chemically modified miRNAs for genome therapy is easy, inexpensive, and practical. The miRNA replacement therapy using these 3′-modified miRNAs may prove useful for the development of anti-cancer RNA medicine.

Keywords RNA interference · siRNA · MicroRNA · Melanoma · Chemical modification

Y. Kitade (✉)
Department of Applied Chemistry, Faculty of Engineering, Aichi Institute of Technology, 1247 Yachigusa, Yakusa-Cho, Toyota, Aichi 470-0392, Japan
e-mail: ykkitade@aitech.ac.jp

Y. Kitade
Department of Chemistry and Biomolecular Science, Faculty of Engineering, Gifu University, 1-1 Yanagido, Gifu 501-1193, Japan

T. Mori
Comparative Cancer Center, Gifu University, 1-1 Yanagido, Gifu 501-1193, Japan

T. Mori
Department of Veterinary Pathology, Faculty of Applied Biological Sciences, Gifu University, 1-1 Yanagido, Gifu 501-1193, Japan

Y. Akao
United Graduate School of Drug Discovery and Medical Information Sciences, Gifu University, 1-1 Yanagido, Gifu 501-1193, Japan

K. Tomioka et al. (eds.), *New Horizons of Process Chemistry*,
DOI 10.1007/978-981-10-3421-3_18

1 Introduction

The discovery of small interfering RNAs, called siRNA, may be one of the major events in biology in the past decade [1, 2]. Digestion of long double-stranded RNAs by Dicer generates siRNAs which contain a 2-nucleotide overhang (3′-dangling end) at the 3′-end of each strand. One of double-strands, an antisense strand, is loaded onto the RNA-induced silencing complex (RISC). The 3′-dangling end structure is especially very important and is recognized by RISC. RNA interference (RNAi) can result in gene silencing or even in the deletion of sequences from the genome. Efforts to understand the mode of action of siRNAs have revealed that they play a central role in gene regulation and host defense (see Fig. 1). The specificity, efficiency, and potency of RNAi make it an attractive tool for analyzing the function of genes. RNAi can be exploited artificially to inhibit the expression of any gene of interest. Therefore, RNAi systems have been used clinically to suppress gene expression as a therapeutic strategy in many hereditary and infectious diseases. The 3′-dangling end of a siRNA guide (antisense) strand, that is, the 3′-overhang region, is recognized by the PAZ domain of Ago2; the 2 nt at the 3′-dangling end of the guide strand are accommodated into a binding pocket composed of hydrophobic amino acids in the PAZ domain [3] (see Fig. 2).

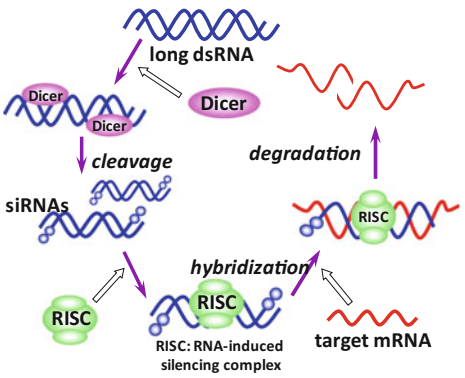

Fig. 1 Gene silencing pathway caused by siRNAs

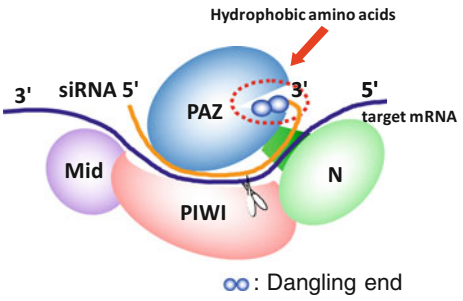

Fig. 2 Structure of siRNA-Ago2 complex

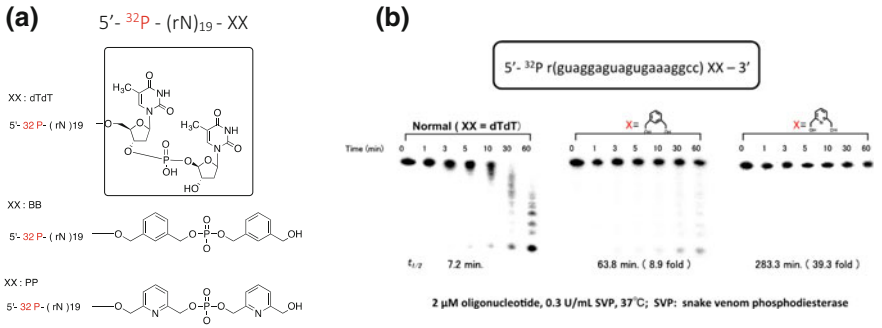

Fig. 3 **a** ^{32}P-Radiolabeled oligonucleotides, **b** Nuclease resistance assay used snake venom phosphodiesterase

2 Chemical Modification for Enhanced Nuclease Resistance

In order to enhance nuclease resistance of RNAs, we attempted the introduction of hydrophobic groups to the 3′-dangling end of RNAs. Chemical modifications at the 3′-dangling end, namely the pyridine-pyridine (PP) type and benzene-benzene (BB) type, were carried out by our group [4] (see Fig. 3a). These analogs were expected to be nuclease resistant and hydrophobic characteristics. For the modification of the 3′-dangling end of RNAs, the phosphoramidites (**1a, b**) and the CPG-resins (**2a, b**) were developed (see Fig. 4). On the basis of the dual-luciferase reporter assay, the benzene-benzene (BB type) and pyridine-pyridine (PP type) analogs demonstrated stronger inhibitory activity than the corresponding non-dangling analogs. Evaluation of nuclease resistance using snake venom phosphodiesterase was carried out. The half-life of the natural type of the RNA oligomer (XX = dTdT) was 7.2 min, that of the benzene-benzene type (XX = BB) was 63.8 min (an approximate 9-fold increase) and that of pyridine-pyridine type (XX = PP) is 283.3 min (an approximate 40-fold increase) (see Fig. 3b). Therefore, these chemical modifications were a useful tool for enhanced nuclease resistance.

3 Role of miRNAs

One of non-coding RNAs ranging from 20–23 nucleotides in length is naturally occurring microRNAs (miRNAs; miRs) that are post-transcriptional regulators of gene expression. Over 2500 miRNAs are predicted to exist in humans. Increasing evidence supports the role of miRNAs in the regulation of a wide range of physiological and pathophysiological processes, including development, cellular apoptosis, cellular differentiation, and cell proliferation. First of all, miRNA is expressed from a much longer RNA-coding gene as a primary transcript known as

Fig. 4 Structure of novel phosphoramidites (**1a, b**) and CPG-resins (**2a, b**)

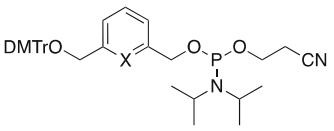

1a ; X = CH
1b ; X = N

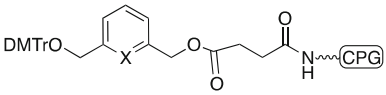

2a ; X = CH
2b ; X = N

pri-miRNA. That is processed in the cell nucleus by the microprocessor complex, which consists of Drosha, to form a 70-nt stem-loop structure called pre-miRNA. This pre-miRNA is transported from nucleus to cytoplasm by exportin 5. The dsRNA portion of pre-miRNA is bound and cleaved by Dicer to produce the mature miRNA molecule. The mature miRNA can then be integrated into the RISC complex and the miRNA-RISC complex mainly inhibits the translation of the corresponding mRNA (see Fig. 5). The 3′-dangling end of an miRNA guide strand is also recognized by the PAZ domain of Ago2; the 2 nt at the 3′-dangling end are also accommodated into a binding pocket composed of hydrophobic amino acids in the PAZ domain (see Fig. 6).

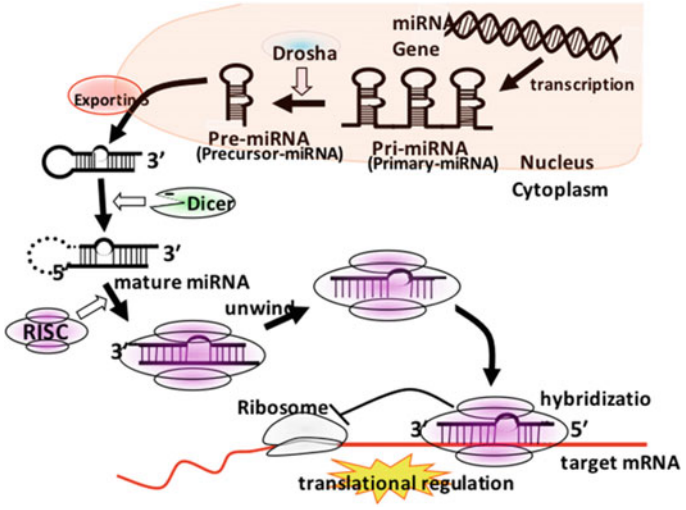

Fig. 5 Biogenesis of miRNA and its function

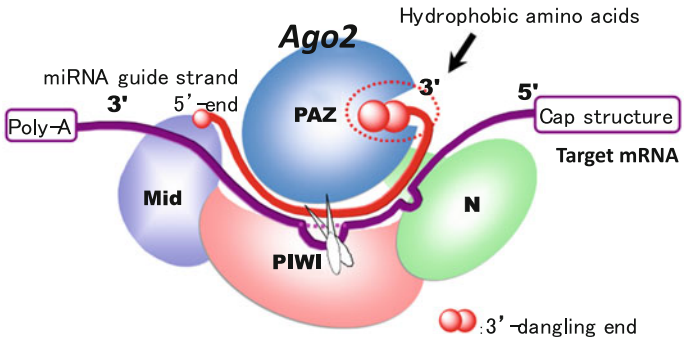

Fig. 6 Structure of miRNA-Ago2 complex

4 MicroRNAs as Tumor Suppressors

Much evidence indicates that miRNAs behave as novel tumor suppressors or oncogenes in human carcinogenesis. Previously, we demonstrated that the expression of miR-143 was severely down-regulated in colon cancers and in smaller adenomas. This observation suggested that miR-143 and -145 were closely associated with the initiation of tumor development. The growth of human colon cancer cells expressing miR-143 at low levels was significantly inhibited by miR-143. These findings indicated the antioncogenic role of miR-143 [5].

5 MicroRNA Replacement Therapy

An aberrantly expressed miRNAs play important roles in the occurrence of human disease. The down-regulation of antioncogenes, such as miR-143 and miR-145, causes imbalance resulting cancer. However, naturally occurring miRNAs are very fragile in vivo. Therefore, we thought administration of chemically modified miRNAs showing nuclease resistance may recover a good balance (see Fig. 7). Restoring the function of a miRNA by using chemically modified miRNAs possessing enhanced nuclease-resistance is a better promising approach. This approach is named microRNA replacement therapy [6, 7]. The addition of just small amount of chemically modified miRNAs modulate to the normal balance. The required properties for the chemically modified RNAs are nuclease-resistance and sufficient the knock-down effect. When a low-expression of miRNA causes human cancer, the microRNA replacement therapy is especially expected as an effective treatment.

Our recent work has revealed that the changing the structure of the passenger strand of the miR-143 duplex enhanced on the growth of human colon cancer DLD-1 cells, and that chemical modification of the 3′-dangling end of miR-143 using aromatic moieties, such as benzene(B)-pyridine(P) analogs (BP-type),

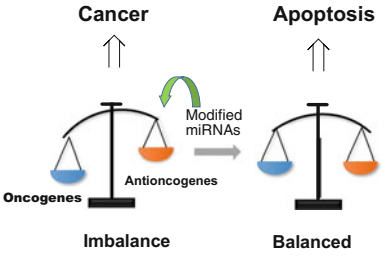

Fig. 7 Replacement therapy by using chemically-modified miRNAs

improved its resistance against nucleases. The administration of such modified miR-143BP via intravenous injection resulted in a potent tumor-suppressive effect on xenografted human colon cancer cells [5].

5.1 *Inhibitory Activity of 3′-Modified miRNA-143 Against Human Colon Cancer Cells*

We synthesized 3′-modified miRNAs possessing hydrophobic groups (benzene and/or pyridine analogs) at the 3′-dangling end. Secondly, we changed the sequences of the passenger (sense) strand at the mismatch portions between the passenger and guide strands (see Fig. 8a). Among these derivatives, the modified miR-143BP (**3**) showed the strongest inhibitory activity against human colon cancer DLD-1 cells (see Fig. 8b).

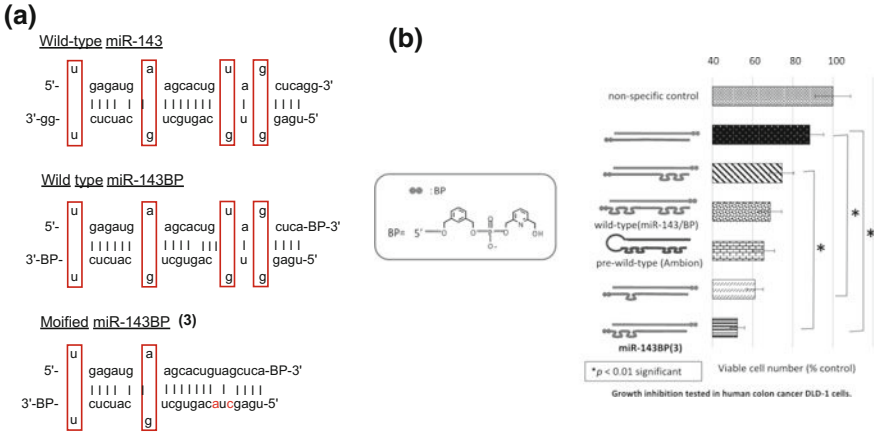

Fig. 8 **a** Sequence design for miR-143, **b** Anti colon-cancer effect for several miR-143s

5.2 Anticancer Activities in Mice Xenografted with Human Colon Cancer

A significant reduction in tumor weight by the miR-143BP (**3**) in comparison with the tumor weight of control animals was observed from 3 weeks after weekly intravenous injections in mice xenografted with human colon cancer tumors. At 2 weeks after the last injection, we evaluated the tumor-suppressive effect of the miR-143BP (**3**). Figure 9 showed that the tumor/body weight ratio of the miR-143BP (**3**)-treated mice was decreased in compared with that for the control miRNA. The addition of BP moiety at the 3′-dangling end of miR-143 improved nuclease resistance, with the amount of miRNA remaining at 5–8-fold more than that obtained with miR-143 from Applied Biosystems [5].

5.3 Anti-melanoma Activity of miR-205BP

Malignant melanoma is one of the most common skin cancers in humans. The incidence of melanoma continues to rise more rapidly than that of all malignancies, expect for lung cancer. The down-regulation of miR-205 is observed frequently in human and canine, i.e. dog, melanoma. Several modified miR-205BPs possessing a benzene-pyridine substituent (BP) at the 3′-dangling end were prepared. Because the modification shows enhanced nuclease-resistance and also binds a hydrophobic binding pocket of PAZ-domain of Ago2. Among the modified microRNAs, modified miR-205BP (**4**) significantly inhibited the growth of human melanoma cells [8] (Fig. 10).

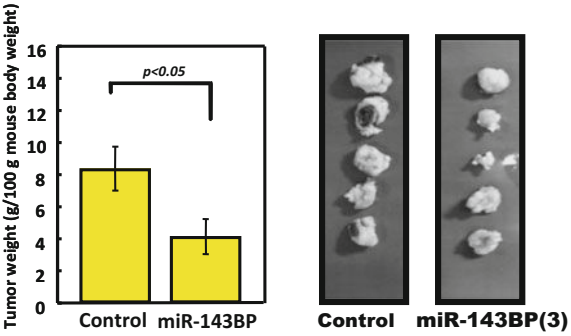

Fig. 9 In vivo miR-143BP (liposome entrapped) assay carried out with intravenous injection (50 μg/a mouse), and total 5 times (one injection per week). Tumor weights measured at 7 weeks after implantation. Control means injection of non-specific miRNA(purchased). *Vertical bars* show tumor weights of implanted colon cancer, and graphics show each developed tissues (tumors)

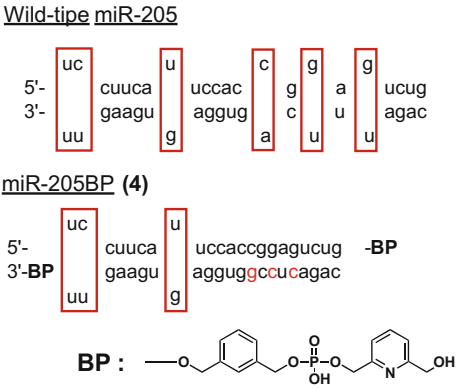

Fig. 10 Sequence design for miR-205

5.4 *Clinical Trial of Modified miR-205BP Against Canine Melanoma*

A clinical trial of miR-205BPs against canine melanoma is now in progress. Since human melanoma and canine melanoma is caused by the reduced expression of the same miR-205. The intratumoral injection of modified miR-205BP (**4**) into a recurrent tumor derived from a naturally occurring canine melanoma has resulted in complete remission in 2 of 5 cases. Once a week to the oral cancer, topical administration of a total of seven times resulted in a complete remission (see Fig. 11). As observed in canines, humans develop melanoma due to the reduced expression of miRNA-205. If the result of the clinical trials in dogs is remarkable, we believe that the transition to clinical trials in humans is in the near future.

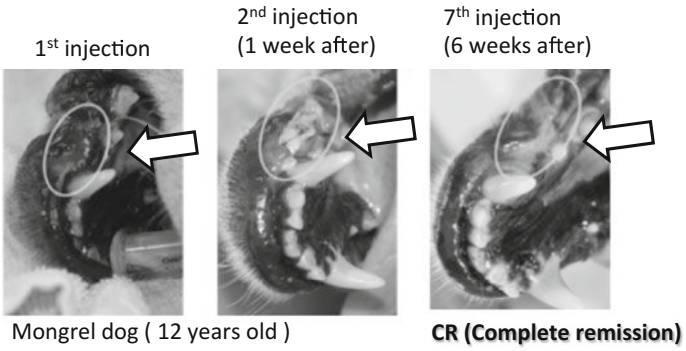

Fig. 11 Clinical trial for a 12-years-old Mongrel dog, carried out with topical administration (2 nmole per injection, liposome entrapped), and total 7 times injection. In this case, we confirmed complete remission

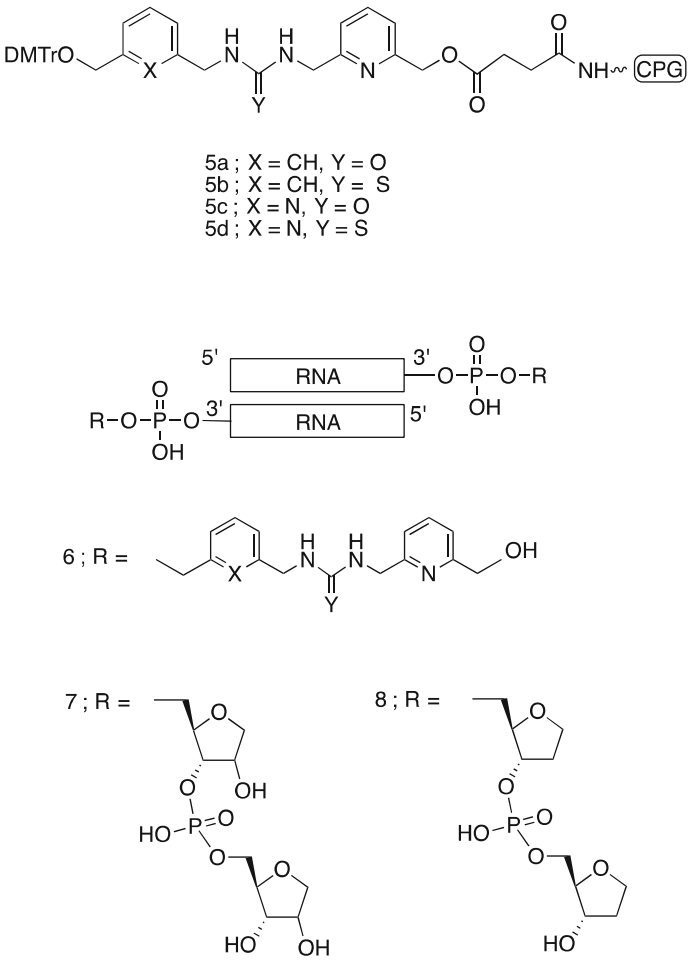

Fig. 12 Urea-substituted miRNAs (**6**) by using urea/thiourea-CPG resins (**5a-b**) and deoxyribofuranose-substituted miRNAs (**7,8**)

6 New Type of the 3′-Modified dsRNAs

6.1 The 3'-Dangling End Bearing Urea/Thiourea-Bridged Aromatic Compounds

When this phosphorodiester bond was converted to form urea bonds, improved cell membrane permeability was observed. Digestive enzyme tolerance was improved when the nucleoside moiety was converted to aromatic rings. We prepared the urea-substituted miRNAs by using urea/thioure-CPG resin (**5a-d**) (see Fig. 12). We prepared controlled pore glass (CPG) solid supports liked to urea/thiourea bridged

(a) Syntesis of Pyrimidine Unit

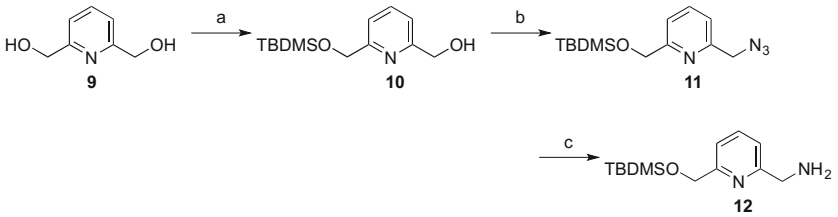

(b) Synthesis of Bezene Unit

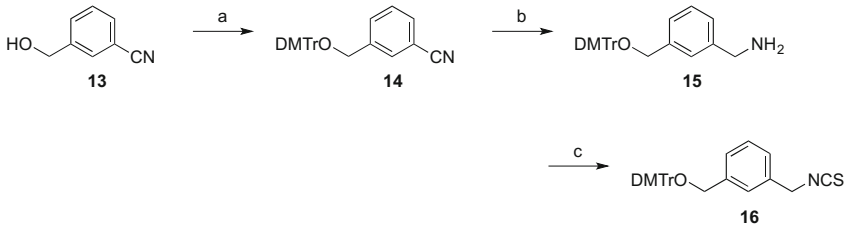

(c) Synthesis of DMTr-BuP derivatives

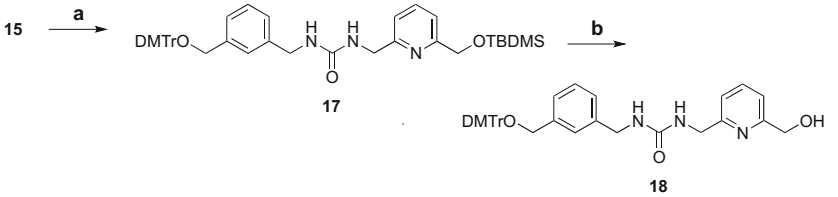

(d) Synthesis of DMTr-BtuP derivatives

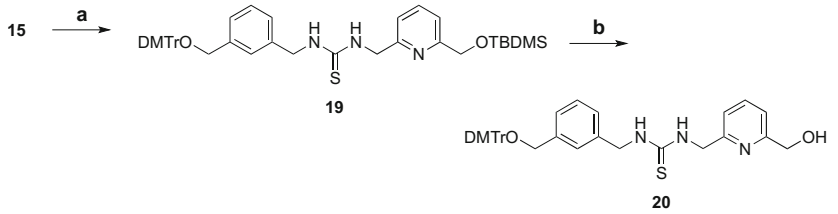

Scheme 1 **a**–**g** Synthesis of urea/thiourea-CPG resins. Reagents and conditions: **a** (a) NaH, DMF, rt, then TBDMSCl, DMF, rt, 49%; (b) CBr4, PPh3, NaN3, Et3N, DMF, rt, 93%; (c) PPh3, THF, H_2O, rt, 93%. **b** (a) DMTrCl, pyridine, DMF, rt, 91%; (b) LiAlH4, THF, rt, 94%; (c) CS2, Et3N, EtOH, rt, then Boc2O, DMAP, EtOH, rt, 96%. **c** (a) CDI, THF, rt, then 12, THF, rt, 54%; (b) TBAF, THF, rt, 98%. **d** (a) 12, CHCl3, reflux, 75%; (b) TBAF, THF, rt, 90%. **e** (a) CDI, THF, rt, 96%; (b) TBAF, THF, rt; (c) DMTrCl, pyridine, DMSO, rt, 43%. **f** (a) CSCl2, Et3N, CH2Cl2, rt, (b) TBAF, THF, rt, 43%, (c) DMTrCl, pyridine, DMF, rt, 18%. **g** (a) (i) succinic anhydride, DMAP, pyridine, rt; (ii) CPG, EDCI, DMF, rt

(e) Synthesis of DMTr-PuP derivatives

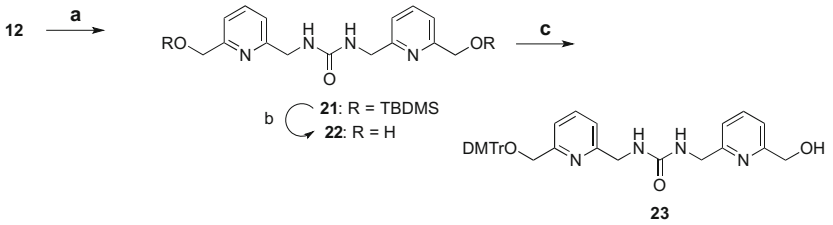

(f) Synthesis of DMTr-PtuP derivatives

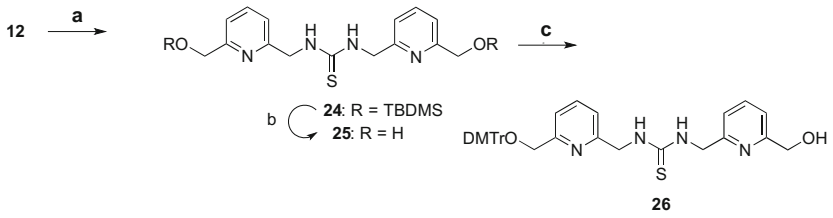

(g) Synthesis of CPG-resins

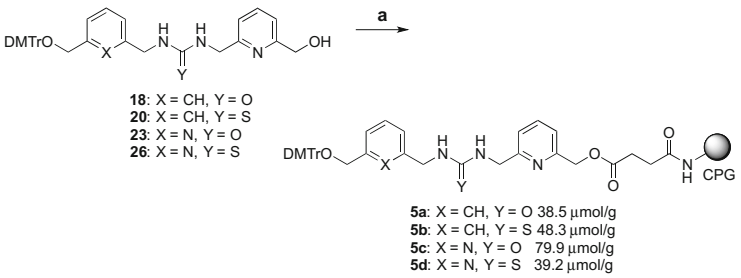

Scheme 1 (continued)

aromatic dimers (**18**, **20**, **23**, and **26** shown in Scheme 1g). To obtain the desired CPG solid supports, we initially prepared pyridine analogs **12** and benzene analogs **15** and **16** (Scheme 1b, c). Urea/thiourea bridged Benzene-Pyridine analogs (**18** and **20**) were synthesized from compounds **15** and **12** (Scheme 1c, d). On the other hand, Pyridine/Pyridine analogs (**23** and **26**) were prepared from compounds **12** (Scheme 1e, f). Detailed synthetic methods for the preparation of urea/thiourea-CPG resins (**5a-d**) are described in the literature [10]. The modified urea/thioure-CPG resins were used to simplify the synthetic process. Thus, in the case of BP-modification, the phoshoramidites (**1a, b**) and the CPG-resins (**2a, b**) are necessary. We have developed chemically modified siRNAs and miRNAs bearing urea/thiourea-bridged aromatic compounds at their 3′-end for RNAi therapy.

Chemically modified RNAs possessing urea/thiourea-bridged aromatic compounds instead of naturally occurring dinucleotides at the 3′-overhang region were easily prepared in good yields and were more resistant to nucleolytic hydrolysis than unmodified RNA. SiRNAs containing urea or thiourea analogs (**6**) showed the expected knockdown effect. Furthermore, these modified miR-143 duplexes carrying the urea/thiourea substituents in each strand inhibited the growth of human bladder cancer T24 cells. We found that incorporation of these urea/thiourea substituents into the 3′-end enhances the nuclease resistance [10, 11].

6.2 The 3′-Dangling End Bearing 1-deoxy-D-Ribofuranoses

To elucidate the role of the sugar moiety in the two natural nucleotides of the 3′-dangling end of siRNA, we synthesized siRNAs that incorporated two abasic nucleosides, 1-deoxy-D-ribofuranose (R^H). We improved the method for preparing an O-protected abasic nucleoside, 1-deoxy-2,3,5-tri-O-benzoyl-β-D-ribofuranose, via the reductive cleavage of the anomeric position of 1-O-acetyl-2,3,5-tri-O-benzoyl-β-D-ribofuranose. To incorporate the deoxyribofuranose into oligonucleotides, the deoxyribofuranose was converted into its phosphoramidite derivative and the solid support linked to a controlled pore glass resin. Chemically modified RNAs (**7**) possessing the deoxyribofuranose at the 3′-dangling end were easily prepared in good yields. These siRNAs showed moderate nuclease-resistance and a desirable knockdown effect [12].

We also developed a practical and reliable method for synthesizing an abasic deoxyribonucleoside, 1,2-dideoxy-D-ribofuranose, via elimination of the nucleobase from thymidine. To synthesize oligonucleotides bearing the 1,2-dideoxyribofuranose by the standard phosphoramidite solid-phase method, the dideoxyribofuranose was converted to the corresponding phosphoramidite derivative and its CPG-resin. Introducing the dideoxyribofuranose to the 3′-end of the antisense strand of siRNA (**8**) reduced its knockdown effect [13].

7 Summary

The 3′-modified oligonucleotides showed prominent nuclease resistance, especially in vivo, and strong RNAi activity. The chemically modified dsRNAs for genome therapy is easy, inexpensive, and practical. The miRNA replacement therapy using these 3′-modified miRNAs may prove useful for the development of anti-cancer RNA medicine.

References

1. Czech, M. P., Aouadi, M., Tesz, G. J., *Nat. Rev. Endocrinol.*, **7**, 473–484 (2011).
2. Lennox, K. A., Behlke, M. A., *Gene Therapy*, **18**, 1111–1120 (2011).
3. Macrea, I. J., Zhou, K., Li, F., Repic, A., Brooks, A. N., Cande, W. Z., Adams, P. D., Doudna, J. A., *Science*, **311**, 195–198 (2006).
4. Ueno, Y., Inoue, T., Yoshida, M., Yoshikawa, K., Shibata, A., Kitamura, Y., and Kitade, Y., *Bioorg. Med. Chem. Lett.*, **18**, 5194–5196 (2008).
5. Akao, Y., Nakagawa, Y., Hirata, I., Iio, A., Itoh, T., Kojima, K., Nakashima, R., Kitade, Y., and Naoe, T., *Cancer Gene Therapy*, **17**, 398–408 (2010).
6. Kitade, Y., Alkao, Y., *J. Pharmacol. Sci.*, **114**, 276–280 (2010).
7. Bader, A. G., Brown, D., Winkler, M., *Cancer Res.*, **70**, 7027–7030 (2010).
8. Noguchi, S., Iwasaki, J., Kumazaki, M., Mori, T, Maruo, K., Sasaki, H., Yamada, N., Shimada, K., Naoe, T., Kitade, Y., Akao, Y., *Molecular Ther.*, **21**, 1204–1211 (2013).
9. Unpublished results.
10. Kitamura, Y., Masegi, Y., Ogawa, S., Nakashima, R., Akao, Y., Ueno, Y., Kitade, Y., *Bioorg. Med. Chem.*, **21**, 4494–4501 (2013).
11. Noguchi, S., Mori, T., Hoshino, Y., Maruo, K., Yamada, N., Kitade, Y., Naoe, T., Akao, Y., *Cancer Lett.*, **307**, 211–220 (2011).
12. Taniho, K., Nakashima, R., Kandeel, M., Kitamura, Y., Kitade, Y., *Bioorg. Med. Chem. Lett.*, **22**, 2518–2521 (2012).
13. Nagaya, Y., Kitamura, Y., Nakashima, R., Shibata, A., Ikeda, M., Kitade, Y., *Nucleosides, Nucleotides and Nucleic Acids*, **35**, 64–75(2016).

Antiviral Agents Towards Chikungunya Virus: Structures, Syntheses, and Isolation from Natural Sources

Jih Ru Hwu, Tapan K. Pradhan, Shwu-Chen Tsay, Mohit Kapoor, Sergey O. Bachurin, Oleg A. Raevsky and Johan Neyts

Abstract Emerging variants of known RNA viruses present an increasing threat to mankind worldwide through their enlarging impact on morbidity and mortality. One of them is the chikungunya disease, which becomes a major public health problem and economic threat. Current world has no approved antiviral drugs available against chikungunya infection. This Book Chapter mainly focuses on discussion of the antiviral compounds that have been reported to inhibit chikungunya virus replication. Various syntheses of antiviral agents, compounds isolated from natural sources, and some structure–activity relationships are illustrated.

Keywords Chikungunya virus · Antivirals · Synthesis · Structure–activity relationship · Mechanism of action

J.R. Hwu (✉) · T.K. Pradhan · S.-C. Tsay · M. Kapoor
Department of Chemistry & Frontier Research Center on Fundamental and Applied Sciences of Matters, National Tsing Hua University, Hsinchu, Taiwan 30013, Republic of China
e-mail: jrhwu@mx.nthu.edu.tw

S.O. Bachurin
Department of Biomedical and Biological Chemistry, Institute of Physiologically Active Compounds, Russian Academy of Science, Chernogolovka, Moscow Region 142432, Russia

O.A. Raevsky
Department of Computer-Aided Molecular Design, Institute of Physiologically Active Compounds, Russian Academy of Science, Chernogolovka, Moscow Region 142432, Russia

J. Neyts
Rega Institute for Medical Research, Katholieke Universiteit Leuven, Minderbroedersstraat 10, Leuven B-3000, Belgium

K. Tomioka et al. (eds.), *New Horizons of Process Chemistry*,
DOI 10.1007/978-981-10-3421-3_19

1 Introduction

Chikungunya virus (CHIKV) is an alphavirus and was first recognized as an epidemic form in East Africa in the early 1950s. Most patients of CHIKV infection suffer from severe persistent arthralgia [1]. Female mosquitoes of the species *Aedes aegypti* and *Aedes albopictus* are mainly responsible for its transmission. The dramatic turn of CHIKV history is its unexpected re-emergence in 2004, which was associated with mutations in the viral genome and a new epidemic strain emerged from the East, Central, South Africa enzootic linage [1, 2]. The outbreaks took place mainly around the Indian Ocean, in particular, the French Island of La Réunion (2005–2006), where about 300,000 cases were confirmed [1, 2]. Since then, thousands of infected travelers imported this virus to many countries of the world. As a result, it is endemic in northern Italy and southern France in 2007. Around the same timeframe, several CHIKV re-emerged incidents happened in Asia, including a local case in Singapore (2008) [3] and hundreds of cases in southern Thailand (2008–2009) [4]. In March 2011, autochthonous transmission of CHIKV was reported in New Caledonia (South Pacific Region), which is also the first report of CHIKV transmission in this region [5]. Another outbreak of autochthonous chikungunya fever with more than 10 cases occurred in Montpellier, France in October 2014 [6]. Beginning in late 2013, the virus started to spread to the Caribbean and into Central and South America, affecting people from 41 countries or more [7, 8]. According to the data of the Pan American Health Organization, about 1.3 million suspected and confirmed cases were reported in these regions by March 2015 [7]. Many factors like commercial transportation, urbanization, deforestation, climate change, have inadvertently formed environments, which brought emerging RNA virus pathogens increasing at an accelerating rate.

In 2008, chikungunya fever is listed as a category C priority pathogen by The U.S. National Institute of Allergy and Infectious Diseases [9]. Considering the global need of new antiviral therapeutics and responding to the health theme of European Union the 7th Framework Call, the Small-molecule Inhibitor Leads Versus Emerging and Neglected RNA Viruses (SILVER) project was conceived in 2010. The SILVER project, led by E. A. Gould and J.-L. Romette, include 24 international research teams and scientists from 12 countries of Europe and Asia. Furthermore, the "Global Virus Network" was initiated in 2011 to identify research gaps and opportunities, including models of infection and disease, epidemiology, candidate vaccines, vector control measures, and antivirals [7].

After being transmitted to the body, CHIKV circulates to the liver, muscle, joints, lymphoid tissue, and brain [9]. There are two phases of infections that were reported in the recent epidemic areas. The first is an acute phase, which lasts from a few days to several weeks. The symptoms include high fever, rigors, headache, photophobia, and petechial/maculopapular rash [9]. The second is a chronic phase, which shows symptoms of polyarthralgia. Although its mortality rate is low, the elderly or those with underlying chronic problems are most likely to have severe complications [9]. During the most recent epidemics in India and in Réunion Island,

severe cases have been described involving encephalitis, myelopathy, peripheral neuropathy, myeloneuropathy, and myopathy [10]. Moreover, some cases of multiorgan failure and eye infections have also been reported [11].

The CHIKV belongs to the *Togaviridae* family and consists of a positive-sense single-stranded RNA genome of about 11.8 kb size. This genome has two open reading frames 5′ and 3′ ends. The 5′ end encodes nsP1, nsP2, nsP3, and nsP4 non-structural proteins; the 3′ end encodes the capsid (C), two glycoproteins E1, E2, and two small cleavage products (E3, 6 K) [11]. Keller et al. [12] present a detailed description of the CHIKV life cycle and identify the key viral target proteins for drug design in a perspective article.

At the present time, there is no vaccine against CHIKV infection licensed for human use. Most of the treatments are symptomatic [13]. Even worse is that the current world has no drug available against CHIKV. Four well-informative review articles covering structures and biological data have been published by Keller [12], Kaur and Chu [13], Neyts [14], Bhakat and Soliman [15], and respective co-authors. The former two are in 2013 and the latter two are in 2015. Moreover, recent review articles involving the discussion and analysis of epidemiology, pathogenesis, global virus network, or cellular mechanisms of action were published by Thiberville et al. [1], Weaver and Forrester [2], McSweegan et al. [7], Schwartz and Albert [9], Couderc and Lecuit [16], Singh and Unni [17], Birendra et al. [18], Parashar and Cherian [19], and Lum and Ng [20].

2 Compound Classes, Structures, Biological Activities, and Mechanisms of Action

In this review article, we illustrate antiviral agents on the basis of their classes of compounds, structures, synthetic routes, natural sources, biological activities, as well as structure–activity relationship (see Table 1). Emphasis will be placed on the newly developed agents reported after the year of 2013 and syntheses of artificially designed compounds. Efficacy in vivo of most of these compounds, however, has not yet been evaluated in animal models on the basis of the information reported in the original articles.

The established antiviral compounds towards CHIKV can mainly classified into five categories: purines/pyrimidines, nucleosides, alkaloids, terpenoids, and flavaglines. Their characteristics and biological data are illustrated as follows. The table contains information of newly developed antiviral agents reported during the past three years and some established compounds studied earlier for comparison.

A. Purines and Pyrimidines

D'hooghe, De Kimpe, and coworkers [21] synthesized a series of purine derivatives, of which antiviral activities were screened against nine different viruses

Table 1 Names, structures, anti-chikungunya virus activities, mechanisms of action, and classes of synthetic and natural compounds

Name (trade name) (year reported)	Structure	Antiviral activities				Mechanism of action
		CC_{50}^{a} (μM)	EC_{50}^{b} (μM)	SI^{c}	IC_{50}^{d} (μM)	
Class A. Purine and pyrimidine						
Purine–β-lactam (2012) [21]	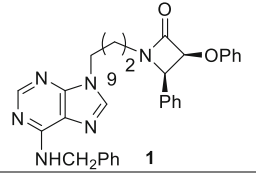 **1**	>98.3	17.1	>5.75	–	Unknown
Purine amino-propanol (2012) [21]	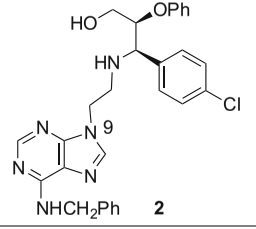 **2**	71.2	11.5	6.19	–	Unknown
Benouracil–coumarin–arene (2015) [22]	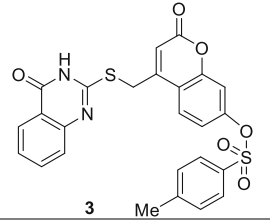 **3**	117	10.2	11.5	–	Unknown

(continued)

Table 1 (continued)

Name (trade name) (year reported)	Structure	Antiviral activities				Mechanism of action
		CC_{50}^{a} (μM)	EC_{50}^{b} (μM)	SI^{c}	IC_{50}^{d} (μM)	
Triazolo-pyrimidine (2014) [23]	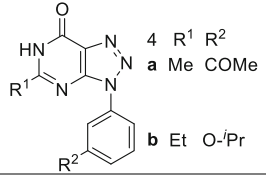 4 R^1 R^2 **a** Me COMe **b** Et O-^{i}Pr	**a**				Unknown
		>743	19	~39.1	–	
		b				
		>668	3	222	–	
Class B. Nucleoside						
Ribavirin (Copegus, Rebetol, Virazole) (2004) [24]	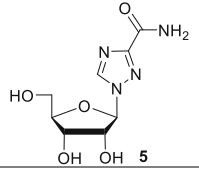 **5**	30.7 (mM)	341	90.0	–	Inhibition of inosine monophosphate dehydrogenase and depletion of guanosine triphosphate pools
6-azauridine (2004) [24]	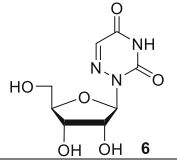 **6**	208	0.82	255	–	Inhibition of orotidine monophosphate decarboxylase and depletion of uridine triphosphate pools
Class C. Alkaloid						
Favipiravir (T-705, Avigan) (2014) [25]	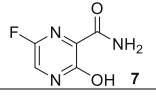 **7**	>636	25	25.4	–	Inhibition of viral genome replication

(continued)

Table 1 (continued)

Name (trade name) (year reported)	Structure	Antiviral activities				Mechanism of action
		CC_{50}^{a} (μM)	EC_{50}^{b} (μM)	SI^{c}	IC_{50}^{d} (μM)	
Umifenovir (arbidol) (2011) [26]	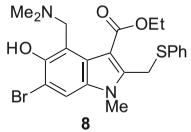 **8**	376	–	–	12.2	Interference with viral entry and alteration of cellular membranes
Thiazolidone (2015) [27]	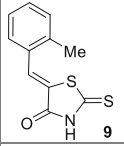 **9**	>100	–	–	0.42	Possible inhibition of nsP2 protease
Thiazolidone (2015) [27]	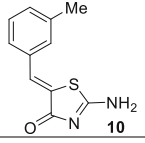 **10**	>100	–	–	6.8	Possible inhibition of nsP2 protease
Harringtonine (2013) [28]	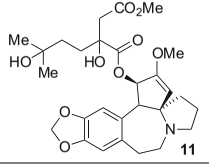 **11**	>10	0.24	>41.6	–	Inhibition of replication cycle, affection of RNA production, and interference with viral protein expression

(continued)

Table 1 (continued)

Name (trade name) (year reported)	Structure	Antiviral activities				Mechanism of action
		CC_{50}^{a} (μM)	EC_{50}^{b} (μM)	SI^{c}	IC_{50}^{d} (μM)	
Class D. Terpenoid						
Jatrophane ester (2014) [29]	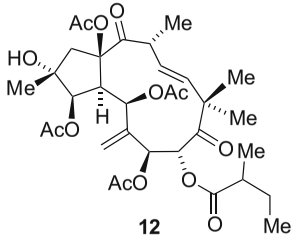 **12**	159	0.76	208	–	Unknown
Aplysiatoxin (2014) [30]	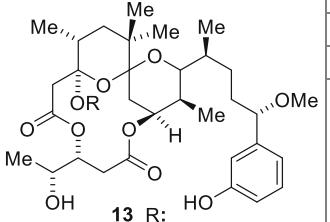 **13** R: **a** H **b** Me	**a**				Unknown
		13.9	1.3	10.9	–	
		b				
		24.8	2.7	9.2	–	

(continued)

Table 1 (continued)

Name (trade name) (year reported)	Structure	Antiviral activities				Mechanism of action
		CC_{50}^{a} (μM)	EC_{50}^{b} (μM)	SI^{c}	IC_{50}^{d} (μM)	
Trigocherrin A (2012) [31]	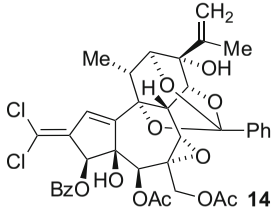 **14**	35	1.5	23.3	–	Unknown
12-*O*-tetradecanoyl-phorbol-13-acetate (2012) [32]	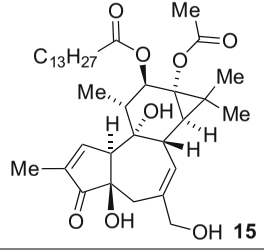 **15**	5.7	0.0029	1965	–	Possible activation of the signal transduction enzyme protein kinase C
Class E. Flavagline						
FL23(2015) [33]	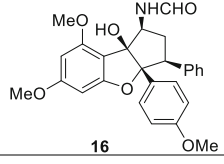 **16**	90.2 (nM)	–	–	~5 (nM)	Interference with the binding of prohibitin-1

(continued)

Table 1 (continued)

Name (trade name) (year reported)	Structure	Antiviral activities				Mechanism of action
		CC_{50}^{a} (μM)	EC_{50}^{b} (μM)	SI^{c}	IC_{50}^{d} (μM)	
FL3 (2015) [33]	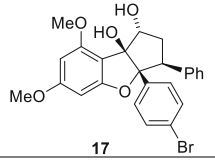 **17**	119 (nM)	–	–	22.4 (nM)	Interference with the binding of prohibitin-1
Others						
CND0335 (2013) [34]	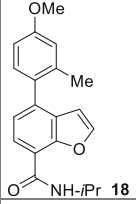 **18**	>50	3.3	>15	–	Unknown
(α-carbonyl)hydrazone (2013) [35]	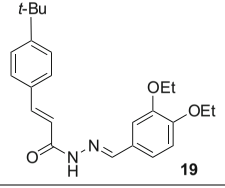 **19**	101	3.2	32	–	Unknown

(continued)

Table 1 (continued)

Name (trade name) (year reported)	Structure	Antiviral activities				Mechanism of action
		CC_{50}^{a} (μM)	EC_{50}^{b} (μM)	SI[c]	IC_{50}^{d} (μM)	
Suramin (Antrypol, 309 F, 309 Fourneau, Bayer 205, Moranyl, Naganin, Naganine) (2015) [36]	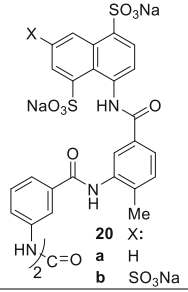	**a**				Inhibition of RNA synthesis, post-attachment step of viral entry, and (re)initiation of RNA synthesis
		>800	210	>3.8	–	
		b				
		>800	79	>10.1	~5	

[a]The concentration of a compound with an adverse effect of 50% was observed on the host cell metabolism, as determined by the MTS method
[b]The concentration of a compound at which virus replication was inhibited by 50% was observed, as determined by real-time quantitative RT–PCR
[c]Selectivity index
[d]Related information are available in original papers

including CHIKV. In 2012, they reported purine β–lactam **1** and purine–amino-propanol **2** with symptom against CHIKV. The key steps for their synthesis shown in Scheme 1 include a Staudinger [2 + 2] cyclocondensation between a Schiff base and a ketene (from $PhOCH_2COCl$) to give a (ω-bromoalkyl)-*cis*-β-lactam with diastereoselectivity. Then *N*-alkylation of a purine derivative with this β-lactam intermediate gives the desired purine–β-lactam **1**. Furthermore, a $LiEt_3BH$-mediated β-lactam ring opening takes place to produce the target purine **2**.

In 2015, Hwu, Tsay, Neyts, and co-workers [22] reported the design and synthesis of a new series of uracil–coumarin–arene conjugates against CHIKV. Five of 22 new hybrid conjugates can inhibit CHIKV in Vero cells with significant potency and low toxicity. As shown in Scheme 2, their synthesis includes a coupling reaction to form a coumarin derivative, its condensation with an organosulfonyl chloride to give sulfonylated intermediate, and a selective *S*-alkylation of 2-thiobenzouracil at the allylic position of (coumarinyl)chloride to yield the desired triply conjugated target **3**. Its molecular framework is determined unambiguously by single X-ray diffraction analysis.

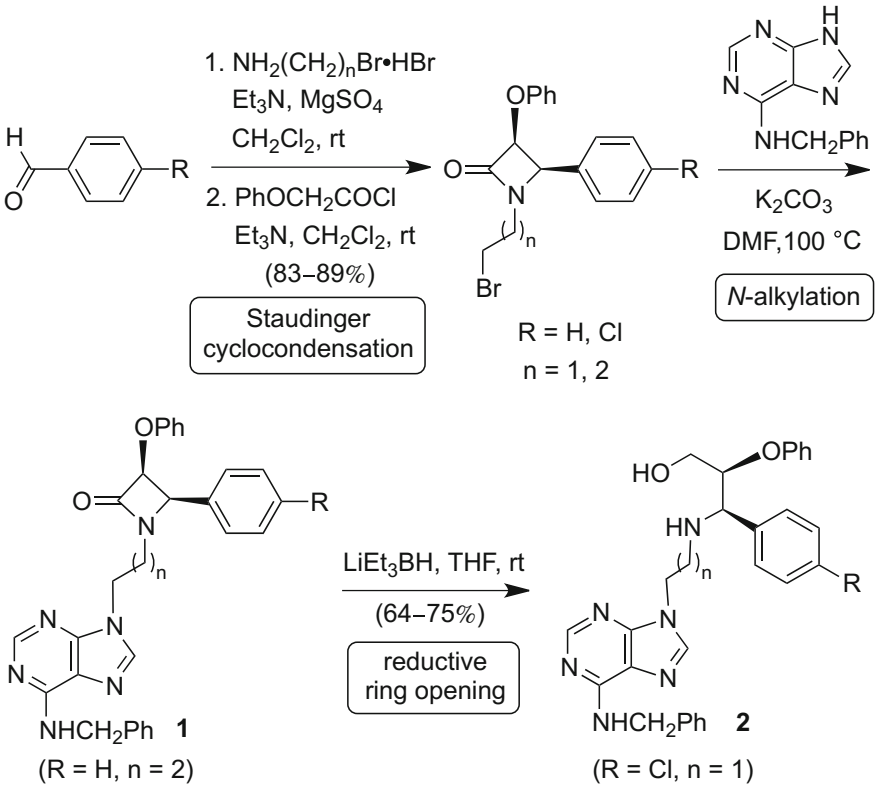

Scheme 1 Synthesis of purine–β-lactam **1** and purine–aminopropanol **2**

The coumarin moiety, $–SCH_2–$, and $–SO_2–$ (but not $–CH_2–$) joints in the conjugated compounds shown in Fig. 1 are essential to their antiviral activity. Use of either an Me or an NO_2 group attached to the arene moiety brings enhanced activity

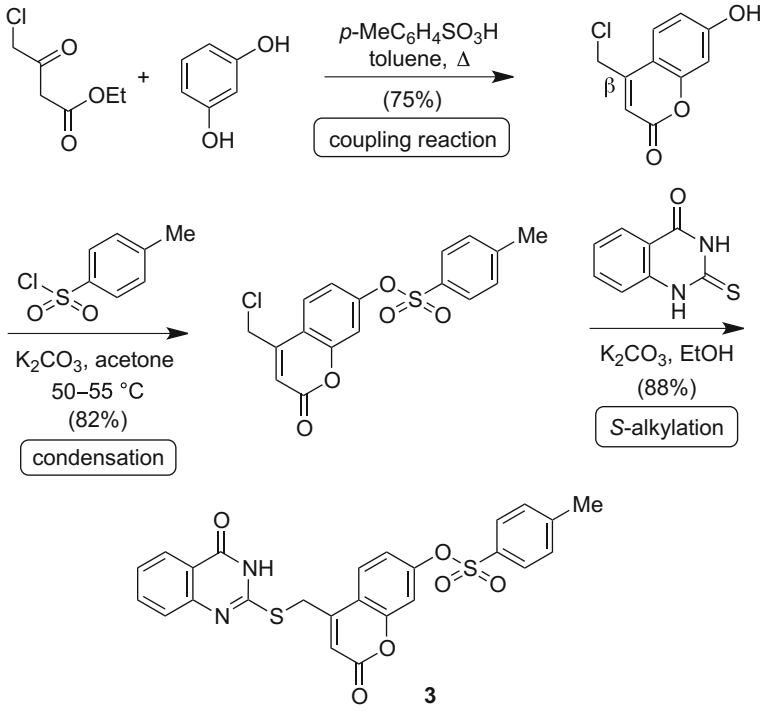

Scheme 2 Synthesis of benzouracil–coumarin–arene conjugates **3**

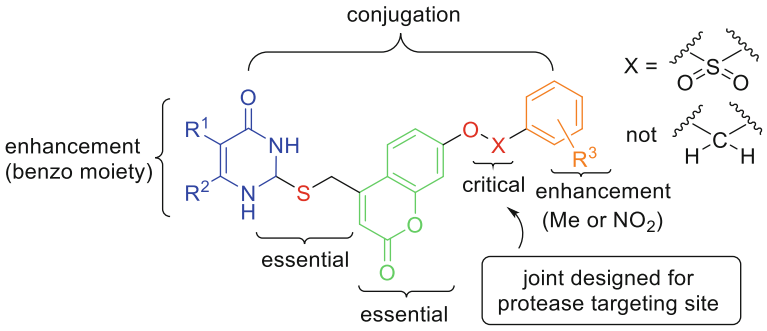

Fig. 1 Structure-activity relationship of uracil–coumarin–arene conjugates

to the target molecules. When coumarin–arenes are conjugated with benzouracil, the resultant hybrids (such as **3**) exhibit better selectivity indexes than their kin with uracil or 5-methyluracil.

In 2014, Pérez–Pérez et al. [23] identified [1,2,3]triazolo[4,5-*d*]pyrimidin-7(6*H*)-ones as active inhibitors of CHIKV replication in the low micromolar range with no cytotoxicity detected up to 668 μM. The synthetic procedure for the most active compounds **4b** as shown in Scheme 3 includes (3 + 2) cycloaddition between an arylazide and a cyanoacetamide to give a 5-aminotriazole amide. Subsequent condensation followed by ring formation produces the target triazolopyrimidine **4b**.

B. Nucleosides

During the past five decades, nucleosides have been used in clinics and, nowadays, become cornerstones of treatment for patients with viral infections. Two drugs in this family were reported with anti-CHIKV activity in 2004 [24]. Ribavirin (**5**), a "synthetic nucleoside" containing a 1*H*-1,2,4-triazole moiety, is effective against a variety of RNA viruses, especially in the genus *Alphavirus*. The combination of ribavirin and interferon-α shows a synergistic anti-chikungunya viral effect [24]. Several studies have elucidated the mechanisms of anti-viral action of ribavirin. They involve predominantly inhibition of inosine monophosphate dehydrogenase (IMPDH) activity, depletion of the intracellular guanosine triphosphate (GTP) pools, inhibition of viral RNA capping, and induction of an error catastrophe [14, 37–39].

6-Azauridine (**6**) [24], containing a 1,2,4-triazine-3,5(2*H*,4*H*)-dione moiety, is an another "synthetic nucleoside" with a broad-spectrum of anti-metabolite. It inhibits both DNA and RNA virus replication. In comparison with ribavirin (**5**), 6-azauridine (**6**) shows a greater potency against CHIKV with EC_{50} = 0.82 μM and

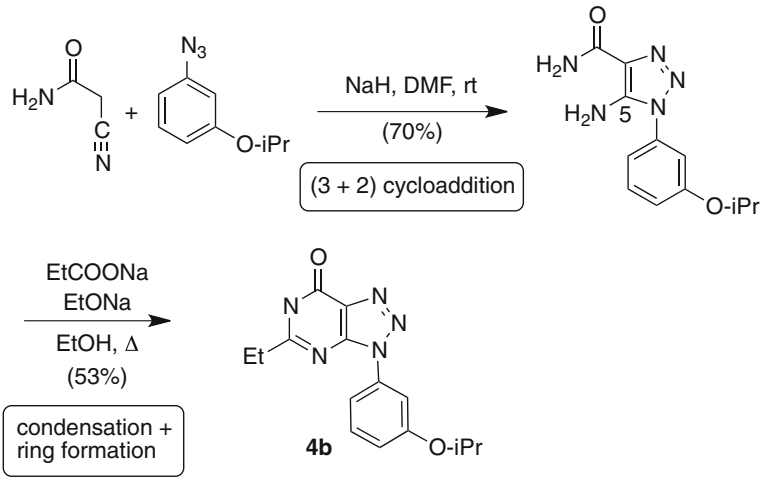

Scheme 3 Synthesis of triazolopyrimidine **4b**

SI = 254. Its activity might be through the inhibition of orotidine monophosphate decarboxylase activity and the depletion of uridine triphosphate pools [40].

C. Alkaloids

Favipiravir (**7**) is a pyrazinecarboxamide derivative, which was discovered and synthesized by Toyama Chemical Co. in Japan as a candidate antiviral drug [41]. It is active against many viruses, including influenza viruses, West Nile virus, yellow fever virus, foot-and-mouth disease virus, flaviviruses, arenaviruses, bunyaviruses, alphaviruses, picornavirus and norovirus [41, 42]. In 2014, favipiravir (**7**) was approved in Japan for the treatment of influenza virus disease. The mechanism of its action is related to the selective inhibition of viral RNA-dependent RNA polymerase. In the same year, Neyts et al. [25] disclosed that favipiravir (**7**) inhibits viral genome replication of laboratory strains and clinical isolates of CHIKV.

The antiviral drug umifenovir (i.e., arbidol, **8**), an indole derivative, was originally developed at the Research Institute of Pharmaceutical Chemistry in Russia about three decades ago [43]. Since 1990, this drug has been used in Russia mainly for the intervention of prophylaxis and acute respiratory infections like influenza [44, 45]. In 2011, Pastorino et al. [26] reported that umifenovir (**8**) presents potent inhibitory activity against CHIKV. The significant anti-viral activity of this drug may be attributed to the diverse mechanisms of action, including interference with the early stages of CHIKV attachment or entry or the replication cycle, as well as alterations of cellular membranes [44, 46]. A synthetic procedure leading to umifenovir (**8**) as illustrated in Scheme 4 includes seven steps, for which the key steps are the Friedel–Crafts alkylation, reductive cyclization, and the Mannich condenation [43, 47]. On the other hand, this drug can also be produced through four steps as shown in the synthetic route in Scheme 5. They involve Nenitzescu indole synthesis, acylation/bromination, *S*-alkylation, and the Mannich condensation [48, 49].

Recently, de Lamballerie, Jayaprakash et al. [27] reported a series of aryl alkylidene alkaloids, among which 1,3-thiazolidin-4-ones **9** and **10** showed anti-chikungunya activity with IC_{50} values of 0.42 and 6.8 μM. These two compounds can be synthesized by simple steps shown in Scheme 6 [50, 51]. The key step is the Knoevenagel condensation. Moreover, the authors performed molecular docking simulation of the active compound **9** with the X-ray crystal structure of CHIKV nsP2 protease. As a result, the mechanism of action may come from the protease inhibition.

Harringtonine (**11**) is a natural alkaloid isolated from the Japanese plum yew, *Cephalotaxus harringtonia* in only 0.0064% yield [52]. In 2013, Chu et al. [28]. reported that it exhibits potent anti-CHIKV activity with an EC_{50} value of 0.24 μM with minimal cytotoxicity. Harringtonine inhibits an early stage of the CHIKV replication cycle, affects CHIKV RNA production, and interferes with viral protein expression.

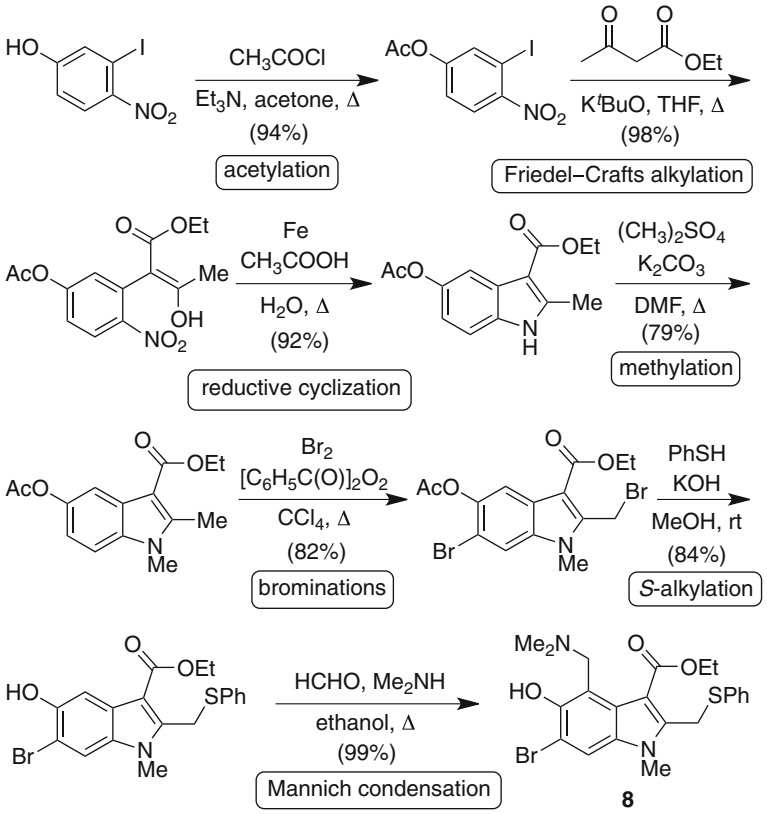

Scheme 4 Total synthesis of umifenovir (**8**)

D. Terpenoids

As a major class of natural compounds, terpenoids display a wide range of biological activity against a variety of infectious diseases. The four representatives shown in Table 1 contribute significantly to the anti-CHIKV development.

In 2014, Litaudon et al. [29] reported their isolation of diterpene jatrophane ester (**12**) in 0.0006% yield from the whole plant of *Euphorbia amygdaloides ssp. Semiperfoliata*, an endemic plant of Corsica and Sardinia. Jatrophane ester (**12**) shows an EC_{50} value of 0.76 μM with a high SI value of 208.

In the same year, Chu et al. [30] disclosed their isolation of two aplysiatoxin-related compounds **13a**,**b** from the marine cyanobacterium *Trichodesmium erythraeum* in ~0.0022% yield. These two 12-membered ring terpenes exhibit significant anti-CHIKV activity in post-treatment of infected SJCRH30 cells with EC_{50} values of 1.3 and 2.7 μM, respectively. Their potency is on the same order as that of the highly-oxygenated natural trigocherrin A (**14**) [31]. This chlorinated daphnane diterpene orthoester was isolated from the bark of *Trigonostemon cherrieri* in

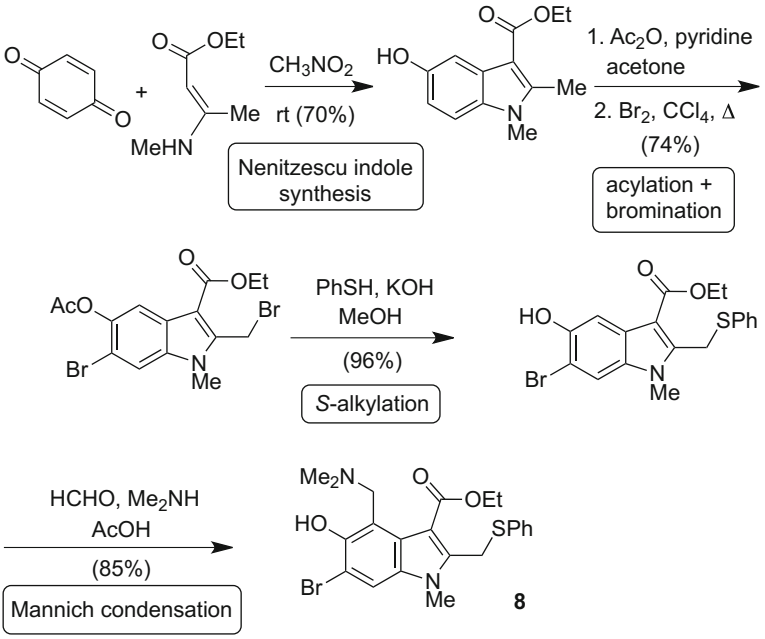

Scheme 5 Total synthesis of umifenovir (**8**)

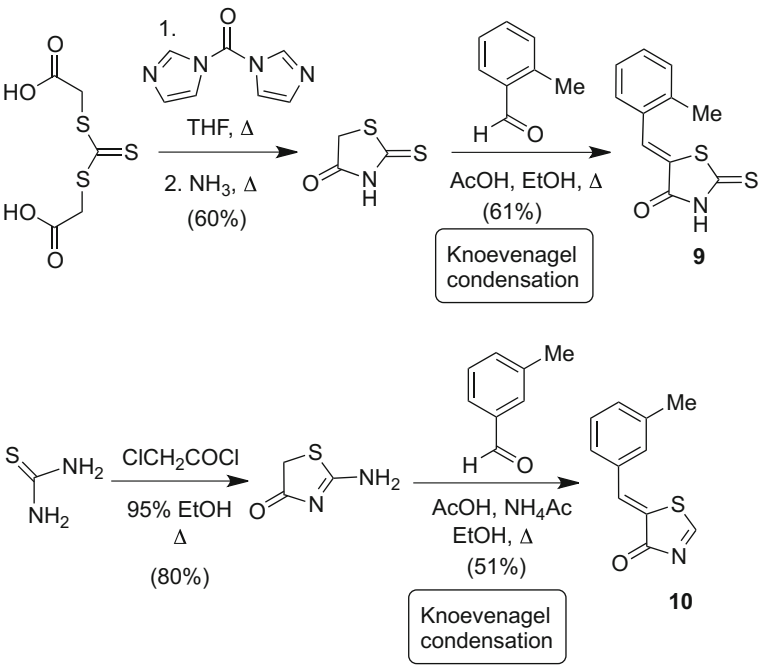

Scheme 6 Synthesis of 1,3-thiazolidin-4-ones **9** and **10**

0.00017% yield, an endemic plant of New Caledonia [53]. Nevertheless, they are much less potent in comparison with 12-*O*-tetradecanoylphorbol 13-acetate (**15**) [54], which was reported by Litaudon et al. in 2012 [32]. Tetradecanoyl phorbol acetate **15** presents an EC_{50} value of 2.9 nM with a very high SI value of 1965. The activation of the signal transduction enzyme protein kinase C could be the mechanism of action on its anti-CHIKV activity.

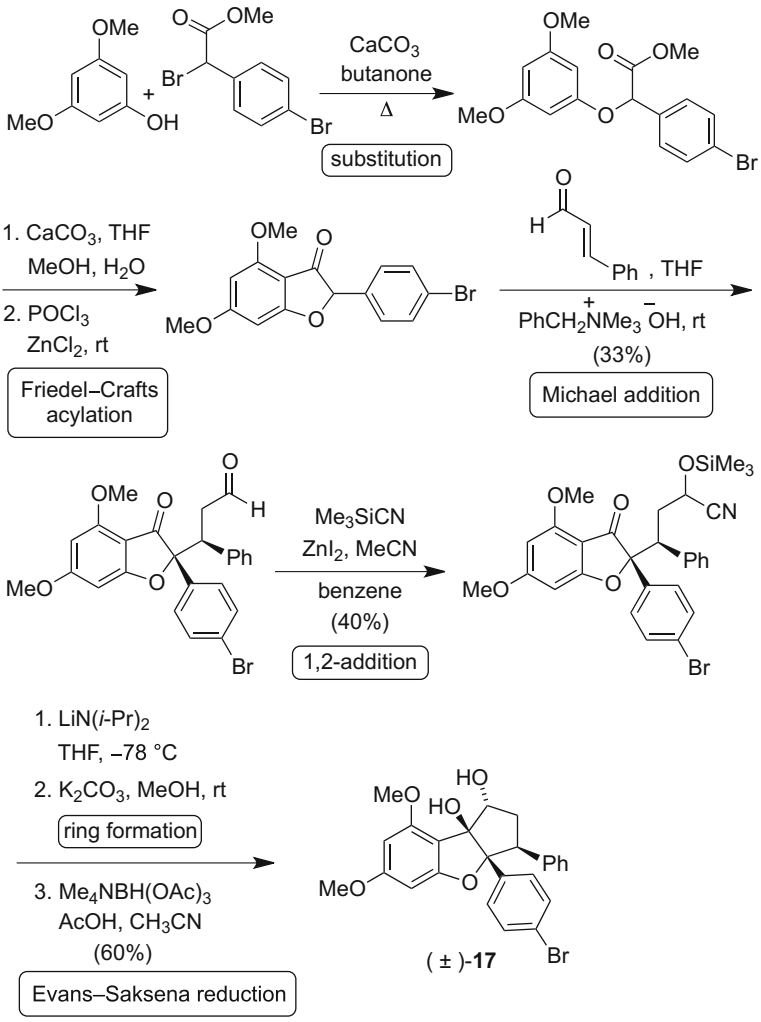

Scheme 7 Synthesis of flavagline (±)−**17**

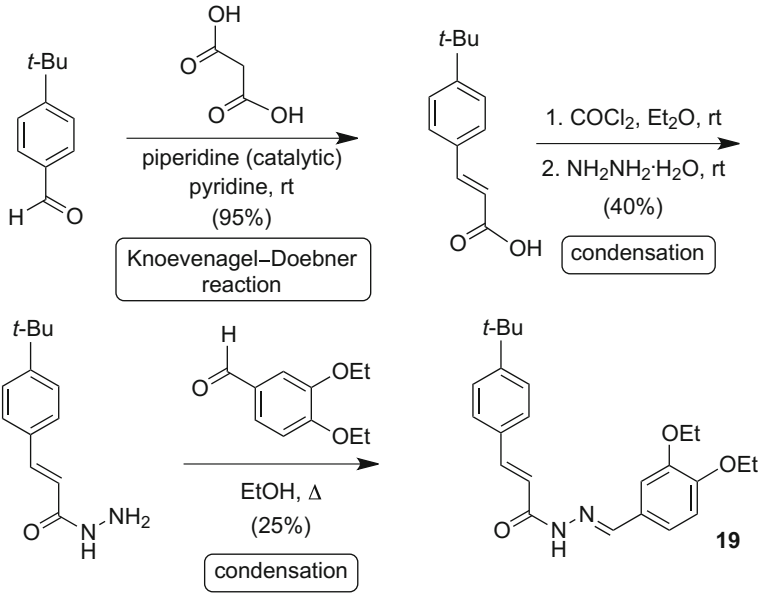

Scheme 8 Preparation of (α-carbonyl)hydrazone **19**

E. Flavagline

Plant natural products flavaglines are characterized with a unique cyclopenta [*b*]benzofuran nuclues. Fused benzofurans display an array of biological effects as insecticidal, antifungal, anti-inflammatory, and neuroprotective agents [55]. In 2015, Smith et al. [33] reported that flavaglines FL23 (**16**) and FL3 (**17**) inhibit the CHIKV by interaction with prohibitin-1, which is a receptor protein used by the virus to enter mammalian cells. The synthetic route to give flavaglines FL3 (±)-(**17**) is shown in Scheme 7. The key steps include the Friedel–Craft acylative cyclization, the Michael addition, and Evans–Saksena reduction reactions [56, 57].

Others

Apart from the above classes of compounds, Freitas–Junior et al. [34] screened a kinase inhibitor library of 4000 compounds against CHIKV infection by using high throughput screening. In 2013, they reported that four benzofuran derivatives were active as inhibitors associated with CHIKV cell death in a dose-dependent manner. Compounds with a scaffold as benzofuran **18** (CND0335) exhibit the EC_{50} values of between 2.2 and 7.1 μM.

Brancale et al. [35] reported their computer-aided identification and design of a series of (α-carbony)hydrazones with selective activity against CHIKV. They initially obtained the hit candidates from a virtual screening simulation of ∼5 million compounds on the CHIKV nsP2. After investigation of their structure–activity relationship in silico and optimization of the candidate compounds, a simplified

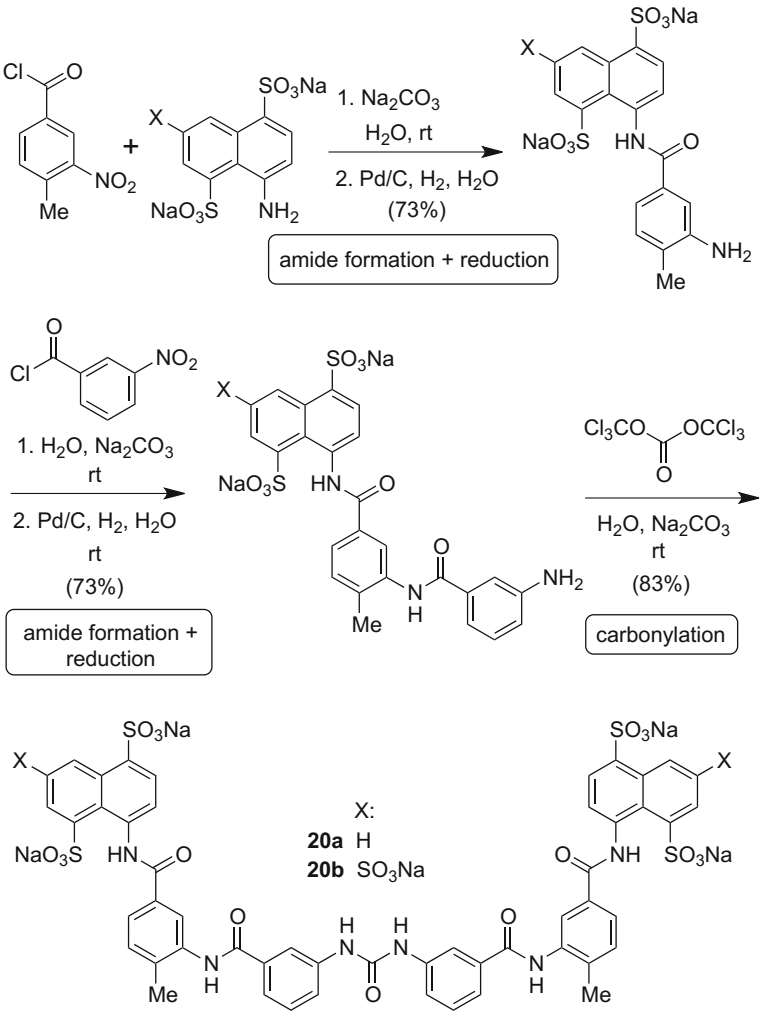

Scheme 9 Synthesis of suramin and its derivative **20a**,**b**

chemical structure (α-carbonyl)hydrazone **19** was attained. Synthesis of compound **19** is illustrated in Scheme 8, in which sequential Knoevenagel–Doebner reaction and condensation reactions are in operation. This compound indeed exhibits promising activity profile as shown in Table 1.

In 2015, van Hemert et al. [36] first reported that the approved anti-parasitic drug suramin (**20b**) inhibits CHIKV RNA synthesis with an IC_{50} value of ~5 μM. It also inhibits replication of various CHIKV isolates in cell culture with an EC_{50} of 79 μM and CC_{50} >800 μM. Furthermore, suramin can inhibit a post-attachment early step of the CHIKV replicative cycle and (re)initiation of CHIKV RNA synthesis by possibly interfering with binding of the template RNA. These findings are

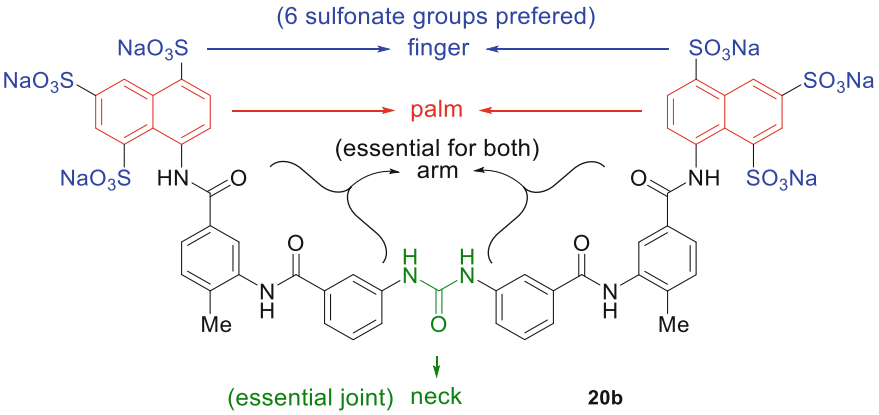

Fig. 2 Structure–activity relationship of suramin and its derivatives

in agreement with the previous studies in vitro that suramin inhibits RNA viral polymerases and helicases [36]. Very soon, closely related results on inhibition of the same virus entry and transmission by suramin (**20b**) is reported by Kuo, Lin et al. [58].

A series of suramin derivatives (e.g., **20a**) were synthesized by Bolognesi, Hwu et al. [59] based on the design of compounds with fewer sulfonate fingers, shorter arms, only one side, or no neck in comparison with suramin. As depicted in Scheme 9, the representative procedure includes amide formation, followed by reduction of nitro compounds and carbonylation. These suramin derivatives were also tested for their ability to inhibit CHIKV RNA synthesis in vitro. Unsymmetrical compounds possessing only one arm were inactive regardless of its length. It has been proved that compound with six sulfonate groups showed greater anti-CHIKV (EC_{50} = 79 μM) than tetrasulfonate (EC_{50} = 210 μM) in the cell culture (see Table 1 and Fig. 2).

3 Concluding Remarks

Development of new antiviral compounds for chikungunya fever meets an urgent need of global societies. It is due to the re-emerged outbreaks occurring in 2004 and recent spreading to the Americas in late 2013. A limited number of natural products exhibit great potency with an appealing selective index value. Unfortunately, their isolation yields are often very low, as represented by the naturally occurring 12-*O*-tetradecanoylphorbol 13-acetate (**15**) obtained in 0.00017% yield. Complex structures associated with these natural products with multiple stereogenic centers, various functional groups, and several rings make their total synthesis very challenging.

As a result, medicinal chemists, biologists, and virologists with interdisciplinary expertise have been seeking for unnatural targets that can be obtained in a large quantity by chemical synthesis. By far, various types of compounds with anti-CHIKV activity have been obtained; among which the ones reported recently are listed in the Table 1. These compounds belong to purine/pyrimidine, nucleoside, alkaloid, flavagline, etc. Nevertheless, none of them has been yet approved as a drug to serve the purpose. The opportunity remains high for scientists to devote their efforts to design and synthesize small molecules to fight for the human battle against CHIKV with success.

Moreover, some molecules in the compound libraries of the Table 1, such as benzouracil–coumarin–arene conjugates, suramin derivatives et al. may be suitable for their development to become potential new drugs for the treatment of neurodegenerative disorders. Multi-functional design, in silico computational screening, in vitro/ex vivo/in vivo experiments, and organic syntheses of these novel candidate compounds are in progress.

References

1. Thiberville S-D, Moyen N, Dupuis–Maguiraga L, Nougairede A, Gould EA, Roques P, de Lamballerie X (2013) Chikungunya fever: epidemiology, clinical syndrome, pathogenesis and therapy. Antiviral Res 99:345–370.
2. Weaver SC, Forrester NL (2015) Chikungunya: evolutionary history and recent epidemic spread. Antiviral Res 120:32–39.
3. Leo YS, Chow ALP, Tan LK, Lye DC, Lin L, Ng LC (2009) Chikungunya outbreak, Singapore, 2008. Emerg Infect Dis 15:836–837.
4. Rianthavorn P, Prianantathavorn K, Wuttirattanakowit N, Theamboonlers A, Poovorawan Y (2010) An outbreak of chikungunya in southern Thailand from 2008 to 2009 caused by African strains with A226 V mutation. Int J Infect Dis 14S:e161–e165.
5. Dupont–Rouzeyrol M, Caro V, Guillaumot L, Vazeille M, D'Ortenzio E, Thiberge J-M, Baroux N, Gourinat A-C, Grandadam M, Failloux A-B (2012) Chikungunya virus and the mosquito vector *Aedes aegypti* in New Caledonia (South Pacific region). Vector Borne Zoonotic Dis 12:1036–1041.
6. Delisle E, Rousseau C, Broche B, Leparc–Goffart I, L'Ambert G, Cochet A, Prat C, Foulongne V, Ferré JB, Catelinois O, Flusin O, Tchernonog E, Moussion IE, Wiegandt A, Septfons A, Mendy A, Moyano MB, Laporte L, Maurel J, Jourdain F, Reynes J, Paty MC, Golliot F (2015) Chikungunya outbreak in Montpellier, France, September to October 2014. Euro Surveill 20: pii=21108.
7. McSweegan E, Weaver SC, Lecuit M, Frieman M, Morrison TE, Hrynkow S (2015) The global virus network: challenging chikungunya. Antiviral Res 120:147–152.
8. Scholte FEM, Tas A, Albulescu IC, Žusinaite E, Merits A, Snijder EJ, van Hemert MJ (2015) Stress granule components G3BP1 and G3BP2 play a proviral role early in chikungunya virus replication. J Virol 89: 4457–4469.
9. Schwartz O, Albert ML (2010) Biology and pathogenesis of chikungunya virus. Nat Rev Microbiol 8: 491–500.
10. Chandak NH, Kashyap RS, Kabra D, Karandikar P, Saha SS, Morey SH, Purohit HJ, Taori GM, Daginawala HF (2009) Neurological complications of chikungunya virus infection. Neurol India 57: 177–180.

11. Pialoux G, Gaüzère BA, Jauréguiberry S, Strobel M (2007) Chikungunya, an epidemic arbovirosis. Lancet Infect Dis 7: 319–327.
12. Rashad AA, Mahalingam S, Keller PA (2014) Chikungunya virus: emerging targets and new opportunities for medicinal chemistry. J Med Chem 57: 1147–1166.
13. Kaur P, Chu JJH (2013) Chikungunya virus: an update on antiviral development and challenges. Drug Discov Today 18: 969–983.
14. Abdelnabi R, Neyts J, Delang L (2015) Towards antivirals against chikungunya virus. Antiviral Res 121: 59–68.
15. Bhakat S, Soliman MES (2015) Chikungunya virus (CHIKV) inhibitors from natural sources: a medicinal chemistry perspective. J Nat Med 69: 451–462.
16. Couderc T, Lecuit M (2015) Chikungunya virus pathogenesis: from bedside to bench. Antiviral Res 121: 120–131.
17. Singh SK, Unni SK (2011) Chikungunya virus: host pathogen interaction. Rev Med Virol 21: 78–88.
18. Birendra VK, Vishwabhan S, Uttam J, Vishal S (2012) A review on chikungunya virus. IRJP 3: 58–60.
19. Parashar D, Cherian S (2014) Antiviral perspectives for chikungunya virus. BioMed Research International http://dx.doi.org/10.1155/2014/631642.
20. Lum FM, Ng LFP (2015) Cellular and molecular mechanisms of chikungunya pathogenesis. Antiviral Res 120: 165–174.
21. D'hooghe M, Mollet K, Vreese RD, Jonckers THM, Dams G, De Kimpe N (2012) Design, synthesis, and antiviral evaluation of purine–β-lactam and purine–aminopropanol hybrids. J Med Chem 55: 5637–5641.
22. Hwu JR, Kapoor M, Tsay S-C, Lin C-C, Hwang KC, Horng J-C, Chen I-C, Shieh F-K, Leyssen P, Neyts J (2015) Benzouracil–coumarin–arene conjugates as inhibiting agents for chikungunya virus. Antiviral Res 118: 103–109.
23. Gigante A, Canela M-D, Delang L, Priego E-M, Camarasa M-J, Querat G, Neyts J, Leyssen P, Pérez–Pérez M-J (2014) Identification of [1,2,3]Triazolo[4,5-*d*]pyrimidin-7(6H)-ones as novel inhibitors of chikungunya virus replication. J Med Chem 57: 4000–4008.
24. Briolant S, Garin D, Scaramozzino N, Jouan A, Crance JM (2004) In vitro inhibition of Chikungunya and Semliki Forest viruses replication by antiviral compounds: synergistic effect of interferon-α and ribavirin combination. Antiviral Res 61: 111–117.
25. Delang L, Guerrero NS, Tas A, Quérat G, Pastorino B, Froeyen M, Dallmeier K, Jochmans D, Herdewijn P, Bello F, Snijder EJ, de Lamballerie X, Martina B, Neyts J, van Hemert MJ, Leyssen P (2014) Mutations in the chikungunya virus non-structural proteins cause resistance to favipiravir (T-705), a broad-spectrum antiviral. J Antimicrob Chemother 69: 2770–2784.
26. Delogu I, Pastorino B, Baronti C, Nougairède A, Bonnet E, de Lamballerie X (2011) In vitro antiviral activity of Arbidol against chikungunya virus and characteristics of a selected resistant mutant. Antiviral Res 90: 99–107.
27. Jadav SS, Sinha BN, Hilgenfeld R, Pastorino B, de Lamballerie X, Jayaprakash V (2015) Thiazolidone derivatives as inhibitors of chikungunya virus. Eur J Med Chem 89: 172–178.
28. Kaur P, Thiruchelvan M, Lee RCH, Chen H, Chen KC, Ng ML, Chu JJH (2013) Inhibition of chikungunya virus replication by harringtonine, a novel antiviral that suppresses viral protein expression. Antimicrob Agents Chemother 57: 155–167.
29. Nothias–Scaglia L-F, Retailleau P, Paolini J, Pannecouque C, Neyts J, Dumontet V, Roussi F, Leyssen P, Costa J, Litaudon M (2014) Jatrophane diterpenes as inhibitors of chikungunya virus replication: structure–activity relationship and discovery of a potent lead. J Nat Prod 77: 1505–1512.
30. Gupta DK, Kaur P, Leong ST, Tan LT, Prinsep MR, Chu JJH (2014) Anti-chikungunya viral activities of aplysiatoxin-related compounds from the marine cyanobacterium *trichodesmium erythraeum.* Mar Drugs 12: 115–127.

31. Allard P-M, Leyssen P, Martin M-T, Bourjot M, Dumontet V, Eydoux C, Guillemot J-C, Canard B, Poullain C, Guéritte F, Litaudon M (2012) Antiviral chlorinated daphnane diterpenoid orthoesters from the bark and wood of *Trigonostemon cherrieri*. Phytochemistry 84: 160–168.
32. Bourjot M, Delang L, Nguyen VH, Neyts J, Guéritte F, Leyssen P, Litaudon M (2012) Prostratin and 12-*O*-tetradecanoylphorbol 13-acetate are potent and selective inhibitors of chikungunya virus replication. J Nat Prod 75: 2183–2187.
33. Wintachai P, Thuaud F, Basmadjian C, Roytrakul S, Ubol S, Désaubry L, Smith DR (2015) Assessment of flavaglines as potential chikungunya virus entry inhibitors. Microbiol Immunol 59: 129–141.
34. Cruz DJM, Bonotto RM, Gomes RGB, da Silva CT, Taniguchi JB, No JH, Lombardot B, Schwartz O, Hansen MAE, Freitas-Junior LH (2013) Identification of novel compounds inhibiting chikungunya virus–induced cell death by high throughput screening of a kinase inhibitor library. PLoS Negl Trop Dis 7: e2471.
35. Bassetto M, Burghgraeve TD, Delang L, Massarotti A, Coluccia A, Zonta N, Gatti V, Colombano G, Sorba G, Silvestri R, Tron GC, Neyts J, Leyssen P, Brancale A (2013) Computer-aided identification, design and synthesis of a novel series of compounds with selective antiviral activity against chikungunya virus. Antiviral Res 98: 12–18.
36. Albulescu IC, van Hoolwerff M, Wolters LA, Bottaro E, Nastruzzi C, Yang SC, Tsay S-C, Hwu JR, Snijder EJ, van Hemert MJ (2015) Suramin inhibits chikungunya virus replication through multiple mechanisms. Antiviral Res 121:39–46.
37. Leyssen P, De Clercq E, Neyts J (2006) The anti-yellow fever virus activity of ribavirin is independent of error-prone replication. Mol Pharmacol 69: 1461–1467.
38. Paeshuyse J, Dallmeier K, Neyts J (2011) Ribavirin for the treatment of chronic hepatitis C virus infection: a review of the proposed mechanisms of action. Curr Opin Virol 1: 590–598.
39. Rothan HA, Bahrani H, Mohamed Z, Teoh TC, Shankar EM, Rahman NA, Yusof R, (2015) A combination of doxycycline and ribavirin alleviated chikungunya infection. PLoS ONE 10: e0126360.
40. Rada B, Dragun M (1977) Antiviral action and selectivity of 6-azauridine. Ann NY Acad Sci 284: 410–417.
41. Furuta Y, Takahashi K, Shiraki K, Sakamoto K, Smee DF, Barnard DL, Gowen BB, Julander JG, Morrey JD (2009) T-705 (favipiravir) and related compounds: novel broad-spectrum inhibitors of RNA viral infections. Antiviral Res 82: 95–102.
42. Furuta Y, Gowen BB, Takahashi K, Shiraki K, Smee DF, Barnard DL (2013) Favipiravir (T-705), a novel viral RNA polymerase inhibitor. Antiviral Res 100: 446–454.
43. Panisheva EK, Nikolaeva IS, Galenko-Yaroshevskii PA, Bartashevich VV, Cherkasova AA, Linchenko SN, Egik'yan AL, Golovanova EA, Pushkina TV (1988) Synthesis and biological activity of substituted 5-hydroxy-6-bromoindoles. Khim-Farm Zh 22: 565–569.
44. Boriskin YS, Leneva IA, Pécheur E-I, Polyak SJ (2008) Arbidol: a broad-spectrum antiviral compound that blocks viral fusion. Curr Med Chem 15: 997–1005.
45. Leneva IA, Russell RJ, Boriskin YS, Hay AJ (2009) Characteristics of Arbidol-resistant mutants of influenza virus: implications for the mechanism of anti-influenza action of Arbidol. Antiviral Res 81: 132–140.
46. Blaising J, Polyak SJ, Pécheur E-I (2014) Arbidol as a broad-spectrum antiviral:an update. Antiviral Res 107: 84–94.
47. Trofimov FA, Tsyshkova NG, Zotova SA, Grinev AN (1993) Synthesis of a new antiviral agent, Arbidole. Khim-farm Zh 27: 70–71.
48. Barraja P, Diana P, Montalbano A, Martorana A, Carbone A, Cirrincione G (2009) Synthesis of the new ring system 2-oxo-[1,4]oxazino[3,2-*e*]indole, heteroanalogue of Angelicin. Tetrahedron Lett 50: 4182–4184.
49. Chai H, Zhao Y, Zhao C, Gong P (2006) Synthesis and in vitro anti-hepatitis B virus activities of some ethyl 6-bromo-5-hydroxy-1*H*-indole-3-carboxylates. Bioorg Med Chem 14: 911–917.

50. Harada K, Kubo H, Abe J, Haneta M, Conception A, Inoue S, Okada S, Nishioka K (2012) Discovery of potent and orally bioavailable 17β-hydroxysteroid dehydrogenase type 3 inhibitors. Bioorg Med Chem 20: 3242–3254.
51. Al-Ansary GH, Ismail MAH, Ella DAAE, Eid S, Abouzid KAM (2013) Molecular design and synthesis of HCV inhibitors based on thiazolone scaffold. Eur J Med Chem 68: 19–32.
52. Powell RG (1972) Structures of homoerythrina alkaloids from *cephalotaxus harringtonia*. Phytochemistry 11: 1467–1472.
53. Allard P-M, Martin M-T, Tran Huu Dau M-E, Leyssen P, Guéritte F, Litaudon M (2012) Trigocherrin A, the first natural chlorinated daphnane diterpene orthoester from *Trigonostemon cherrieri*. Org Lett 14: 342–345.
54. El-Mekkawy S, Meselhy MR, Nakamura N, Hattori M, Kawahata T, Otake T (2000) Anti-HIV-1 phorbol esters from the seeds of *Croton tiglium*. Phytochemistry 53: 457–464.
55. Ribeiro N, Thuaud F, Nebigil C, Désaubry L (2012) Recent advances in the biology and chemistry of the flavaglines. Bioorg Med Chem 20: 1857–1864.
56. Bruce I, Cederbaum F, Cooke NG, Diorazio LJ, Dobler M, Hall RG, Szczepanski H (2000) Cyclopentabenzofuran-derivatives. Ger Offen DE 199 34 952 A 1 3 Feb 2000.
57. Thuaud F, Bernard Y, Turkeri G, Dirr R, eve Aubert G, Cresteil T, Baguet A, Tomasetto C, Svitkin Y, Sonenberg N, Nebigil CG, Désaubry L (2009) Synthetic analogue of rocaglaol displays a potent and selective cytotoxicity in cancer cells: involvement of apoptosis inducing factor and caspase-12. J Med Chem 52: 5176–5187.
58. Ho YJ, Wang YM, Lu JW, Wu TY, Lin LI, Kuo SC, Lin CC (2015) Suramin inhibits chikungunya virus entry and transmission. PLoS ONE 10: e0133511.
59. Croci R, Pezzullo M, Tarantino D, Milani M, Tsay S-C, Sureshbabu R, Tsai YJ, Mastrangelo E, Rohayem J, Bolognesi M, Hwu JR (2014) Structural bases of norovirus RNA dependent RNA polymerase inhibition by novel suramin-related compounds. PLoS ONE 9: e91765.

Analytical Standards Purity Determination Using Quantitative Nuclear Magnetic Resonance

Toru Miura, Naoki Sugimoto, Takako Suematsu, Kevin K. Millis, Katsuo Asakura and Yuko Yamada

Abstract Quantitative nuclear magnetic resonance (qNMR) with Internal Standard named as AQARI (*A*ccurate *Q*u*A*ntitative NM*R* with *I*nternal standard material) has been adopted by the Japanese Pharmacopoeia and the Japanese Standard of Food Additives as an official analytical method because of reliability and efficiency. We have developed Certified Reference Material (CRM) suitable for AQARI and utilitized AQARI with developed CRM to characterize analytical standards and certified reference materials (CRMs) for use in developing qNMR and chromatographic calibration standards. AQARI was used to determine the chemical purity of analytical standards for more than 500 compounds, including the following seven Japanese Pharmacopoeia crude drug products: magnolol, geniposide, paeonol, magnoflorine Iodide, saikosaponin b_2, (*E*)-cinnamic acid and rosmarinic acid.

Keywords qNMR · AQARI · Internal standard · CRM · Analytical standard

1 Introduction

With the revision of the Food Sanitation Act, a "positive list system" relating to pesticide residues came into force in Japan in May of 2006 [1], resulting in tightened regulations for the distribution of approximately 800 types of pesticides,

T. Miura (✉) · Y. Yamada
Wako Pure Chemical Industries Ltd., 1633, Matoba, Kawagoe-shi
Saitama 350-1101, Japan
e-mail: miura.toru@wako-chem.co.jp

N. Sugimoto
National Institute of Health Science (NIHS), 1-18-1, Kamiyoga,
Setagaya-ku, Tokyo 158-8501, Japan

T. Suematsu · K. Asakura
JEOL RESONANCE Inc., 3-1-2, Musashino, Akishima-shi, Tokyo 196-8558, Japan

K.K. Millis
Cambridge Isotope Laboratories Inc., 3 Highwood Drive, Tewksbury, MA 01876, USA

K. Tomioka et al. (eds.), *New Horizons of Process Chemistry*,
DOI 10.1007/978-981-10-3421-3_20

both inside and outside Japan. Internationally, the number of chemicals subject to regulations, such as persistent organic pesticides (POPs), and the chemicals listed in the Restriction of Hazardous Substances (RoHS) directive and the Registration, Evaluation, Authorization and Restriction of Chemicals (REACH) legislation are continually increasing. Generally, the analysis of these hazardous substances must be performed in accordance with official analytical methods which include gas chromatography (GC) and high-performance liquid chromatography (HPLC).

The advantages of GC and HPLC, such as high sensitivity and analyte separation, are very suitable for the analysis of both single- and multi-component solutions. In this type of analysis, a calibration curve using an analytical standard that is identical to the target analyte is required to conduct accurate quantitative measurements [2]. Depending on the results of such analyses, this type of analysis may lead to development of international issues through regulation of the distribution of imported products. It also relates directly to food safety assurance, and thus accurate measurement results are needed and are extremely important to assure the reliability of characteristic values for the analytical standard used [2]. In addition, as the number of controlled substances under the regulations has increased significantly, these analytical standards should be supplied to the market promptly. Based on these background issues, we have been proactively supplying analytical standards for the measurement of pesticide residues. Historically, we have utilized GC and HPLC methods that confer purity by normalization of peak areas according to the official analytical method such as official gazette, however, the purity measured with these methods can be prone to error because the degree of sensitivity differs depending on the main constituent and the impurities. This situation has led us to start using the other analytical method for determining the chemical purity of our analytical standards which is more robust than chromatographic methods. The first option we tried to utilize was the mass balance method which is able to determine the absolute purity. But this method is complicated and time-consuming one. Therefore we tried to utilize AQARI as second option which is able to determine the absolute purity with reliability and efficiency.

2 AQARI

Quantitative nuclear magnetic resonance (qNMR) refers to when NMR data is collected and processed in a manner that yields quantitative information. qNMR relies on a reference NMR signal as an intensity calibration reference. The reference NMR signal may be purely electronic or may originate from a reference standard. The reference standard may be "external" (i.e., the standard solution is in a sealed capillary tube that is run separately or together with the sample) or "internal" (i.e., the reference standard is dissolved in the sample). AQARI (*A*ccurate *Q*u*A*ntitative NM*R* with *I*nternal standard material) [3] is a ^{1}H qNMR method that uses an internal standard.

qNMR requires the NMR data to be acquired under quantitative conditions [4]. When this is achieved, peak areas for resonances become proportional to the number of hydrogen nuclei producing the resonances [5]. Therefore, when measuring mixtures under quantitative conditions, the area of well-resolved resonances arising from different molecules are not only proportional to the number of hydrogen nuclei giving rise to the resonances, but are also proportional to the concentration of the different molecules that are present in the sample [5]. Utilizing this property enables standard measurement of the mass of the target substance and the mass of other substances that could be present in the sample [5].

AQARI requires a substance that has been allocated an accurate degree of purity (hereafter referred to as the Internal Standard) to be quantitatively added and dissolved in the sample solution before the ^{1}H NMR measurement is conducted. Once the spectrum is obtained, the molar ratio of the target molecule to the internal standard is calculated from the peak area ratio originating from each substance. Finally, the chemical purity of the measured substance can be calculated using this molar ratio.

qNMR can be used to rapidly conduct purity determination, which was previously conducted via complicated quantification methods, such as Area Normalization Method of GC or HPLC. Attractive features of qNMR include easy sample preparation, the ability to achieve absolute quantification with traceability to the International System of Units (SI), and the ability to quantitate more than one analyte in a single measurement. Due to the overall reliability of qNMR, and its ability to achieve absolution quantitation, qNMR has recently been adopted as an official analytical method by the Japanese Pharmacopoeia and the Japanese Standard of Food Additives [6, 7]. There are also plans for qNMR to be adopted by the Japanese Industrial Standards, as qNMR is currently seeing widespread use in the field of industrial chemistry.

We have started to shift towards a higher level of quality assurance by applying the superior characteristics of qNMR to the purity assessment of analytical standards.

3 Development of Certified Reference Material for AQARI, Sample Preparation, NMR Measurement, and Data Processing Conditions

The equation used to determine chemical purity using AQARI is shown in Fig. 1 [8]. In this equation, S_A, S_R, m_A, m_R, and P_R are the only variables that create variability and bias in the purity result. Therefore, to obtain accurate quantitative values with qNMR, the following conditions must be met:

3.1 A reliable internal standard with traceability to the International System of Units (SI) should be used

$$P = \frac{S_A}{S_R} \times \frac{H_R}{H_A} \times \frac{m_R}{m_A} \times \frac{Mw_A}{Mw_R} \times P_R$$

P : Calculated value of purity (mass fraction %)
S_A : Signal area of the sample target analyte
S_R : Signal area of the internal standard
H_A : Hydrogen number shown in the sample target analyte
H_R : Hydrogen number shown in the internal standard
m_A : Weighed the sample target analyte mass (mg)
m_R : Weighed the internal standard mass (mg)
Mw_A : Molar mass of the sample target analyte
Mw_R : Molar mass of the internal standard
P_R : Purity of the internal standard (mass fraction %)

Fig. 1 Purity equation for qNMR analysis

3.2 The mass of the analyte and internal standard used in sample preparation must be accurately measured
3.3 The NMR data must be acquired under quantitative NMR conditions
3.4 The NMR data must be processed under conditions suitable for quantitative measurements

We will now explain the development and setting of conditions for our internal standard, while explaining the elements shown below.

3.1 The Internal Standard

When we first began investigating the utility of qNMR, a dedicated internal standard for qNMR had not been distributed on the global market. This situation led us to develop qNMR standards for use in AQARI. The most important requirements for an ideal qNMR internal standard are the following: 1. The internal standard must have a simple 1H-NMR spectrum, preferably a single resonance; 2. The ^{1}H-NMR resonance from the internal standard must be baseline-resolved from all other resonances in the sample of which it is placed; 3. The internal standard must be chemically inert; 4. The internal standard must be stable in solution; 5. The internal standard substance must be easily handled and weighed to produce stable and accurate mass measurements; and 6. The internal standard must be soluble in deuterated solvents. Based on these requirements, we selected a number of candidate substances to determine if we could develop them into internal standards for qNMR. We used the freezing point depression method in DSC (Differential Scanning Calorimetry) to determine the purity of the internal standard candidates as one of the primary methods of measurement [2].

We also determined the associated expanded uncertainty for chemical purity. The uncertainty associated with the chemical purity of a standard determined by qNMR is a composite of uncertainties that arise from the purity of the internal standard, the analytical balances, and in the NMR measurement. The results of comparing the content acquired by qNMR to the content acquired with chromatography were synthesized with uncertainty to prevent a lowering of the accuracy due to the substance containing analogous compounds, thereby assuring the reliability of that

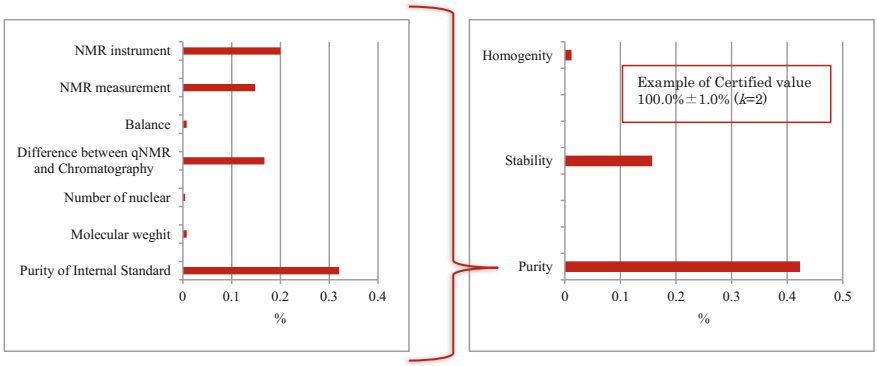

Fig. 2 Representative values for uncertainty components in developing certified reference materials for qNMR

value. Representative values of the contributions of uncertainties in the qNMR purity results for our Certified Reference Materials (CRMs) are shown in Fig. 2. Given that both qNMR and freezing point depression are measurement methods that, in principle, are traceable to the SI, it became possible to assure the measurement traceability of the analytical value, and develop a highly reliable internal standard for qNMR that conforms to, or is compliant with, ISO requirement [9].

As a result of these investigations, we started distributing 1,4-bis(trimethylsilyl) benzene-d_4 (1,4-BTMSB-d_4) and sodium 3-(trimethylsilyl)-1-propane-1,1,2,2,3,3-d_6-sulfonate (DSS-d_6), which were the first internal standards for AQARI for the first time on the global market in 2009. The typical ^{1}H NMR spectra of these two internal standards are shown in Figs. 3 and 4. As of 2016, we have developed four CRMs (Table 1), five standards for qNMR (Table 2).

These internal standards are extremely versatile, particularly 1,4-BTMSB-d_4 and DSS-d_6, which produce a specific signal close to 0 ppm, making them applicable to many types of compounds, and have been adopted in official methods, such as by the Japanese Pharmacopoeia [10]. Also, 3,5-bis(trifluoromethyl)benzoic acid, an NMIJ CRM, is a hybrid internal standard for qNMR compatible with both ^{1}H qNMR and ^{19}F qNMR, and has also attracted a great deal of international attention because it is currently the only CRM for qNMR that is offered by a national metrological institution.

3.2 Gravimetry of the Analyte and Internal Standard in Sample Preparation

The general qNMR measurement work-flow adopted by the Japanese Pharmacopoeia is shown in Fig. 5 [11]. It is only possible to obtain accurate results if all sample preparations, NMR measurements and data processing steps are

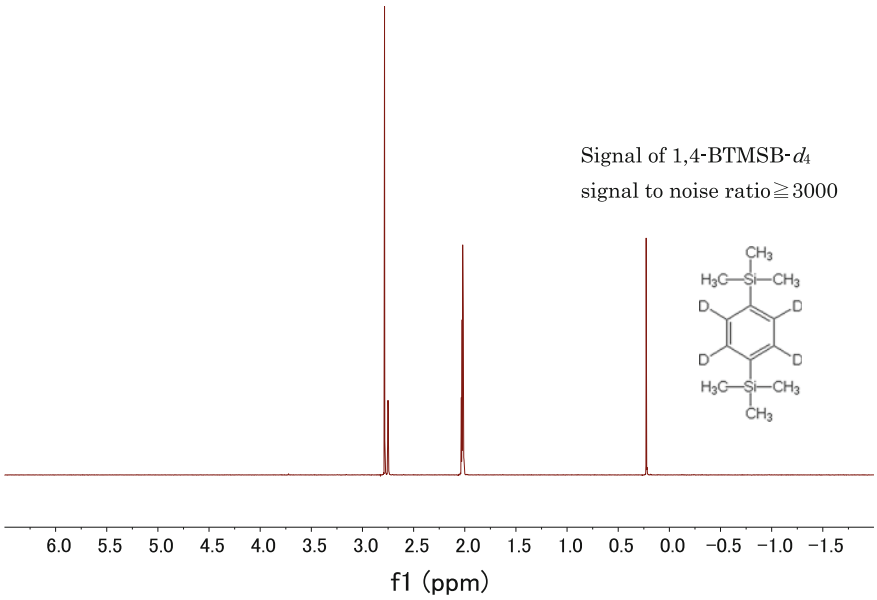

Fig. 3 ^{1}H NMR spectrum of 0.05%w/v 1,4-BTMSB-d_4 reference material in Acetone-d_6 measured by 400 MHz NMR instrument (JNM-ECS400 with NM-03510TH5 Probe) using the acquisition and processing parameters listed in Tables 3 and 4

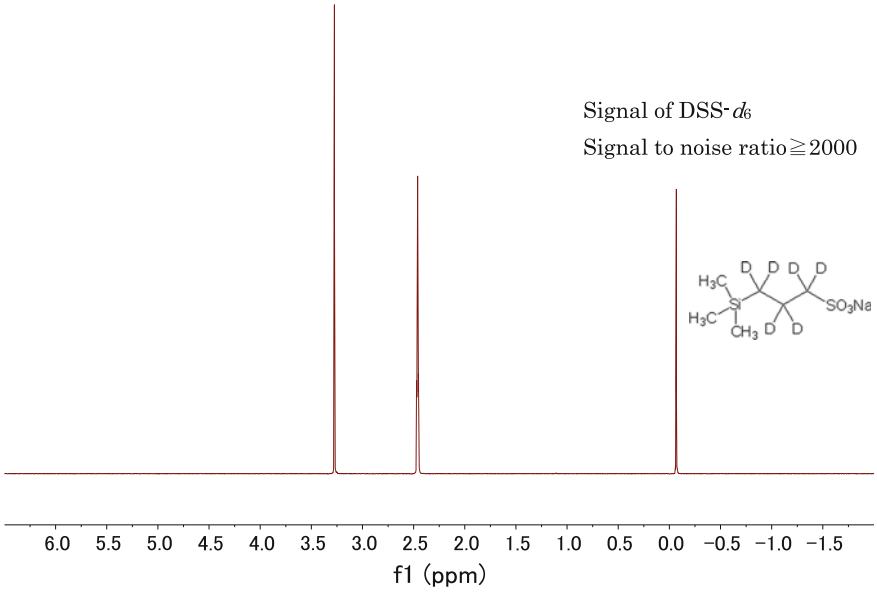

Fig. 4 ^{1}H NMR spectrum of 0.05%w/v DSS-d_6 reference material in Dimethyl Sulfoxide-d_6 measured by 400 MHz NMR instrument (JNM-ECS400 with NM-03510TH5 Probe) using the acquisition and processing parameters listed in Tables 3 and 4

Table 1 Certified reference materials for qNMR

Product name	Chemical shift δppm[a]
1,4-BTMSB-d_4 reference material	0.2
DSS-d_6 reference material	0.0
Dimethyl sulfone reference material	3.1
Maleic acid reference material	6.4

[a]It means that Chemical shifts may vary according to solvent type

Table 2 Standards for qNMR

Product name	Chemical shift δppm[a]
1,3,5-trimethoxybenzene standard	3.7, 6.1
Triphenylmethane Standard	5.6, 7.1–7.3
Benzoic acid standard	7.5, 7.6, 8.0
Dimethyl terephthalate standard	3.9, 8.1
Potassium hydrogen phthalate standard	7.5, 7.8

[a]Chemical shifts may vary according to solvent type

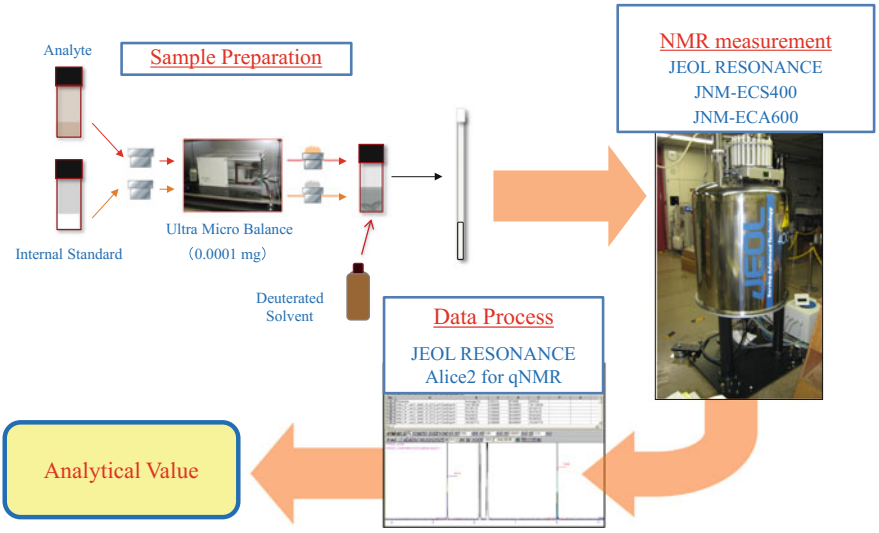

Fig. 5 General qNMR (AQARI) measurement work-flow

carefully implemented using practices compatible with qNMR. To ensure accurate gravimetry of the sample and internal standard, a stable balance read-out is necessary. Therefore, we developed an aluminum weighing dish for qNMR, which has a low mass and is less prone to static electricity than plastic weighing dishes. These aluminum weighing dishes are inert to all commonly used deuterated solvents. It is normal practice to measure solutions with concentrations of approximately 1 mg/mL. Therefore, an analytical balance that is capable of accurately measuring

Table 3 General qNMR acquisition parameters

Observer nucleus	^{1}H
Decoupled nucleus	^{13}C
^{13}C Decoupling pulse sequence	MPF8
Field strength	400 MHz
Spectral width	20 ppm
DSP	ON
Offset	5 ppm
Flip angle	90°
Acquisition time	4 s
Digital resolution	0.25 Hz
Relaxation delay	60 s
Probe temperature	25 °C
Number of transitions	8
Dummy scans	2

1 mg of a substance is essential. For this reason, it is also clearly stated in the Japanese Pharmacopoeia that qNMR measurements are to be taken using an ultra-micro balance [12].

3.3 *Quantitative NMR Data Acquisition*

The general measurement conditions adopted in the Japanese Pharmacopoeia [12, 13] are shown in Table 3. Two basic requirements for acquiring qNMR data is that all of the signal strength from both the analyte and internal standard must be collected and that the signals themselves are not saturated. To ensure all the signal is collected, the free induction decay (FID) must be long enough to prevent signal truncation. An acquisition time of 4 s is sufficiently long for this purpose. To prevent signal saturation, the sum of the interpulse relaxation delay and acquisition time should be 10 times longer than the spin-lattice relaxation time (T1) of the resonances that are monitored from both the analyte and internal standard [8]. Because ^{1}H T1 times for small molecules in solution are on the order of only a few seconds, the relaxation delay was set to a value of 60 s [8]. Furthermore, ^{13}C satellites (corresponding to approximately 0.55% of the main signal) which are normally observed on both sides of the main signal are eliminated through decoupling using the MPF8 pulse sequence [14] to ensure accurate integrals are obtained [15].

3.4 *Data Processing Under Conditions Suitable for Quantitative Measurements*

Generally, in qualitative NMR, the FID prior to Fourier transform is processed with a window function, which serves to improve either the S/N ratios or the spectral

Table 4 General qNMR data processing conditions

Software	Alice 2 for qNMR and Mnova NMR
Window function	OFF
Phase correction	Manual optimization for leveling baseline
Integral range	Integrals up to the point to where the baseline is lowered by eyesight
Baseline Correction	Auto

resolution, depending on the type of window function used. However, the use of window functions can introduce error in the integrals such that the resonance peaks areas are no longer proportional to the number of ^{1}H nuclei giving rise to the resonance. Therefore, window function processing usually not performed in qNMR [16].

Proper phase correction of the spectrum is essential to obtaining accurate results. Generally, in qualitative NMR, phase optimization is achieved via auto processing, but in reality it is difficult to achieve complete optimization with auto processing. Therefore, in qNMR it is necessary to conduct phase optimization manually while conducting visual checks to ensure proper phasing of the spectrum [17].

In qualitative NMR, the integral range is usually set automatically, but to obtain an accurate signal area with qNMR, it is necessary to set the limits of an integral for a resonance (or a group of resonances) where the integral curve starts to rise and stops rising which is where the peak intensity is greater than the baseline. Furthermore, it is necessary to be cautious with baseline correction. In NMR measurements, baseline correction processing is conducted to flatten out NMR spectral distortion, but, depending on the algorithm used, the signal area may change by a few percentage points. Therefore it is essential in qNMR to ensure that the baseline correction point does not enter within the integral range of each signal [18].

The processing parameters and we applied are shown in Table 4. Specialized analysis software for qNMR is now marketed by a number of software manufacturers, and it is possible to implement data processing suitable for quantitative measurements using this software [19].

4 Application of AQARI to Creating Analytical Standards

The internal standards for qNMR and the set of qNMR conditions we have developed since 2011 are now being used to measure chemical purity of analytical standards in GC and HPLC, as well as other qNMR reference standards. The applicable scope of purity determination using qNMR is broad, and in the five years up to 2016, this method has been demonstrated to confer absolute purity, with assured traceability to the SI, for new and existing analytical standards of more than 500 compounds [20]. These products are diverse, including pesticides, crude drugs, active drug ingredients, catechin, mycotoxins, and amino acids. In particular, a supply of analytical standards using qNMR for seven crude drug products

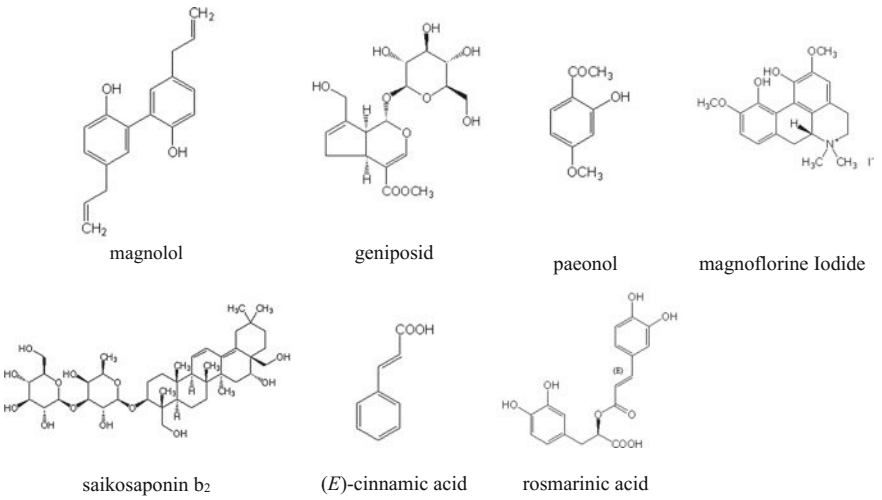

Fig. 6 Structural formulas of seven crude drugs

(magnolol, geniposide, paeonol, magnoflorine iodide, saikosaponin b_2, (*E*)-cinnamic acid and rosmarinic acid whose Structural formulas shown in Fig. 6 has commenced [21]; The former three crude drugs are the first analytical standards in Japan that were produced in an ISO/IEC17025 [22] -accredited laboratory. Also, the values obtained by qNMR are generally consistent with those obtained by freezing point depression and mass balance methods using DSC, which are the absolute quantification methods used until now. Thus, these results demonstrate that it is possible to promptly and efficiently obtain highly reliable absolute purity.

5 Summary

We have used AQARI, a qNMR method employing an internal standard, to characterize new qNMR standards and to characterize over 500 chromatographic analytical standards which have reliability because of having traceability to the International System of Units (SI). We expect to broaden our use of qNMR to include the characterization of reagents because qNMR is scheduled to be listed in the General Rules and Reagent Standards of the Japanese Industrial Standards.

References

1. Department of food safety, ministry of health, labor and welfare, Introduction of the Positive List Systems for Agricultural Chemical Residues in Food (2006).
2. T. Ihara, T. Saito, N. Sugimoto, *Synthesiology*. 2: 12–22 (2009).

3. T. Suematsu, H. Goda, N. Sugimoto, T. Miura *et al*., *qNMR Primary Guide*. 1: 19–22 (2015).
4. Grzegorz Maniara, Kannan Rajamoorthi, Srinivasan Rajan, Gerald W. Stockton, *Anal. Chem.* 70: 4921–4928 (1998).
5. Saito T, Ihara T, Koike M, Kinugasa S, Fujimine Y, Nose K, Hirai, *Accred Qual Assur*. 14: 79–86 (2009).
6. The Japanese Pharmacopoeia 16th Ed., Supplement 2 (2014).
7. The Cabinet Office and the Ministry of Health, Labor and Welfare, Order to partially revise the Ordinance for Enforcement of the Food Sanitation Act and the Ministerial Ordinance concerning Compositional Standards, Etc. for Milk and Milk Products: Order No. 5 (2011)., and Ministry of Health, Labor and Welfare, Notification Specifications and Standards for Food and Food Additives: Notification No. 307, 011 (2011).
8. T. Saito, T. Ihara, T. Miura, Y. Yamada, K. Chiba, *Accred Qual Assur*. 16: 421–428 (2011).
9. General requirements for the competence of testing and calibration laboratories, ISO/IEC 17025 (2005).
10. The Japanese Pharmacopoeia 16th Ed., Supplement 2:18 (2014).
11. The Japanese Pharmacopoeia 16th Ed., Supplement 2:20 (2014).
12. The Japanese Pharmacopoeia 16th Ed., Supplement 2:21 (2014).
13. The Japanese Pharmacopoeia 16th Ed., Supplement 2:12 (2014).
14. Fujiwara T, Anai T, Nagayama K, *J Magn Reson A*. 104: 103–105 (1993).
15. Pauli, G. F., *et al*., *J. Nat Prod.* 75(4): 834–851 (2012).
16. T. Suematsu, H. Goda, N. Sugimoto, T. Miura *et al*., *qNMR Primary Guide*. 1: 50–51 (2015).
17. T. Suematsu, H. Goda, N. Sugimoto, T. Miura *et al*., *qNMR Primary Guide.* 1: 101–102 (2015).
18. T. Suematsu, H. Goda, N. Sugimoto, T. Miura *et al*., *qNMR Primary Guide.* 1: 102–103 (2015).
19. JEOL RESONANCE, Alice 2 for qNMR and Mestrelab Research, Mnova NMR.
20. Wako Pure Chemical Industries, Ltd., Product list of analytical standard of pesticide and animal drug.
21. (2016), http://www.wako-chem.co.jp/siyaku/info/env/pdf/positivelist_1_1.pdf.
22. J. Hosoe, N. Sugimoto, T. Suematsu, Y. Yamada, T. Miura, M. Hayakawa, H. Suzuki, T. Katsuhara, H. Nishimura, T. Yamasihita, Y. Goda, *Pharmaceutical and Medical Device Regulatory Science*. 45: 243–250 (2014).